Title Models and Optimisation Methods for Interference Coordination in Self-organising Cellular Networks

Name David Lopez-Perez

Practical Models and Optimisation Methods for Inter-Cell Interference Coordination in Self-organising Cellular Networks

David López Pérez

Department of Computer Science and Technology

University of Bedfordshire

A thesis submitted for the degree of

Doctor of Philosophy

April 1st, 2011

I would especially like to dedicate this thesis to the memory of my aunt Lorenza, whose inner strength I will always admire, to my parents Juan José and Antonia, for whom there are no sufficient words to express my infinite gratitude and love, and also to my sister Charo and Emilia for their continuous support during these years.

Acknowledgements

I would like to thank my Director of Studies, Professor Jie Zhang, for the chance he gave me to join the Centre for Wireless Network Design (CWiND) and for his confidence and support in my investigations during these 3 years. I will always be grateful to him for it.

I would also like to thank Xiaoli Chu from King's College London for her support, help and kindness in the difficult times. She is one of the persons I came to admire the most. She helped me to significantly improve both my technical and writing skills and always provided me with wise advises. I really wish I could somehow pay back the help and support she gave me.

I would also like to thank my colleagues, house mates and friends Fernando Gordejuela, Alvaro Valcarce, Guillaume de la Roche, Ákos Ladányi and Lorenzo Galati for their friendship and good times in 15 Sotckwood Crescent. I would also like to extend this acknowledgement and thank the friendship of everyone I got to know in CWiND, the University, Luton and London.

I also like to express my admiration for Álpar Jüttner and Ákos Ladányi. Álpar for his always available advices and for our interesting discussions. Ákos for his useful suggestions and for his tireless work in our research. I would also like to thank Raymond Kwan for his comments and reviews.

I would like to thank M. Foster for his friendly talks and English corrections, and Luca Reggiani and Lorenzo Gallati for kindly reviwing this PhD thesis.

I would like to thank Jean Marie Gorce for inviting me to his lab in Lyon.

I would like to thank Holger Claussen and Carsten Maple for his comments. Although it was difficult to perform the review, I learnt quite a lot things. They pushed me to the limit, but I 'survived' with hard work and optimism. I will never forget this last 6 months.

I thank my colleagues in VODAFONE Spain in Alicante (Jose Manuel, Lydia and Jesus), who taught me the fundamentals of cellular networks.

I want to thank Emilia for her truly love and attention. She has always been there for me when it was needed. She is a very good person and an example to follow. This thesis would never be written without her support.

I want to thank my aunt Lorenza for her loving care and those long afternoon talks in her flat, my aunt Esperanza for her attention and those wonderful summers in Zarzadilla picking up almonds, my cousin Ramón for his wise advices and those extraordinary days in Carboneras on holidays, my cousins Andres, Elena and Daniel for his continuos and real friendship, In many ways, all these people have lit up my dreams across the years.

I express my gratitude to my family for their support throughout the years: to my parents, sister, grandparents, uncles, aunts, cousins and families too. I know that without their love, I cannot even live in this world. Thank you!

From the bottom of my heart, I am very thankful to each and every one of my friends of Zarzadilla de Totana. I want to thank all of them: Petete, Zorro, Amaro, Gerofo, Maeras, Peseta, Cecos, Abo, Botite, Giovanni, Roque and many others for their friendship, encouragement and loving care. Somehow, they have built my character and the person who I am now.

Finally, let me acknowledge the European Commission for supporting me; This research is funded by the EU FP6 Marie Curie RANPLAN-HEC project on Automatic 3G/4G Radio Access Network Planning and Optimisation - A High End Computing Approach (MEST-CT-2005-020958).

Abstract

We are at that moment of network evolution when we have realised that our telecommunication systems should mimic features of human kind, e.g., the ability to understand the medium and take advantage of its changes. Looking towards the future, the mobile industry envisions the use of fully automatised cells able to self-organise all their parameters and procedures.

A fully self-organised network is the one that is able to avoid human involvement and react to the fluctuations of network, traffic and channel through the automatic/autonomous nature of its functioning. Nowadays, the mobile community is far from this fully self-organised kind of network, but they are taken the first steps to achieve this target in the near future. This thesis hopes to contribute to the automatisation of cellular networks, providing models and tools to understand the behaviour of these networks, and algorithms and optimisation approaches to enhance their performance.

This work focuses on the next generation of cellular networks, in more detail, in the DownLink (DL) of Orthogonal Frequency Division Multiple Access (OFDMA) based networks. Within this type of cellular system, attention is paid to interference mitigation in self-organising macrocell scenarios and femtocell deployments. Moreover, this thesis investigates the interference issues that arise when these two cell types are jointly deployed, complementing each other in what is currently known as a two-tier network. This thesis also provides new practical approaches to the inter-cell interference problem in both macrocell and femtocell OFDMA systems as well as in two-tier networks by means of the design of a novel framework and the use of mathematical optimisation. Special attention is paid to the formulation of optimisation problems and the development of well-performing solving methods (accurate and fast).

Book chapters published

[1] David López-Pérez and Jie Zhang. *Femtocells: Technologies and Deployment*, chapter Self-Organization, pages 225–259. Wiley, January 2010.

[2] David López-Pérez, Guillaume de la Roche, and Hui Song. *Femtocells: Technologies and Deployment*, chapter System-Level Simulation for Femtocell Scenarios, pages 105–143. Wiley, January 2010.

[3] Alvaro Valcarce and David López-Pérez. *Femtocells: Technologies and Deployment*, chapter Interference in the presence of femtocells, pages 145–178. Wiley, January 2010.

Journal articles published/submitted

[1] Xiaoli Chu, Yuhua Wu, David López-Pérez, and Xiaofeng Tao. On Providing Downlink Services in Collocated Spectrum-Sharing Macro and Femto Networks. *Submitted to IEEE Transactions on Wireless Communications*, 2011.

[2] David López-Pérez, Xiaoli Chu, and Ismail Güvenc. On the Expanded Region of Picocells in Heterogeneous Networks. *Submitted to IEEE Transactions on Communications*, 2011.

[3] David López-Pérez, Xiaoli Chu, and Jie Zhang. Dynamic Frequency Planning and Power Assignment in OFDMA Cellular Networks. *Submitted IEEE Transactions on Vehicular Technology*, 2011.

[4] David López-Pérez, Ismail Güvenc, Guillaume de la Roche, Marios Kountouris, Tony Q.S. Quek, and Jie Zhang. Enhanced Inter-cell Interference Coordination Challenges in Heterogeneous Networks. *To appear in IEEE Wireless Commun. Mag. (Special Issue on HetNets)*, July 2011.

[5] Liqiang Zhao, Zhang Chi, David López Pérez, Xin Zhang, and Hailin Zhang. AirWiMAX: Low-Medium Altitude Platforms based PMP/Mesh Hybrid Access Networks. *Submitted to IET Communications*, 2010.

[6] David López-Pérez, Ákos Ladányi, Guillaume de La Roche, and Jie Zhang. Intracell Handover for Interference and Handover Mitigation in OFDMA Two-Tier Networks. *EURASIP Journal of Wireless Communications and Networking. Special issue on Femtocells*, March 2010.

[7] Guillaume de la Roche, Alvaro Valcarce, David López-Pérez, and Jie Zhang. Access Control Mechanisms for Femtocells. *IEEE Communications Magazine*, 48(1):33–39, January 2010.

[8] David López-Pérez, Alvaro Valcarce, Guillaume de la Roche, and Jie Zhang. OFDMA Femtocells: A Roadmap on Interference Avoidance. *IEEE Communications Magazine*, 47(9):41–48, September 2009.

[9] Alvaro Valcarce, Guillaume de La Roche, Alpár Jüttner, David López-Pérez, and Jie Zhang. Applying FDTD to the coverage prediction of WiMAX femtocells. *EURASIP Journal of Wireless Communications and Networking. Special issue on Advances in Propagation Modelling for Wireless Systems*, February 2009.

Conference articles published/submitted

[1] Xiaoli Chu, Yuhua Wu, David López-Pérez, and Haibo Wang. Decentralized Femtocell Transmission Regulation in Spectrum-Sharing Macro and Femto Networks. In *IEEE 74st Vehicular Technology Conference (VTC 2011) (submitted)*, San Francisco USA, September 2011.

[2] David López-Pérez and Xiaoli Chu. Inter-Cell Interference Coordination for Expanded Region Picocells in Heterogeneous Networks. In *IEEE ICCCN 2011 Workshop on Cooperative Heterogeneous Networks (submitted)*, Hawaii, USA, August 2011.

[3] David López-Pérez, Xiaoli Chu, and Thanos Vasilakos. On the Decentralized and Cooperative Resource Allocation for Interference Mitigation in Self-Organizing LTE Networks. In *ACM SIGCOMM 2011 (submitted)*, Toronto Canada, August 2011.

[4] David López-Pérez, Ákos Ladányi, Alpár Jüttner, Herve Rivano, and Jie Zhang. Optimization Method for the Joint Allocation of Modulation Schemes, Coding Rates, Resource Blocks and Power in Self-Organizing LTE Networks. In *IEEE Conference on Computer Communications (INFOCOM 2011)*, Shanghai, China, April 2011.

[5] Guillaume de La Roche, Akos Ladanyi, David López-Pérez, Chia-Chin Chong, and Jie Zhang. Self-organization for LTE Enterprise Femtocells. In *IEEE Globecom 2010 Workshop on Femtocell Networks*, Miami, USA, December 2010.

[6] David López-Pérez, Ákos Ladányi, Alpár Jüttner, and Jie Zhang. OFDMA femtocells: Intracell Handover for Interference and Handover Mitigation in Two-Tier Networks. In *IEEE Wireless Communications and Networking Conference (WCNC)*, Sydney, Australia, April 2010.

[7] David López-Pérez, Ákos Ladányi, Alpár Jüttner, and Jie Zhang. OFDMA femtocells: A self-organizing approach for frequency assignment. In *IEEE Personal, Indoor and Mobile Radio Communications Symposium (PIMRC)*, Tokyo, Japan, September 2009.

[8] Alvaro Valcarce, David López-Pérez, Guillaume De La Roche, and Jie Zhang. Limited Access to OFDMA femtocells. In *IEEE Personal, Indoor and Mobile Radio Communications (PIMRC)*, Tokyo (Japan), September 2009.

[9] Lorenzo Galati, David López-Pérez, Luca Reggiani, Laura Dossi, Alpár Jüttner, and J. Zhang. Two-Dimensional Radio Resource Allocation Algorithms with Contiguity Constraint for IEEE 802.16e Systems. In *IEEE Personal, Indoor and Mobile Radio Communications Symposium (PIMRC)*, Tokyo, Japan, September 2009.

[10] David López-Pérez, Ákos Ladányi, Alpár Jüttner, and Jie Zhang. Self-organisation of the Sub-channel Assignment in OFDMA Femtocellsi Advantages and Drawbacks of Different Channel Monitoring Techniques. In *FemtoCells Europe*, London, UK, June 2009.

[11] David López-Pérez, Alpár Jüttner, and Jie Zhang. Dynamic System Level Simulation of Dynamic Frequency Planing for Real Time Services in WiMAX Networks. In *International Conference on Wireless Communications and Mobile Computing (IWCMC)*, pages 1397–1403, Leipzig, Germany, 2009.

[12] Fernando Gordejuela-Sánchez, David López-Pérez, and Jie Zhang. A Two-Step Method for the Optimization of Antenna Azimuth/Tilt and

[6] D_.id López-Pérez, Ákos L nyi, Alpár Jüttner, and Jie Zhang. OFDMA femtocells: Intracell Handover for Interference and Handover Mitigation in Two-Tier Networks. In *IEEE Wireless Communications and Networking Conference (WCNC)*, Sydney, Australia, April 2010.

[7] David López-Pérez, Ákos Ladányi, Alpár Jüttner, and Jie Zhang. OFDMA femtocells: A self-organizing approach for frequency assignment. In *IEEE Personal, Indoor and Mobile Radio Communications Symposium (PIMRC)*, Tokyo, Japan, September 2009.

[8] Alvaro Valcarce, David López-Pérez, Guillaume De La Roche, and Jie Zhang. Limited Access to OFDMA femtocells. In *IEEE Personal, Indoor and Mobile Radio Communications (PIMRC)*, Tokyo (Japan), September 2009.

[9] Lorenzo Galati, David López-Pérez, Luca Reggiani, Laura Dossi, Alpár Jüttner, and J. Zhang. Two-Dimensional Radio Resource Allocation Algorithms with Contiguity Constraint for IEEE 802.16e Systems. In *IEEE Personal, Indoor and Mobile Radio Communications Symposium (PIMRC)*, Tokyo, Japan, September 2009.

[10] David López-Pérez, Ákos Ladányi, Alpár Jüttner, and Jie Zhang. Self-organisation of the Sub-channel Assignment in OFDMA Femtocells: Advantages and Drawbacks of Different Channel Monitoring Techniques. In *FemtoCells Europe*, London, UK, June 2009.

[11] David López-Pérez, Alpár Jüttner, and Jie Zhang. Dynamic System Level Simulation of Dynamic Frequency Planing for Real Time Services in WiMAX Networks. In *International Conference on Wireless Communications and Mobile Computing (IWCMC)*, pages 1397–1403, Leipzig, Germany, 2009.

[12] Fernando Gordejuela-Sánchez, David López-Pérez, and Jie Zhang. A Two-Step Method for the Optimization of Antenna Azimuth/Tilt and

Frequency Planning in OFDMA Multihop Networks. In *IEEE International Wireless Communications and Mobile Computing Conference (IWCMC)*, pages 1404–1409, Leipzig, Germany, June 2009.

[13] David López-Pérez, Alpár Jüttner, and Jie Zhang. Dynamic Frequency Planning Versus Frequency Re-use Schemes in OFDMA Networks. In *IEEE Vehicular Technical Conference (VTC 2009-Spring)*, Barcelona, Spain, April 2009.

[14] Alvaro Valcarce, David López-Pérez, Guillaume De La Roche, and Jie Zhang. Predicting small-scale fading distributions with Finite-Difference methods in Indoor-to-Outdoor scenarios. In *IEEE Vehicular Technical Conference (VTC 2009-Spring)*, Barcelona, Spain, April 2009.

[15] Fernando Gordejuela-Sánchez, David López-Pérez, and Jie Zhang. Frequency Planning in IEEE 802.16j Networks: An Optimisation Framework and Performance Analysis. In *IEEE Wireless Communications and Networking Conference (WCNC)*, Budapest, Hungary, April 2009.

[16] David López-Pérez, Guillaume de la Roche, Alvaro Valcarce, Álpar Jüttner, and J. Zhang. Interference Avoidance and Dynamic Frequency Planning for WiMAX Femtocells Networks. In *11th IEEE Singapore International Conference on Communication Systems (ICCS)*, pages 1579–1584, Guangzhou, China, November 2008.

[17] David López-Pérez, Alvaro Valcarce, Guillaume De La Roche, Enjie Liu, and Jie Zhang. Access Methods to WiMAX Femtocells: A downlink system-level case study. In *11th IEEE Singapore International Conference on Communication Systems (ICCS)*, pages 1657–1662, November 2008.

[18] Fernando Gordejuela-Sánchez, David López-Pérez, Liquiang Zhao, and Jie Zhang. Efficient Mobile Wimax Capacity Estimations in a Multihop Environment. In *11th IEEE Singapore International Conference*

on Communication Systems (ICCS), pages 1640–1646, Guangzhou, China, November 2008.

[19] David López-Pérez, Alpár Jüttner, and Jie Zhang. Optimisation Methods for Dynamic Frequency Planning in OFDMA Networks. In *13th International Telecommunications Network Strategy and Planning Symposium (Networks 2008)*, pages 1–28, Budapest, Hungary, September 2008.

Declaration

I, David López Pérez, declare that the thesis entitled *Self-organization in cellular networks: models and optimization* and the work presented in the thesis are both my own, and have been generated by me as the result of my own original research.

I confirm that:

- this work was done wholly or mainly while in candidature for a research degree at this University;
- where any part of this thesis has previously been submitted for a degree or any other qualification at this University or any other institution, this has been clearly stated;
- where I have consulted the published work of others, this is always clearly attributed;
- where I have quoted from the work of others, the source is always given. With the exception of such quotations, this thesis is entirely my own work;
- I have acknowledged all main sources of help;
- where the thesis is based on work done by myself jointly with others, I have made clear exactly what was done by others and what I have contributed myself;

Signed: .....

April 30, 2011

Acronyms

3GPP	3rd Generation Partnership Project
ABSF	Almost Blank Subframes
AMC	Adaptive Modulation and Coding
APA	Adaptive Power Assignment
auRRAA	autonomous Radio Resource Allocation Architecture
auRAP	autonomous Resource Allocation Problem
auRPAP	autonomous RB and Power Allocation Problem
BLER	BLock Error Rate
BS	Base Station
CAPEX	CAPital EXpenditure
CDF	Cumulative Distribution Function
CDMA	Code Division Multiple Access
CoMP	Coordinated Multi-Point transmission/reception
coRRAA	cooperative Radio Resource Allocation Architecture
coRAP	cooperative Resource Allocation Problem
coRPAP	cooperative RB and Power Allocation Problem

CQI	Channel Quality Indicator
CSG	Closed Subscriber Group
DAS	Distributed Antenna System
DFP	Dynamic Frequency Planning
DL	DownLink
DSA	Dynamic Subcarrier Assignment
DSL	Digital Subscriber Line
eDFP	enhanced Dynamic Frequency Planning
FAP	Femtocell Access Point
FDD	Frequency Division Duplexing
FDTD	Finite-Difference Time-Domain
FEC	Forward Error Correction
FFRS	Fractional Frequency Reuse Scheme
FRS	Frequency Reuse Scheme
GSM	Global System for Mobile communication
HARQ	Hybrid Automatic Repeat reQuest
HBS	Home Base Station
HII	High Interference Indicator
HO	Handover
HSPA	High Speed Packet Access
IEEE	Institute of Electrical and Electronics Engineers
ILP	Integer Linear Programming

IM	Interference Minimisation
IP	Internet Protocol
KPI	Key Performance Indicator
LLS	Link-Level Simulation
LP	Linear Programming
LTE	Long Term Evolution
LUT	Look Up Table
MAC	Medium Access Control
MCS	Modulation and Coding Scheme
MIMO	Multiple Input Multiple Output
MIP	Mixed Integer Program
MR	Measurement Report
NCL	Neighbouring Cell List
NGMN	Next Generation Mobile Networks
OAM	Operating, Administering, and Maintaining
OFDM	Orthogonal Frequency Division Multiplexing
OFDMA	Orthogonal Frequency Division Multiple Access
OPEX	OPerational EXpenditure
PHY	Physical
QoS	Quality of Service
RB	Resource Block
RF	Radio Frequency

RNC	Radio Network Controller
RPAP	RB and Power Allocation Problem
SA	Simulated Annealing
SINR	Signal to Interference plus Noise Ratio
SLS	System-Level Simulation
TDD	Time Division Duplexing
TS	Tabu Search
UL	UpLink
UMTS	Universal Mobile Telecommunication System
VoIP	Voice over IP
WiFi	Wireless Fidelity
WiMAX	Wireless Interoperability for Microwave Access

List of Symbols

$\mathcal{A}$	Restriction matrix
A_c	An interfering femtocell of user U_u
$A^{h,max}$	Maximum attenuation offset of the horizontal antenna pattern
$A^{v,max}$	Maximum attenuation offset of the vertical antenna pattern
$A^h(\theta)$	Attenuation offset introduced by the horizontal antenna pattern
$A^v(\theta)$	Attenuation offset introduced by the vertical antenna pattern
$a_{m,n}$	Interference restriction between macrocells M_m and macrocell M_n in terms of percentage of interference time
B_k	Bandwidth of RB or subchannel k
$BLER_{u,h,k}$	Block error rate of user U_u in subchannel k when using MCS h
$BR_{u,h,k}$	Bit rate of user U_u in subchannel k when using MCS h
C_u^{intrf}	Number of interfering cells of user U_u
$C_{u,k}$	Capacity in bps of user U_u^m in RB or subchannel k

$\mathcal{D}$	Demand vector
D_m	Number of RBs required by macrocell M_m to satisfy the bandwidth demand of its outer-zone users
D^{max}	Maximum number of RBs that a macrocell can require to meet the bandwidth demand of its outer-zone users
D_u	Number of RBs required by macrocell M_m to satisfy the throughput demand TP_u^{req} of its user U_u^m
d_{ID}	Number of bits needed to encode N_b
d_k	Number of bits needed to encode k
d_w	Number of bits needed to encode $w_{f,k}$
$d_{\Delta P}$	Number of bits needed to encode ΔP_k
$d_{\Delta T_{IHO}}$	Number of bits needed to encode ΔT_{PC}
$d_{m,u}$	Distance in kilometers between macrocell M_m and user U_u
$\mathcal{F}$	Set of femtocells
F_f	A femtocell
$f(x)$	Cost function value of solution x, i.e. overall inter-cell interference
$f(\rho)$	Cost function value of solution ρ, i.e. macrocell power consumption
g	Antenna gain
$g(k)$	Sequence number of subchannel k according to its ordering in terms of badness value

$\mathcal{H}$	Set of modulation and coding schemes
h	A modulation and coding scheme
$IE_{m,b}$	Interference event between macrocell M_m and its neighboring macrocell $N_b^m \in \mathcal{N}_m$
$IEC_{m,b}$	Counter used by macrocell M_m to count the number of interference events between itself and its neighboring macrocell $N_b^m \in \mathcal{N}_m$
$\mathcal{K}$	Set of subchannels or resource blocks
k	A subchannel or resource block
l	Equipment loss
$\mathcal{M}$	Set of macrocells
M_m	A macrocell
MR_u	Measurement report sent by user U_u
$MRC_{m,b}$	Counter used by macrocell M_m to count the number of measurement reports among itself and its neighboring macrocell $N_b^m \in \mathcal{N}_m$
$\mathcal{N}_m$	Set of neighboring cells of macrocell M_m
N_m	Number of neighboring cells of macrocell M_m
N_b^m	A neighboring cell of macrocell M_m
$\mathcal{N}_x$	Set of visited neighbors of a solution x per iteration in TS
N_x	Number of visited neighbors of a solution x per iteration in TS

$\mathcal{N}_\rho$	Set of visited neighbors of a solution ρ per iteration in TS
N_ρ	Number of visited neighbors of a solution ρ per iteration in TS
p_m^{total}	Total available power in macrocell M_m
$p_{m,k}^{max}$	Power resulting from dividing the total available power p_m^{total} in macrocell M_m by the number of available subcarriers R
$p_{u,k}^{m,centre}$	Power applied by macrocell M_m to a cell-centre subcarrier when using FFRSs
$p_{u,k}^{m,edge}$	Power applied by macrocell M_m to a cell-edge subacarrier when using FFRSs
p_m^{pilot}	Power applied by macrocell M_m to each one of the subcarriers of the pilot symbols
$p_{u,k}^{m}$	Power applied by macrocell M_m to each one of the subcarriers of the subchannel k allocated to user $U_u m$
$p_{u,k,h}^{m}$	Power that macrocell M_m has to allocate in each of the subcarriers of RB k for user U_u^m to achieve the SINR threshold γ_h^{mcs} of MCS h
$p_k^{m,max}$	Power constraint: Maximum power that macrocell M_m should allocate to RB k
$\mathcal{R}$	Set of subcarriers
R_{DL}^{tot}	Number of total subcarriers
R_{DL}^{data}	Number of data subcarriers
r	A subcarrier
s	Number of cells per base station
$\mathcal{T}_{\mathcal{DL}}$	Set of downlink OFDM symbols

T_{DL}^{data}	Number of data OFDM symbols
T_{ca}	Time interval in which each macrocell M_m measures the number D_m of utilized RBs by its outer-zone users
T_{ca}^{w}	Size of the temporal moving window used to remember the number D_m of utilized RBs by its outer-zone users
T_{dfp}	Time between the execution of two consecutive DFP procedures
T_{ie}^{w}	Size of the temporal moving windows used to remember both $MRC_{m,b}$ and $IEC_{m,b}$
$T_{MR,up}^{f}$	Maximum time between consecutive updates in femtocell F_f for the measurement report approach
$T_{NLM,up}^{f}$	Maximum time between consecutive updates in femtocell F_f for the network listening mode
T_{rpap}	Maximum time between consecutive updates in a cell for RPAP
T_{corap}	Maximum time between consecutive updates in a cell for coRAP
T_{aurap}	Maximum time between consecutive updates in a cell for auRAP
T_{corpap}	Maximum time between consecutive updates in a cell for coRPAP
T_{aurpap}	Maximum time between consecutive updates in a cell for auRPAP
$T_{subframe}$	Time duration of the DL subframe
$\hat{T}$	Poisson process: time interval of the process used to generate users
TP_{u}^{req}	Throughput demand of user U_u
$TP_{u,h,k}$	Throughput of user U_u in subchannel k when using MCS h

t_{dl}	A downlink OFDM symbol
t_u	Exponential distribution: holding time of a user in the network
$T_{u,cqi}$	Time between consecutive channel quality indicators of user U_u
$T_{u,mr}$	Time between consecutive measurement reports of user U_u
$\mathcal{U}$	Set of users
U_u	A user
$\mathcal{U}^m$	Set of users connected to macrocell M_m
U_u^m	A user connected to macrocell M_m
U_m	Maximum number of users in macrocell M_m
$w_{u,k}$	Power of the interference suffered by user U_u^m in subchannel k
$w_{u,k}^m$	Power of the signal received by user U_u^m in subchannel k due to serving macrocell M_m
$w_{u,m}^p ilot$	Power of the signal received by user U_u^m due to the pilot signal of macrocell M_m
$w_{u,k}^{max}$	The maximum interference that user U_u^f can tolerate to meet its quality of service demand
$w_{u,k}^{C-max}$	The maximum interference that a single interfering cell A_c is allowed to cause to macrocell user U_u^m to guarantee its quality of service demand
x	A solution consisting of an RB assignment to every sector fulfilling all DFP constraints
$x_{m,k}$	Binary variable that is equal to 1 if macrocell M_m is using RB k, or equal to 0 otherwise

$y_{m,b,k}$	Binary variable that is equal to 1 if macrocell M_m and its neighboring cell N_b^m are using RB k, or equal to 0 otherwise
α	Path loss exponent
γ^{edge}	Boundary between cell-centre and cell-edge
$\Gamma_{m,u}$	Channel gain between macrocell M_m and user U_u
γ_h	SINR threshold of MCS h
$\gamma_{u,k}^m$	SINR suffered by user U_u^m connected to macrocell M_m in subchannel k
γ_u^{pc}	SINR guarantied through macrocell-femtocell cooperation to nonsubscriber U_u^m
$\delta_{m,u}$	Path loss between cell M_m and user U_u^m
Δp_k	Power reduction asked by macrocell M_m to each one of its interfering femtocells $A_c \in \theta_u$ in subchannel k
ΔQ	Interference protection margin in the DFP approach
ΔT_{PC}	Period of time for which macrocell-femtocell cooperation last
Δw	Inter-cell interference margin used in order to compute cooperative constraints between cells
κ_u	Binary variable that is equal to 1 if user U_u can be allocated to the RBs reserved for cell-edge use via DFP, or equal to 0 otherwise
Ξ	The solution space of the MCS assigment problem in coRAP/auRAP problem
$\theta_{m,u}^h$	Angle of arrival in the azimuth plain between macrocell M_m and user U_u^m

$\theta^v_{m,u}$	Angle of arrival in the vertical plain between macrocell M_m and user U^m_u
θ^h_{3dB}	Beam width of the horizontal antenna pattern within which at least half of the maximum power is transmitted
θ^v_{3dB}	Beam width of the vertical antenna pattern within which at least half of the maximum power is transmitted
λ	Poisson process: intensity of the process used to generate users
μ	Exponential distribution: mean holding time of a user in the network
$\xi_{m,u}$	Shadow fading between macrocell M_m and user U^m_u
ρ	A solution consisting of an MCS assignment to every user of a macrocell fulfilling all coRAP (auRAP) constraints
$\rho_{u,h}$	Binary variable that is equal to 1 if user U_u uses MCS h, or equal to 0 otherwise
σ	Background noise density
σ_s	Shadowing standard deviation
τ	Sensitivity of the receiver of a base station
Υ_u	Set of interfering cells of user U_u
$\phi_{u,k}$	Binary variable that is equal to 1 if U_u uses RB k, or equal to 0 otherwise
$\chi_{u,k,h}$	Binary variable that is equal to 1 if user U_u is using MCS h in RB k, or equal to 0 otherwise
Ψ_f	Interference matrix of cell F_f for the interference minimisation based approach
Ω	The solution space of the DFP problem

Contents

Acronyms xiv

List of symbols xxxii

1 Introduction 1

1.1 Cellular Networks 1

1.2 Self-organisation 3

1.3 Fundamentals of OFDMA: The LTE and WiMAX perspective 5

1.3.1 LTE (3GPP Release 8) 7

1.3.2 WiMAX (IEEE 802.16e) 10

1.3.3 Channel-state Estimation 12

1.4 Femtocell Access Points: A New Challenge in Cellular Networks 14

1.4.1 Femtocell Related Terminology 17

1.5 Principal Objectives of This Thesis 18

1.6 Structure of This Thesis 19

2 Interference Avoidance: State of the Art and Research Challenges 22

2.1 Interference Avoidance in Macrocell Deployments 23

2.1.1 Frequency Reuse Schemes 23

2.1.1.1 Universal Reuse 23

2.1.1.2 Frequency Reuse 23

2.1.2 Fractional Frequency Reuse 24

2.1.2.1 Fractional Frequency Reuse Scheme (FFRS) s-A 25
2.1.2.2 FFRS s-B 25
2.1.3 Dynamic Approaches 25
2.1.3.1 Centralised Approaches 26
2.1.3.2 Distributed Approaches 28
2.2 Interference Mitigation in Femtocell Deployments 29
2.2.1 Spectrum Assignment to Femtocells . . . i 29
2.2.1.1 Assignment of Carrier Frequencies 29
2.2.1.2 Assignment of OFDM Subchannels 31
2.2.2 Access Methods to Femtocells . . ii . . i 32
2.2.2.1 Interference in Closed Access Femtocells 32
2.2.2.2 Interference in Open Access Femtocells 33
2.2.2.3 Interference in Hybrid Access Femtocells 34
2.2.3 State-of-the-Art in Self-organising Interference Avoidance Techniques for Femtocells 35

3 Network Modelling: Dynamic System-Level Simulation 39
3.1 Network Definition 40
3.2 Simulation Assumptions 40
3.3 Traffic load Modelling 41
3.4 Path Loss Modelling 42
3.5 Signal Strength Modelling 43
3.6 Interference Modelling 45
3.7 Signal Quality Modeling 45
3.8 Bit Rate Modeling 46
3.9 Throughput Modeling 46
3.10 Measurement Reports 47
3.11 Channel Quality Indicators 47

4 Centralised Interference Mitigation Architecture for Macrocells: enhanced Dynamic Frequency Planning **49**

4.1 Enhanced Dynamic Frequency Planning 50

4.2 Dynamic Frequency Planning 51

4.2.1 DFP Inputs 51

4.2.1.1 Demand Vector 52

4.2.1.2 Restriction Matrix 53

4.2.2 DFP Optimisation 55

4.3 Distributed Resource Block and Power Allocation 56

4.4 Solving DFP 60

4.4.1 Integer Linear Programming 61

4.4.2 Metaheuristics 61

4.4.2.1 Simulated Annealing 62

4.4.2.2 Tabu Search 63

4.4.3 Greedy Algorithms 64

4.4.3.1 Insertion Algorithms 64

4.4.3.2 Removal Algorithms 66

4.5 Solving RPAP 67

4.6 Simulation and Numerical Results 68

4.6.1 Scenario 68

4.6.2 Optimisation Performance 71

4.6.2.1 Solving DFP 71

4.6.2.2 Solving RPAP 75

4.6.3 Network Performance 75

4.6.3.1 Techniques Used for Comparison 75

4.6.3.2 Cell-Centre and Cell-Edge Zones: γ^{edge} 77

4.6.3.3 Transmit Power 77

4.6.3.4 Inter-Cell Interference 78

4.6.3.5 System-Level Performance 78

4.7 Conclusions 83

5 Decentralised Interference Mitigation Architecture for Macrocells: enhanced Resource Allocation Problem 85

5.1 Fundamentals of Our Decentralised Allocation Schemes 86

5.1.1 Transmit Power Minimisation 86

5.1.2 Inter-BS Cooperation . . . . r 87

5.2 Cooperative Resource Allocation Problem 89

5.3 Cooperative RB and Power Allocation Problem 92

5.3.1 Solving coRPAP optimally 93

5.4 Solving coRAP 95

5.5 Resource Management Architecture 98

5.5.1 Signalling Overhead 99

5.6 Simulation and Numerical Results 99

5.6.1 Scenario 99

5.6.2 Optimisation Performance 100

5.6.2.1 Solving coRPAP 100

5.6.2.2 Solving coRAP 100

5.6.3 Network Performance 101

5.6.3.1 Techniques Used for Comparison 101

5.6.3.2 Cell-Centre and Cell-Edge Zones: γ^{edge} 101

5.6.3.3 Subroutine Updating Frequency: T_{corpap} and T_{aurpap} . . 102

5.6.3.4 Transmit Power 103

5.6.3.5 Inter-Cell Interference 104

5.6.3.6 Resource Block Allocation 105

5.6.3.7 System-Level Performance 107

5.6.3.8 Signalling Overhead 110

5.7 Conclusions 110

6 Radio Resource Management for Femtocells: Co-Tier Interference 113

6.1 Radio Resource Management Issues in Femtocell Scenarios 115

6.1.1 Network Listening Mode 115

6.1.2 Message Passing 116

6.1.3 User Measurements 116

6.2 coRRAA and auRRAA 118

6.3 Femtocell Radio Resource Management Techniques Proposed for Performance Comparison 121

6.3.1 Network Listening Mode-Based Method 121

6.3.2 IM-Based Method . . . r 122

6.4 Simulation and Numerical Results 124

6.4.1 Scenario 124

6.4.2 Optimisation Performance 126

6.4.2.1 Solving auRPAP 126

6.4.2.2 Solving auRAP 127

6.4.3 Network Performance 127

6.4.3.1 Techniques Used for Comparison 127

6.4.3.2 Cell-Centre and Cell-Edge Zones: γ^{edge} 128

6.4.3.3 Transmit Power 128

6.4.3.4 Inter-Cell Interference 129

6.4.3.5 Resource Block Allocation 130

6.4.3.6 System-Level Performance 130

6.4.3.7 Signalling Overhead 132

6.5 Conclusions 133

7 Radio Resource Management for Femtocells: Cross-Tier Interference 135

7.1 Introduction 135

7.2 Overview on Handover and Cross-Tier Interference Coordination in Femtocell Deployments 137

7.2.1 Handover 137
7.2.2 Cross-Tier Interference Coordination 138
7.3 Cooperative Radio Resource Allocation Architecture for Two-Tier Networks 139
7.3.1 Macrocell and Femtocell Communication 145
7.4 Simulation and Numerical Results 146
7.4.1 Scenario 146
7.4.2 Network Performance 149
7.4.2.1 Techniques Used for Comparison 149
7.4.2.2 coRRAA Basis 150
7.4.2.3 Subroutine Updating Frequency: T_{corpap} 152
7.4.2.4 System-Level Performance 155
7.4.3 Signalling Overhead 160
7.5 Conclusions 162

8 Discussion **164**
8.1 Trade-offs 164
8.2 Limitations 166

9 Conclusions and Future Work **170**
9.1 Conclusions 170
9.2 Future Work 172

A Techniques Used for Comparison **174**
A.1 Ronald's Approach 174
A.2 Hussain's Approach 176
A.3 Stolyar's Approach 179

References **191**

Chapter 1

Introduction

1.1 Cellular Networks

In the early years of wireless communications when this field was only a research area, the efficiency of networks was not an issue and engineers were only worried about making them work. However, over the last decades, this field has rapidly matured, and the number of customers and their needs have exponentially increased. Consequently, the planning and optimisation of current networks have become an important issue, not only for making networks functional, but also for making them more efficient.

In the early nineties, Global System for Mobile communication (GSM) [1] networks were deployed in order to satisfy the demands of users mostly based on voice services. At that time, the acquisition of new cell locations and the installation of new cell sites in order to extend radio coverage were one of the major concerns of network operators. In addition, Radio Frequency (RF) engineers expended a great effort in the area of automatic frequency planning [2] and antenna azimuth/tilt optimisation [3] as a way of mitigating electromagnetic interference and thus enhancing network performance. These tasks, together with the assignment of cell identities, set up of neighbouring cell lists and tuning of handover parameters represented one of the first works carried out in the area of what is known nowadays as *network planning and optimisation*. Nevertheless, the capacity improvements through optimisation were not enough to cope with the ever-increasing traffic demands of users. Thus, the development of new technologies that could complement and/or replace this type of network was necessary.

At the beginning of this millennium, Code Division Multiple Access (CDMA) appeared as the most promising technology to be deployed to replace GSM networks [4]. CDMA-based networks[1] are used nowadays to fulfil the new demands of users imposed by the use of mobile Internet applications. Given the huge number of parameters to be configured and the trade-off between coverage/capacity, cell breathing phenomena [6], this kind of network would not be able to work efficiently without the help of advanced network planning and optimisation tools. These tools cover a wide range of topics, from base station location or power control algorithms to scrambling code allocations. However, the use of these tools requires a large human involvement as well as expertise.

In the last five years, High Speed Packet Access (HSPA) networks have emerged as a new solution to improve user throughputs and thus allow a high speed connectivity [7]. This new technology moves some Medium Access Control (MAC) capabilities from the Radio Network Controller (RNC) to the base stations (NodeBs), e.g., fast scheduling, fast Hybrid Automatic Repeat reQuest (HARQ). In this way, these functionalities are closer to the air interface, thus making the system more responsive to fluctuations in traffic and channel due to delay minimisation. In addition, new techniques were introduced such as Adaptive Modulation and Coding (AMC) and fast power control, Operators had to expend new efforts to combine both systems, CDMA and HSPA, hence increasing work loads of engineers and their OPerational EXpenditures (OPEXs) and CAPital EXpenditures (CAPEXs) too.

Additionally, it is predicted that in the near future the traffic loads of networks and the requirements of customers will continue growing (Figure 1.1). Furthermore, new services, requiring improved Quality of Services (QoSs) and bit rates, will appear. To satisfy these requirements, vendors and operators are working on the development of new standards such as Wireless Interoperability for Microwave Access (WiMAX) [8] and Long Term Evolution (LTE) [9], which are considered the most suitable solutions for future deployments of cellular networks. They are both based on an Orthogonal Frequency Division Multiplexing (OFDM) Physical (PHY) layer that supports several key features necessary for delivering broadband services to high speed users [10], e.g., high spectral efficiency, intra-cell interference avoidance, multi-path robustness.

[1]Universal Mobile Telecommunication System (UMTS) is an example of CDMA-based network [5].

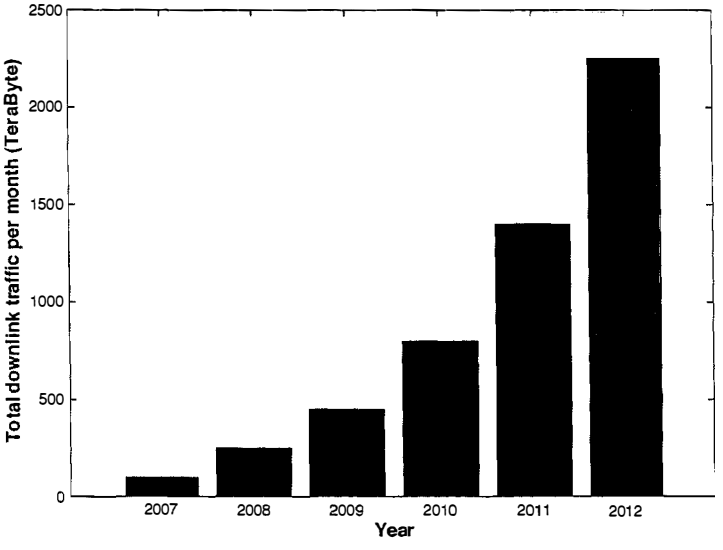

Figure 1.1: Cellular network traffic prediction from 2007 to 2012.[a]

[a]This figure has been obtained from [11]

These technologies will enable the possibility of a truly mobile broadband connectivity. However, it may be again at the expense of increasing the complexity/cost of networks.

1.2 Self-organisation

Nowadays, the pressure to be competitive forces operators to take the reduction of the complexity and cost of current networks as the key driver for future deployments. Becase of this fact, the minimisation of both CAPEX and OPEX, and the enhancement of network performance via self-organising approaches is of particular interest. Organisations such as Institute of Electrical and Electronics Engineers (IEEE) [12]; 3rd Generation Partnership Project (3GPP) [13]; Next Generation Mobile Networks (NGMN) [14] and the Socrates project [15] have already identified self-organisation as a need for the deployment, maintenance and sustainability of future cellular networks.

A *self-organising* network is defined as a network that requires minimal human involvement because of the *autonomous* and/or *automatic*[2] nature of its functioning.

[2]An autonomous activity is one that does not require any human involvement, while in an auto-

In these types of networks, base stations will integrate the processes of network planning and optimisation in sets of autonomous and/or automatic functions that will allow them to scan the air interface and tune their parameters according to the dynamic behaviour of the network, traffic and channel.

The need for self-organisation in future wireless networks is driven by the following aspects [16]:

- To achieve a substantial reduction in the CAPEX and OPEX of operators by reducing human involvement.
- To optimise the performance of networks in terms of coverage, capacity and QoS.
- To allow both operators and users the deployment of large numbers of small cells.

Due to the complexity of current cellular networks and the huge number of parameters to be configured, network operators invest large amounts of money in planning the deployment of new cell sites and optimising the performance of operative base stations. In addition, when new technologies such as LTE will be deployed by network operators, it is expected that in many regions more than three different technologies will coexist. This translates into a large human involvement that should incur an additional OPEX. However, the reduction of human involvement by means of self-organisation will permit network operators to remain competitive due to the reduction of these overheads [17].

Moreover, automating processes such as the configuration of frequency assignments, neighbouring cell lists or handover parameters will allow networks to rapidly adapt themselves to time-dependent network, traffic and channel fluctuations. In this way, avoiding long periods of time between manual optimisation procedures, base stations will be more responsive, and thus the performances of networks will be improved [18].

Self-organisation will also allow the final customer to install by himself a new type of base station known as Home Base Station (HBS) or Femtocell Access Point (FAP). This is possible since these devices will be able to integrate themselves into the existing networks without the help of operators. Also, because these access points will be both paid and maintained by users, these small base stations will aid to reduce CAPEX [19].

matic process, part of the activity is handled by the machine and part by the human being.

1.3 Fundamentals of OFDMA: The LTE and WiMAX perspective

Orthogonal Frequency Division Multiple Access (OFDMA) is the multi-user access technique adopted by the next generation of cellular networks, LTE [20] and WiMAX [8].

OFDMA relies on an OFDM PHY layer, which is a multi-carrier transmission technique that divides the available spectrum into a large number of small radio channels, each of them modulated by a low data rate. OFDM uses the spectrum very efficiently by spacing all these small channels very close to each other, making their carriers orthogonal to one another, therefore preventing intra-cell interference among them [21]. The orthogonality among carriers means that a carrier spectrum has a null at the centre frequency of adjacent ones (Figure 1.2).

In OFDMA-based networks, the radio spectrum is broken down into orthogonal *subcarriers* that are in turn combined into groups generally known as *subchannels*. Moreover, the time domain is split up into consecutive frames that are in turn divided into time slots called OFDM symbols. Since OFDMA is based on an OFDM PHY layer, it also inherits some of its fundamental properties [22]. Among them, it is worth noting:

- its *scalable spectrum allocation*, which permits a flexible spectrum assignment to base stations from relatively small bandwidths, 1.25 MHz, to large ones, 20 MHz.
- its *resistance to multipath* due to the use of large OFDM symbols in the order of 100 μseand a cycle prefix[1] of about 10 μs, which can support large delay spreads.
- its *fully orthogonal subcarriers*, which remove intra-cell interference from neighbouring subcarriers and allow them to be spaced as close as theoretically possible.

Due to frequency-selective interference and fading fluctuations along the spectrum, different users could suffer from very diverse channel conditions in a given subcarrier.

[1] The addition of a cycle prefix at the beginning of each symbol in OFDM is used to remove inter-symbol and inter-carrier interference. By repeating the end of a symbol at the beginning of the next one, the convolution of the channel impulse response with the signal at the end of a symbol does not affect the data at the beginning of the next symbol.

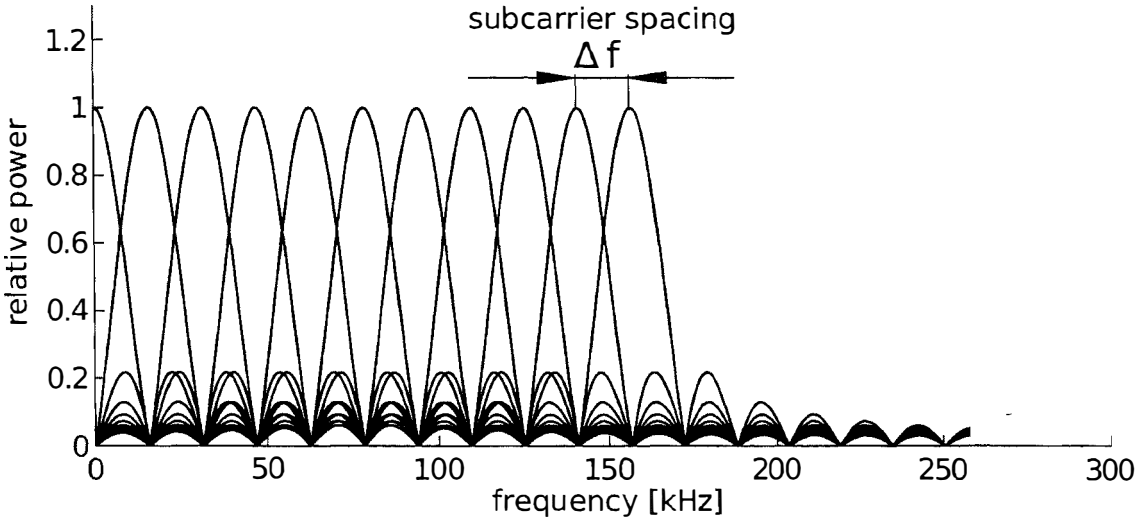

Figure 1.2: OFDM orthogonal subcarriers modulating rectangular pulses.

A single user could also experience diverse channel conditions in distinct subcarriers. Because it is unlikely that a user enjoys excellent signal qualities over all subcarriers, it is more reasonable to provide users with subcarriers that maximise their received Signal to Interference plus Noise Ratios (SINRs) instead of letting a single user use all the spectrum at a given time (Figure 1.3).

As a multi-access method, OFDMA offers the possibility of enhancing the spectral efficiency of networks by assigning distinct OFDM symbols or subchannels to distinct mobiles, thus taking advantage of their diverse time and frequency channel conditions. In this way and on the contrary to CDMA[1], OFDMA provides access to the frequency domain, and enables an additional degree of freedom to channel-dependent schedulers, which allows exploiting multi-user diversity.

Since the performance of an OFDMA-based network depends on this subchannel allocation procedure, there is a necessity for dynamic frequency assignment algorithms

[1] In CDMA, intra-cell interference is handled by using special pseudo-random orthogonal codes, and inter-cell interference can be mitigated by applying orthogonal time domain resource allocations. In OFDMA, intra-cell interference is handled by using orthogonal subcarriers, and inter-cell interference can be mitigated by applying both orthogonal time and frequency domain resource allocations. Moreover, power allocation strategies, antenna optimisation techniques, etc. can be used in both technologies to further reduce inter-cell interference.

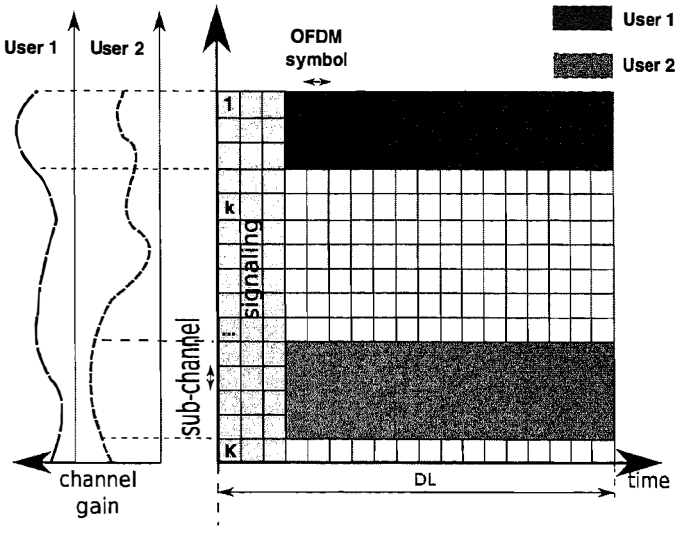

Figure 1.3: OFDMA frequency-time grid.[a]

[a]In OFDMA, different subchannels can be allocated to different users, preferably in the range where they have channel gain.

that can intelligently decide which subchannels are suitable for each user at each time.

Let us note that distinct network standards have distinct understandings of how to utilise OFDMA. In the following, the bases of LTE and WiMAX with regard to their use of OFDMA as multi-user access technology are introduced. These concepts, definitions and constraints will be employed from now on throughout this manuscript.

1.3.1 LTE (3GPP Release 8)

LTE offers round trip times below 10 ms as well as peak data rates of 50 Mbps in the UpLink (UL) and 100 Mbps in the DownLink (DL). It provides better spectrum efficiency and flexibility than legacy systems by allowing spectrum allocations to cells from 1.4 MHz up to 20 MHz. It enables sophisticated channel-dependent scheduling and rate adaptation to meet the rapid varying resource demands posed by packet data. It supports load management among neighbouring cells to permit inter-cell interference coordination by providing information about resource use and traffic load conditions. Furthermore, it also considers both Frequency Division Duplexing (FDD) and Time

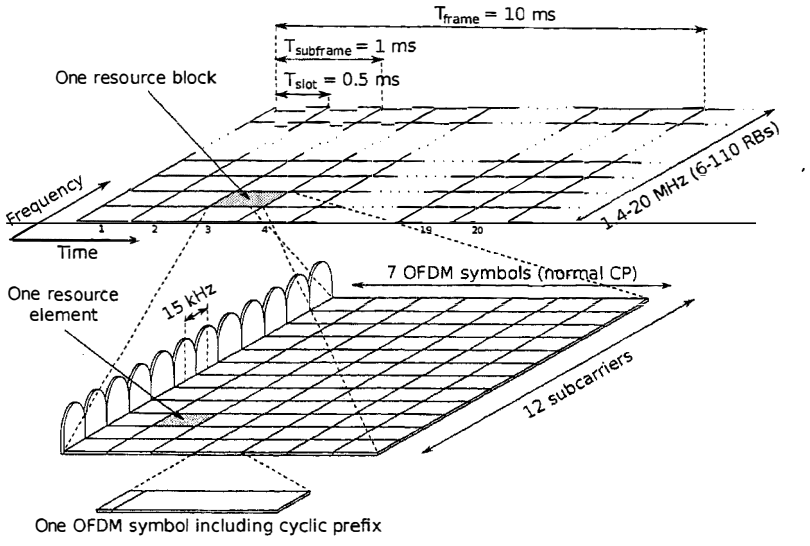

Figure 1.4: Physical layer structure of LTE (3GPP Release 8)i

Division Duplexing (TDD) modes for uplink-downlink duplexing with a large commonality of operations between both modes. [23; 24]

LTE DL transmissions are based on OFDMA, thus the set of DL physical resources can be seen as a frequency-time resource grid (Figure 1.4)i An element of this grid, a resource element, is built of one OFDM subcarrier lasting for one OFDM symbol. Due to efficiency reasons, the resource assignment works on groups of these resource elements called Resource Blocks (RBs)[1]. An RB is a rectangular block of resource elements, which spreads 12 adjacent subcarriers in the frequency domain and 7 OFDM symbols[2] in the time domain (180 kHz×0.5 ms). Depending on the transmission bandwidth, a DL carrier is comprised of a variable number of RBs in the frequency domain. The minimum bandwidth of 1.4 MHz corresponds to 6 RBs, while the maximum one of 20 MHz to 110 RBs. The subcarrier spacing is always 15 kHz[3], which fixes the OFDM

[1]In LTE, a subchannel is generally called an RB.

[2]Each RB has a time slot duration of 0.5 ms, which corresponds to 6 or 7 OFDM symbols [20]. However, this depends on whether an extended or normal cyclic prefix is adopted in order to transmit.

[3]In addition to the 15 kHz subcarrier spacing, a reduced subcarrier spacing of 7.5 kHz with twice as long OFDM symbol time is also defined for LTE. The reduced subcarrier spacing specifically targets Multicast-Broadcast Single-Frequency Network (MBSFN)-based multicast/broadcast transmissions. The remaining discussions within the following chapters will consider the 15 kHz subcarrier spacing.

Table 1.1: Modulation and coding schemes for LTE (3GPP Release 8)

MCS	**Modulation**	**Code Rate**	γ_h = **SINR threshold** [dB]	**Efficiency** [bits/symbol]
MCS1	QPSK	1/12	-6.50	0.15
MCS2	QPSK	1/9	-4.00	0.23
MCS3	QPSK	1/6	-2.60	0.38
MCS4	QPSK	1/3	-1.00	0.60
MCS5	QPSK	1/2	1.00	0.88
MCS6	QPSK	3/5	3.00	1.18
MCS7	16QAM	1/3	6.60	1.48
MCS8	16QAM	1/2	10.00	1.91
MCS9	16QAM	3/5	11.40	2.41
MCS10	64QAM	1/2	11.80	2.73
MCS11	64QAM	1/2	13.00	3.32
MCS12	64QAM	3/5	13.80	3.90
MCS13	64QAM	3/4	15.60	4.52
MCS14	64QAM	5/6	16.80	5.12
MCS15	64QAM	11/12	17.60	5.55

symbol duration and minimises the impact of bandwidth scaling in upper layers. [25]

At a high-level time-domain, LTE transmissions are structured in frames of 10 ms, each one of them containing 10 subframes of 1 ms [26]:

- In case of FDD operation, there are 2 carrier frequencies, 1 for UL and 1 for DL. Therefore, during each frame, there are 10 UL subframes and 10 DL subframes that are transmitted simultaneously in each base station using these 2 carriers.
- In case of TDD operation, there is only one carrier, thus during each frame some subframes are dedicated to the UL and some others to the DL transmissions. Because the same carrier is utilised for UL and DL, base stations and users need to continuously switch from transmission mode to reception mode and vice versa.

The assignment of RBs to users is carried out by the MAC scheduler, and it is performed on a subframe by subframe basis, i.e., each 1 ms (Figure 1.4). The scheduler decides which users are allowed to transmit and which RBs to assign to each user. It must be noted that the minimum resource scheduling unit[1] that the scheduler can

[1]For the sake of simplicity, from now on, when we refer to an RB, we refer to this minimum

assign to a user is comprised of 2 consecutive RBs and thus spans an entire subframe. Moreover, LTE supports AMC (Table 1.1), i.e.e it supports multiple modulation and Forward Error Correction (FEC) coding schemes and allows the network to change them on a per user and per subframe basis to cope with varying channel conditions. As a result, the scheduler must also decide the quantity of power to be applied to each RB as well as the Modulation and Coding Scheme (MCS) to be assigned to each user. Nevertheless, it must be noted that a constraint for LTE DL scheduling is that when a user is allocated to more than one RB, all of them have to have the same MCS. [27]

1.3.2 WiMAX (IEEE 802.16e)

WiMAX offers scalability in both radio access technology and network architecture, thus providing flexibility in network deployment and offering a large service variety. WiMAX defines service flows to enable QoS and end-to-end IP-based service mapping, provides a flexible spectrum allocation to cells that can operate in different channellisation from 1.25 MHz to 20 MHz in order to satisfy different operator requirements, enables mechanisms for channel-dependent scheduling on a frame by frame basis, and supports long range communications of up to 50 km and high data rates with peaks of 70 Mbps in the DL and 70 Mbps in the UL.

WiMAX transmissions are also based on OFDMA, thus the set of physical resources can be seen as a frequency-time resource grid (Figure 1.5)e The minimum frequency-time resource unit that the MAC scheduler can allocate to a user is known as a slot. Each slot consists of one subchannel over the frequency domain and one, two or three OFDM symbols over the time domain[1]. A contiguous set of slots allocated to a user is called data region. The MAC scheduler allocates different data regions to different users based on their channel conditions. Depending on the number of OFDM symbols in each slot, the number of subcarriers in each subchannel varies from 16 to 32 or 48. Similarly to LTE, the available spectrum scales from 128 subcarriers, 1.25 MHz, up to 2048 subcarriers, 20 MHz. The subcarrier spacing is always 10.94 kHz, which fixes the OFDM symbol duration and reduces the bandwidth scaling impact in upper layers. [28]

At a high-level time-domain, WiMAX transmissions are structured in frames of 5 ms, each one of them comprised of 48 OFDM symbols [29]:

scheduling unit of 2 consecutive RBs, spanning 1 ms.

[1]The number of subcarriers and OFDM symbols per slot depends on the network configuration.

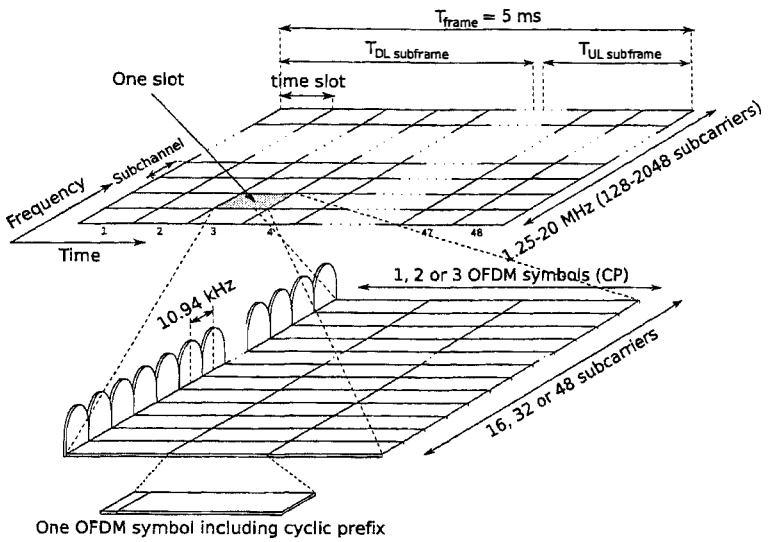

Figure 1.5: Physical layer structure of WiMAX (IEEE 802.16e).

Table 1.2: Modulation and coding schemes for WiMAX (IEEE 802.16e)

MCS	**Modulation**	**Code Rate**	γ_h = **SINR threshold** [dB]	**Efficiency** [bits/symbol]
MCS1	QPSK	1/2	2.88	1.00
MCS2	QPSK	3/4	5.74	1.50
MCS3	16QAM	1/2	8.79	2.00
MCS4	16QAM	3/4	12.22	3.00
MCS5	64QAM	1/2	15.88	4.00
MCS6	64QAM	3/4	17.50	4.50

- In case of FDD operation, there are 2 carrier frequencies, 1 for UL and 1 for DL, and thus UL and DL frames are transmitted simultaneously over distinct carriers.
- In case of TDD operation, since the same carrier is utilised for both UL and DL, the frame is divided into a DL subframe that is followed by an UL subframe[1]. Thus, the equipment also needs to switch often from transmission to reception.

The assignment of data regions to users is carried out by the MAC scheduler, and it is performed on a frame by frame basis, i.e., each 5 ms (Figure 1.4). The scheduler

[1] The number of OFDM symbols in each subframe depends on the network configuration used by the operator and varies according to an downlink-to-uplink ratio to support different traffic profiles.

decides which users are able to transmit and which data region to assign to each user. It must be noted that a constraint in WiMAX scheduling is that a data region must be a two-dimensional allocation of contiguous subchannels and OFDM symbols [8]. In addition, WiMAX also supports AMC, i.e., it supports several MCSs (Table 1.2). Therefore and similarly to an LTE network, a WiMAX network can also change MCSs on a per user and per frame basis to deal with time-fluctuating channel conditions. Thus, the scheduler must also decide the amount of power to be applied to each slot and the MCS to be allocated to each user. Nevertheless, it must be noted that a constraint for WiMAX DL scheduling is that when a user is assigned to more than one slot, all of them must have the same MCS [8].

The constraints imposed by these two network standards, LTE and WiMAX, on the allocation of subcarriers to users make the problem of resource assignment complex. *This is a research topic that this thesis addresses from a self-organisation viewpoint.*

1.3.3 Channel-state Estimation

In order to estimate user channel conditions, in both standards LTE and WiMAX, user terminals are able to estimate the instantaneous SINR of all subcarriers [30] [8]. Moreover, inserting known reference symbols, as well referred to as pilot symbols, at regular intervals within the OFDM frequency-time grid (Figure 1.6), user terminals can directly measure the channel conditions in both the frequency and the time domain.

Measurements over the OFDM reference symbols can be used for different purposes (let us note that the following definitions will be used throughout this manuscript):

Channel dependent scheduling In order to allow channel-dependent scheduling, i.e., the scheduler is able to select for each frequency region and time instant the user with the best channel conditions, both standards LTE and WiMAX grant to user terminals the capability of providing the network with channel-status reports indicating the instantaneous DL channel quality in both the frequency and the time domain [27].

Within a channel-status report, the Channel Quality Indicator (CQI) must be noted. The CQI contains the user recommended MCS that the cell should allocate to its DL transmissions in a given subchannel.

A CQI for each subchannel could be theoretically fed back from a user to its cell,

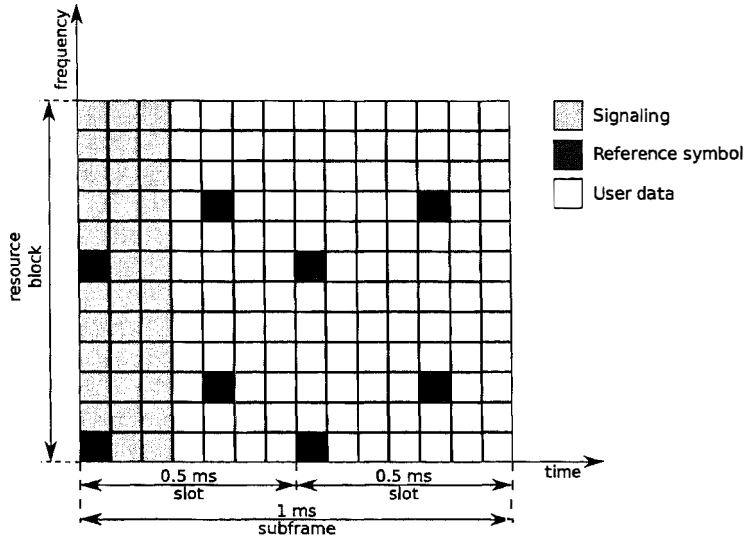

Figure 1.6: Reference symbols in LTE (3GPP Release 8).

but in practice only the CQIs of a subset of them can be fed back in each channel-status report due to UL signalling concerns[1].

Let us note that channel-status reports are either periodic or eventually triggered. For example, in LTE, users are instructed to perform a periodic channel-status report as regularly as once every 2 ms in order to assist the channel dependent scheduling [27].

Cell re-selection and handover In order to select the best serving cell when a user terminal is idle or to aid the handover procedure when a user terminal is active, user terminals are continuously measuring and reporting back to their serving cells the received signal strength of the cell-specific reference signals[2] of their neighbouring cells.

In order to simplify and speed up the task of user terminals when monitoring the air interface, the serving cell periodically broadcasts to its connected user terminals the list of specific neighbouring cells and reference symbols that they have to measure. This list is called the Neighbouring Cell List (NCL).

[1] Limited feedback needs a smaller bandwidth at the expense of degraded system performance [31].

[2] A cell-specific reference signal consists of a known sequence of reference symbols. In LTE, there are 504 different cell-specific reference signals, where each sequence corresponds to one physical-layer cell identity. It must be noted that cell-specific reference signals are used to identify different cells, and thus neighbouring cells have different cell-specific reference signals [27].

After receiving the NCL, user terminals periodically perform the appropriate measurements and feed back the results to their serving cells using a *measurement report*. Thereafter, using this information, the serving cell decides whether to start a new cell selection or handover procedure or to take no action.

For example, in LTE, users are instructed to perform measurement reports as regularly as once every 480 ms in order to aid cell selection and handover procedures [32].

Due to the relevant role played by the NCL in the cell selection and handover procedure, the proper configuration and set up of these NCLs is of a vital importance. This task has traditionally been performed off-line by operators using network planning and optimisation tools. However, current research attempts to automatise this task, thus allowing every base station to independently self-organise its own NCL [33] [34]. *For the sake of simplicity, in this manuscript, it is assumed that all base stations have perfect knowledge of the existence and identity of all their neighbouring base stations.*

It must be noted that the above definitions have focused on an LTE point of view. However, the idea behind these concepts also applies to WiMAX networks.

1.4 Femtocell Access Points: A New Challenge in Cellular Networks

According to recent surveys, in the following years, 50 % of phone calls as well as 70 % of data services will take place indoors [35]. Hence, it is important for network operators to provide good indoor coverage for voice, video and high speed data services. Furthermore, some other surveys show that 45 % of households and 30 % of businesses experience poor indoor coverage [36]. In addition, note that poor indoor coverage will affect operator revenues, reduce subscriber loyalty and increase subscriber churn. Therefore, new solutions for this indoor coverage and capacity problem are required.

A straightforward solution to enhance indoor coverage is to increase the number of existing outdoor base stations. This leads to the creation of more small outdoor cells providing a larger capacity to the network. Unfortunately, this approach is expensive for operators because they have to deploy more cells. Moreover, this solution will also generate new problems due to interference, as more cells overlap with one another [37].

Hence, indoor solutions such as Distributed Antenna Systems (DASs) and picocells

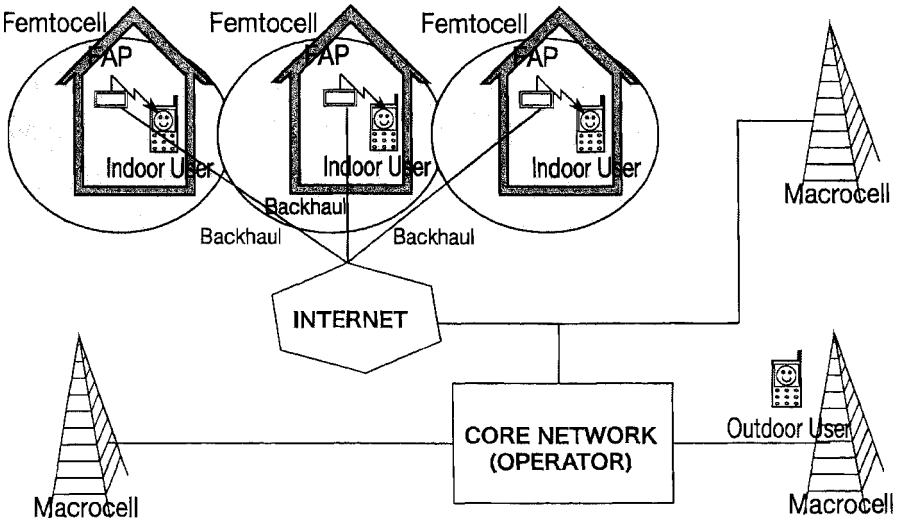

Figure 1.7: Femtocell architecture.

become an attractive solution in hotspots such as office buildings and shopping malls. These solutions deployed by operators improve in-building coverage, off load traffic from outdoor macrocells, enhance service quality and allow high data rate services due to the improved performance of radio links.

Even though the above indicated indoor solutions are more cost effective than using outdoor macrocells to provide indoor coverage for high speed data services, these solutions are still too expensive to be used in scenarios such as small offices or homes. This is because they have to be planned, installed and maintained by operators [37].

The market pressures for improved coverage and capacity to satisfy the demands of large numbers of handsets and laptops using mobile cellular standards has resulted in an intensive effort to solve this problem. Over the last years, femtocells have gained the attention of the mobile industry and the research community due to their features. The development of so-called femtocells provides an attractive solution for low cost indoor coverage and capacity extension [38].

FAPs[1] are low-cost, low-power base stations designed for indoor usage that allow cellular network operators to extend indoor coverage where it is limited or unavailable. On the air interface, FAPs provide radio coverage of a certain cellular standard type,

[1] In this thesis, FAP is used to denote the device itself, while femtocell refers to the coverage area.

e.g. HSPA, WiMAX, LTE. On the backhaul, they are connected to the network operator via a broadband connection such as optical fiber or Digital Subscriber Line (DSL). FAPs, unlike DAS or picocells, will be deployed in a similar way to Wireless Fidelity (WiFi)[1] access points, meaning that individual customers will deploy their own FAPs in an ad-hoc fashion in random locations without the supervision of any network operator.

The use of femtocells will offer different advantages to both users and operators. Signal qualities will improve due to the short distance between transmitter and receiver, the result of this being communications with enhanced reliabilities and throughputs. This will also provide power savings that may reduce the electromagnetic interference as well as the energy consumption of base stations and other network equipment. In this way, more users will access the same radio resources or utilise higher MCSs, while operators will benefit from a larger network capacity and spectral efficiency. Furthermore, since indoor traffic will be transmitted over the IP backhaul, femtocells will help operators manage the exponential growth of traffic within their macrocells. Additionally, because femtocells will be paid and maintained by the users, femtocells will also reduce the cost of networks [39].

Nevertheless, these benefits are not easy to realise and there are many technical challenges that operators must face before successfully deploying a wide femtocell network over the existing macrocell tier [40]. For example, the management of inter-cell interference between the macrocell and the femtocell tier as well as between femtocells themselves will play a very important role, since this interference could counteract the above mentioned benefits and downgrade the overall performance of the network [41].

Furthermore, due to the individualistic nature of femtocells and due to the uncertainty on the number and location of these devices, operators must use new approaches rather than classic network planning and optimisation in order to mitigate interference. It is impossible to perform a centralised planning of a user-deployed femtocell network. As a result, FAPs must be self-organising devices that integrate the processes of planning, configuration and optimisation in a set of in-built autonomous functionalities. These self-organising techniques will allow femtocells to monitor their environment

[1] The technical differences between both femtocell and WiFi access points are of many kinds. Nevertheless, let us highlight that FAPs operate in a licensed band using mobile cellular standards, while WiFi operates in an unlicensed band and thus is a device out of the mobile operator portfolio. Mobile operators will use femtocells in order to extend indoor coverage/capacity and hence they can expect a revenue out of it, but not from the WiFi.

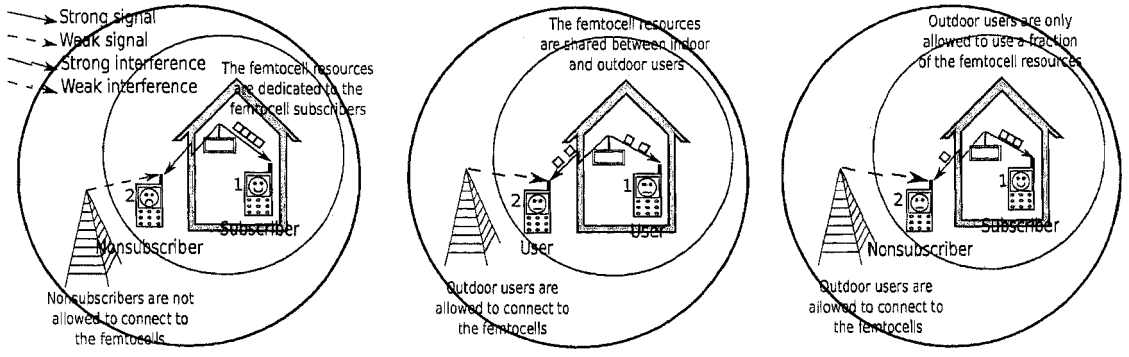

(a) Closed Subscribers Group. (b) Open Access. (c) Hybrid Access.

Figure 1.8: Access Methods.

and fine tune their parameters according to network, traffic and channel fluctuations, therefore reducing human involvement and their impact on neighbouring cells [40].

Finally, let us highlight the main differences between both macrocells and femtocells (Figure 1.7):

- Femtocells will be deployed in much larger numbers compared with macrocells.
- They can be turned on and off or moved at any time by the customer.
- Femtocells are initially designed to provide indoor coverage.
- They are low-cost and low-power devices.
- A femtocell may be used only by a few users (subscribers).
- The physical access to the femtocells is not possible for the operator.
- Femtocell access can be restricted to a given set of users decided by the owner.

1.4.1 Femtocell Related Terminology

For the sake of clarity, the terminology that will be used throughout this manuscript with regard to two-tier networks is presented in the following.

First of all, the main femtocell access policies are described (Figure 1.8):

Closed access mode Also referred to as Closed Subscriber Group (CSG) [42]. Only some specific clients of an operator can connect to a given closed access femtocell. The list of allowed clients is regulated and modified *in situ* by each femtocell owner.

Open access mode: All clients of an operator have the right to connect to all open access femtocells of this operator.

Hybrid access mode Part of the femtocell resources are operated in closed access, while the remaining femtocell resources are operated in an open access mode [43] [44]. This results in a preferential access for allowed users and a limited access for the others.

Furthermore, in closed and hybrid access modes, users are classified as follows:

Femtocell subscriber A subscriber of a femtocell is a user registered in it, and they are usually terminals that belong to the femtocell owner, its family or its friends.

Femtocell nonsubscriber A nonsubscriber of a femtocell is a user not registered in it, and hence it is only allowed to connect to the network through the macrocell tier.

Moreover, the types of interference in two-tier networks are classified as follows:

Cross-tier interference This occurs when the aggressor, e.g., a FAP, and the victim of the interference, e.g., a passing macrocell user, belong to different tiers.

Co-tier interference This occurs when the aggressor, e.g., a FAP, and the victim of the interference, e.g., a neighbouring femtocell user, are both of the same tier.

1.5 Principal Objectives of This Thesis

The principal objectives of this thesis can be summarised as follows:

1. To overview the current approaches to the self-organisation of cellular networks, discuss their capability to satisfy the new requirements of future applications, and introduce the motivation for new self-organising models and/or techniques.

2. To study the interference mitigation and resource allocation problem in OFDMA macrocellular networks and femtocell roll-outs from a self-organising perspective, and create new resource management models and optimisation techniques that help to enhance network performance. This objective is studied making use of centralised, cooperative and/or distributed self-organising network architectures, and taking resources such as MCSs, subchannels and transmit power into account.

3. To show that in realistic network deployments with a limited number of users, large capacity improvements can be gained by assigning different transmit powers to different subchannels according to users' throughput demands and positions.

4. To propose novel algorithms for mitigating co- and cross-tier interference and improve network performance in two-tier OFDMA macrocell-femtocell scenarios.

5. To implement all these models and techniques in a system-level simulation tool to verify the boost in capacity that they produce with respect to other approaches.

1.6 Structure of This Thesis

This thesis is structured as follows:

- In Chapter 2, the interference problems that arise in both macrocell and femtocell deployments and their current solutions are analysed. Also, the state-of-the-art with regard to self-organising and interference mitigation techniques is reviewed.

- Chapter 3 introduces the methodology utilised for modelling the performance of macrocell and femtocell networks, as well as the principles of the dynamic system-level simulation tool developed during this research, to test proposed algorithms.

- In Chapter 4, a new approach to the joint frequency and power allocation problem is presented that indicates that large benefits in macrocell performance can be achieved through the sophisticated joint allocation of subchannels and power. Our solution first allocates subchannels to cells so that inter-cell interference suffered by cell-edge users is minimised, and later each cell independently assigns subcarriers and power to users so that its own total transmit power is minimised, while the throughput requirements of its connected user terminals are satisfied.

Optimisation schemes use user MRs and CQIs to assess interference conditions. Extensive system-level simulation results show the boost in network capacity when using the proposed scheme with respect to other approaches in literature.

Contribution: A semi-distributed self-organising scheme, called enhanced Dynamic Frequency Planning (eDFP), for the assignment of resources and the avoidance of interference in OFDMA macrocell deployments.

- Chapter 5 further improves the work presented in the previous chapter and proposes a fully decentralised joint MCS, subcarrier and power allocation scheme, where each cell independently and dynamically allocates resources to its users so that its transmit power is minimised, while meeting its user rate requirements. In order to enhance network stability, cooperation among cells may occur via message passing so that a cell is able to inform neighbouring ones that downlink transmissions of its cell-edge users will be scheduled in certain subchannels, and thus neighbouring cells may abstain from using high powers to these subchannels. Extensive system-level simulation results show the boost in network capacity when using the proposed scheme with respect to other approaches in literature.

  Contribution: Two decentralised architectures, cooperative Radio Resource Allocation Architecture (coRRAA) and autonomous Radio Resource Allocation Architecture (auRRAA), able to operate with few or no signalling among cell, respectively, and provide inter-cell interference mitigation in macrocell scenarios.

- In Chapter 6, we research the potential of applying the decentralised radio resource management framework proposed in the previous chapter to femtocell scenarios to mitigate co-tier interference. This decentralised framework provides a practical approach to the femtocell co-tier interference avoidance problem since it involves a few or no signalling among neighbouring user-deployed FAPs. Dynamic simulations in a realistic enterprise femtocell scenario indicate that large performance enhancements can also be gained when using the proposed approach compared to other schemes in literature.

  Contribution: Tailoring and evaluating the performance of the two proposed decentralised architectures, coRRAA and auRRAA, in femtocell scenarios for co-tier interference mitigation.

- Chapter 7 further improves the work presented in the previous chapter and proposes a macrocell-femtocell cooparation method to mitigate cross-tier interference and avoid macrocell user outages in two-tier macro-femto network deployments. In this method, macrocells could set subchannel specific transmit power limits in neighbouring femtocells so that the communications of mobile macrocell users can be protected with a certain SINR. Dynamic simulations in a realistic residential femtocell scenario indicate that this protection comes at the expense of low throughput reductions at femtocells.

  Contribution: A power-controlled macrocell-femtocell cooperative approach to avoid the cross-tier interference suffered by macrocell users in two-tier networks.

- In Chapter 9, the conclusions are drawn, and open issues and future work are described.

Chapter 2

Interference Avoidance: State of the Art and Research Challenges

In literature, the solutions to the interference problem fall mainly into two categories: *interference cancellation* and *mitigation*.

When using interference cancellation, the receiver side subtracts the interfering signal from the received one so that the useful information can be successfully decoded. This allows a communication system to operate under high levels of interference [45]. From an information-theoretic point of view, the capacity enhancement achieved by interference cancellation is studied in [46]. The use of these interference cancelation techniques in wireless communication systems has been further analysed in [47] [48]. Nevertheless, implementing these techniques in real communication systems may not be practical due to the complexity of the processes used to estimate the interfering signal and cancel it from the received one. Errors may also occur during cancellation. Thus, the tendency is to drop its use [49].

Due to the high complexity of interference cancellation, interference mitigation has gained lot of attention from both the mobile industry and the research community. Let us define an interference mitigation technique as one that attempts to avoid interference by preventing it from occurring. For instance, antenna planning, power control and radio resource management are tools often used to mitigate interference.

2.1 Interference Avoidance in Macrocell Deployments

In literature, there are several categories of inter-cell interference mitigation schemes:

- At the low end of complexity, techniques based on frequency reuse patterns do not involve any signalling among cells. Nevertheless, because of their fixed allocation of bandwidth and power established during the initial network planning phase, they are not able to dynamically adapt to time-varying network conditions [50].
- At the high end of complexity, techniques based on coordinated scheduling within cell neighbourhoods determine the bandwidth and power allocation for each cell. These schemes result in a better system performance, but they are difficult to implement and typically incur a large delay and signalling overhead among cells.

2.1.1 Frequency Reuse Schemes

In order to mitigate inter-cell interference, Orthogonal Frequency Division Multiple Access (OFDMA)-based networks can exploit their Physical (PHY) layer flexibility and permit the utilisation of a large variety of Frequency Reuse Schemes (FRSs) [51]e In the following, the most representative FRSs used in OFDMA networks are described. All these schemes will be used in the following chapters for performance comparison.

2.1.1.1 Universal Reuse

Using universal reuse, all cells[1] of a network have access to all available subcarriers. Hence, inter-cell interference may be an issue that could degrade network performance. This approach is also called reuse 1. [51]

2.1.1.2 Frequency Reuse

With frequency reuse schemes, the channel bandwidth is divided into s segments, being s the number of BS cells, and each segment is assigned to one cell in each BS. This approach eliminates the possibility of subcarrier collision among adjacent cells

[1]The term cell and sector are synonyms here, e.g., a macrocellular BS has three cells or sectors.

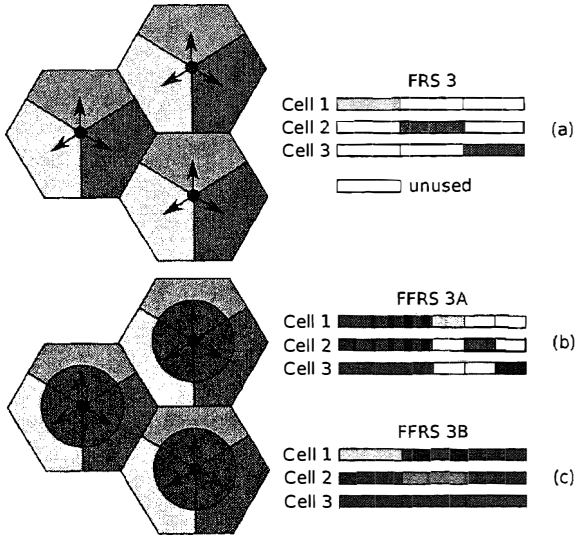

Figure 2.1: Frequency reuse and fractional frequency reuse schemes.

at the expense of a reduced cell capacity. This approach is also known as reuse s. Figure 2.1 (a) shows the case of $s = 3$. [52]

2.1.2 Fractional Frequency Reuse

The generic Fractional Frequency Reuse Scheme (FFRS) [53] explores the trade-off between spectrum usage that may be obtained with reuse 1, and interference mitigation that can be achieved using reuse s. When using FFRSs, users are divided into 2 groups according to their locations and geometries:

- Users with good geometries, e.g., close to the cell-centre, belong to the inner-zone group.
- Users with bad geometries, e.g., those in the cell-edge, belong to the outer-zone group.

The boundary that separates the inner- and outer-zones is a design parameter that has to be fine tuned by operators based on distances, signal strengths, signal qualities, etc. Two popular FFRSs are [53]:

2.1.2.1 FFRS s-A

No overlapping between cell-centre and cell-edge bands in neighbouring cells is allowed. In neighbouring cells, cell-centre users share the same band, whereas cell-edge users are separated into orthogonal ones. Hence, a spectrum portion is unused in each cell, but spatial reuse is improved compared to FRS s. Figure 2.1 b) illustrates FFRS3-A.

2.1.2.2 FFRS s-B

Partial overlapping between cell-centre and cell-edge bands in neighbouring cells is permitted. Therefore, the entire available spectrum can be used by a cell. Moreover, the orthogonality among neighbouring outer-zone bands is maintained by allocating cell-centre users in those spectrum bands that are not allocated to cell-edge users. Figure 2.1 c) illustrates FFRS3-B.

The power applied to those subcarriers allocated to inner-zone users may be lower than that applied to those subcarriers allocated to outer-zone users. In this way, inter-cell interference from inner-zones to neighbouring outer-zones may be mitigated. This power reduction should not significantly affect inner-zone users since they are located close to their BSs and have good SINRs. The power applied to the subcarriers allocated to each zone is also a design parameter that has to be fine tuned by operators.

2.1.3 Dynamic Approaches

As it has been presented above, one way to control inter-cell interference is to imply certain frequency domain restrictions and transmit power limits to Base Stations (BSs). Frequency reuse patterns such as FRSs and FFRSs are a way to set such constraints. Nevertheless, these patterns are mostly based on static pre-planned frequency allocations that slowly evolve through time. As a result, they cannot efficiently cope with time-fluctuating factors such as traffic spatial distributions, user Quality of Service (QoS) demands and channel conditions [54]i

To solve this issue, several OFDMA-based Dynamic Subcarrier Assignment (DSA) and Adaptive Power Assignment (APA) schemes have been proposed in literature. However, simpler solutions involving DSA with equal power per subcarrier have gained lager attention than intricate joint DSA and APA approaches due to mathematical

tractability and/or easier implementation. Furthermore, these simpler DSA solutions have also been sheltered by some studies, e.g., [55] [56], which showed that improvements in system capacity due to the allocation of distinct powers to distinct subcarriers is low in scenarios with a wide range of users that necessitate diverse signal qualities. Some of the most representative dynamic approaches are introduced in the following.

2.1.3.1 Centralised Approaches

Numerous papers have been published on resource allocation in OFDMA systems. However, most of them are focused on single cell scheduling and typically do not consider the effect of inter-cell interference. Although not in the context of OFDMA, several papers have been published on coordinated resource allocation, e.g., [57], [58]. These papers propose algorithms that are based on centralised network architectures and an intricate exchange of messages between cells and the network coordinator. In OFDMA literature, most of the proposed centralised resource allocation schemes assume a perfect channel knowledge for all users in all subcarriers, e.g., [59], [60]. Nevertheless, this assumption may pose a serious threat to centralised architectures since large quantities of signalling are necessary to capture the global network state and distribute scheduling decisions to all BSs. Other works propose dynamic allocations of resources to cells, but they do not provide information on how measurements are collected and processed or how methods adapt themselves over time, e.g., [61], [62]. The analysis of these techniques is performed using static snapshot-based simulations where there is no time domain concept and channel conditions are known a priori. More comprehensible approaches to OFDMA networks have been recently proposed in [53], [63], [31] where more realistic and tailored approaches to OFDMA allocation constraints are considered.

In [53], Chang et al. present a dynamic frequency allocation scheme for a fractional frequency reused OFDMA-based network. This technique improves the performance of conventional FFRSs by enabling adaptive subchannel sharing between macrocells taking their load conditions into account. This technique is based on a uniform distribution of cell power among subcarriers and also a centralised network architecture, where a radio resource broker solves on a regular basis a graph colouring problem that adapts subchannel allocations to cell loads. Although a few user feedback is required, the central radio resource broker is in charge of directly assigning subchannels to user,

which may originate severe delay issues. Also, the resource assignment needs that users are allocated to one subchannel and thus no minimum user bit rate is guaranteed.

In [63], Hussain et al. present another centralised dynamic fractional frequency reuse approach for OFDMA networks, in which transmit power is also uniformly distributed among subcarriers. This approach first of all allocates subcarriers to cells in a way that long-term throughput is maximised, and then independently and opportunistically each cell schedules assigned subcarriers to users. Furthermore, a minimum bit rate is guaranteed to connected users. Since subcarriers assigned to cells to guarantee these users' QoS demands cannot be reused in cells with different orientations, i.e., the assignment to the cells of one BS is replicated for every BS in the network, this scheme may make some cells monopoly all resources, whereas other cells starve. Also, large amounts of uplink feedback are required since inter-cell interference data is necessitated on every user-subcarrier pair.

In [31] and on the contrary to the previous approaches, Kwan et al. investigate the impact in performance of the user Modulation and Coding Scheme (MCS) constraint presented in Chapter 1, i.e., all Resource Blocks (RBs) of a user employ the same MCS. Also, the authors propose a sub-optimal reduced complexity multiuser scheduler that maximises cell throughput in scenarios where users have distinct fading in each RB. This paper also assumes a uniform distribution of transmit power among subcarriers. But, inter-cell interference is not considered.

Since all presented methods uniformly distribute transmit power among subcarriers, spatial spectrum reuse losses are necessary to achieve inter-cell interference mitigation, i.e., some subchannels allocated to a given cell cannot be reused by neighbouring cells. *This thesis proposes a semi-distributed approach for dynamic resource allocation, where a central node assigns RBs to cells to minimise inter-cell interference to cell-edge users, while independently and more frequently cells assign transmit power and RBs to users so that their transmit power is minimised, while meeting their user QoS requirements. This solution indicates that large benefits in network performance can be achieved through a sophisticated and joint assignment of RBs and transmit power (Chapter 4).*

2.1.3.2 Distributed Approaches

Centralised approaches may be more powerful from the optimisation point of view, providing a coordinated scheduling across multiple cells where bandwidth and power assignments are jointly determined. However, they are based on a low latency communication between cells and a central broker or between cells, hence incurring large delays and also signalling overheads. Therefore and to minimise signalling overheads, distributed approaches that do not involve any coordination among cells are preferred.

Dynamic distributed resource allocation in the context of Gaussian interference channels has been considered in [64] and [65]. However, neither of these works consider a model with multiple interfering BSs each one serving several, differently located users.

Some other papers such as [66] and [67] propose distributed inter-cell interference avoidance schemes that operate under low load conditions. Due to low load conditions, cells can always find RBs that suffer from low interference through user measurements. Nevertheless, due to their uniform distribution of power among subcarriers, these methods do not work in highly loaded scenarios.

In order to provide a better spatial reuse via a joint allocation of RBs and power, Stolyar et al. introduce in [68] a network, where cells constantly perform a selfish optimisation of the assignment of its user packets to its resource sets. This approach targets to minimise cell transmit power and does not need any frequency planning. Moreover, it does not involve signalling or any explicit coordination between cells. This is because minimising cell transmit power leads to choosing for user transmission the subcarriers with the least interference. A cell that targets to minimise its own transmit power tends to use those subcarriers that are not used by neighbouring cells, because less power is needed in a non-interfered/faded subcarrier to get a given SINR. In this way, the entire network settles into a stable allocation pattern that changes dynamically according to cell traffic loads. In order to assess user channel conditions, the proposed dynamic approach rely on user measurements regularly fed back to cells. Nevertheless, this work is not tailored to the constraints of neither LTE nor WiMAX: there is no concept of RB or subchannel, thus directly assigning subcarriers to users, does not consider the use of distinct MCSs, and uses random frequency hopping from slot to slot by permuting subcarrier indices independently across sub-bands[1] and cells.

[1] In their simulation, they consider an OFDMA system with 48 subcarriers divided into 3 sub-bands having exactly 16 subcarriers in each sub-band.

This thesis takes this scheme further and proposes new models for the joint allocation of MCSs, subchannels and power from cells to user terminals in OFDMA networks. In more detail, two models based on cooperative and distributed architectures, where cells also target to independently minimise their own transmit power are proposed. When utilising the cooperative architecture, message exchange between cells is allowed, but not when utilising the distributed one. Such models provide inter-cell interference mitigation and network capacity enhancement through the decentralised self-organisation of radio resource assignments (Chapter 5).

2.2 Interference Mitigation in Femtocell Deployments

Figure 2.2 shows that a femtocell not only provides coverage at the customer premises, but that it also radiates energy towards neighbouring households as well as outdoors, thus introducing interference. Due to this fact and because femtocells are deployed within the coverage area of existing macrocells, femtocells can significantly degrade the performance of macrocells. In addition, the deployment of new femtocells can also disrupt the operation of neighbouring ones, thus compromising their performance too. Hence, in order to reduce the appearance of dead zones within existing macrocells and to successfully deploy a wide femtocell tier, cross- and co-tier inter-cell interference generated by femtocells should be minimised.

In two-tier networks, the severity of this interference depends on two main factors: the strategy utilised for allocating spectrum resources to both tiers and the method used for accessing each one of the femtocells.

2.2.1 Spectrum Assignment to Femtocells

2.2.1.1 Assignment of Carrier Frequencies

Network operators having more than one licensed spectrum band, i.e., owning several carrier frequencies, have the following options for spectrum allocation (Figure 2.3) [69]:

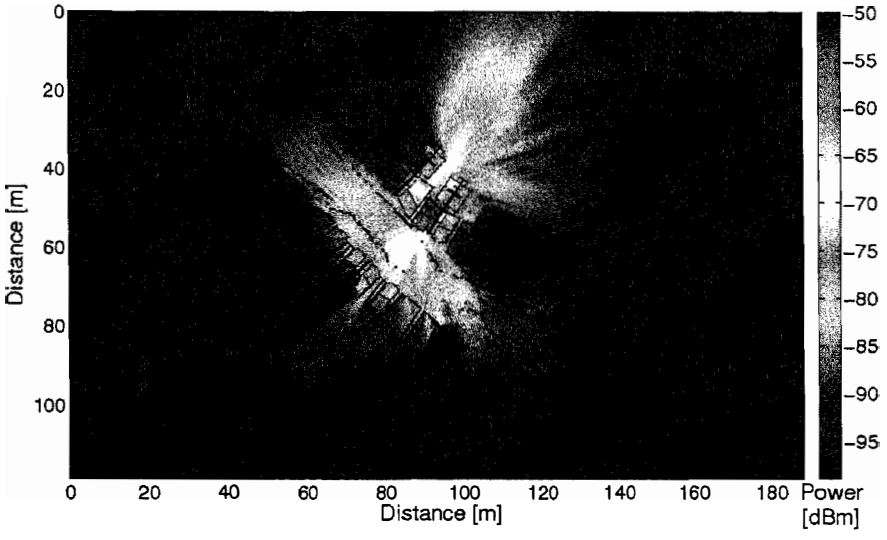

Figure 2.2: Femtocell coverage.

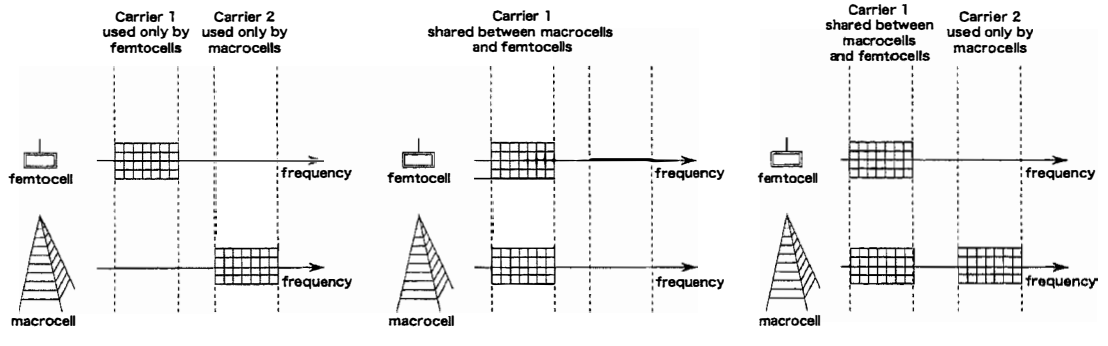

(a) Fully dedicated spectrum. (b) Shared spectrum. (c) Partially shared spectrum.

Figure 2.3: Assignment of carrier frequencies.

Fully dedicated spectrum: In this approach, some spectrum bands are assigned to macrocells, whereas different spectrum bands are assigned to femtocells. In this way, cross-tier interference is completely avoided, since both tiers operate at a different frequency. However, this approach may result in a low network spectral efficiency because the cells in one tier can only access a subset of the overall frequency resources.

Shared spectrum: This approach can reach a higher network spectral efficiency than the dedicated spectrum approach because both tiers can access all resources. Nevertheless, when using this approach, cross-tier interference may occur, which could degrade the overall network performance unless this interference is efficiently handled.

Partially shared spectrum: This is an intermediate solution. In this approach, the macrocell tier has access to all spectrum bands, while the femtocell tier operates in a subset of them. The benefits of this approach compared to the above ones are:

- A larger spectral efficiency with respect to the dedicated spectrum approach because the macrocell tier can access all resources.
- A lower cross-tier interference with respect to the shared spectrum approach because macrocell users creating or suffering from large cross-tier interference can be moved to the dedicated macrocell spectrum.

Since not all operators have more than one spectral band to divide among tiers, and because the shared spectrum approach could result in a larger spectral efficiency, *this thesis focuses exclusively in the mitigation of co-tier (Chapter 6) and cross-tier (Chapter 7) interference in shared spectrum deployments with one carrier frequency.*

2.2.1.2 Assignment of OFDM Subchannels

Operators deploying a two-tier OFDMA network and owning only one carrier frequency also have different choices for assigning subchannels among both tiers (Figure 2.3) [40]:

Orthogonal assignment: A fraction of the available subchannels is only used by the macrocell tier, while the remaining subchannels are only used by the femtocell tier.

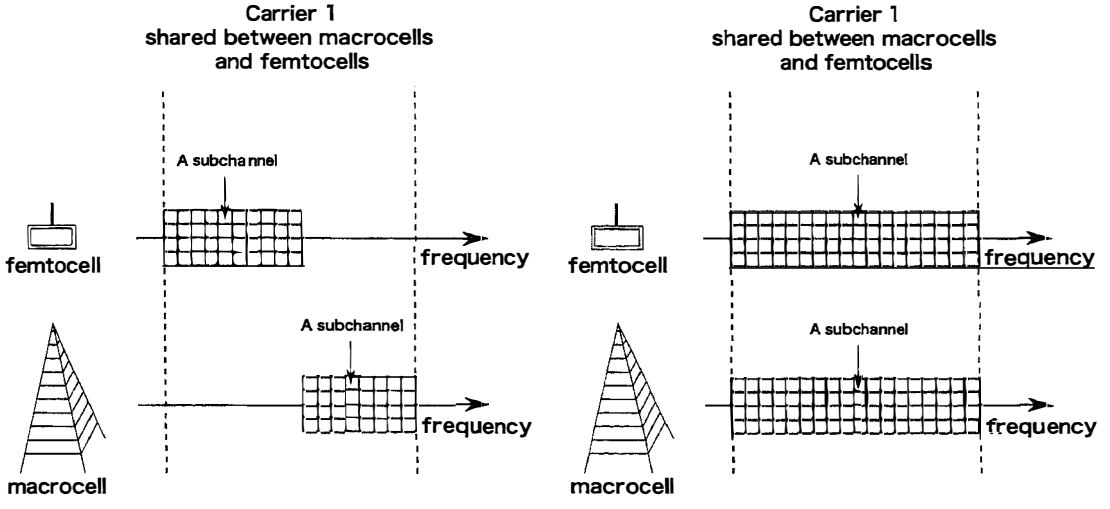

(a) Orthogonal assignment.

(b) Co-channel assignment.

Figure 2.4: Assignment of OFDMA subchannels.

Co-channel assignment: All macrocells and femtocells can access all subchannels.

Similarly to the shared spectrum case, a co-channel assignment of subchannels always results in a larger spectral efficiency if cross-tier interference is properly handled. *This thesis focuses exclusively in the mitigation of co-tier (Chapter 6) and cross-tier (Chapter 7) interference in shared spectrum deployments with co-channel assignments.*

Let us note that in [70]ę a hybrid approach has been proposed in which femtocells far from their umbrella macro BS use co-channel assignments, while those femtocells nearby a macro BS use orthogonal ones.

2.2.2 Access Methods to Femtocells

2.2.2.1 Interference in Closed Access Femtocells

With closed access, nonsubscribers cannot connect to the network via every femtocell, even if they provide a stronger received pilot strength than that of the closest macrocell. Hence, a strong component of cross-tier interference is generated between both tiers. For example, in the DownLink (DL), femtocells could disrupt the communication of

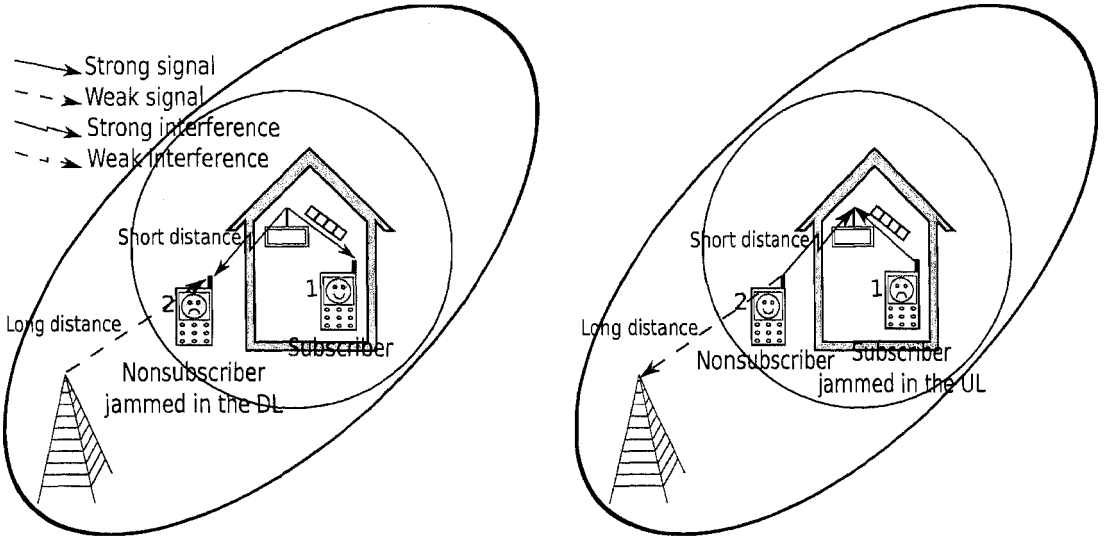

(a) Downlink interference case

(b) Uplink interference case.

Figure 2.5: Interference in closed access femtocells.

passing nonsubscribers connected to a distant macro BS, or in the UpLink (UL), nonsubscribers located close to a femto BS could jam the communication of its connected users (Figure 2.5) [71]. The most challenging case of cross-tier interference in both the DL and the UL of Closed Subscriber Group (CSG) femtocells takes place when a nonsubscriber enters a house hosting a CSG femtocell. In this particular case, the power of the interfering signal may be larger than the power of the carrier signal.

Co-tier interference also pops up among neighbouring femtocells in dense femtocells deployments. In many cases, users will install their femtocells in challenging positions within their homes, e.g., close to a room of a neighbour or to a window. In this case, femtocell subscribers are likely to suffer severe jams from their neighbouring femtocells.

2.2.2.2 Interference in Open Access Femtocells

The use of open access reduces the interference problems caused by CSG femtocells. In this case, all passing users are authorised to connect to any open access femtocell, thus reducing the negative impact of the femtocell tier on the existing macrocell tier. As a result, all users are always connected to the strongest macrocell or femtocell, therefore mitigating cross-tier interference and enhancing network throughput [71].

However, open access has some major drawbacks:

- Since femtocells are paid and maintained by subscribers, they will not be keen on paying for a service that is to be used free of charge by others, i.e., nonsubscribers. It is thus expected that operators would reduce the fees paid by subscribers or provide them with other benefits to make open access femtocells more appealing.
- Open access reduces the performance of femtocell owners due to sharing of femtocell resources with nonsubscribers.
- Open access increases the amount of handovers between cells and thus signalling due to the mobility of outdoor users. Outdoor users moving in residential areas hand over from a femtocell to another or to the umbrella macrocell (Figure 2.6). Also, it should be noted that there is the possibility of that a handover fails. According to [72], the probability of a handover resulting in a dropped call is 2%.

Furthermore, in large deployments of open access femtocells, even if nonsubscribers may connect to femtocells, the aggregate of co-tier interference coming from neighbouring femtocells can disrupt their services too.

As a conclusion, both access methods, open and closed access, have drawbacks: closed access femtocells are more appealing to users but increase cross-tier interference, while open access femtocells mitigate cross-tier interference but increase handovers [71]. *Thus, in order to allow an extensive deployment of femtocells within existing networks, new solutions are required to manage cross- and co-tier interference and also handovers.*

2.2.2.3 Interference in Hybrid Access Femtocells

A hybrid access model can be defined as a closed access with a cap on the amount of resources allocated to nonsubscribers [73]. On the one hand, hybrid access femtocells are able to deal with the cross-tier interference problem of closed access femtocells, since all users are always able to connect to the strongest macrocell or femtocell. On the other hand, they are more appealing to customers than open access femtocells, since the number of nonsubscribers connected to their femtocells is regulated [44][43]. Nevertheless, in hybrid access femtocells, in a similar way to open access femtocells, The probability of handover failure will still affect the performance of nonsubscribers.

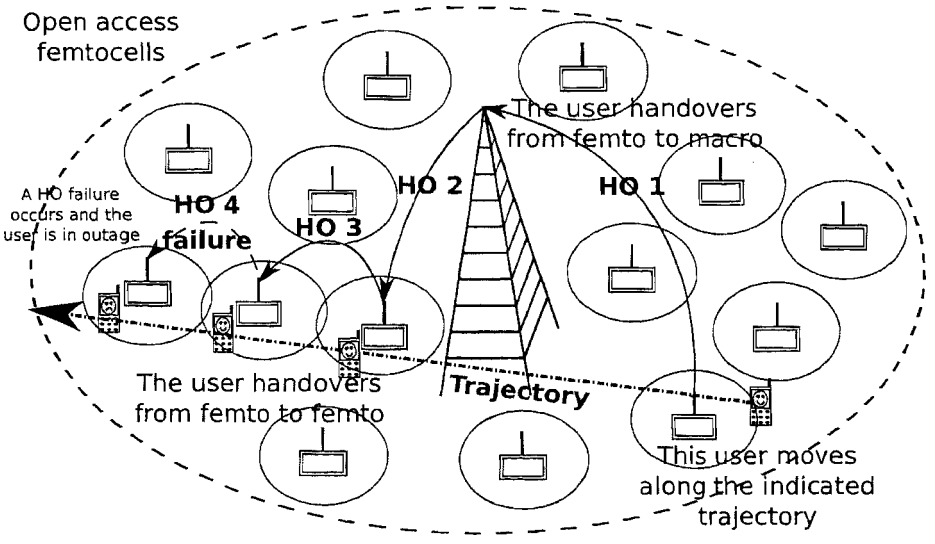

Figure 2.6: Handover failure in open access femtocells. Handover failure may occur due to different reasons such as physicall cell indentity confusion, wrong handover synchronisation, back-haul delay issues, speech codec or encryption mismatch, etc.

2.2.3 State-of-the-Art in Self-organising Interference Avoidance Techniques for Femtocells

In order to mitigate the effects of inter-cell interference imposed by femtocell roll-outs, the implementation of interference cancelation techniques was initially proposed. However, these techniques were disregarded due to errors in the cancellation process. Moreover, these techniques are expensive to implement due to its complex functioning, thus increasing the cost of the receiver side. Hence, interference mitigation techniques are considered as a most suitable approach to deal with the interference problem [74].

The self-organisation of the femtocell transmit power will play a very important role to successfully deploy a wide femtocell tier. In order to mitigate inter-cell interference, femtocells should be able to dynamically tune their own transmit power according to the changing conditions of the environment (passing users, neighbouring cells, channel). Self-organising femtocell transmit power will help to adapt the femtocell coverage to household shapes, mitigate inter-cell interference towards macrocell users passing by and reduce the attempts of macrocell-femtocell handovers by underlay macrocell users.

In [75], Claussen et al. introduce a self-organising power control mechanism for pilot and data channels for UMTS that ensures a constant femtocell coverage radius. Each femtocell sets its power to a value that on average is equal to the power received from the closest macrocell at a target femtocell radius. In this way, cross-tier interference is mitigated using power management.

In [76], Claussen et al. present a self-organising method for coverage adaptation for UMTS that uses information on mobility events of outdoor and indoor users. Each femtocell sets its power to a value that on average minimises the number of attempts of passing macrocell users to connect to a femtocell. In this way, cross-tier interference is mitigated using power management.

However, these two approaches may lead eventually to insufficient indoor coverage. Because FAPs are typically equipped with only one omnidirectional antenna and because customers may not locate their FAPs right in the middle of their households, over reducing femtocell transmit power may lead to coverage holes inside user premisses.

In order to solve this problem, multiple antenna elements could be installed in Femtocell Access Points (FAPs) to create diverse antenna patterns to adapt the femtocell coverage to the user premises. However, installing multiple antenna elements may be inconvenient in this case due to the tight size and low price constraints required to successfully commercialise FAPs. Thus, these multiple antenna elements must be of reduced volume and also cost, and the system used to handle this array of antennas must be of a very low complexity.

In [77], Claussen et al. suggest using a simple switching antenna system in FAPs based on multiple patch and inverted-F antennas able to generate distinct patterns. These patterns can be used to adapt the femtocell coverage to the household layout, hence reducing the leakage of power outdoors and thus avoiding cross-tier interference. However, this is achieved at the expense of utilising a more complex hardware in FAPs.

In [78], Chandrasekhar et al. also analyse the impact of using time-hopping and installing sectorial antennas in FAPs on the performance of an Code Division Multiple Access (CDMA) two-tier network. The usage of sectorial antennas with N_{sec} sectors in FAPs will reduce the probability of cross-tier interference caused by close macrocell users in the UL by a factor of N_{sec}. However, using sectorial antennas will also require a more complex hardware in FAPs.

Unfortunately, more complex hardware approaches imply an increase in FAP costs, which may currently prevent these types of approaches from man implementation. Moreover, the low cost requirement of FAPs also bans other sophisticated techniques, e.g., Multiple Input Multiple Output (MIMO). Interesting areas for future research are thus the non-expensive implementation of diversity schemes such as space-time codes, beamforming or spatial multiplexing.

OFDMA femtocells also provide two dimensions for managing radio resources, i.e., frequency and time. Thus, interference mitigation can be handled not only through power or antenna approaches but also through sophisticated subchannel allocation [40]. In this way, the drawbacks of power control and antenna management can be overcame.

In [79], Chandrasekhar et al. propose an OFDMA subchannel allocation strategy based on an orthogonal assignment of radio resources to macrocells and femtocells that maximises the spatial frequency reuse. The spatial frequency reuse of a network represents the average throughput per frequency and area unit, i.e., bit/s/Hz/m^2. Assigning orthogonal spectrum resources between the macrocell and femtocell tiers, cross-tier interference is completely negated. In this method, it is assumed that a total of $F = F_M + F_f$ subchannels are available, being F_M subchannels allocated to the macrocell tier and F_f to the femtocell tier. The portion of spectrum assigned to the macrocell tier is defined as$r\rho = F_M/F$ and one important planning decision should be a proper dimensioning of such parameter ρ. In this research, ρ is chosen dynamically depending on the specific QoS requirement of one tier with respect to the other one. This is performed by means of a variable η, which represents the ratio between the expected throughput per user in one tier to the overall expected throughput per user. However, this approach requires a central entity able to perform such optimisation, but centralised architectures may not be the most appropriate for user-deployed femtocells. With regard to the assignment of subchannels to users within the femtocell tier, each femtocell accesses a random set of subchannels within the allowed femtocell spectrum. In this way, persistent collision among neighbouring femtocells is not efficiently avoided, thus if the load of the femtocell tier is large, co-tier interference becomes a problem. *This thesis will show that utilising self-organisation within a femtocell tier mitigates co-tier interference and enhances network performance compared to random assignments.*

In [80], Ling et al. study the co-tier interference and subchannel allocation problem in scenarios with dense femtocell roll-outs operating on a dedicated frequency band.

In more detail, they assess femto-to-femto interference in suburban and urban areas, and introduce a self-organising algorithm for the assignment of subchannels to users. This is a measurement based autonomous algorithm where the target of each femtocell is to minimise its own suffered interference. In this case, each femtocell independently takes measurements over all subchannels and choose the ones with lowest interference. Because these measurements are performed by femtocell themselves and not by users, subchannel allocations are therefore independent of network traffic or user locations. Therefore, femtocell assignments may be good but not optimal for all connected users.

In [81], Su et al. study the cross-tier interference and resource allocation problem in two-tier networks, in which both macrocells and femtocells share the same carrier. An optimisation scheme for two-tier networks is proposed that is targeted to minimise the interference suffered by macrocell users and guaranteeing a given SINR for all users. Co-tier femtocell interference is not considered since it is found to be small in their case[1]. In addition, in order to simplify the model, each femtocell utilises only one subchannel. In this case, the optimisation problem has been formulated as a Lagrangian problem and it is solved up to the optimality using the subgradient method presented in [82]. The exact implementation of the proposed algorithm in a two-tier network is as follows: Macrocell users regularly measure the power of the interference suffered from femtocells, and send this data to the their macrocells. Then, the serving macrocell recalculates the Lagrange multiplier of this problem and broadcasts its new value to all femtocells. Femtocells then determine their new subchannel assignments based on this multiplier. This process is repeated until convergence. But, since several iterations may be needed by the scheme to converge that involve user measurements, feedback and processing, this scheme may suffer from serious delays, and hence it may be not responsive enough. For instance, a Voice over IP (VoIP) macrocell user is considered to suffer from outage, if it cannot transmit its voice data packets for a period of time greater than 200 ms. *This thesis proposes a fast-reacting algorithm to cope with cross- and co-tier interference based on a cooperative macro-femto RB and power allocation scheme (Chapters 6 & 7), which is an extension of the assignment approaches presented in previous chapters.*

[1] Since the authors considered a high path loss exponent $\alpha = 3.5$ in their numerical evaluation, co-tier femtocell interference is almost non-existent. Note that the situation may vary for other values.

Chapter 3

Network Modelling: Dynamic System-Level Simulation

This research was conducted to design models and optimisation techniques for cellular Orthogonal Frequency Division Multiple Access (OFDMA) networks. It was also part of the objectives to analyse the advantages and disadvantages as well as the reliability of the proposed self-organising algorithms.

In order to evaluate the performance of the self-organising techniques of this thesis, an event driven dynamic System-Level Simulation (SLS) was used. In this kind of simulation, the 'life' of the network through time is modelled as series of events [83] [84]. An event for example happens when a user connects to the network, a mobile changes its current position, an optimisation procedure is triggered in the network or a cell, etc. Samples of user performance in terms of power consumption, Signal to Interference plus Noise Ratio (SINR), throughput and other indicators are also taken on a regular basis to estimate system-level performance.

Let us note that this dynamic SLS tool was created from scratch by David López together with Á. Ladanyi and A. Jüttner. This dynamic SLS tool is written in C++, and models the DownLink (DL) communication of OFDMA based networks, i.e., Long Term Evolution (LTE) and Wireless Interoperability for Microwave Access (WiMAX). In the following, a general overview of this dynamic SLS and the methodology used to model network performance are presented.

3.1 Network Definition

For the sake of clarity, let us introduce here some general notation that will be used in this thesis. Let us define an OFDMA two-tier macrocell-femtocell network as a set of:

- macrocells: $\mathcal{M} = \{M_1, ..., M_m, M_n, ..., M_M\}$,
- where $\mathcal{N}_m = \{N_1^m, ..., N_b^m, ..., N_{N_m}^m\}$ is the set of neighbouring cells of macrocell M_m,
- femtocells: $\mathcal{F} = \{F_1, ..., F_f, F_g, ..., F_F\}$,
- where $\mathcal{N}_f = \{N_1^f, ..., N_b^f, ..., N_{N_f}^f\}$ is the set of neighbouring cells of femtocell F_f,
- users of macrocell M_m: $\mathcal{U}^m = \{U_1^m, ..., U_u^m, ..., U_{U_m}^m\}$,
- users of femtocell F_f: $\mathcal{U}^f = \{U_1^f, ..., U_u^f, ..., U_{U_f}^f\}$,
- subcarriers: $\mathcal{R} = \{1, ..., r, ..., R\}$,
- subchannels or Resource Blocks (RBs): $\mathcal{K} = \{1, ..., k, ..., K\}$,
- Orthogonal Frequency Division Multiplexing (OFDM) symbols per subchannel or RB: $\mathcal{T}_{\mathcal{DL}} = \{1, ..., t_{dl}, ..., T_{DL}\}$,
- Modulation and Coding Schemes (MCSs): $\mathcal{H} = \{1, ..., h, ..., H\}$ (Table 1.1 [85] and Table 1.2 [85]).

3.2 Simulation Assumptions

For the sake of simplicity, several assumptions have been made, which do not involve any loss of generality in order to assess the functioning of an OFDMA based network:

1. A full buffer based model is employed in order to simulate the DL traffic of users, i.e., there is always data available to be transmitted to all users [54].
2. A subchannel is always comprised of the same subcarriers across the network, independently of the permutation scheme utilised by the network [52].

3. The OFDMA network is synchronous. In other words, inter-cell interference will only occur when several users are allocated to the same subchannel at the same time in different cells.

4. The coherence bandwidth of the channel is larger than the subchannel bandwidth, thus being the fading of all subcarriers within a subchannel constant.

5. The coherence time of the channel is larger than the duration of a subframe, hence being the fading of all OFDM symbols of a subframe constant.

These assumptions are widely used in literature when analysing the performance of a network at the system level [31; 53; 63].

3.3 Traffic load Modelling

In this dynamic SLS, users can be generated in different ways according to the following models:

1. A fixed number of users is uniformly distributed within the coverage area of each cell, and they hold in the system from the beginning till the end of the simulation.

2. A fixed number of users is uniformly distributed within the coverage area of each cell, holding in the system for some time t_u. When the user holding time expires, a new one is generated in a random position within the same cell coverage area.

3. Users are generated in this case according to a homogeneous Poisson process [86] and they are uniformly distributed within the coverage of random selected cells. Users hold in the system for some time t_u.

   The probability of exactly $\hat{s}$ users appearing in a period of time $\hat{T}$ is given by:

$$P(\hat{s}, \lambda\hat{T}) = P_{\hat{s}} = \frac{\left(\lambda \cdot \hat{T}\right)^{\hat{s}} \cdot e^{-\lambda\hat{T}}}{\hat{s}!} \tag{3.1}$$

   where $\lambda \cdot \hat{T}$ is the mean call arrival rate of users, also known as 'process intensity'.

The holding time t_u of user U_u in the network is described by an exponential distributed random variable generated from the following probability density function:

$$f_{t_u}(t_u) = \mu e^{(-\mu \cdot t_u)} \tag{3.2}$$

being μ the mean holding time of users.

For the sake of clarity, the model utilised in each chapter of this thesis is explicitly indicated in its section, simulation results.

3.4 Path Loss Modelling

In this dynamic SLS, path losses of radio signals are modeled according to the following models[1]:

1. For macrocell environments operating at 3.5 GHz, the model recommended by [87] is utilised. This is an empirical model, and it is based on the following formula:

$$(\delta_{m,u})_{\mathrm{dB}} = 105.45 + 39.11 \cdot log_{10}(5 \cdot d_{m,u}) \tag{3.3}$$

   where $d_{m,u}$ represents the distance in kilometres between cell M_m and user U_u^m, and $\delta_{m,u}$ is the path loss between them.

2. For macrocell environments operating at 2.0 GHz, the model recommended by [88] is utilised. This is an empirical model, and it is based on the following formula:

$$(\delta_{m,u})_{\mathrm{dB}} = 128.1 + 37.6 \cdot log_{10}(d_{m,u}) \tag{3.4}$$

   where $d_{m,u}$ represents the distance in kilometres between cell M_m and user U_u^m, and $\delta_{m,u}$ is the path loss between them.

3. Femtocell coverages at a frequency of 3.5 GHz and 2.0 GHz are predicted with deterministic Finite-Difference Time-Domain (FDTD) based propagation models, which were calibrated making use of indoor and indoor-to-outdoor measurements. These FDTD based models capture wall effects in indoor and small cell scenarios.

[1] It must be noted that low case indicates linear units, while upper case represents decibel units.

In case of working at 3.5 GHz or 2.0 GHz, the radio propagation tools presented in [89] and [90] are used, respectively. Details about their calibration procedures are also provided in both [89] and [90].

For the sake of clarity, the model utilised in each chapter of this thesis is explicitly indicated in its section, simulation results.

In addition, the shawdow[1] fading $\xi_{m,u}$ between cell M_m and user U_u^m is modeled utilising a lognormal distribution $LogN(0, \sigma_s^2)$ of mean 0 and standard deviation σ_s.

$$(\xi_{m,u})_{\text{dB}} = LogN(0, \sigma_s^2) \tag{3.5}$$

However, this shadowing model does not apply to FDTD based propagation models because these models based on Maxwell's equations already predict shadowing effects.

When using sectorial antennas in macrocell scenarios, the horizontal (3.6) and vertical (3.7) antenna patterns are simulated according to the models proposed in [91], i.e.,

$$(A^h(\theta^h_{u,m}))_{\text{dB}} = -min[12\frac{\theta^h_{u,m}}{\theta^h_{3\text{dB}}}, A^{h,max}],\ \theta^h_{3\text{dB}} = 70^\circ,\ A^{h,max} = 20\,\text{dB} \tag{3.6}$$

$$(A^v(\theta^v_{u,m}))_{\text{dB}} = max[-12 \cdot ((\frac{\theta^v_{u,m} - \theta_{\text{tilt}}}{\theta^v_{3\text{dB}}})^2, A^{v,max}],\ \theta^v_{3\text{dB}} = 62^\circ,\ A^{v,max} = -18\,\text{dB} \tag{3.7}$$

in which A^h and A^v represent the attenuation offsets introduced by the horizontal and vertical antenna patterns with respect to the maximum antenna gain, respectively, $\theta^h_{u,m}$ and $\theta^v_{u,m}$ represent the angles of arrival in the horizontal and the vertical plane between macrocell M_m and user U_u^m, respectively, θ_{tilt} is the angle between the axis of radiation of the main lobe of the vertical antenna pattern and the horizontal plane, $\theta_{3\text{dB}}$ represents the beam width of the antenna pattern within which at least half of the maximum transmit power is radiated, and A^{max} is the maximum offset of the pattern.

3.5 Signal Strength Modelling

Let us assume that cell M_m is transmitting to its connected user U_u^m in subchannel k.

[1] Shadowing is the effect that the received signal power fluctuates due to objects obstructing the propagation path between transmitter and receiver.

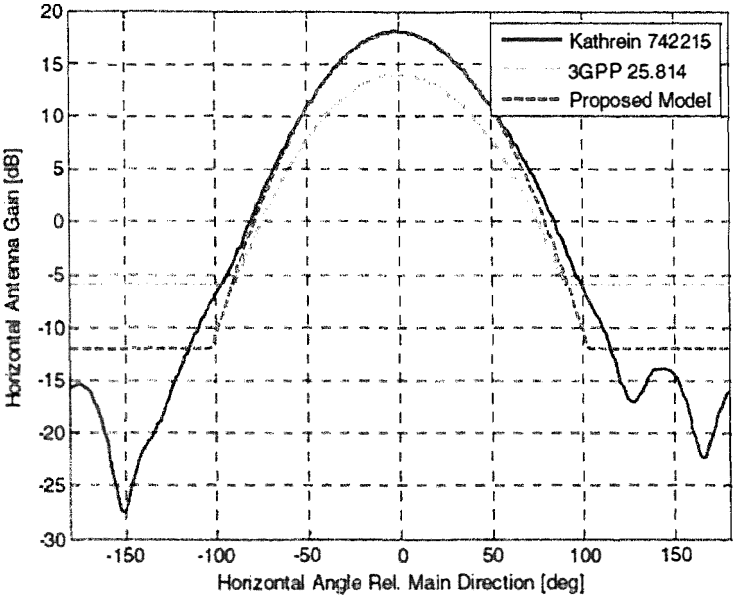

Figure 3.1: Horizontal antenna pattern of the adopted model, 3GPP 25.814 and Kathrein 742215 [91].

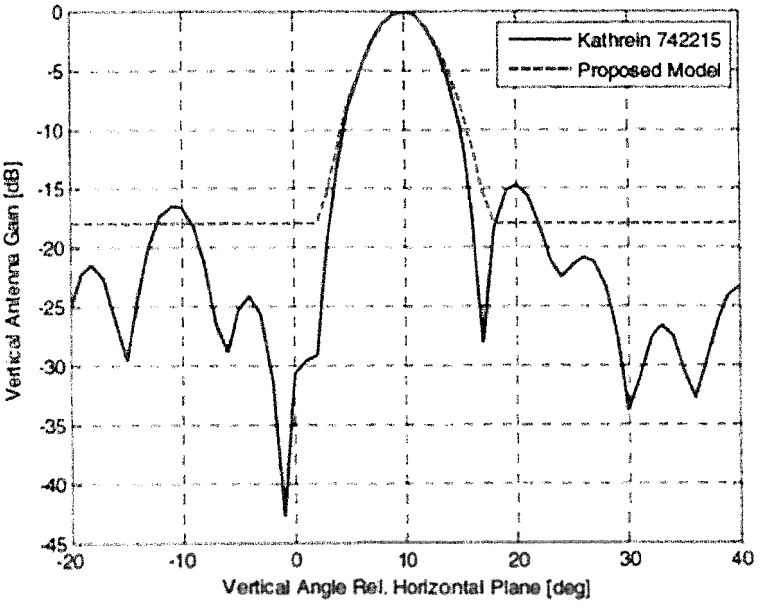

Figure 3.2: Normalised vertical antenna pattern of the used model and Kathrein 742215 with 10° downtilt [91].

The strength of the carrier signal received by user U_u^m from its serving cell M_m in subchannel k is modeled as:

$$w_{u,k}^m = \frac{p_{u,k}^m \cdot g_{m,u} \cdot g_{u,m}}{l_m \cdot \delta_{m,u} \cdot \xi_{m,u} \cdot l_u} = p_{u,k}^m \cdot \Gamma_{m,u} \tag{3.8}$$

being $p_{u,k}^m$ the power applied by cell M_m to each of the subcarriers of subchannel k, $\delta_{m,u}$ represents the path loss between cell M_m and user U_u^m, $\xi_{m,u}$ denotes the shadowing between cell M_m and user U_u^m, g and l stand for the antenna gains and for the equipment losses, respectively, and $\Gamma_{m,u}$ denotes the channel gain between cell M_m and user U_u^m.

In order to successfully decode a DL signal at the receiver of user terminal U_u^m, its strength $w_{u,k}^m$ has to be larger than the sensitivity τ_u of the receiver at user U_u^m plus a margin ζ added to consider the effects of signals close to the receiver sensitivity, i.e.,

$$w_{u,k}^m > \tau_u \cdot \zeta \tag{3.9}$$

where, in this thesis, ζ was tuned to 10 dB.

3.6 Interference Modelling

Inter-cell interference in the DL takes place when the signals transmitted towards different users by different cells overlap in both the frequency and the time domain.

The strength of the interference received by user U_u^m from its neighbouring cell M_n in subchannel k is modeled as:

$$w_{u,k}^n = \frac{p_{u',k}^n \cdot g_n \cdot g_u}{l_n \cdot \delta_{n,u} \cdot \xi_{m,u} \cdot l_u} = p_{u',k}^n \cdot \Gamma_{n,u} \tag{3.10}$$

being $p_{u',k}^n$ the power applied by cell M_n to each of the subcarriers of subchannel k, $\delta_{n,u}$ represents the path loss between cell M_n and user U_u^m, $\xi_{n,u}$ denotes the shadowing between cell M_n and user U_u^m, g and l stand for the antenna gains and for the equipment losses, respectively, and $\Gamma_{n,u}$ denotes the channel gain between cell M_n and user U_u^m.

3.7 Signal Quality Modeling

The signal quality in terms of SINR $\gamma_{u,k}^m$ of user U_u^m in subchannel k is thus modeled as:

$$\gamma_{u,k}^{m} = \frac{p_{u,k}^{m} \cdot \Gamma_{m,u}}{\sum_{n=1,n\neq m}^{M} p_{u',k}^{n} \cdot \Gamma_{n,u} + \sigma^2} = \frac{w_{u,k}^{m}}{\sum_{n=1,n\neq m}^{M} w_{u,k}^{n} + \sigma^2} = \frac{w_{u,k}^{m}}{w_{u,k} + \sigma^2} \tag{3.11}$$

where σ is the background noise density, and $w_{u,k}$ is the sum of the inter-cell interference suffered by user U_u^m in subchannel k.

It is assumed that thermal noise is an additive white Gaussian noise and that inter-cell interference is a zero-mean Gaussian process, whose variance equals the sum of the powers received from all surrounding cells.

3.8 Bit Rate Modeling

The bit rate $BR_{u,k,h}$ of user U_u^m in subchannel k when using MCS h is modeled as:

$$BR_{u,k,h} = \Theta \cdot eff_h = \frac{\mathrm{R}_{\mathrm{DL}}^{\mathrm{data}} \cdot \mathrm{T}_{\mathrm{DL}}^{\mathrm{data}}}{\mathrm{T}_{\mathrm{subframe}}} \cdot eff_h \tag{3.12}$$

where Θ denotes a fixed parameter that depends on the configuration of the network, $\mathrm{R}_{\mathrm{DL}}^{\mathrm{data}}$ and $\mathrm{T}_{\mathrm{DL}}^{\mathrm{data}}$ are the number of data subcarriers and OFDM symbols per subchannel, respectively, eff_h represents the efficiency in bits per symbol of the selected MCS h, and $T_{subframe}$ is the DL subframe duration.

3.9 Throughput Modeling

The throughput $TP_{u,k,h}$ of user U_u^m in subchannel k when using MCS h is modeled as:

$$TP_{u,k,h} = BR_{u,k,h} \cdot (1 - BLER(h, \gamma_{u,k}^{m})) \tag{3.13}$$

where $BR_{u,k,h}$ denotes the bit rate of user U_u^m in subchannel k when utilizing MCS h, while $BLER(r, \gamma_{u,k}^{m})$ is the BLock Error Rate (BLER) of user U_u^m in subchannel k, which is function of MCS h and SINR $\gamma_{u,k}^{m}$.

Furthermore, it should be noted that these BLER values were obtained from [85] and that they are made available to SLSs through the use of Look Up Tables (LUTs). Examples of these LUTs for LTE and WiMAX SLSs are shown in Figures 3.4 and 3.5, respectively.

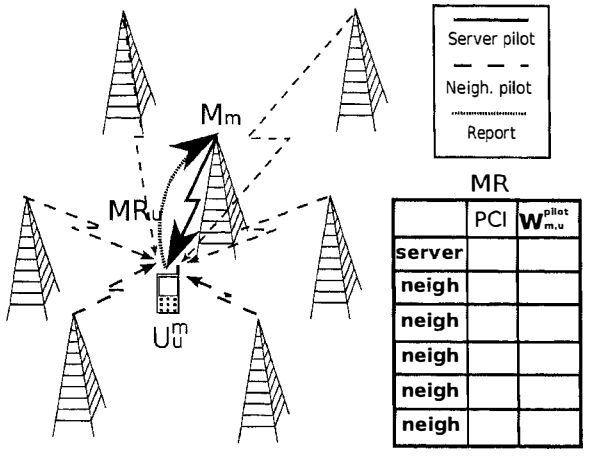

Figure 3.3: User measurement report over neighbouring pilot signals.

3.10 Measurement Reports

Cell-specfic reference signals are comprised of known sequences of reference symbols, denote unique Physical Cell Identities (PCIs), and are utilised for identifying different neighbouring cells during both cell selection and handover procedures (Section 1.3.3). Cell-specfic reference signals are emitted over fixed resource elements at a fixed power, behaving as BS beacons for mobile terminals. In order to avoid confusion or collision, neighbouring cells should have different PCIs.

In order to assist the network in mentioned cell selection and handover procedures, user U_u^m feeds back regularly, every $T_{u,mr}$, a user Measurement Report (MR), MR_u, to its serving cell M_m (Figure 3.3), which indicates the power $w_{u,m}^{pilot}$ received by user U_u^m from the reference signals of its serving cell M_m and its neighbouring ones $M_n \in \mathcal{N}_m$.

3.11 Channel Quality Indicators

User U_u^m feeds back regularly, every $T_{u,cqi}$, a Channel Quality Indicator (CQI), CQI_u, to its server M_m to assess channel status. In this thesis, wideband CQIs are utilised to report the power $w_{u,k} \forall k \in \mathcal{K}$ of the interference suffered by user U_u^m in RB k [27]; i.e., a user reports K values (Section 1.3.3).

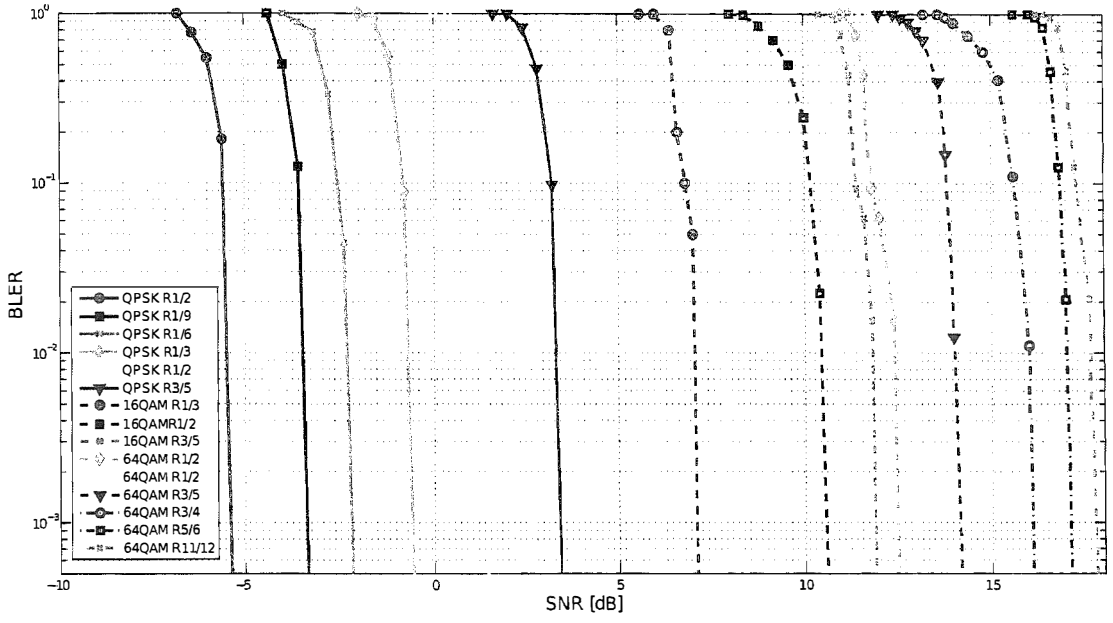

Figure 3.4: Block error rate look-up-table for LTE system-level simulations.

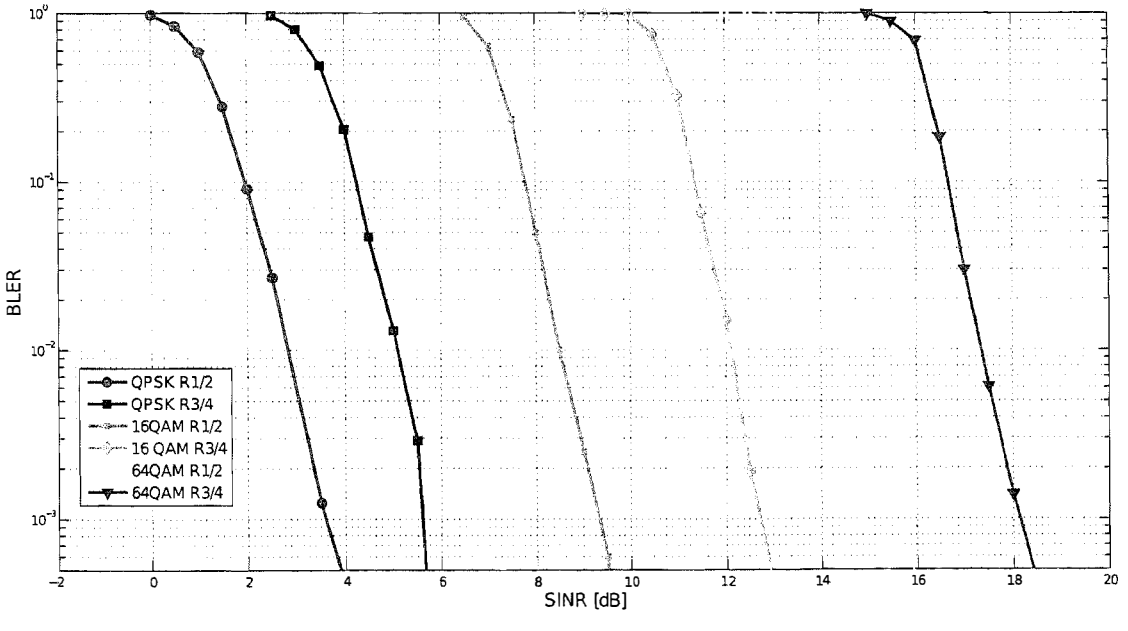

Figure 3.5: Block error rate look-up-table for WiMAX system-level simulations.

Chapter 4

Centralised Interference Mitigation Architecture for Macrocells: enhanced Dynamic Frequency Planning

In this chapter, we investigate the potential of improving network performance by achieving a reuse factor of one in every cell[1] of all Base Stations (BSs) of a network. Motivation for the use of a reuse factor of one in all cells steams from the fact that users may have different bit rate demands or suffer from different channel conditions. Then, users requiring large powers due to large bit rate demands or adverse channels, e.g., users at cell-edge, can coexist in the same frequency with neighbouring cell users using low powers due to low bit rate demands or good channels, e.g., users at cell-centre. Our work is different from others in that we do not incur spatial reuse losses to provide inter-cell interference mitigation, i.e., we do not sacrifice Resource Blocks (RBs) in one cell to reduce interference in neighbouring ones. Instead, we provide interference mitigation by sophisticatedly allocating both RBs and power to user terminals taking their Quality of Service (QoS) requirements and geographical positions into account.

In order to fulfil this aim, we designed enhanced Dynamic Frequency Planning (eDFP), a semi-distributed architecture for dynamic radio resource management, where

[1]The term cell and sector are synonyms here, e.g., a macrocellular BS has three cells or sectors.

a central node assigns RBs to cells to minimise inter-cell interference to cell-edge users, while independently and more frequently cells assign transmit power and RBs to users so that their transmit power is minimised, while meeting their user QoS requirements. An advantage of this model is that it requires minimum feedback information between cells and the central node because the inputs of the centralised optimisation problem are gathered and post-processed by BSs based on their user Measurement Reports (MRs)i

It should be noted that in this chapter the nomenclature of Long Term Evolution (LTE) networks is used, and that without loss of generality with respect to our novel approach, this chapter focuses on the DownLink (DL).

It should be noted that the idea of this approach was developed by David López, while A. Jüttner and Á. Ladányi provided a close collaboration.

4.1 Enhanced Dynamic Frequency Planning

eDFP decomposes the radio resource allocation problem in Orthogonal Frequency Division Multiple Access (OFDMA)-based networks into two subproblems:

1. **Dynamic Frequency Planning (DFP)**

   The first subproblem is referred to as DFP. This subproblem is solved by a central resource broker, which has a network wide perspective, operates in large time scales, and intelligently distributes RBs among cells so that long-term inter-cell interference suffered by cell-edge users is minimised.

2. **RB and Power Allocation Problem (RPAP)**

   The second subproblem is named as RPAP. This subproblem is solved on a more frequent basis than DFP at the cell level, i.e., it is solved independently by each cell, and allocates Modulation and Coding Schemes (MCSs), RBs and power to users. For decision making, each cell uses the suggestions of the central resource broker and also user Channel Quality Indicators (CQIs).

Note that eDFP is the architecture resulting from using DFP and RPAP together. In the following two sections, both DFP and RPAP are presented.

4.2 Dynamic Frequency Planning

When running DFP and similarly to Fractional Frequency Reuse Schemes (FFRSs), cells divide their sets of connected users into two groups: inner-zone and outer-zone. Since cell-edge users are more prone to suffer from strong inter-cell interference and because they are typically assigned with larger powers that tend to inject instability, DFP is targeted to obtain RB assignments that minimise long-term time-averaged inter-cell interference suffered by cell-edge users.

The main idea is that using a cooperative architecture, a central broker can receive information from all cells. Thereafter, the central broker will solve the DFP problem and indicate to every BS which RBs are permitted for their own outer-zone usage. This process is repeated on a regular basis, i.e., every T_{dfp} time units, in order to adapt cell-edge RB assignments to the long-term fluctuations of network, traffic and channel.

The central broker can be located in the Operating, Administering, and Maintaining (OAM) subsystem, or in a BS that acts as the master of a cluster of BSs in a region. Information between BSs can be exchanged either using the operator's back-haul that connects macro BSs to the OAM subsystem, or BS-to-BS interfaces, e.g., LTE-X2 [92]. Because DFP operates in long time scales, for instance, tens of seconds or minutes, the time delay incurred by DFP processing and signalling should not be a problem. In the proposed eDFP architecture, the fast fluctuations of the channel will be handled at cell level by RPAP, the low latency resource scheduler to be presented in Section 4.3.

In the following, first the inputs and later the formulation of the proposed DFP problem are introduced.

4.2.1 DFP Inputs

The DFP problem has two inputs:

- The *demand vector* $\mathcal{D}$ of size M, which indicates the number of RBs D_m needed by each cell M_m to satisfy the throughput requirements of its outer-zone users.
- The *restriction matrix* $\mathcal{A}$ of size $M \times M$, which models long-term time-averaged inter-cell interference $a_{m,n}$ between each pair of cells $< M_m, M_n >, \forall m, n \in \mathcal{M}$. The restriction matrix will be used to identify for each cell which neighbouring

ones pose a big threat in terms of inter-cell interference. This is particularly useful when BSs are not deployed according to an ideal and perfect regular grid.

Every cell M_m will estimate D_m and $a_{m,n}, \forall M_n \in \mathcal{N}_m$ on a regular basis, and will feed back this information to the central broker every time it performs a DFP update.

4.2.1.1 Demand Vector

The first question that needs to be addressed when estimating the number of RBs D_m required by each cell M_m to satisfy the throughput demands of its outer-zone users is: who are the cell-edge users? A common approach is to classify users into inner-zone or outer-zone users upon their distances to their servers. Nevertheless, this approach does not fit well to sectored BSs, since users nearby BSs but in the boundary between sectors may suffer from large interference due to imperfect isolation between co-located sectors provided by sectored antennas patterns. Hence, we identify cell-edge users based on Signal to Interference plus Noise Ratio (SINR) measurements over reference signals, also referred to as pilot signals (Section 1.3.3).

Because pilot signals are transmitted over fixed resource elements at a fixed power, pilot signal measurements are relatively stable over time and can be used to provide a good indication of the worst interfering conditions that users can possibly suffer from. User pilot SINR measurements may be averaged over time to mitigate fading effects. Hence, if user U_u^m's pilot SINR γ_u^{pilot} is lower than an outer-zone SINR threshold γ^{edge}, then this user U_u^m is considered as an outer-zone user, otherwise, as an inner-zone user, where γ_u^{pilot} can be derived from user MRs, i.e.,

$$\gamma_u^{\text{pilot}} = \frac{p_m^{\text{pilot}} \cdot \Gamma_{m,u}}{\sum_{n=1,n\neq m}^{M} p_n^{\text{pilot}} \cdot \Gamma_{n,u} + \sigma^2} = \frac{w_{u,m}^{\text{pilot}}}{\sum_{n=1,n\neq m}^{M} w_{u,n}^{\text{pilot}} + \sigma^2} \tag{4.1}$$

where p_m^{pilot} is the power allocated by cell M_m to every subcarrier of its pilot signal, $\Gamma_{m,u}$ denotes the channel gain between cell M_m and user U_u^m, $w_{u,m}^{\text{pilot}}$ is the power received by user U_u^m from the pilot signal of its cell M_m, and σ^2 denotes the power of the noise.

Since DFP runs at regular time intervals, i.e., every T_{dfp} time units, it must be considered when estimating D_m that users may connect or disconnect during the time period between two consecutive DFP updates. The cell-edge RB demands of cells may also vary due to mobility of associated users or time-varying interference conditions.

Hence, in order to estimate D_m, we propose that each cell M_m measures the number of allocated RBs to its outer-zone users at a regular time interval $T_{ca} << T_{dfp}$, and keeps record of these estimations using a moving average window of size T_{ca}^{w} time units (Note that the allocation of RBs to users is done by RPAP at each cell (Section 4.3)). Because DFP is designed to minimise long-term time-averaged inter-cell interference, we do not want to know D_m at every time, but how this demand D_m evolves with it. Nonetheless, if the size T_{ca}^{w} of the moving average window is very large, DFP may not be responsive enough to variations of traffic. On the contrary, if T_{ca}^{w} is very small, sporadic traffic peaks that do not represent cell loads may affect DFP performance.

Then, when the central broker is ready to carry out a DFP update, each cell M_m computes the average of its moving average window values and forwards the result D_m to the central broker using the proper interface, e.g., cell back-haul or X2-LTE. In order to avoid unfair RB assignments among cells, where some cells monopolise all resources while others starve, an upper bound D^{max} is set to the number of RBs D_m that a cell M_m can request to satisfy the throughput demands of its outer-zone users.

Since D_m is calculated based on estimates of the own RB usage of each cell, this process could be implemented in BSs.

4.2.1.2 Restriction Matrix

Because DFP is designed to minimise long-term time-averaged inter-cell interference where shadowing and fast-fading effect are averaged out, its principal aim is to mitigate RB collisions between those neighbouring cells more prone to inter-cell interference. The idea here is hence to have cell-edge RB assignments as orthogonal as possible among those cells that suffer from larger long-term time-averaged inter-cell interference.

Long-term time-averaged inter-cell interference between pairs of cells is characterised in terms of percentage of time, i.e., the percentage of time in which the users of a cell are 'interfered' by the pilot signals of a neighbouring one (Section 1.3.3). This model will allow us to estimate inter-cell interference utilising standardised MRs over cell-specific pilot signals, which are always emitted by all cells at a fixed power and do not vary with time-dependent scheduler decisions, simplifying the estimation of the interference coupling between cells.

Interference Event: An interference event $IE_{m,n}$ occurs between two cells, e.g., M_m and M_n, if the received power $(w_{u,m}^{pilot})_{dB}$ from the serving cell pilot signal is lower than the one $(w_{u,n}^{pilot})_{dB}$ from a neighbouring cell pilot signal plus margin $(\Delta Q)_{dB}$, i.e.,

$$(w_{u,m}^{pilot})_{dB} < (w_{u,n}^{pilot})_{dB} + (\Delta Q)_{dB} \tag{4.2}$$

where threshold ΔQ can be considered as a protection margin to fight both the aggregated interference coming from neighbouring cells and the fading of the radio channel, and it should be set by the operator depending on planning targets.

DFP Cell Counters: Every cell M_m has a measurement report counter $MRC_{m,n}$ as well as an interference event counter $IEC_{m,n}$ for each neighbouring cell $M_n \in \mathcal{N}_m$. Hence, when an MR arrives at cell M_m, it carries out two actions:

- Each time an incoming user MR informs about neighbouring cell M_n, cell M_m increases its counter $MRC_{m,n}$ by 1 unit.
- Each time an interference event occurs between itself M_m and cell M_n, cell M_m increases its counter $IEC_{m,n}$ by 1 unit.

Restriction Matrix: When the central broker is ready to carry out a DFP update, cell M_m calculates the percentage of interference time $a_{m,n}$ between itself M_m and its neighbouring cells $M_n \in \mathcal{N}_m$.

$$a_{m,n} = \frac{IEC_{m,n}}{MRC_{m,n}} \tag{4.3}$$

where $a_{m,n}$ are elements of the $M \times M$ restriction matrix $\mathcal{A}$, and sends these values, i.e., $a_{m,n}$, $\forall\, M_n \in \mathcal{N}_m$, to the central broker.

Note that if the number of interference event increases, i.e., $IEC_{m,n}$, the percentage of interference time increases, thus indicating that cell M_n represents a bigger threat.

Similarly to the demand vector $\mathcal{D}$ computation, $MRC_{m,n}$ and $IEC_{m,n}$ use a moving average window of size T_{ie}^{w} time units. Nonetheless, since MRs depend on user locations, the more MRs collected from different geographical locations and from different users, the better characterisation of the interference coupling among cells in terms of time. Thus, it is worth collecting MRs for a large time to average out the correlation between the restriction matrix $\mathcal{A}$ and user locations. Therefore, T_{ie}^{w} should be larger than T_{ca}^{w}.

Since users frequently feed back MRs to their serving cells in cellular networks, this process could be implemented in BSs.

4.2.2 DFP Optimisation

Once both DFP inputs $\mathcal{D}$ and $\mathcal{A}$ are known, the DFP problem can be formulated as a Mixed Integer Program (MIP) problem, in which the objective is to obtain a solution that minimises a cost function representing the overall interference in the network, i.e.,

$$\min_{y_{m,n,k}} \sum_{k=1}^{K} \sum_{m=1}^{M} \sum_{n=1}^{M} \frac{D_n}{K} \cdot a_{m,n} \cdot y_{m,n,k} \tag{4.4a}$$

subject to:

$$\sum_{k=1}^{K} x_{m,k} = D_m \qquad \forall m \tag{4.4b}$$

$$\max\{0, x_{m,k} + x_{n,k} - 1\} = y_{m,n,k} \qquad \forall m, n, k \tag{4.4c}$$

$$y_{m,n,k} \in \{0, 1\} \qquad \forall m, n, k \tag{4.4d}$$

$$x_{m,k} \in \{0, 1\} \qquad \forall m, k \tag{4.4e}$$

where

- $x_{m,k}$ is a binary variable that is equal to 1 if user M_m is using RB k, 0 otherwise.
- $y_{m,n,k}$ is a binary variable that indicates whether both cells M_m and M_n use RB k, 0 otherwise.
- Constraint (4.4b) guarantees that each cell M_m is allocated to exactly D_m RBs.

Each element of summation (4.4a) indicates the percentage of interference time resulting from M_n if RB k is used in M_m. Obtaining lower values of cost function (4.4a) is therefore proportional to decreased inter-cell interference throughout the network. Note that the percentage of interference time $a_{m,n}$ was estimated under worst case scenario conditions, since $a_{m,n}$ was computed with user measurements over pilot signals, which are always transmitted over the channel and thus always 'interfere' each other (Pilots signals act as BS beacon signals and are not affected by scheduler decisions). As a consequence, in order to correctly characterise the percentage of interference time

resulting from ... if RB k is used in ..., the per ... ference time $a_{m,n}$, computed over pilot signals, is thinned by the probability of interferer M_n using RB k. Provided that cells choose RBs independently and a priori with an equal probability (since DFP targets to minimise long-term interference, and thus shadowing/fading effect can be averaged, it considers that all RBs can be used with equal probability), the probability of cell M_n using RB k is $\frac{D_n}{K}$. This is the reason why in (4.4a), the probability $\frac{D_n}{K}$ of cell M_n allocating RB k multiplies the percentage of interference time $a_{m,n}$. Consequently, the larger the number of RBs D_n employed by interfering macrocell M_n, the larger the RB collision probability and the larger the percentage of interference time.

How this problem is solved is presented in Section 4.4.

4.3 Distributed Resource Block and Power Allocation

In a more regular basis and considering the cell-edge frequency planning given by DFP, every cell solves RPAP independently to assign MCSs, RBs and power to its users. RPAP is used as a low latency scheduler to deal with fast fluctuations of the channel.

Due to the good self-organising features of the radio resource management scheme presented in [68] in distributed architectures, in which cells independently minimise their total transmit powers while meeting the throughput requirements of their users, RPAP uses a similar approach but tailored to LTE and WiMAX standard constraints. For instance, in [68], it is considered that the spectrum is divided in three sub-bands, and also that a random-based frequency hopping is implemented on a slot by slot basis by permuting the subcarrier indices independently across different sub-bands and cells. In our case, the spectrum is divided in RBs and all subcarriers within an used RB are modulated, i.e., no frequency hopping is used[1].

The reasons for minimising transmit power independently at each cell are as follows:

1. A cell that targets to minimise its transmit power reduces inter-cell interference towards neighbouring cells, because less power is applied to those RBs allocated

[1]More details about the allocation scheme in [68] will be presented in the following chapter when analysing the performance of fully decentralised radio resource management architectures.

to users that are closer to their BSs and/or have lower throughput requirements. Indeed, this is obvious from the Shannon-Hartley theorem [93].

2. A cell that targets to minimise its transmit power tends to use those RBs that are not being used by neighbouring cells, because less transmit power is required in less interfered or faded RBs to achieve an aimed user SINR.

According to Shannon-Hartley theorem,

$$C_{u,k} = B_k \cdot log_2(1 + \frac{p^m_{u,k} \cdot \Gamma_{m,u}}{w_{u,k} + \sigma^2}) \tag{4.5}$$

where $C_{u,k}$ is the user U^m_u capacity (bps) in RB k, B_k is the bandwidth (Hz) of RB k, $p^m_{u,k}$ is the power allocated by cell M_m to every subcarrier of RB k assigned to user U^m_u, $\Gamma_{m,u}$ is the channel gain between M_m and user U^m_u, σ^2 denotes the power of the noise, and $w_{u,k}$ represents the power of the inter-cell interference suffered by user U^m_u in RB k, we can prove the previous two statements:

If users are closer to their BSs, i.e., if $\Gamma_{m,u}$ increases, the required transmit power $p^m_{u,k}$ to obtain a given capacity $C_{u,k}$ decreases. If users have lower capacity requirements, i.e., if $C_{u,k}$ decreases, the required transmit power $p^m_{u,k}$ for a given gain $\Gamma_{m,u}$ decreases. Algebraic manipulations of (4.5) show that (note that $w_{u,k}$, B_k and σ^2 are kept fixed):

$$p^m_{u,k} = \frac{(w_{u,k} + \sigma^2) \cdot (2^{\frac{C_{u,k}}{B_k}} - 1)}{\Gamma_{m,u}} \tag{4.6}$$

Furthermore, it can also be demonstrated carrying out a simple transformation that inter-cell interference $w_{u,k}$ also decreases, if transmit power $p^m_{u,k}$ is minimised:

$$w_{u,k} = \frac{p^m_{u,k} \cdot \Gamma_{m,u}}{2^{\frac{C_{u,k}}{B_k}} - 1} - \sigma^2 \tag{4.7}$$

Using this kind of power-controlled approach has clear advantages over uniform power distribution approaches. For example, let us assume a network comprised of 2 cells M_m and M_n each one providing service to 2 distinct users with 2 RBs k and k'. In each cell, one user is close to the cell-centre, while the other one is at the cell-edge. Then, if

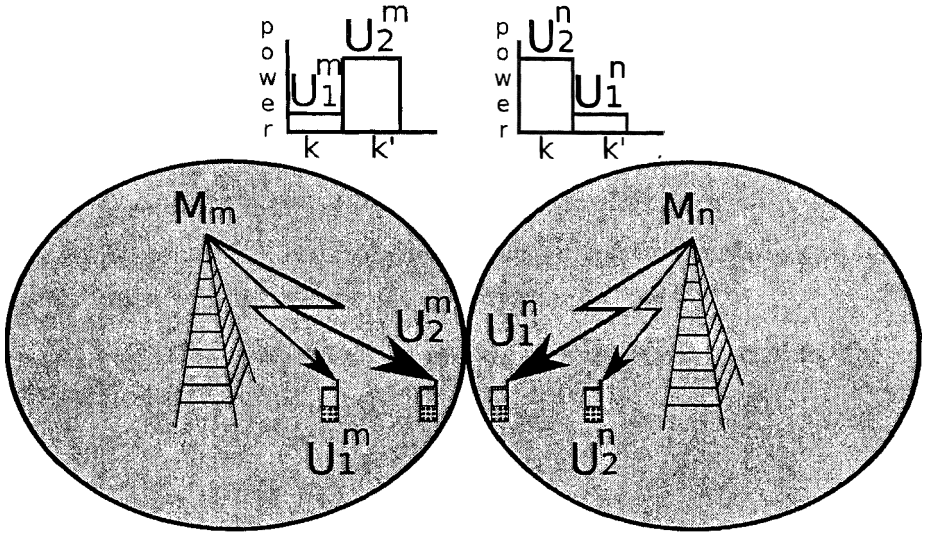

Figure 4.1: Users coexisting in the same RB.

Case A) cells target to minimise their transmit powers: According to statement 1), users close to the cell-centre will be assigned less power than those at the cell-edge. According to statement 2), when cell M_m decides how to assign k and k' to its users, it will see higher inter-cell interference in one RB, e.g., k, than in the other, i.e., k', due to the different powers applied by neighbouring cell M_n in both RBs k and k'. Therefore, cell M_m will assign its cell-edge user to RB k' and its cell-centre user to k (Figure 4.1). Following this approach, users in the cell-edge are not much interfered due to the low power applied by neighbouring cells to the corresponding RBs.

Case B) cells uniformly distribute transmit power among subcarriers: In this case, both cells will assign the same power to their users independently of their positions, throughput requirements or channel conditions. As a result, users positioned at the cell-edge will suffer from larger inter-cell interference than in the previous case.

Because macrocell deployments are designed to cater to large coverage areas and since user may be uniformly distributed within the coverage area of their servers [78], the scenario given in *Case A)* is likely to occur.

In the following, our model for the joint radio resource allocation in M_m is given, i.e., RPAP, which is targeted to minimise transmit power independently at each cell.

The transmit power $p^m_{u,k,h}$ that cell M_m should apply to each subcarrier of RB k

allocated in the DL to user U_u^m to obtain the SINR threshold γ_h of assigned MCS h is

$$p_{u,k,h}^m = \gamma_h \cdot \frac{w_{u,k} + \sigma^2}{\Gamma_{m,u}} \tag{4.8}$$

where $w_{u,k}$ and $\Gamma_{m,u}$ are known by cell M_m because of its user CQIs (Section 3.11).

Similarly to [68], user U_u^m is allocated to the MCS h that requires the least number of RBs and the least power to meet its throughput target TP_u^{req}.

Clearly, MCS h determines the number D_u of RBs needed to meet the throughput target TP_u^{req} of user U_u^m, i.e.,

$$D_u := \left\lceil \frac{TP_u^{req}}{\Theta \cdot eff_h} \right\rceil \tag{4.9}$$

Note that, in this case, the BLock Error Rate (BLER) has not been considered since it is negligible when a user is provided with the SINR target of its aimed MCS.

Moreover, we should also ensure that the RB allocation provided by DFP for cell-edge users is respected. Therefore, we should ensure that users with the lowest pilot SINR γ_u^{pilot} are allocated to the RBs reserved for them via DFP. Because DFP booked D_m RBs for outer-zone usage of cell M_m, we must identify the users with the lowest γ_u^{pilot} value and assign them to these RBs. Hence, let us define $g(u)$ as the sequence order of user U_u^m according to its ascending order in terms of its estimated γ_u^{pilot}, i.e.,

$$\begin{aligned} g : \{1, \cdots, U\} &\mapsto \{1, \cdots, U\} \\ g(u) = g(u\prime) &\Rightarrow u = u\prime \\ g(u) < g(u\prime) &\Rightarrow \gamma_u^{pilot} \leq \gamma_{u\prime}^{pilot} \\ \forall u, u\prime &\in \{1, \cdots, U\} \end{aligned} \tag{4.10}$$

where U_u^m and $U_{u\prime}^m$ are users of cell M_m, while $g(u)$ and $g(u\prime)$ are their sequence orders. Then, in order to realise the outer-zone assignment suggested by DFP, let us define $\kappa_u \in \{0, 1\}\ \forall u \in \mathcal{U}^m$ as a binary variable that is equal to 1 if $g(u) \leq D_m$, 0 otherwise.

Hence, the proposed RPAP to be solved in each cell M_m can be formulated as the following integer linear problem:

$$\min_{\phi_{u,k}} \sum_{u=1}^{U} \sum_{k=1}^{K} p_{u,k,h}^m \cdot \phi_{u,k} \tag{4.11a}$$

subject to:

$$\sum_{u=1}^{M} \phi_{u,k} \leq 1 \qquad \forall k \qquad (4.11b)$$

$$\sum_{k=1}^{K} \phi_{u,k} = D_u \qquad \forall u \qquad (4.11c)$$

$$\phi_{u,k} = \overline{\kappa_u \oplus x_{m,k}} \qquad \forall u,k \qquad (4.11d)$$

$$\phi_{u,k} \in \{0,1\} \qquad \forall u,k \qquad (4.11e)$$

where

- $\phi_{u,k}$ is a binary variable that is equal to 1 if user U_u^m is using RB k, 0 otherwise.
- Constraint (4.11b) ensures that RB k is only allocated to at most one user U_u^m.
- Constraint (4.11c) guarantees that each user U_u^m is allocated to exactly D_u RBs.
- Constraint (4.11d) makes sure that the D_m users with lowest pilot SINR γ_u^{pilot} are assigned to the RBs reserved by DFP (where $\overline{\oplus}$ represents an XNOR operation).

User feedback, CQIs, has been used to determine the MCS h, number of RBs D_u and transmit power $p_{u,k,h}^m$ required for users to meet their throughput targets TP_u^{req}. In order to mitigate the effects of fast fading, user feedbacks are averaged over time, therefore avoiding fast variations of $p_{u,k,h}^m$ and rapid fluctuations of resource allocations in response to fast-fading, which may introduce ping-pong problems into the system. Hence, average channel quality estimations in the form of instantaneous $w_{u,k}$ averaged over tens of CQIs are utilised to derive $p_{u,k,h}^m$ (over intervals of the order of 1 second)s

In order to avoid that several cells change their resource assignment simultaneously, RPAP runs in every cell at a random time uniformly distributed in $[1,2T_{rpap}]$ time units.

How this problem is solved is presented in Section 4.5.

4.4 Solving DFP

This section presents techniques that can be used to solve the centralised DFP problem: Integer Linear Programming (ILP) solvers, metaheuristics and also greedy algorithms. These techniques have a different tradeoff between solution quality and running time.

4.4.1 Integer Linear Programming

The formulation (4.4) of the DFP problem can be solved directly using ILP solvers [94]. Applying standard ILP techniques readily available in both commercial [95][96] and free [97][98] software packages, the DFP problem can be solved up to optimality. Unfortunately, the running times of these ILP solvers are unpredictable in most cases (exponential in the worst case), which renders them inappropriate for their usage in real base stations within acceptable times.

For example, in practice, they can only solve DFP for networks with a few cells. When utilising ILP solvers for realistic network deployments, the required computing resources are out of a viable range. As a result, new solving strategies with good performances within reasonable running times are required for realistic deployments.

4.4.2 Metaheuristics

Since using techniques designed to guarantee the optimality of the solution may be impossible for realistic network scenarios, the use of *metaheuristics* is proposed here. Metaheuristics are general optimisation frameworks used to find good solutions in reasonable times to complex optimisation problems. These methods are based on a search within the solution space, and although they do not guarantee optimality, they often achieve competitive solutions in practice. In the following, the principal features of the two metaheuristics proposed to solve the DFP problem are analysed. These metaheuristics are Simulated Annealing (SA) [99] and Tabu Search (TS) [100].

Before describing these metaheuristics, let us note that in our case:

- A solution x consists of a cell-edge RB assignment to cells fulfilling all constraints.

$$x := (x_{m,k})_{M\times K}\Big|_{(4.4b),\,(4.4c),\,(4.4d),\,(4.4e)}, \quad 1 \le m \le M, \quad 1 \le k \le K \tag{4.12}$$

- The solution space Ω of the DFP problem is comprised of all feasible solutions x.

$$\Omega := \{x \in \mathbb{R}^{M\times K} | (4.4b),\ (4.4c),\ (4.4d),\ (4.4e)\} \tag{4.13}$$

- Two solutions $x \in \Omega$ and $x' \in \Omega$ are called neighbours if and only if they differ at the assignment of a single RB of a single cell.

- The cost $f(x)$ of a solution $x \in \Omega$ corresponds to the overall system interference associated with such solution x, and it is computed by using equation (4.4a). For an interference free allocation x, $f(x)$ is zero.

4.4.2.1 Simulated Annealing

When applying SA to a minimisation problem such as DFP, SA moves in each iteration from the current solution x to a neighbouring one x' based on a probabilistic process. Let us note that neighbouring solutions are always randomly selected by choosing a random cell M_m and randomly changing one of its assigned RBs k for a different one k'. In more detail, movements are defined by a given acceptance probability function $P_{SA}(f(x), f(x'), T)$ that depends on $f(x)$, $f(x')$ and a factor T known as temperature. The fundamental properties of a good acceptance probability function are the following:

- P_{SA} must be larger than 1 if $f(x) > f(x')$, meaning that SA must move from the current solution x to a neighbouring one x', when x' is of better quality than x.
- P_{SA} may be larger than 0 if $f(x) \leq f(x')$, meaning that SA might move from the current solution x to a neighbouring one x', even if x' is of worse quality than x. This condition prevents the search within Ω from getting stuck in local minima. Nevertheless, the higher the difference between $f(x)$ and $f(x')$, the lower the probability of moving from x to x'.
- The temperature T is a parameter that decreases with the number of iterations in an exponential fashion dictated by the so called *annealing factor* parameter. The smaller the temperature, the more likely SA will reject worsening neighbours. Let us note that the initial temperature and the annealing factor must be tuned. In general, the slower the annealing factor, the better solution we may expect, but then the algorithm will require a longer time to converge to a stable solution.

SA is thus expected to wander initially around a broad region of the solution space, thereafter drift towards better regions of the solution space having better solutions and finally move downhill towards a solution similarly to the steepest descent heuristic.

SA stops iterating when a given ending condition is reached. This ending condition could be a given number of iterations, a final temperature or solution quality.

Algorithm 1 Simulated Annealing for DFP

```
x = x_rnd; f_curr = f(x)                          {initial solution (random)}
x_best = x; f_bestS= f(x)                         {initialize best solution}
t = t_init                                        {initialize temperature}
while t > t_end do
  x' = neighbor(x)                                {select a neighbor}
  f_neig = f(x')                                  {compute its cost}
  p_SA = e^((f_curr - f_neig)/t)                  {compute its cost}
  if p_SA > random(0,1) then                      {is this a valid movement?}
    x = x'; f_curr = f_neig                       {yes, save it}
    if f_curr < f_best then                       {is this the best solution so far?}
      x_best = x; f_best = f_curr                 {yes, save it}
    end if
  end if
  t = t · annealingFactor                         {lower the temperature}
end while
```

A general SA algorithm that can be directly used to solve the DFP problem is given in Algorithm 1.

4.4.2.2 Tabu Search

When applying TS to a minimisation problem as DFP, TS moves in each iteration from the current solution x to a neighbouring one x' based on a tabu selection process. Let us note that neighbouring solutions are always randomly selected by choosing a random cell M_m and randomly changing one of its assigned RBs k for a different one k'. Firstly, in each iteration, the neighbourhood $\mathcal{N}_x$ of current solution x must be found. In small problems, all neighbours of the current solution can be visited in each iteration. In large problems, the set of visited neighbours is generally reduced to a given subset. This fact decreases the quality of the search, but significantly reduces the running time. In our case, the number of visited neighbours per iteration is limited to a value of N_x. Then, TS always moves from current solution x to its best neighbouring one $x' \in \mathcal{N}_x$, i.e, the one with the lowest cost within $\mathcal{N}_x$. Note that the cost function value $f(x')$ of the best neighbour x' does not need to improve the one $f(x)$ of the current solution x.

In TS, the search process may move from a current solution x to a neighbouring one x' even when worsening the cost function value to avoid getting stuck in a local minima. The action of moving from a solution x to its best neighbour x' is known as movement.

In addition, TS introduces the concept of tabu list in order to prevent the problem of possible cycling and/or infinite loop [100]. In its simplest form, the tabu list does not allow solutions that have certain attributes or that have been visited/checked recently. In this case, the tabu list forbids those movements that have been performed recently for a number of iterations equal to the size N_x of the subset $\mathcal{N}_x$ of visited neighbours. In this case, a movement is described by the difference between both x and x', that is: the cell M_m whose allocation was modified and how it was modified, i.e., the old RB k that was randomly changed by a new one, k'.

TS stops iterating when a given ending condition is reached. This ending condition could be a given number of iterations, a running time or solution quality.

A general TS algorithm that can be directly used to solve the DFP problem is given in Algorithm 2.

4.4.3 Greedy Algorithms

In order to obtain good approximate solutions of the DFP problem (4.4) within a reduced amount of computing time, we have also devised greedy and reverse greedy procedures that construct a solution.

The reason why we are interested in these greedy rules to solve the DFP problem is not only because they are faster than metaheuristics, but also because they are of lower complexity and therefore easier to implement in off-the-shelf base stations.

In the following, the main features of the six greedy algorithms created in this research are presented:

4.4.3.1 Insertion Algorithms

Insertion schemes maintain a list of assigned RBs per cell. This list is initially empty, i.e., no RBs are assigned to any cell.

At each iteration, we first calculate the *the best* RB k_m to be added to each sector M_m, i.e., the RB k_m which increases the cost function the least. Then, we choose a cell

Algorithm 2 Tabu search algorithm for DFP

$x = x_{rnd}$; $f_{curr} = f(x)$ {initial solution (random)}
$x_{best} = x$; $f_{best} = f(x)$ {initialize best solution}
$tabu = []$; $iter = 0$ {initialize tabu list and iteration counter}
while $iter < iter_{max}$ **do**
  $iter = iter + 1$
  $cn = 0$ {initialize checked neighbour counter}
  x_{neig}^{best} = NULL; $f_{neig}^{best} = 999999$ {best neighbor}
  while $cn < N_\kappa$ **do**
    $cn = cn + 1$
    $x' = neighbor(x)$ {select a neighbor}
    $f_{neig} = f(x')$ {compute its cost}
    if $f_{neig} < f_{best}$ **then** {is this the best solution so far?}
      $x_{best} = x'$; $f_{best} = f_{neig}$ {yes, save it}
      $x_{neig}^{best} = x'$; $f_{neig}^{best} = f_{neig}$ {also the best neighbor}
      break {stop looking for neighbours}
    end if
    if $movement(x, x')$ **in** $tabu$ **then** {is this movement forbidden?}
      continue {yes, skip it}
    end if
    if $f_{neig} < f_{neig}^{best}$ **then** {is this the best neighbor?}
      $x_{neig}^{best} = x'$; $f_{neig}^{best} = f_{neig}$ {yes, save it}
    end if
  end while
  $m = movement(x, x_{neig}^{best})$
  $x = x_{neig}^{best}$; $f_{curr} = f_{neig}^{best}$ {move to best neighbor}
  $tabu = tabu + [m]$ {add movement to tabu list}
  $remove\_old(tabu)$ {remove too old entries}
end while

M_m according to the rules RI, $MinI$ or $MaxI$ (see below) and assign the chosen RB k_m to its list.

Random Insertion (RI) A random sector is selected at each iteration.

Minimum Insertion (MinI) The sector increasing the cost function *the least* is selected.

Maximum Insertion (MaxI) In contrast to $MinI$, here the sector increasing the cost function *the most* is selected.

Intuitively, we can say that $MinI$ tries to delay the difficulties by choosing first cells to which it is cheap to allocate new RBs. On the contrary, $MaxI$ faces the difficulties by choosing first cells to which it is costly to assign new RBs.

With respect to the complexity of these greedy rules: RI has a complexity of $\mathcal{O}((\sum_m D_m) \cdot K)$, while both MinI and MaxI have a complexity of $\mathcal{O}((\sum_m D_m) \cdot (M \cdot K + M)$. $\sum_m D_m$ represents the number of insertions (RB assignments) to be done, while M and K are the number of cells and RBs, respectively.

4.4.3.2 Removal Algorithms

Removal schemes maintain a list of assigned RBs per cell. This list is initially full, i.e., all RBs are allocated to all cells.

At each iteration, we first derive the *the best* RB k_m to be deleted from each sector M_m, i.e., the RB k_m which decreases the cost function the most. Then, we select a cell M_m according to the rules RI, $MinI$ or $MaxI$ (see below) and remove the chosen RB k_m from its list.

Random Removal (RR) A random sector is selected at each iteration.

Maximum Removal (MaxR) The sector decreasing the cost function *the most* is selected.

Minimum Removal (MinR) In contrast to $MaxR$, here the sector decreasing the cost function *the least* is selected.

With respect to the complexity of these greedy rules: RI has a complexity of $\mathcal{O}((M \cdot K - \sum_m D_m) \cdot K)$, while both MinI and MaxI have a complexity of $\mathcal{O}((M \cdot K - \sum_m D_m) \cdot (M \cdot K + M)$. $M \cdot K - \sum_m D_m$ represents the number of removals (RB subtractions) to be performed.

In the insertion algorithms, the RB assignment is started from scratch, and then we allocate RBs to all cells until they have the number of RBs that they require.

In the removal algorithms, we assume that all cells are utilising all RBs, and then we remove RBs from all cells until they have the number of RBs that they need.

4.5 Solving RPAP

RPAP can be solved efficiently up to optimality using the following observation.

Claim 1 *Let us define the following* network flow *problem* $F = (V, E)$ *[101] with:*

- *Vertex set*

$$V := \mathcal{U}^M \cup \mathcal{K} \cup \{\hat{s}, \hat{t}\}, \tag{4.14a}$$

being $\hat{s}, \hat{t} \in V$ *the source and the sink of* V*, respectively.*

For the sake of simplicity a user U_u^m *of the studied cell* M_m *is denoted as user* u*.*

- *Edge set*

$$\begin{aligned} E := &\{(\hat{s}u) : u \in \mathcal{U}\} \cup \{(uk) : u \in \mathcal{U}, k \in \mathcal{K} \big| \kappa_u = x_{m,k}\} \cup \\ &\{(k\hat{t}) : k \in \mathcal{K}\}, \end{aligned} \tag{4.14b}$$

where edges with $\kappa_u \neq x_{m,k}$ *are broken. This means that there is no flow between user* u *and RB* k *either if* $x_{m,k} = 1$ *and* $g(u) > D_m$*, or* $x_{m,k} = 0$ *and* $g(u) \leq D_m$*. If any of these two conditions is met, then user* u *cannot make use of RB* k*, respecting the advice provided by DFP.*

- *Capacity function*

$$cap(ab) := \begin{cases} D_b, & \text{if } a = \hat{s}, b \in \mathcal{U} \\ 1 & \text{otherwise,} \end{cases} \tag{4.14c}$$

- *Cost function*

$$cost(uk) := \begin{cases} p^m_{u,k,h}, & \text{if } u \in \mathcal{U}, k \in \mathcal{K} \\ 0 & \text{otherwise.} \end{cases} \tag{4.14d}$$

Then, a minimal cost network flow with value $\min \sum_{u \in \mathcal{U}} D_u$ *will provide an optimal solution to RPAP.*

In order to solve this problem, the *network simplex* algorithm [102] implemented in the LEMON library [103] has been adopted in our simulations.

In order to avoid frequent radio resource reassignments in cell M_m, new allocations are loaded into it, only if they result in significant enhancement over existing ones. Improvements are estimated over cost function (4.11a) and must be at least of a 10%.

4.6 Simulation and Numerical Results

4.6.1 Scenario

We considered a hexagonal LTE cellular network comprised of 19 tri-sectored eNodeBs. Different simulations with 3, 6, 9 or 12 static users connected per cell were performed, representing in this case a cell user load of 25%, 50%, 75% and 100%, receptively, since the studied network had 12 RBs per DL time slot in a bandwidth of 2.5 MHz. Users were uniformly distributed within the coverage area of each cell. A user held its connection for a time dictated by an exponential distribution of meanμ and then disconnected. After its disconnection, a new user was generated at a random location. A full-buffer user-traffic model was used and the demand of each user was 250 kbps. Users suffered from outage if they could not transmit at a throughput no less than their requirements[1] for a time period T_{outage}. When a given user suffered from outage, its resources were freed and a new user was not generated till its holding time expired.

[1]Applications based on real-time or streaming services are insensitive to bit rate slow downs if the expected QoS, i.e., transmission rate, is achieved.

Table 4.1: SIMULATION PARAMETERS

Parameter	Value	Parameter	Value
eNodeB	19	UE Body Loss	0 dB
Simulation time	600 s	Path Loss Model	Empirical
Site-to-site distance	500,1000 m	Shadowing s.d.	8 dB
Carrier Frequency	2.0 GHz	Users per sector (U)	3,4,9,12
Channel Bandwidth	2.5 MHz	User distribution	Uniform
Frame Duration	1 ms	Min. dist. UE to eNodeB	35 m
Subcarriers	150	Mean Holding Time	90 s
RB (K)	12	Type of Service	Full buffer
DL OFDM data symbols	11	Min Service TP	250 kbps
BS Tx Power (P_m^{tot})	43 dBm	T_{outage}	9 s
BS Ant. Base Gain	18 dBi	$T_{u,mr}$	480 ms
BS Ant. Pattern	Sectorized	$T_{u,cqi}$	10 ms
BS Ant. Height	30 m	T_{dfp}	10 s
BS Ant. Tilt	10	T_{rpap}	100 ms
BS Noise Figure	5 dB	T_{ca}	500 ms
BS Cable Loss	3 dB	T_{ca}^{w}	60 s
Thermal Noise Density	-174.0 dBm/Hz	T_{ie}^{w}	1 h
UE Ant. Gain	0 dBi	$(\Delta Q)_{dB}$	12 dB
UE Ant. Pattern	Omni	D^{max}	50% of K
UE Ant. Height	1.5 m	γ^{edge}	2 dB
UE Noise Figure	9 dB	-	-

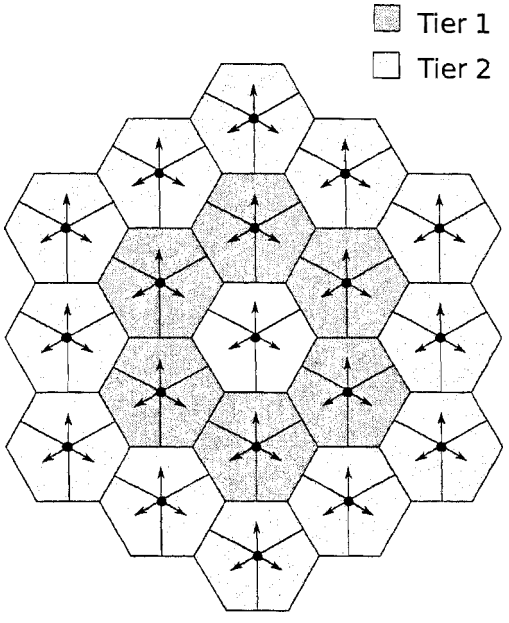

Figure 4.2: System-level simulation scenario.

The system model was implemented as a subframe-level simulator using the event-driven simulation presented in Chapter 3. 600 s of network operation were simulated. User performance in terms of throughput, outage, transmit power and other indicators was assessed on a regular basis, every 1 s. In order to avoid scenario border effects, statistics were collected from the central eNodeB and the first tier of interfering ones, but not from the second tier.

Path losses and antenna patterns were modelled according to models in Chapter 3, and fading was modelled using a log-normal shadowing with standard deviation of 8dB. When solving the proposed RPAP, average channel quality estimations in the form of instantaneous $w_{u,k}$ averaged over a time window of 1 s were used to derive $p^m_{u,k,h}$ [68]. Users were not located closer than 35 m to any eNodeB to avoid tower shadow effects. Subframe errors were modelled based on BLER Look Up Tables (LUTs) from Link-Level Simulations (LLSs) [85]. Further details about the scenario and parameters used in our simulations are presented in Figure 4.2, Table 4.1, respectively and Chapter 3.

Network performance was assessed through 3 Key Performance Indicators (KPIs):

1. User outages, which represents the absolute number of outages incurred to user

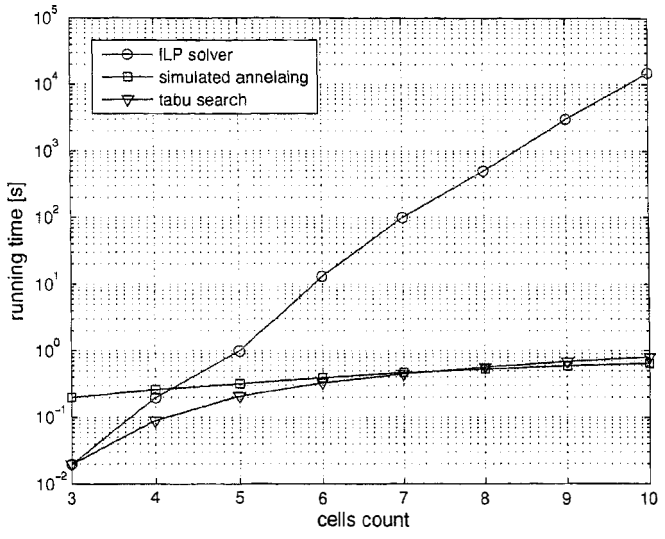

Figure 4.3: ILP, TS and SA running times

handsets during the entire simulation.

2. Connected users, which denotes the average number of users simultaneously connected to the network along the simulation.

3. Network throughput, which indicates the average sum throughput carried by the network during the entire simulation.

Because of the nature of user traffic, i.e., constant throughput demand, reducing the number of outages, i.e., user dissatisfaction, and hence increasing the average number of connected users, has a larger added-value here than enhancing user throughputs, because real-time user services will not benefit from lager bit rates than the demanded.

4.6.2 Optimisation Performance

4.6.2.1 Solving DFP

Figure 4.3 illustrates the running time of the ILP solver, SA and TS when solving DFP in scenarios with a different number of cells. The following parameters were used in the simulations performed to get this figure: 8 RBs and 3 to 11 network cells where their cell-edge RB demands, i.e., D_m, were uniformly distributed within interval $[1, 5]$.

The restriction matrices of this numerical evaluation were obtained utilising subsets of cells of the scenario introduced in Figure 4.2. SA and TS were tuned for the analysis, and curves were obtained by averaging of 20 realisations with different subsets of cells. Moreover, it should be noted that the computer utilised for these simulations contained an AMD Opteron 275 dual-core processor running at $2.2\,GHz$ with $16\,GB$ of RAM.

Figure 4.3 illustrates that the running time of the ILP solver increases rapidly with the number of cells in the network, while that of TS and SA increases much slower. Greedy rule running times are not shown, since they are in the order of milliseconds and because they are analysed afterwards.

The ILP solver ran out of memory for 11 cells, being unable to obtain solutions. Indeed, the ILP solver running time increased exponentially with the number of cells. Hence, we may consider it useless for realistic scenarios with much more than 11 cells. For these small network scenarios, TS and SA were able to find very good solutions. SA was able to obtain the optimal solution in all studied cases, while TS was able to obtain it until 9 cells. For 10 cells, it was at most 3.10 % away from the optimal solution. TS running time depends on the number of neighbouring solutions visited per iteration, which is small when the number of cells is small. On the other hand, SA running time mostly depends on the initial fine tuning of the temperature and the annealing factor. In both cases, SA and TS, the running time increased in a much more slower fashion than that of the ILP solver, hence allowing the analysis of much larger cell deployments.

Figure 4.4 illustrates the performance of both metaheuristics, SA and TS, in terms of cost function (4.4a) versus iterations number.

The numerical tests performed to obtain Figure 4.4 used the following parameters: 50 RBs, 57 cells where their cell-edge RB demand was uniformly distributed in $[15, 20]$ and the restriction matrix was obtained according to the scenario given in Figure 4.2. Figure 4.4 illustrates that the solution qualities obtained by SA and TS are similar. However, their performances are sensitive to the fine tuning:

- With regard to SA, Figure 4.4 shows that SA obtains a worse solution when the annealing factor is decreased from 0.99990 to 0.99950. If the annealing factor increases to 0.99995, SA (green line) does not converge within the expected time.
- With regard to TS, a better solution is found when both the number of visited neighbours per iteration and the size of the tabu list increased from 25 to 75.

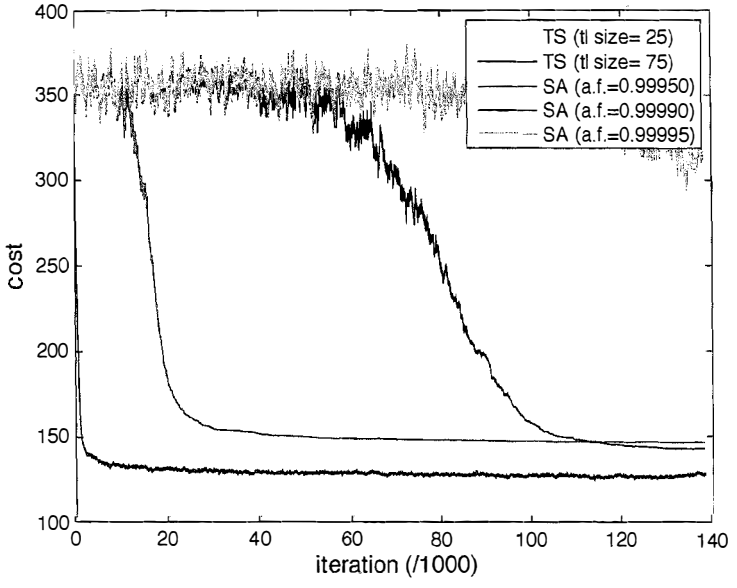

Figure 4.4: TS versus SA

In this case, further increasing these values did not provide a significant solution quality improvement with respect to the running time.

Hence, for SA, the temperature and annealing factor were set to 1000 and 0.99990, respectively, while for TS, both the number of visited neighbours per iteration and the size of the tabu list were set to 75.

Table 4.2 and 4.3 depict the performance of both metaheuristics, SA and TS, and greedy heuristic rules in terms of cost function (4.4a) and running time, respectively. Eight different network scenarios were utilised in this case to test their performances. The first four scenarios had 7 BSs and 21 sectors, i.e., one tier of interfering cells, whereas the second four had 21 BSs and 57 sectors, i.e., two tiers of interfering cells. Four variants of both set-ups were studied with distinct RB demands D_m per cell, which were uniformly distributed within intervals [15,20], [20,25], [25,30] and [30,35]. The total number of RBs was 50. The entry 'random' indicates the value of cost function (4.4a) averaged over 100 random RB allocations. Table 4.2 shows that major improvements are obtained when using optimisation instead of random allocations. Depending on sector loads, the value of cost function (4.4a) decreased up to 81 %.

Table 4.2: Solution quality of TS, SA, greedy rules

Scenario	21 sectors				57 sectors			
min/max req. RBs	15/20	20/25	25/30	30/35	15/20	20/25	25/30	30/35
Methods	**Solution quality in terms of cost function (4.4a)**							
random	58.02	133.77	234.94	397.73	351.14	1587.41	2389.94	3356.39
SA	**10.87**	48.20	**132.27**	**300.99**	142.69	**454.03**	**1017.78**	1870.80
TS	12.10	**44.90**	133.02	302.15	**140.93**	457.33	1017.78	**1870.80**
best metah.	10.87	44.90	132.27	300.99	140.93	454.03	1017.78	1870.80
RI	15.23	50.58	**138.27**	319.73	210.44	**497.46**	**1034.65**	1948.78
MinI	**12.35**	57.01	151.22	322.10	187.45	539.83	1143.84	2016.53
MaxI	13.01	51.21	139.10	320.20	**182.75**	534.63	1126.27	**1900.72**
RR	18.31	**49.97**	139.07	**317.10**	223.66	498.54	1074.26	1934
MaxR	16.82	59.11	151.02	325.09	202.47	536.83	1100.34	1953.25
MinR	20.01	53.41	158.02	333.64	326.81	563.97	1167.34	2001.45
best greedy	12.35	49.97	138.27	317.10	182.75	497.46	1034.65	1900.72
Reduction (%) random vs. best metah.	81.27	66.37	43.70	24.32	59.87	71.40	57.41	44.26
Reduction (%) rrandom vs. best greedy	78.71	62.64	41.15	20.27	47.96	68.66	56.71	43.37
Reduction (%) best greedy vs. best metah.	11.9	10.14	4.34	5.08	22.88	8.73	1.63	1.57

Table 4.3: Running time of TS, SA, greedy rules

Scenario	21 sectors				57 sectors			
min/max req. RBs	15/20	20/25	25/30	30/35	15/20	20/25	25/30	30/35
Methods	**Running time**							
SA	524 ms	561 ms	693 ms	721 ms	2536 ms	2921 ms	3544 ms	4045 ms
TS	555 ms	701 ms	865 ms	954 ms	2964 ms	3401 ms	4102 ms	4899 ms
RI	0.32 ms	0.45 ms	0.59 ms	0.71 ms	1.36 ms	1.82 ms	2.29 ms	2.71 ms
MinI	0.48 ms	0.52 ms	0.63 ms	0.85 ms	2.17 ms	3.01 ms	3.95 ms	4.50 ms
MaxI	0.56 ms	0.45 ms	0.81 ms	0.87 ms	2.33 ms	3.22 ms	3.67 ms	4.23 ms
RR	0.66 ms	0.65 ms	0.51 ms	0.41 ms	3.17 ms	2.99 ms	2.63 ms	2.29 ms
MaxR	0.97 ms	0.83 ms	0.79 ms	0.82 ms	5.73 ms	5.07 ms	4.45 ms	3.76 ms
MinR	1.01 ms	0.86 ms	0.70 ms	0.67 ms	5.29 ms	4.93 ms	4.51 ms	3.81 ms
sum of greedy	4.00 ms	3.76 ms	4.03 ms	4.33 ms	20.05 ms	21.04 ms	21.50 ms	21.30 ms
Reduction (%) sum of greedy vs. SA	99.24	99.33	99.42	99.4	99.21	99.28	99.39	99.47
Reduction (%) sum of greedy vs. TS	99.28	99.47	99.53	99.55	99.32	99.38	99.48	99.57

Also, as shown in Figure 4.4, Table 4.2 indicates that SA and TS perform similarly. Indeed, there is no absolute winner among both of them.

Comparing the performance of our greedy heuristic rules, we can see that there is no absolute winner among them either. Nonetheless, they run so quick that one can afford to execute all of them sequentially and thereafter selecting the best solution. The sum running time of all greedy rules was at most 0.79 % and 0.72 % of the running time of SA and TS, respectively.

Most importantly, Table 4.2 indicates that the solution qualities provided by the best greedy heuristic rule in each scenario is not far from that given by metaheuristics. On average, the best greedy rule was only 8.28% worse than the devised metaheuristics.

As a conclusion, greedy rules are faster, easier to implement and provide solutions very similar to those of metaheuristics, therefore in practice one may prefer these greedy rules to solve DFP. In the following simulations, the proposed greedy rules will be used.

4.6.2.2 Solving RPAP

When using network simplex, the average running time of a RB and power allocation, i.e., RPAP, estimated over one million assignments in different cells was 0.31 ms. Thus, since RPAP can be solved faster than the minimum feedback frequency in LTE, i.e., 2 ms [27], it can be used as a low latency scheduler to cope with channel variations originated due to shadowing, fast fading or quick fluctuations of inter-cell interference. Regarding solution quality, lets us recall that network simplex ensures the optimallity.

4.6.3 Network Performance

4.6.3.1 Techniques Used for Comparison

The approaches described in the following were included for performance comparison. Let us note that some of these approaches were initially described in (Section 2.1.3). Also, Reuse/Static/IM and Reuse/Dynamic/IM represent two different flavours of the reuse schemes presented in Section 2.1.1, i.e., reuse 1, reuse 3, FFRS3-A and FFRS3-B.

Reuse/Static/IM When using reuse 3, FFRS3-A, or FFRS3-B, the total bandwidth is divided into 3 segments. We make use of the SINR threshold γ^{edge} to divide users

into inner- and outer-zones. If the RBs reserved for the inner-zone are all occupied, RBs reserved for outer-zone users are not permitted for inner-zone use and vice versa. Cells uniformly distribute their total transmit power among subcarriers of each zone, but transmit powers applied to subcarriers of the inner- and outer-zones are different. In this case, these powers $p_{u,k}^{m,\text{centre}}$ and $p_{u,k}^{m,\text{edge}}$ were tuned using the approach in [104],

$$p_{u,k}^{m,\text{centre}} = \frac{\frac{3 \cdot p_m^{\text{tot}}}{R_{\text{DL}}^{\text{tot}}}}{s+2}, \quad p_{u,k}^{m,\text{edge}} = s \cdot \frac{\frac{3 \cdot P_m^{\text{tot}}}{R_{\text{DL}}^{\text{tot}}}}{s+2} \tag{4.15}$$

where p_m^{tot} is the total transmit power of cell M_m, s is the number of spectrum segments, and $R_{\text{DL}}^{\text{tot}}$ is the number of total subcarriers.

Each cell independently performs an Interference Minimisation (IM) process so that RBs are assigned to terminals while minimising the sum interference suffered by them. This assignment scheme is assisted by CQIs, and is formally presented in Section 6.3.2.

Reuse/Dynamic/IM This approach only differs from the previous one in that if the RBs reserved for the inner-zone are all occupied, RBs reserved for outer-zone users may be allocated to inner-zone users and vice versa.

Note that Reuse/Static/IM and Reuse/Dynamic/IM behave the same in case of reuse 1 and reuse 3 because these two reuse schemes do not separate connected users in cell-centre and cell-edge zones.

Ronald's Approach [53]: Its exact implementation is presented in Appendix A.1. However, let us note that this scheme is based on a centralised architecture and uniformly distributes power among subcarriers.

Hussain's Approach [63]: Its exact implementation is presented in Appendix A.2. It also uses a centralised architecture and an uniform power distribution among subcarriers. But, in our implementation, RBs instead of subcarriers are assigned to users.

Note that eDFP will also be compared to Stolyar's approach [68] in the following chapter when analysing fully decentralised radio resource management architectures.

Table 4.4: Network Performance vs. γ^{edge}

γ^{edge} [dB]	0	0.5	1.0	1.5	2.0	2.5	3.0
User outage	29	22	17	14	**7**	27	32
Connected users	245.23	246.85	247.99	248.38	**249.61**	245.76	245.01
Network throughput [Mbps]	56.54	56.76	57.89	58.61	**59.17**	56.96	56.23

4.6.3.2 Cell-Centre and Cell-Edge Zones: γ^{edge}

Parameter γ^{edge} plays a key role in system performance because it defines the cell-centre and cell-edge boundary. Recall that γ_u^{pilot} denotes the user SINR estimated over pilot signals that are transmitted by each cell over fixed resource elements at a fixed power. If $\gamma_u^{\text{pilot}} \leq \gamma^{\text{edge}}$, user U_u^m is considered as a cell-edge user, otherwise, a cell-centre user.

Because only cell-edge users are involved in the DFP resource allocation procedure presented in Section 4.2, if γ^{edge} is too small, few users will benefit from DFP planning. On the other hand, if γ^{edge} is too large, the number of cell-edge RB requested per cell will be large, close to D^{max}, and the quality of the obtained DFP will be compromised.

In order to fine tune γ^{edge}, we run several simulations in the proposed scenario. The set-up with 12 users per cell and an inter-BS distance of 500 m was used here. Table 4.4 illustrates that $\gamma^{\text{edge}} = 2\,\text{dB}$ provides the best network-wide performance. For instance, the number of user outages considerably decreased from 32 to 7 when γ^{edge} was fine tuned from 3.0 dB to 2.0 dB.

In the following simulations, the cell-centre and cell-edge boundary γ^{edge} is set to 2 dB.

4.6.3.3 Transmit Power

Figure 4.5 shows the Cumulative Distribution Function (CDF) of the power allocated to subcarriers along the simulation. When using reuse schemes the transmit power applied to RBs is fixed and does not vary according to interference or load fluctuations. On the contrary, when using eDFP not only the power applied to each RB changes depending on such conditions, but becomes much smaller. Like this, interference to neighbouring cells is mitigated. Moreover, it can be observed that according to [104], FFRS3-A and FFRS3-B assign different constant powers to the inner and outer-zone.

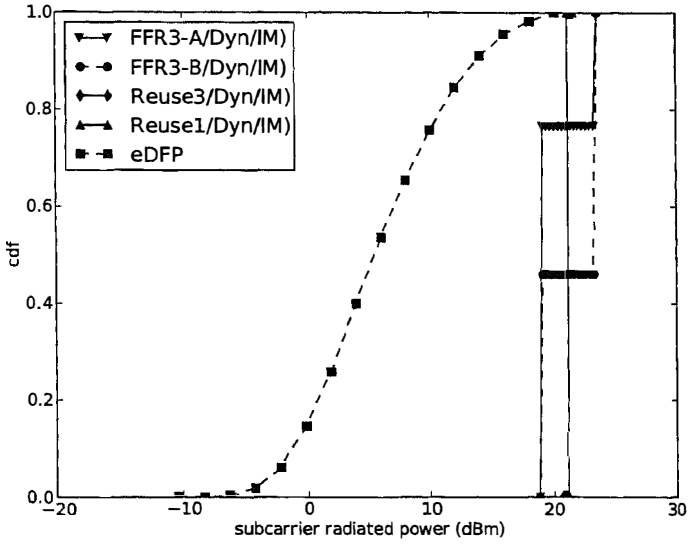

Figure 4.5: CDF of the radiated power per subcarrier during the simulation in the 12 user/sector scenario.

4.6.3.4 Inter-Cell Interference

Figure 4.6 corroborates what has been stated in the previous sections: minimising total transmit power in every cell mitigates inter-cell interference towards neighbouring cells. Figure 4.6 illustrates that the inter-cell interference suffered by subcarriers decreases when using the proposed allocation scheme with respect to the other approaches. This inter-cell interference reduction is significant with respect to reuse 1 and FFRS3-B, specifically a median reduction of 11 dB. Note that reuse 3 supplies the best inter-cell interference mitigation at the expense of thinning the cell bandwidth by a factor of 3. Because reuse 3 offers interference coordination, by avoiding a cell reusing RBs that can be used in neighboring cells, reuse 3 results in a significant network capacity loss. This is shown in the following subsection.

4.6.3.5 System-Level Performance

When running eDFP, the following parameters were used: T_{dfp}=10 s, T_{ca} = 500 ms, T_{ca}^{w} = 60 s, T_{ie}^{w} = 1 h, $(\Delta Q)_{dB}$ = 12 dB, D^{max} = 50%, γ^{edge} = 2 dB and T_{rpap} = 100 ms.

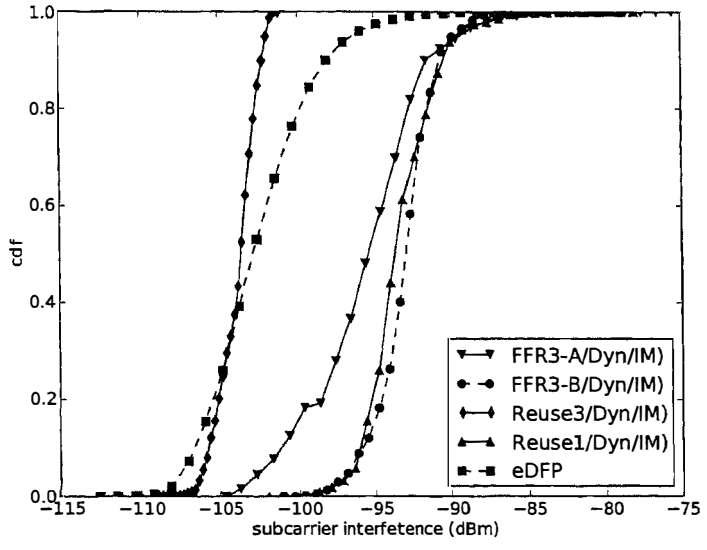

Figure 4.6: CDF of the interference suffered per subcarrier during the simulation in the 12 user/sector scenario.

Tables 4.5, 4.6, 4.7 and 4.8 illustrate the network performance when using eDFP and the presented schemes in terms of outages, average number of network connected users and average network throughput. Note that 12 RBs were available and that 3, 6, 9 or 12 users attempted to connect per cell, representing a 25 %, 50 %, 75 % and 100 % cell user load of its maximum, respectively. The distance among BSs was set to 500 m. In these tables, columns denote proposed approaches, e.g., eDFP, Ronald's, Hussain's, and rows denote its frequency reuse form, i.e., reuse 1, reuse 3, FFRS3-A, FFRS3-B Note that DNA stands for Does Not Apply and it means that a given approach cannot be utilised in a given frequency reuse form because it was not proposed/designed for it.

We can see that all tables follow exactly the same trend, being eDFP the method that provides the best performance. Nonetheless, when the number of users increased, the number of user outages also increased because of the larger inter-cell interference.

In the 12 users/cell case, i.e., the most challenging scenario, eDFP resulted in a performance improvement over the second best method, i.e., FFRS3-B/Dynamic/IM, of 50.66 more average connected users and a 22.18% higher average network throughput.

eDFP outperforms all other approaches because it permits a better spatial reuse.

It allows all cells to allocate all available RBs to their users in an intelligent manner: Cells minimise transmit power and hence assign less power to those RBs allocated to users having good geometries or with lower demands, therefore neighbouring cells will 'see' low interference in such RBs and will allocate them to their bad geometry users. This kind of spatial reuse is not possible by making use of uniform power distributions when all network cells are highly loaded.

Since Ronald's approach does not use any user feedback to assess channel conditions, spatial reuse loss is necessary to obtain inter-cell interference avoidance, which may be affordable when cell traffic loads are low compared to the total number of available radio resources, but not when traffic loads are large and homogeneously distributed. Since RBs allocated to cell-edge users in a cell cannot be reused in its 6 adjacent cells, Ronald's approach results therefore in a large spatial reuse and throughput loss. For similar reasons, reuse 3 and FFRS 3-A perform poorly when the network is loaded. For instance, in case of reuse 3, since only one third of the RBs can be used in a cell, at most 4 users can be connected to it. Therefore, resulting in a large throughput loss when a larger number of users attempt to connect per cell, i.e., 6, 9 or 12 users/cell.

In Hussain's approach, RBs allocated to a cell of a BS to satisfy the minimum throughput requirements of its users cannot be reused in other cells of the same BS. Moreover, the RB assignment for all cells of a BS is replicated for all BSs in the network. Hence, this approach performs well when the number of available RBs is much larger than what requested by the users, but if some cells are loaded and necessitate all RBs, this algorithm may allocate all RBs to such specific cells, whereas other network cells, e.g., cells with different antenna bearing than those ones that first hoard all resources, may be left starving without no RBs at all.

Table 4.9 also illustrates the network performance of eDFP and the above approaches in terms of outages, average number of network connected users and average network throughput. In this case, 12 user terminals attempted to connect per cell and the distance between neighbouring BSs was set to 1000 m. The increase in cell radius reduced inter-cell interference. Consequently, for almost all techniques considered, outages reduced and system capacity in terms of both average network connected users and average network throughout improved.

For eDFP, because the number of outages was low in Table 4.8, increased user path losses had a larger impact in terms of outages at cell-edges than reduced inter-

Table 4.5: System-level simulation results: 3 users per cell.

Scheme	KPI	Reuse Static IM	Reuse Dynamic IM	Ronald Approach	Hussain Approach	eDFP
Reuse 1	Outage	0 (0.00 %)	0 (0.00 %)	DNA	DNA	DNA
	Users	63	63			
	Mbps	15.73	15.73			
Reuse 3	Outage	0 (0.00 %)	0 (0.00 %)	DNA	DNA	DNA
	Users	63	63			
	Mbps	15.75	15.75			
FFR3A	Outage	14 (3.18 %)	0 (0.00 %)	10 (2.27 %)	DNA	DNA
	Users	61.88	63	60.54		
	Mbps	15.43	15.75	14.97		
FFR3B	Outage	0 (0.00 %)	0 (0.00 %)	28 (6.36 %)	0 (0.00 %)	0 (0.00 %)
	Users	63	63	57.47	63	63
	Mbps	15.72	15.73	14.02	15.74	15.74

Table 4.6: System-level simulation results: 6 users per cell.

Scheme	KPI	Reuse Static IM	Reuse Dynamic IM	Ronald Approach	Hussain Approach	eDFP
Reuse 1	Outage	18 (2.16 %)	18 (2.16 %)	DNA	DNA	DNA
	Users	122.92	122.92			
	Mbps	30.35	30.35			
Reuse 3	Outage	257 (30.82 %)	257 (30.82 %)	DNA	DNA	DNA
	Users	84	84			
	Mbps	21.00	21.00			
FFR3A	Outage	93 (11.15 %)	19 (2.28 %)	81 (9.71 %)	DNA	DNA
	Users	111.03	122.54	99.58		
	Mbps	27.60	30.09	24.49		
FFR3B	Outage	41 (4.92 %)	16 (1.92 %)	132 (15.83 %)	58 (6.95 %)	0 (0.00 %)
	Users	119.97	124.63	102.24	116.32	126
	Mbps	29.73	30.84	24.84	28.36	31.46

Table 4.7: System-level simulation results: 9 users per cell.

Scheme	KPI	Reuse Static IM	Reuse Dynamic IM	Ronald Approach	Hussain Approach	eDFP
Reuse 1	Outage	161 (13.76 %)	161 (13.76 %)	DNA	DNA	DNA
	Users	161.19	161.19			
	Mbps	39.74	39.74			
Reuse 3	Outage	640 (54.70 %)	640 (54.70 %)	DNA	DNA	DNA
	Users	84	84			
	Mbps	21	21			
FFR3A	Outage	324 (27.69 %)	206 (17.61 %)	379 (32.39 %)	DNA	DNA
	Users	132.73	152.87	98.91		
	Mbps	32.95	37.39	24.36		
FFR3B	Outage	199 (17.01 %)	117 (10.00 %)	302 (25.81 %)	235 (20.09 %)	0 (0 %)
	Users	158.40	165.91	138.34	149.77	189
	Mbps	39.13	40.89	33.55	36.29	46.50

Table 4.8: System-level simulation results: 12 users per cell.

Scheme	KPI	Reuse Static IM	Reuse Dynamic IM	Ronald Approach	Hussain Approach	eDFP
Reuse 1	Outage	412 (23.44 %)	412 (23.44 %)	DNA	DNA	DNA
	Users	194.79	194.79			
	Mbps	47.79	47.79			
Reuse 3	Outage	1195 (67.97 %)	1195 (67.97 %)	DNA	DNA	DNA
	Users	84	84			
	Mbps	21	21			
FFR3A	Outage	749 (42.61 %)	514 (29.24 %)	773 (43.97 %)	DNA	DNA
	Users	142.16	171.82	99.87		
	Mbps	35.21	42.02	24.54		
FFR3B	Outage	451 (25.65 %)	337 (19.17 %)	516 (29.35 %)	411 (23.38 %)	7 (0.40 %)
	Users	182.08	198.95	176.81	194.56	249.61
	Mbps	44.88	48.43	42.88	47.00	59.17

Table 4.9: System-level simulation results: 12 users per cell (1000m).

Scheme	KPI	Reuse Static IM	Reuse Dynamic IM	Ronald Approach	Hussain Approach	eDFP
Reuse 1	Outage	329 (18.71 %)	329 (18.71 %)	DNA	DNA	DNA
	Users	204.16	204.16			
	Mbps	50.27	50.27			
Reuse 3	Outage	1195 (67.97 %)	1195 (67.97 %)	DNA	DNA	DNA
	Users	84	84			
	Mbps	21	21			
FFR3A	Outage	741 (42.15 %)	474 (26.96 %)	648 (36.86 %)	DNA	DNA
	Users	145.92	173.65	109.80		
	Mbps	36.11	42.81	26.90		
FFR3B	Outage	436 (24.80 %)	242 (13.77 %)	399 (22.69 %)	326 (18.59 %)	13 (0.74 %)
	Users	189.47	215.75	192.40	204.48	248.78
	Mbps	46.62	52.49	46.98	49.13	61.85

cell interference, hence increasing users outages very slightly from 7 to 13 occurrences. Nevertheless, because of the mentioned reduced inter-cell interference, in this case, the average network throughput increased with cell radius from 59.17 to 61.85 Mbps.

Finally, let us note that the impact on network performance of the centralised RB planning provided by DFP, it is analysed in the following Chapter in comparison with decentralised architectures where cells operate independently in a distributed manner.

4.7 Conclusions

This chapter has presented a new approach to the radio resource assignment for OFDMA networks called eDFP. On the one hand, DFP was proposed as a novel scheme for cell-edge inter-cell interference minimisation. On the other hand, RPAP has been proposed as a low latency scheme for allocating RBs and power to users. Tailored metaheuristics such as SA and TS, and greedy heuristics have been utilised to solve the DFP optimisation problem, whereas a network simplex based approach has been adopted to find optimal solutions to our RPAP. Simulations corroborate that eDFP enhances network performance compared to other schemes proposed in literature.

The results of optimisation and system-level simulations have shown the following

evidences about eDFP:

Conclusion 1: The modelling of long-term time-averaged inter-cell interference between pairs of cells based on pilot signal measurements does not need extra signalling. Moreover, the cost function used for characterising the overall network interference based on this pilot signal model has been shown to be adequate for the purpose of interference minimisation.

Conclusion 2: The DFP optimisation becomes too complex and cannot be solved directly using integer linear programming approaches in realistic cellular deployments. Contrarily, the proposed SA, TS and greedy algorithms have been shown to be able to find well-performing network solutions of the DFP assignment problem within a reduced amount of time.

Conclusion 3: The implementation of a power controlled resource allocation scheme that minimises transmit power at each cell is the key to allow a better spatial reuse. Minimising transmit power independently at each cell reduces interference in those RBs allocated to users with good channel conditions or low throughput requirements, hence generating RB allocation opportunities that may be used by neighbouring cells for their cell-edge users.

Conclusion 4: eDFP mitigates inter-cell interference and significantly improves network capacity in terms of average number of network connected users and average network throughput ($\simeq$22 %) with respect to a variety of resource allocation methods in the OFDMA literature.

Chapter 5

Decentralised Interference Mitigation Architecture for Macrocells: enhanced Resource Allocation Problem

Different techniques with different degrees of complexity can be utilised to mitigate interference in Orthogonal Frequency Division Multiple Access (OFDMA) networks. These schemes fundamentally differ in how radio resource assignments are determined within cell neighbourhoods. Centralised approaches may be more powerful from the optimisation point of view, providing a coordinated scheduling across multiple cells. However, they are based on low latency communications between cells and a central broker or among cells that incur signalling.

In order to decrease signalling overhead, and also prevent single points of failure, decentralised schemes that need few or no coordination among cells are more practical. In this case, cells should take radio resource management decisions independently, i.e., Modulation and Coding Schemes (MCSs), Resource Blocks (RBs) as well as power, while targeting at the enhancement of system performance throughout the network. Due to the good inter-cell interference mitigation features shown by eDFP in Chapter 4, in this chapter, we investigate the potential of improving network performance through a decentralised and joint MCS, RB and power assignment based on power minimisation. Our work differs from other in that we devised a joint MCS, RB and power allocation

able to improve network performance under standardised assignment constraints, e.g., all RBs allocated to a user terminal have to have the same MCS (Section 1.3). Furthermore, two decentralised radio resource management architectures are proposed:

- An autonomous Radio Resource Allocation Architecture (auRRAA), where cells independently allocate resources to users based on local knowledge of subchannel usage in neighbouring cells fed back by their associated users.
- A cooperative Radio Resource Allocation Architecture (coRRAA), where cells additionally are able to exchange information via a message passing approach to coordinate assignments.

It must be noted that in this chapter the nomenclature of Long Term Evolution (LTE) networks is used, and that without loss of generality with respect to our novel approach, this chapter focuses on the DownLink (DL).

It must be noted that the idea of this approach was developed by David López, while A. Jüttner and Á. Ladányi provided a close collaboration.

5.1 Fundamentals of Our Decentralised Allocation Schemes

5.1.1 Transmit Power Minimisation

In order to achieve a self-organised resource allocation pattern across the network through the independent and dynamic optimisation of resource assignments at cells, implying the least signalling overhead or no communication among Base Stations (BSs), it is necessary that this optimisation is done according to an objective that presents a good self-organising behaviour. For example, in a skein of birds flying in V formation, a bird bases its behaviour on its own observations and very simple rules rather than on the commands given by a 'central leading bird'. The self-organising rule for a bird is to line up on one side of the bird ahead, in this way a given bird can benefit from the upwash behind the wing tips of the bird ahead, therefore having better aerodynamics. In our case, an similarly to [68] and eDFP, we propose that each cell independently minimises its transmit power across all RBs, as self-organising rule.

Our cell optimisation objective is thus to allocate MCS, RBs and power to users, while minimising its own transmit power and meeting its user throughput demands. Let us note that the reasons for minimising transmit power independently at each cell were previously presented in Section 4.3, but let us briefly recall them in the following:

1. A cell that targets to minimise its transmit power reduces inter-cell interference towards neighbouring cells, because less power is applied to those RBs allocated to users that are closer to their BSs and/or have lower throughput requirements. Indeed, this is obvious from the Shannon-Hartley theorem [93].

2. A cell that targets to minimise its transmit power tends to use those RBs that are not being used by neighbouring cells, because less transmit power is required in less interfered or faded RBs to achieve an aimed user Signal to Interference plus Noise Ratio (SINR).

However, because in our model we also consider the allocation of MCSs to users, the optimisation problem to be solved at each cell is more intricate than that of [68]. It is hence expected that the self-organised MCS, RB and power assignment to users proposed in this chapter may tend to assign more RBs (increasing the cell RB usage), each one of them modulated with a low-order MCS and using the least possible power (reducing inter-cell interference).

Due to the dynamics of the scheduling schemes that will be proposed in this chapter, cells can quickly react to the appearance of incoming users, avoiding overload issues related to high cell RB usage. Since some amount of bandwidth is set aside to ensure that users are not dropped during handovers, new users can also rely on this bandwidth until they are scheduled by the allocation schemes to be proposed in this chapter [105].

5.1.2 Inter-BS Cooperation

In the following, we describe the message passing approach that will be used to coordinate inter-cell interference in coRRAA. This method will not be used in auRRAA.

The message passing approach to be presented here is targeted at coordinating cell-edge inter-cell interference, similar to eDFP (Chapter 4), because users at cell-edges are more prone to inter-cell interference and are usually assigned with larger powers that tend to inject instability in the network.

In order to enhance system performance, we thus propose that neighbouring cells coordinate their allocations in terms of frequency and power to their cell-edge users, through a message passing approach via inter-BS interfaces, e.g., LTE X2 interface [92], so that inter-cell interference suffered by cell-edge users is coordinated and mitigated.

In this case, collaboration is only established among neighbouring cells instead of using a centralised resource broker. Only local information is exchanged, thus involving a few signalling and avoiding single points of failure. Since cells only communicate with their neighbours, this cooperative approach is more scalable than the proposed eDFP. It should be noted that signalling overhead is to be analysed in Section 5.5.1 and 5.6.3.8.

Similarly to eDFP in the previous chapter, user U_u^m is considered as a cell-edge user, if its time-averaged pilot SINR γ_u^{pilot} is smaller than cell-edge SINR threshold γ^{edge}. Otherwise, user U_u^m is considered as an inner-zone user (Section 4.2.1).

In the following, our message passing approach to coordinate inter-cell interference is introduced.

When cell-edge user U_u^m connects to cell M_m, it is allocated to a specific RB k and it is given a transmit power $p_{u,k,h}^m$, which results from dividing the total cell power among the number of subcarriers (uniform distribution). Based on RB k interference, we estimate the MCS h to be assigned to this user to meet its throughput requirement. Soon after, in the next scheduling procedure, the MCS, RB and transmit power assignment to this user is updated according to the approach to be presented in Section 5.2.

Based on this init assignment, cell $M_$ computes the maximu $_{u,k}$ that user U_u^m can su r in RB k so that its SINR is no less than the SINR threshold γ_h of its selected MCS h, i.e,

$$w_{u,k}^{max} = (\frac{p_{u,k,h}^m \cdot \Gamma_{m,u}}{\gamma_h} - \sigma^2) + \Delta w \tag{5.1}$$

where $\Gamma_{m,u}$ is known by serving cell M_m due to Channel Quality Indicators (CQIs), and Δw represents an additional inter-cell interference protection margin set to 3 dB (Note that the notation was presented in previous chapters).

Thereafter, this maximum interference $w_{u,k}^{max}$ is divided by the number of potential interferers C_u^{intrf} of user U_u^m

$$w_{u,k}^{C-max} = \frac{w_{u,k}^{max}}{C_u^{intrf}} \tag{5.2}$$

where $\Upsilon_u \in \mathcal{M}$ is the set of interfering cells of U_u^m and C_u^{intrf} denotes its cardinality. In this case, Υ_u is comprised of the 6 physically adjacent cells of the serving cell M_m.

Then, based on user U_u^m's channel gain to each of these interfering cells $M_n \in \Upsilon_u$, which can be derived using measurement reports over pilot signals fed back by user U_u^m, cell M_m calculates the maximum transmit power $p_k^{n,max}$ that interfering cell $M_n \in \Upsilon_u$ can apply to RB k in order to prevent the outage of cell-edge user U_u^m in cell M_m, i.e,

$$p_k^{n,max} = w_{u,k}^{C-max} \cdot \Gamma_{n,u} \tag{5.3}$$

and sends this information, i.e., k and $p_k^{n,max}$, to all its potential interferers $M_n \in \Upsilon_u$.

As mentioned earlier, in LTE, eNodeBs are connected to each other through a low-latency operator-deployed X2 interface. Also, in order to facilitate a dynamic interference coordination among eNodeBs, LTE has standardised control messages to indicate challenging interference conditions, e.g., High Interference Indicator (HII). A given cell will use HIIs to inform neighbouring ones that uplink transmission of one of its cell-edge users will be scheduled in the near future, and thus neighbouring cells should not assign their own cell-edge users or high powers to those specified RBs [106]. Similarly, in our approach, we propose using DL-HIIs to indicate to each cell $M_n \in \Upsilon_u$, that they should not allocate a power $p_{u,k,h}^n$ greater than $p_k^{n,max}$ in a specified RB k. A given DL-HIIs will contain two values, i.e., $p_k^{n,max}$ and k, in their simplest form, and will be sent to a specific cell $M_n \in \Upsilon_u$. Cell M_m will indicate to each cell $M_n \in \Upsilon_u$ when a power constraint expires through a DL-HII where $p_k^{n,max}$ is set to a null value. Furthermore, when receiving several DL-HIIs for the same RB k, cell $M_n \in \Upsilon_u$ will always follow the lowest power constraint.

5.2 Cooperative Resource Allocation Problem

This section defines our model for the joint MCS, RB and power allocation to users, i.e., an optimisation problem called cooperative Resource Allocation Problem (coRAP). The main idea of the model proposed in this chapter is that each cell M_m will independently update from its neighbouring cells $\mathcal{N}_m$ the MCS, RB and power assignment to its users $\mathcal{U}^m$ according to the CQIs of its users and DL HIIs of its neighbouring cells, while minimising its own transmit power and meeting its user throughput demands.

Recall that the power $p_{u,k,h}^m$ that cell M_m should apply to each subcarrier of RB k

allocated in the DL to user U_u^m to obtain the SINR threshold γ_h of assigned MCS h is

$$p_{u,k,h}^m = \gamma_h \cdot \frac{w_{u,k} + \sigma^2}{\Gamma_{m,u}} \tag{5.4}$$

where $w_{u,k}$ and $\Gamma_{m,u}$ are known by cell M_m because of its user CQIs (Section 3.11). Then, the optimisation problem of the joint MCS, RB and power assignment to users that runs independently in each cell M_m can be formulated as the following Integer Linear Programming (ILP) problem, i.e.,

$$\min_{\chi_{u,k,h}} \sum_{u=1}^{U} \sum_{k=1}^{K} \sum_{h=1}^{H} p_{u,k,h}^m \cdot \chi_{u,k,h} \tag{5.5a}$$

subject to:

$$\sum_{u=1}^{U} \sum_{h=1}^{H} \chi_{u,k,h} \leq 1 \qquad \forall k \tag{5.5b}$$

$$\sum_{h=1}^{H} \rho_{u,h} \leq 1 \qquad \forall u \tag{5.5c}$$

$$\chi_{u,k,h} \leq \rho_{u,h} \qquad \forall u,k,h \tag{5.5d}$$

$$\sum_{k=1}^{K} \sum_{h=1}^{H} \Theta \cdot eff_h \cdot \chi_{u,k,h} \geq TP_u^{req} \qquad \forall u \tag{5.5e}$$

$$p_{u,k,h}^m \leq p_k^{m,max} \qquad \forall u,k,h \tag{5.5f}$$

$$\rho_{u,h} \in \{0,1\} \qquad \forall u,h \tag{5.5g}$$

$$\chi_{u,k,h} \in \{0,1\} \qquad \forall u,k,h \tag{5.5h}$$

where

- $\chi_{u,k,h}$ is a binary variable (5.5h) that is equal to 1 if user U_u^m uses MCS h in RB k, or 0 otherwise.
- $\rho_{u,h}$ is a binary variable (5.5g) that is equal to 1 if user U_u^m makes use of MCS h, or 0 otherwise.
- Constraint (5.5b) ensures that RB k is only allocated to at most one user U_u^m.
- Constraint (5.5c) and constraint (5.5d) both together make sure that each user U_u^m is allocated to at most one MCS h.

- Constraint (5.5e) ensures that user U_u^m achieves its throughput demand TP_u^{req}. Note that, in this case, the BLock Error Rate (BLER) has not been considered since it is negligible when users are provided with the SINR targets of their MCSs.

- Constraint (5.5f) guarantees that power constraints set by neighbouring cells through the DL-HIIs presented in Section 5.1.2 are respected.

Remark 1: Note that if constraint (5.5f) is omitted from the problem formulation, the presented cooperative assignment problem transforms into an autonomous one because DL-HIIs are not taken into account, and hence every cell acts independently. This new problem is referred to as autonomous Resource Allocation Problem (auRAP).

In this case, this joint radio resource assignment scheme tends to allocate users that are closer to their BSs or have lower data-rate demands (therefore requiring lower MSCs and transmit powers) to RBs occupied by cell-edge user in neighbouring cells. In order to avoid the effects of fast fading, user feedbacks may be averaged over time, thus avoiding fast variations of $p_{u,k,h}^m$ and rapid fluctuations of resource assignments in response to fast-fading, which may introduce ping-pong problems into the system. Hence, average channel quality estimations in the form of instantaneous $w_{u,k}$ averaged over tens of CQIs are used to derive $p_{u,k,h}^m$.

Furthermore, in order to inject stability in the network and avoid the exchange of a large number of DL-HIIs, the power assignment to a cell-edge user is only updated if $p_{u,k,h}^m$ significantly varies with respect to its current value. Like this, we avoid sending numerous DL-HIIs in response to the time-dependent fluctuations of the radio channel. In this case, a given cell updates $p_{u,k,h}^m$ and sents out a new DL-HII only if its new value varies 1 dB with respect to its current one.

The formulation (5.5) of coRAP can be solved directly making use of ILP solvers [94]. Applying standard ILP techniques readily available in both commercial [95][96] and free [97][98] software packages, the presented coRAP can be solved up to optimality. Unfortunately, the running times of these ILP solvers are unpredictable in most cases (exponential in the worst case), which renders them inappropriate for their usage in real base stations within acceptable times. As a result, new solving strategies with good quality/running time performances are necessary for realistic network scenarios.

Performance details of an ILP solver when solving coRAP are given in Section 5.6.2.

5.3 Cooperative RB and Power Allocation Problem

This section discusses an important subproblem of coRAP referred to as cooperative RB and Power Allocation Problem (coRPAP), that occurs when MCSs assigned to all users are known a priori as part of the input.

An efficient solution to this subproblem has two important applications:

- It can be used as a subroutine in order to solve the coRAP problem, as will be presented in Section 5.4.
- It can be utilised as a low latency RB and power allocation algorithm, as will be discussed in Section 5.5.

Assuming that an MCS h has been selected for each user U_u^m and fixed a priori as part of the input, i.e., $\rho_{u,h}$ $\forall u$ $\forall h$is known, coRAP transforms into a simpler form. Clearly, the selected MCS h determines the number D_u of RBs needed for satisfying the throughput demand TP_u^{req} of user U_u^m. Namely,

$$D_u := \left\lceil \frac{TP_u^{req}}{\sum_{h=1}^{H} \Theta \cdot eff_h \cdot \rho_{u,h}} \right\rceil = \left\lceil \frac{TP_u^{req}}{\Theta \cdot eff_h} \right\rceil \tag{5.6}$$

where these parameters were defined in Chapter 3.

Furthermore, let us introduce the binary variable $\phi_{u,k} \in [0,1]$, which indicates whether user U_u^m is using RB k or not, i.e.,

$$\phi_{u,k} := \sum_{h=1}^{H} \chi_{u,k,h} \tag{5.7}$$

Substituting these 2tequations (5.6) and (5.7) into (5.5a)-(5.5h), we obtain the following RB and power allocation problem.

$$C_{\mathcal{S}} = \min_{\phi_{u,k}} \sum_{u=1}^{U} \sum_{k=1}^{K} p_{u,k,h}^{m} \cdot \phi_{u,k} \tag{5.5a*}$$

subject to:

$$\sum_{u=1}^{U} \phi_{u,k} \leq 1 \qquad \forall k \qquad (5.5b^*)$$

$$\sum_{k=1}^{K} \phi_{u,k} = D_u \qquad \forall u \qquad (5.5e^*)$$

$$p^m_{u,k,h} \leq p^{m,max}_k \qquad \forall u,k,r \qquad (5.5f^*)$$

$$\phi_{u,k} \in \{0,1\} \qquad \forall u,k \qquad (5.5h^*)$$

where

- Constraint (5.5b*) ensures that RB k is only allocated to at most one user U^m_u.
- Constraint (5.5e*) guarantees that each user U^m_u is allocated to exactly D_u RBs.
- Constraint (5.5f*) makes sure that power constraints set by neighbouring cells through the DL-HIIs presented in Section 5.1.2 are respected.

Remark 2: Note that if constraint (4.11e) is omitted from the problem formulation, the presented cooperative assignment problem transforms into an autonomous one because DL-HIIs are not taken into account, and hence every cell acts independently. This new problem is named autonomous RB and Power Allocation Problem (auRPAP).

Moreover and due to the totally unimodular property [107] of the constraint matrix, optimal solutions of coRPAP can always be chosen to be integral.

Therefore, the integrality constraint (5.5h*) can be replaced by

$$\phi_{u,k} \geq 0 \qquad \forall u,k, \qquad (5.5h^{**})$$

As a result, this formulation is now efficiently solvable by a general purpose Linear Programming (LP) solving tool.

5.3.1 Solving coRPAP optimally

The following observation makes possible to solve coRPAP optimally more efficiently.

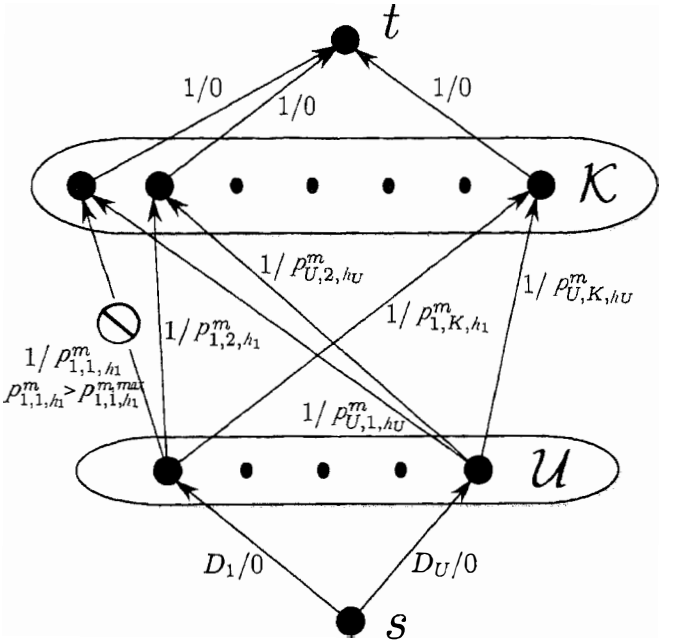

Figure 5.1: Network flow diagram of coRPAP.

Claim 2 *Let us define the following* network flow *problem* $F = (V, E)$ *[101] with:*

- *Vertex set*

$$V := \mathcal{U}^M \cup \mathcal{K} \cup \{\hat{s}, \hat{t}\}, \tag{5.8a}$$

being $\hat{s}, \hat{t} \in V$ *the source and the sink of* V*, respectively.*

For the sake of simplicity a user U^m_u *of the studied cell* M_m *is denoted as user* u*.*

- *Edge set*

$$E := \{(\hat{s}u) : u \in \mathcal{U}^M\} \cup \{(uk)\text{i}: u \in \mathcal{U}^M, k \in \mathcal{K} \mid p^m_{u,k,h} \leq p^{m,max}_{u,k,h}\} \cup \{(k\hat{t}) : k \in \mathcal{K}\}, \tag{5.8b}$$

where if $p^m_{u,k,h} > p^{m,max}_k$*, then the edge between user* u *and RB* k *is broken, meaning that user* u *according to DL-HIIs cannot make use of RB* k *(Figure 5.1).*

- *Capacity function*

$$cap(ab) := \begin{cases} D_b, & \text{if } a = \hat{s}, b \in \mathcal{U} \\ 1 & \text{otherwise,} \end{cases} \tag{5.8c}$$

- *Cost function*

$$cost(uk) := \begin{cases} p_{u,m,k}, & \text{if } u \in \mathcal{U}, k \in \mathcal{K} \\ 0 & \text{otherwise.} \end{cases} \tag{5.8d}$$

Then, a minimal cost network flow with value $\min \sum_{u \in \mathcal{U}} D_u$ *will provide an optimal solution to coRPAP.*

In order to solve this problem, the *network simplex* algorithm [102] implemented in the LEMON library [103] has been adopted in our simulations.

Remark 3: Similarly, we can also efficiently solve auRPAP, if we replace edge set $E := \{(\hat{s}u) : u \in \mathcal{U}^M\} \cup \{(uk) : u \in \mathcal{U}^M, k \in \mathcal{K} \mid p^m_{u,k,h} \leq p_k^{m,max}\} \cup \{(k\hat{t}) : k \in \mathcal{K}\}$ *by this new edge set* $E := \{(\hat{s}u) : u \in \mathcal{U}^M\} \cup \{(uk) : u \in \mathcal{U}^M, k \in \mathcal{K}\} \cup \{(k\hat{t}) : k \in \mathcal{K}\}$.

5.4 Solving coRAP

In this section, a metaheuristic based approach is proposed in order to solve the joint MCS, RB and power assignment problem, i.e., coRAP, based on a subroutine able to optimally compute RB and power assignments given an MCS allocation, i.e., coRPAP.

The key idea behind this approach is that a metaheuristic can be used to search over the MCS assignment solution space. Meanwhile, for each MCS assignment, an optimal RB and power assignment can be obtained by solving coRPAP (Section 5.3). Let us recall again that the target of coRAP is to find an MCS assignment together with its associated RB and power assignment so that cells' transmit power is minimised. In the following, we sketch the Tabu Search (TS) [100] employed to solve coRAP. However, let us note that the main contribution of this chapter is not to provide a metaheuristic to solve the complex problem, but the transformation of this problem into one of reduced complexity by means of a two-level decomposition approach[1].

Before describing this metaheuristic, let us note that in our case:

- A solution ρ consists of an MCS assignment to every user fulfilling all constraints.

$$\rho := (\rho_{u,h})_{U_m \times H}\Big|_{(5.5b),(5.5c),(5.5d),(5.5e),(5.5h)}, \quad 1 \leq u \leq U_m, \quad 1 \leq h \leq H \tag{5.9}$$

[1]Let us note that other metaheuristics can be applied to solve RAP, e.g. Simulated Annealing (SA).

- The solution space Ξ of our coRAP is therefore the set of all feasible solutions ρ.

$$\Xi := \{\rho \in \mathbb{R}^{U_m \times H} | (5.5b),\ (5.5c),\ (5.5d),\ (5.5e),\ (5.5h)\} \tag{5.10}$$

- Two solutions $\rho \in \Xi$ and $\rho' \in \Xi$ are called neighbours if and only if they differ at the assignment of a single MCS of a single user.

- The cost $f(\rho)$ of a solution $\rho \in \Xi$ corresponds to the sum of the transmit power associated with all users connected to cell M_m over all the allocated RBs $\in \mathcal{K}$, and it is computed utilising the cost function (5.5a*) of the subroutine, i.e., coRPAP.

In this approach, the MCS h of each user U_u^m of cell M_m is selected according to a TS heuristic rule, building a given MCS solution ρ. Thereafter, by solving coRPAP, the optimal RB and power assignment associated to this MCS allocation is obtained. Afterward, the quality of MCS allocation ρ is evaluated according to the cost value $f(\rho)$ of this optimal RB and power assignment obtained by coRPAP, i.e., (5.5a*). Following this procedure and employing TS, distinct MCS assignments can be tested in a sophisticated way to obtain a good solution ρ from the solution space Ξ of coRAP.

When applying TS to a minimisation problem such as coRAP, TS moves in each iteration from a solution ρ to a new neighbouring solution ρ' based on a tabu process. It must be noted that neighbouring solutions are always randomly selected by choosing a random user U_u^m and randomly changing its assigned MCS h for a different one h'. Note that a neighbouring solution is not feasible and cannot be 'visited' either if there are not sufficient RBs ($\sum_{u=1}^{U} D_u > K$) and/or power ($f(\rho) > P_m^{total}$) in order to satisfy the throughput demands TP_u^{req} of all user terminals $U_u^m \in \mathcal{U}^m$ associated to cell M_m.

The action of moving from a current solution ρ to a neighbouring one ρ' is known as *movement*. Because the number of neighbours of solution ρ could be significant, TS may not visit all neighbours of a solution in an iteration due to time constraints. $\mathcal{N}_\rho$ represents the set of neighbours of ρ visited per iteration and $_\rho$ its cardinality. This fact reduces the quality of the search, but significantly decreases the running time. Thereafter, TS moves from current solution ρ to its best neighbouring one $\rho' \in \mathcal{N}_\rho$, i.e., the one with the lowest cost within $\mathcal{N}_\rho$. Note that the cost function value $f(\rho')$ of the best neighbour may not improve the cost function value $f(\rho)$ of the current one. TS may move from a current solution to a neighbouring one even when worsening the

Algorithm 3 Tabu search algorithm

$\rho = \rho_0$; $f_{curr} = f(\rho)$ {initial solution}
$\rho_{best} = s$; $f_{best} = f_\rho$ {initialise best solution}
$tabu = [\,]$; $iter = 0$ {initialize tabu list and iteration counter}
while $iter < iter_{max}$ **do**
  $iter = iter + 1$
  $cn = 0$ {initialize checked neighbour counter}
  $\rho^{best}_{neigh} =$ NULL; $f^{best}_{neigh} = 999999$ {best neighbour}
  while $cn < N_\rho$ **do**
    $cn = cn + 1$
    $\rho' = neighbour(\rho)$ {select a neighbour}
    $f_{neig} = f(\rho')$ {compute its cost (solve RPAP)}
    if $needed\_RBs(\rho') > K$ **or** $f_{neig} > P^{total}_m$ **then** {is this a feasible solution?}
      continue {yes, skip it}
    end if
    if $f_{neig} < f_{best}$ **then** {is this the best solution so far?}
      $\rho_{best} = \rho'$; $f_{best} = f_{neig}$ {yes, save it}
      $\rho^{best}_{neigh} = \rho'$; $f^{best}_{neigh} = f_{neig}$ {also the best neighbour}
      break {stop looking for neighbours}
    end if
    if $movement(\rho, \rho')$ **in** $tabu$ **then** {is this movement forbidden?}
      continue {yes, skip it}
    end if
    if $f_{neig} < f^{best}_{neigh}$ **then** {is this the best neighbour?}
      $\rho^{best}_{neigh} = \rho'$; $f^{best}_{neigh} = f_{neigh}$ {yes, save it}
    end if
  end while
  $m = movement(\rho, \rho^{best}_{neigh})$
  $\rho = \rho^{best}_{neigh}$; $f_{curr} = f^{best}_{neigh}$ {move to best neighbour}
  $tabu = tabu + [m]$ {add movement to tabu list}
  $remove\_old(tabu)$ {remove too old entries}
end while

cost function value of the current solution to avoid getting stuck in a local minima. Furthermore, the tabu list forbids those movements that have been performed recently for a number of iterations equal to the size N_ρ of the subset $\mathcal{N}_\rho$ of visited neighbours. In this case, a movement is described by the difference between both ρ and ρ', that is: the user U_u^m whose allocation was modified and how it was changed, i.e., the old MCS h that was randomly changed by a new one, h'.

A general TS algorithm that can be directly utilised to solve coRAP is presented in Algorithm 3.

After executing TS, a good MCS assignment ρ is found by macrocell M_m with its associated RB and power allocation. Thereafter, macrocell M_m allocates this good resource assignment to its connected users. Then, macrocell M_m continues gathering new CQIs in order to learn interference conditions and perform the next optimisation.

5.5 Resource Management Architecture

Because coRPAP can be solved very quickly, which will be shown in Section 5.6.2, and much more frequently than coRAP, we suggest utilising the following architecture to implement the proposed self-organisation.

- By solving coRAP, users' MCSs can be updated in a hundreds of frame basis in order to cope with the time-dependent traffic load fluctuations within the cell, or the slow path loss variations of users due to mobility.

  If a new user wants to connect to a cell, this cell will raise the MCSs of its users to free some RBs to accommodate this new connection.

- By solving coRPAP, the RB and power allocation to users can be updated independently and in a much faster basis than the assignment of MCS in order to cope with the fast variations of the channel due to interference and/or fading. In this case, coRPAP will use the MCS assignment previously found by coRAP. This should not greatly affect capacity, because coRAP is updated frequently, a hundreds of frames basis.

In order to enhance stability and avoid frequent reassignments in the network, a new assignment is loaded in macrocell M_m only if this new assignment provides a

significant improvement over the cost function value of the current one (in here, a 10%).

coRAP and coRPAP allocations occur in each cell after a random time uniformly distributed in $[0.5, T_{corap}]$ srand $[1, T_{corpap}]$ ms after the previous allocation, respectively. In this way, the probability of cells changing their allocations at the same time reduces, hence enhancing the network coordination.

Moreover, when solving coRPAP, average channel quality estimations in the form of instantaneous $w_{u,k}$ averaged over a time window of 1 s are used to derive $p^m_{u,k,h}$ [68].

The same architecture will be used for auRRAA.

5.5.1 Signalling Overhead

The input data required for our architectures to work are two, DL-HIIs and user CQIs. In case of coRRAA, both of them are needed, while auRRAA only requires user CQIs. Because in standard cellular networks CQIs are regularly fed back from users to cells to assist channel dependent scheduling [27], new signalling overhead incurred by our architectures comes from inter-BS DL-HIIs. Recall that a DL-HII contains 2 items, the power constraint $p^{m,max}_k$ and RB index k.

Assuming that we make use of 10 bits for encoding $p^{m,max}_k$, i.e., 1024 discrete levels, and 7 bits for encoding k (up to 100 RBs), the number of bits needed per DL-HHI is $(10 + 7) \cdot D_u$ bits, being D_u the number of RBs of cell-edge user U^m_u (Section 5.3).

5.6 Simulation and Numerical Results

5.6.1 Scenario

In order to allow performance comparisons with the centralised radio resource management scheme proposed in Chapter 4.2, i.e., eDFP, the same system-level simulation, network scenario and parameter setting than those presented in Section 4.6.1 are used.

5.6.2 Optimisation Performance

5.6.2.1 Solving coRPAP

In order to analyse the performance of network simplex when solving coRPAP, we extracted one million problem instances from simulations of the scenario in Section 4.6.1. The running time[1] of one million coRPAP RB and power allocations in different cells was estimated to be 253.45 s. Therefore, the average running time of network simplex for a single coRPAP RB and power allocation procedure in one cell is around 0.25 ms.

Let us conclude that since coRPAP can be solved faster than the maximum feedback frequency in LTE, i.e. 2 ms [27], it can be used as a way of 'fighting' fading fluctuations.

Note that very similar results were obtained with auRPAP.

5.6.2.2 Solving coRAP

A way to get solutions of the joint MCS, RB and power allocation problem, i.e, coRAP, is to solve formulation (5.5) directly using ILP solvers. Although this method ensures the optimality of the solution, it may take a considerable amount of time to solve this assignment problem in a realistic scenario, thus being unsuitable for online operation.

To compare the performance of our proposed two-level optimisation approach to that of an ILP solver when solving coRAP, we have extracted 100 problem instances from the scenario described in Section 4.6.1. The ILP solver utilised was CPLEX [95] version 9.130, while in case of our two-level optimisation approach the proposed TS and network simplex schemes were utilised.

The average running time of the ILP solver was 456.28 s, while that one of our two-level optimisation approach was 0.51 s. In addition, on average, the total power requirement of the solution provided by our two-level optimisation approach was only 5.34 % higher/worse than the optimal one.

These results show that our two-level optimisation approach provides a significant running time improvement over an ILP solver with only a slight loss in solution quality. Nevertheless, it must be noted that the running time of the entire procedure may change depending on the number of iterations and neighbouring solutions visited by the TS.

[1] It must be noted that the computer utilised for this simulation contained an AMD Opteron 275 dual-core processor running at $2.2\,GHz$ with $16\,GB$ of RAM.

Therefore, the performance of our two-level decomposition approach is subjected to a tradeoff between running time and solution quality that should be tuned by operators.

Note that very similar results were obtained with auRPAP.

5.6.3 Network Performance

5.6.3.1 Techniques Used for Comparison

Because the scenario and settings employed for this network performance evaluation are the same as the ones presented in the previous chapter in Section 4.6.3, results about coRRAA and auRRAA are comparable to all methods presented in Section 4.6.3.1. In the following and for the shake of clarity, only the methods that provided the best performance, i.e., FFRS3-B/Dyn/IM, Ronald's, Hussain's and eDFP, will be displayed. Also, the decentralised approach proposed by Stolyar was included for comparison (Section 2.1.3):

Stolyar's Approach [68]: Its exact implementation is presented in Appendix A.3. However, let us note that this scheme does not divide users into inner- and outer-zones, and is based on a distributed architecture and a dynamic allocation of power to users. Sub-bands[1] in Stolyar's approach correspond to RBs in our implementation. RBs are assigned to users according to a cell power minimisation procedure similar to auRPAP. But, in contrast to our proposed approach, it does not tune the MCS allocated to users and uses frequency hopping within sub-bands, thus the least number of subcarriers in a RB are used to meet users' aimed data rates and permit an efficient frequency hopping.

5.6.3.2 Cell-Centre and Cell-Edge Zones: γ^{edge}

Since only cell-edge users are involved in the cooperative resource allocation procedure presented in Section 5.1.2, if γ^{edge} is too small few users will benefit from cooperation. On the other hand, if γ^{edge} is too large the number of power constraints set in neighbouring cells will be significant, therefore degrading the overall system performance.

Similarly to the procedure introduced in Section 4.6.3.2 of the previous chapter,

[1] In [68], a sub-band was comprised of 16 subcarriers, while in our approach a RB is comprised of 12, so they are similar units in terms of subcarriers.

in order to fine tune γ^{edge}, we run a number of simulations in the proposed scenario. The set-up with 12 users per cell was used

Table 5.1 illustrates that $\gamma^{edge} = 2\,dB$ provides the best network-wide performance. For instance, the number of user outages considerably decreased from 81 to 23 when γ^{edge} was fine tuned from 3.0 dB to 2.0 dB. (This result is inline with Section 4.6.3.2).

In the following simulations, the cell-centre and cell-edge boundary γ^{edge} is set to 2 dB.

Table 5.1: Network Performance vs. γ^{edge}

γ^{edge} [dB]	0	0.5	1.0	1.5	2.0	2.5	3.0
User outage	60	48	33	32	**23**	53	81
Connected users	243.55	243.85	246.26	246.38	**247.24**	244.34	240.62
Network throughput [Mbps]	54.71	54.94	55.94	56.47	**58.29**	54.66	54.13

5.6.3.3 Subroutine Updating Frequency: T_{corpap} and T_{aurpap}

In this section, we investigate the impact in network performance of the updating frequency of coRPAP and auRPAP, i.e., the subroutine able to compute optimum RB and power allocations given an MCS assignment.

Recall that coRPAP (auRPAP) allocations occur in each cell after a random time uniformly distributed within $[1,T_{corpap}]$ ms ($[1,T_{aurpap}]$ ms) after the previous allocation. Tables 5.2 and 5.3 show that increasing T_{corpap} (T_{aurpap}) degrades system performance, since the RB and power allocation to users is updated less often. When using coRRAA, using T_{corpap} =500 ms already provided the best performance, while a more frequent update was necessary using auRRAA to obtain the best result, T_{aurpap} =100 ms. coRPAP requires less often updates because it provides a better system stability through DL HHI-based inter-BS coordination. On the contrary, auRPAP requires more often updates to find an efficient solution via a fully decentralised optimisation.

Let us note that because no fast fading was simulated, network performance was not significantly affected by less frequent updates. In Chapter 7, it will be shown that fast RB and power updates are necessary to cope with fast-fading when user mobility is considered.

Table 5.2: coRPAP frequency (Inter-BS distance 500m).

Cell load	RPAP freq.	50 ms	100 ms	500 ms	750 ms	No RPAP
12 users/macro 100 % load	Outage	23(1.31 %)	23(1.31 %)	23(1.31 %)	29(1.31 %)	34(1.31 %)
	Users	247.24	247.24	247.24	245.67	243.98
	Mbps	58.29	58.29	58.29	57.02	55.92

Table 5.3: auRPAP frequency (Inter-BS distance 500m).

Cell load	RPAP freq.	50 ms	100 ms	500 ms	750 ms	No RPAP
12 users/macro 100 % load	Outage	82 (4.66 %)	82 (4.66 %)	92 (5.23 %)	108 (6.14 %)	118 (6.71 %)
	Users	241.07	241.07	238.01	233.98	230.75
	Mbps	54.46	54.46	53.22	52.21	51.01

According to these results, when running auRRAA, each cell independently solves auRPAP after a random time interval uniformly distributed in [1,100] ms after its previous auRPAP updating event. In addition, each cell solves auRAP after a random time interval uniformly distributed in [0.5,1] s after its previous auRAP updating event. The same configuration will be utilised for coRRAA for a fair comparison.

5.6.3.4 Transmit Power

Figure 5.2 shows the Cumulative Distribution Function (CDF) of the power allocated to subcarriers along the simulation. When using reuse schemes the transmit power applied to RBs is fixed and does not vary according to interference or load fluctuations. On the contrary, when using coRRAA not only the power applied to each RB changes depending on such conditions, but becomes much smaller. Like this, interference to neighbouring cells is mitigated. Note that the performances of coRRAA and auRRAA are similar to that of the centralised architecture presented in Chapter 4.2, i.e., eDFP.

Because eDFP results in less user outages and therefore in a larger cell user load, it uses slightly more power than coRRAA to deal with the larger inter-cell interference. The reason why coRRAA applies more transmit power than auRRAA is the same. Details on network performance in terms of user outages are given in Section 5.6.3.7.

On the other hand, Stolyar's approach uses more transmit power per subcarrier because its objective was to allocate as less subcarriers as possible within a given RB

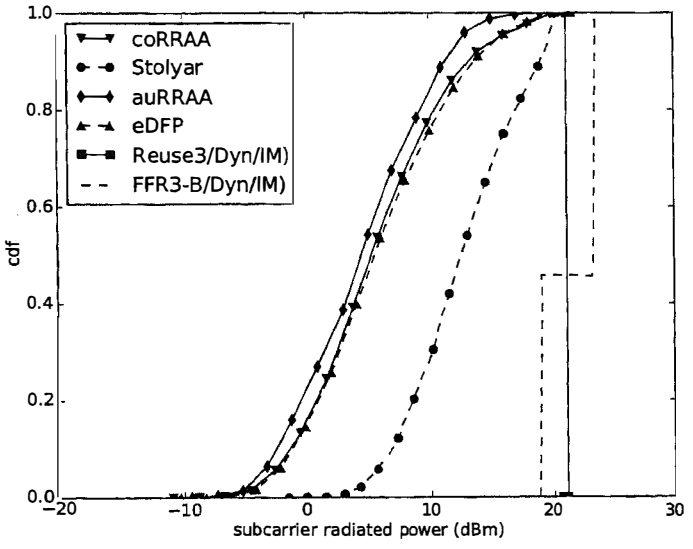

Figure 5.2: CDF of the radiated power per subcarrier during the simulation in the 12 user/sector scenario.

in order to satisfy user throughput demands, hence allocating larger MCSs and power.

5.6.3.5 Inter-Cell Interference

Figure 5.3 corroborates what has been stated in the previous sections: minimising total transmit power in every cell mitigates inter-cell interference towards neighbouring cells. Figure 5.3 illustrates that the inter-cell interference suffered by subcarriers decreases when using the proposed coRRAA and auRRAA in comparison to the other approaches. This inter-cell interference reduction is specially significant with respect to FFRS3, specifically a median reduction of 10 dB. Contrarily, reuse 3 supplies the best inter-cell interference mitigation at the expense of thinning cell bandwidth by a factor of 3. Following subsections show that this has a negative impact on network performance.

Since eDFP results in a larger traffic load because it results in less user outages, inter-cell interference is slightly larger in the eDFP case than in the coRRAA case. The reason why coRRAA suffers from more interference than auRRAA is the same. Details on network performance in terms of user outages are given in Section 5.6.3.7.

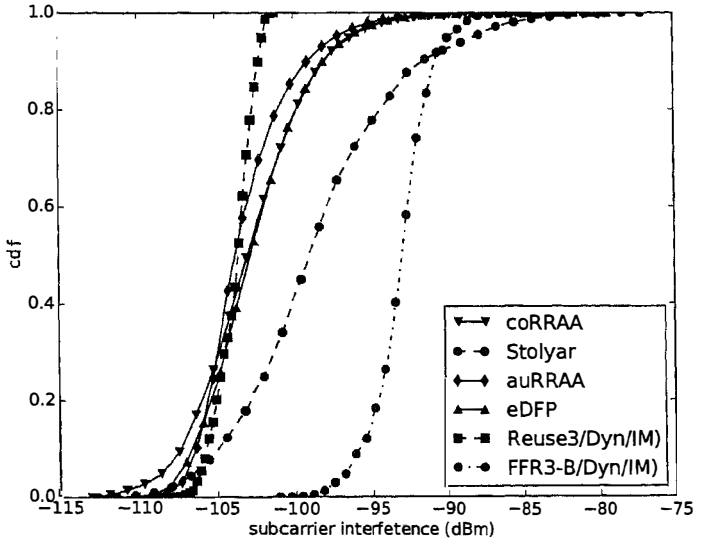

Figure 5.3: CDF of the interference suffered per subcarrier during the simulation in the 12 user/sector scenario.

On the other hand, note that frequency hopping in Stolyar's approach does not efficiently deal with inter-cell interference. This is because the throughput target and cell load are high and 12 subcarriers per RB does not provide enough 'space' for hopping.

5.6.3.6 Resource Block Allocation

In order to illustrate the resource allocation bases of coRRAA, Figures 5.4 and 5.5 depict the power applied by 3 neighbouring cells to each RB at a given time instant. In Figure 5.5, 12 users per cell were deployed, while in Figure 5.5, only 6 users per cell. In both cases, inter-BS distances were 500 m.

Note that inter-cell interference avoidance is not only provided by the reduction of transmit power applied to each RB, but also because when targeting at minimising transmit power in all base stations, the system settles into an RB allocation pattern that provides inter-cell interference avoidance. This result is in line with that of [68]. It can be observed from both figures that the proposed coRRAA obtains an efficient frequency planning, while achieving a frequency reuse of 1 in the 3 cells. In this case,

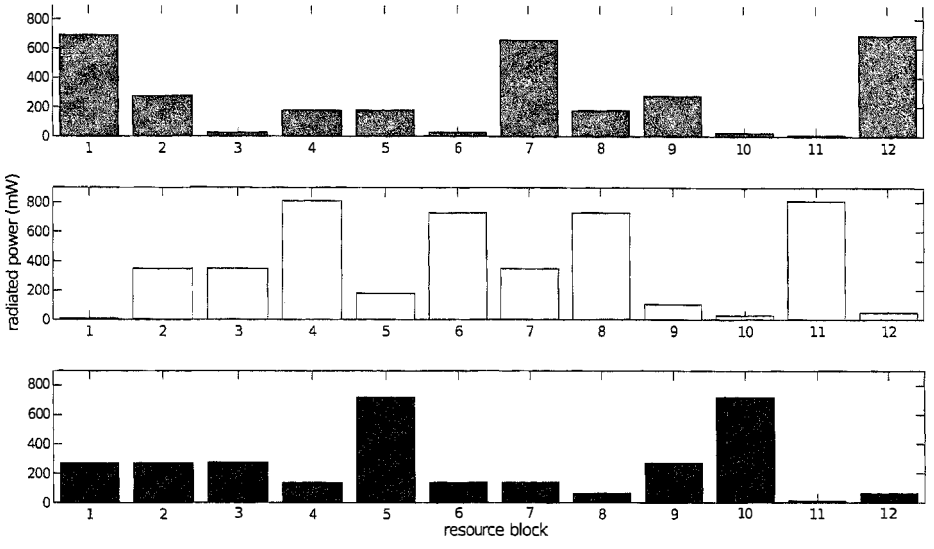

Figure 5.4: RB allocation of three neighbouring sectors with 6 users each.

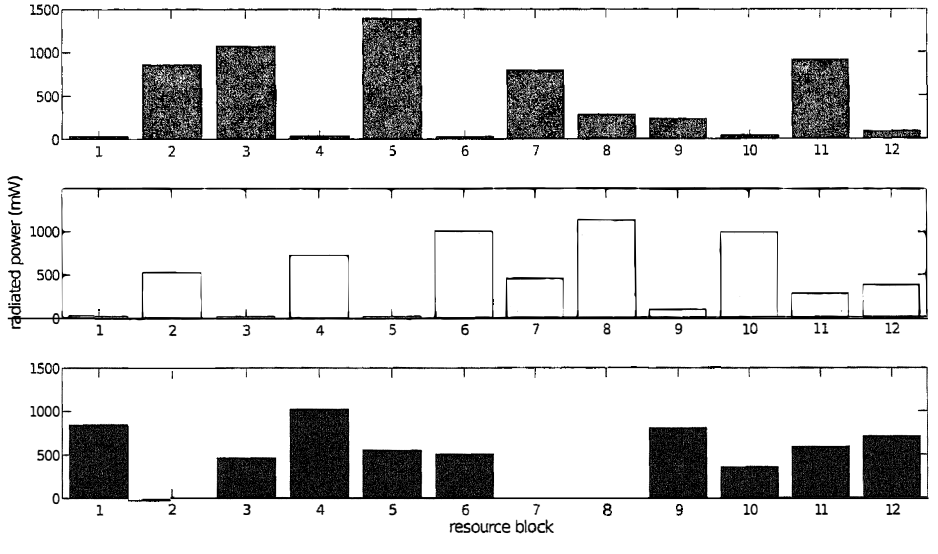

Figure 5.5: RB allocation of three neighbouring sectors with 12 users each.

we can see that cells tend to allocate their cell-edge users with large powers in those RBs in which neighbouring cells allocate their cell-centre users with low transmit powers. In this way, users connected to different cells can coexist making use of the same RB, while meeting their throughput requirements.

Also, note that the average transmit power increases from Figures 5.4 to Figure 5.5. This is because the more users in the network, the larger transmit power is required by cells to overcome the more challenging inter-cell interference conditions in the network.

The same logic also applies to auRRAA.

5.6.3.7 System-Level Performance

Table 5.4: System-level simulation results (Inter-BS distance 500m).

Scheme	KPI	FFRS3-B Dynamic IM	Ronald Approach	Hussain Approach	Stolyar Approach	auRRAA	coRRAA	eDFP
3 users/cell, 25% traffic load	Outage	0 (0.00%)	28 (6.36%)	0 (0.00%)	0 (0.00%)	0 (0.00%)	0 (0.00%)	0 (0%)
	Users	63	57.47	63	63	63	63	63
	Mbps	15.73	14.02	14.74	14.74	14.74	14.74	14.74
6 users/cell, 50% traffic load	Outage	16 (1.92%)	132 (15.83%)	58 (6.95%)	1 (0.12%)	0 (0%)	0 (0%)	0 (0%)
	Users	124.63	102.24	116.32	125.87	126	126	126
	Mbps	30.84	24.84	28.36	30.96	31.15	31.35	31.46
9 users/cell, 75% traffic load	Outage	117 (10.00%)	302 (25.81%)	235 (20.09%)	34 (2.91%)	23 (2.05%)	13 (1.11%)	0 (0%)
	Users	165.91	138.34	149.77	182.74	185.29	187.46	189
	Mbps	40.89	33.55	36.29	41.77	43.47	45.30	46.50
12 users/cell, 100% traffic load	Outage	337 (19.17%)	516 (29.35%)	411 (23.38%)	295 (16.78%)	82 (4.66%)	23(1.31%)	7 (0.40%)
	Users	198.95	176.81	194.56	211.69	241.07	247.24	249.61
	Mbps	48.43	42.88	47.00	49.00	54.46	58.29	59.17

Table 5.4 illustrates the network performance when making use of coRRAA, auRRAA and the presented schemes in terms of outages, average number of network connected users and average network throughput. Note that 12 RBs were available and that 3, 6, 9 or 12 users attempted to connect per cell, representing a 25 %, 50 %, 75 % and 100 % cell user load of its maximum, respectively. The distance among BSs was set to 500m. In these tables, columns denote proposed approaches, e.g., coRRAA, auRRAA, eDFP, while rows represent the user load of cells.

We can see that network performance follows the same trend for all cell user loads. being eDFP the best performing approach. But, when the number of users increased, the number of user outages also increased because of the larger inter-cell interference.

Nevertheless, our decentralised schemes, i.e., coRRAA and auRRAA, provided the second and third best performance, respectively, being not far from that of eDFP. Specifically, the performance improvement of eDFP over coRRAA was of 2.37 average connected users and 0.88 Mbps (1.51 %), whereas over auRRAA was of 8.54 average connected users and 4.71 Mbps (8.64 %).

coRRAA provided a significant improvement in network performance over all methods used for comparison. Specifically, coRRAA gave an average performance improvement over FFRS3-B of 48.29 connected users and 9.86 Mbps (20.36%). The average performance improvement over Stolyar's approach was about 35.55 connected users and 9.28 Mbps (18.96%). Enhancements were measured over the 12 user per cell case.

auRRAA also provided a large improvement in network performance over all methods used for comparison. Specifically, auRRAA gave an average performance improvement over FFRS3-B of 42.12 connected users and 6.03 Mbps (12.45%). The average performance improvement over Stolyar's approach was about 29.38 connected users and 5.46 Mbps (11.14%). Enhancements were measured over the 12 user per cell case.

The reason why coRRAA outperformed auRRAA is because the cooperation provided by our DL-HHI based approach introduces stability throughout the network. When new users with bad geometry appear in the network, they are allocated to RBs that suffer from low interference due to cell cooperation. This cooperation aids to converge to stable solutions. On the contrary, when using auRRAA, it may take some time to reach a new efficient radio resource assignment over decentralised optimisation. Since eDFP provides a better coordination between cells due to its centralised nature, eDFP outperformed coRRAA and auRRAA.

Because centralised architectures such as eDFP rely on a low latency communication among all BSs and a central resource broker, and involve a larger signalling overhead they may be difficult to implement or deploy. On the contrary, decentralised schemes allow for plug-and-play roll-outs of eNodeBs and thus for reduced CAPEX and OPEX. Since coRAA and auRRAA result in a network performance not far form that of eDFP, our decentralised solutions may thus have a larger added-value than centralised ones. In particular, auRRAA may be very useful in scenarios were inter-BS coordination is not feasible due to unreliable back-haul or inter-BS interfaces, e.g., femtocell networks.

Stolyar's, coRRAA, auRRAA and eDFP outperformed all other schemes because they allow all cells to allocate all available RBs to their users in an intelligent manner:

Table 5.5: System-level simulation results (Inter-BS distance 1000m).

Scheme	KPI	FFRS3-B Dynamic IM	Ronald Approach	Hussain Approach	Stolyar Approach	auRRAA	coRRAA	eDFP
12 users/cell,	Outage	242 (13.77%)	399 (22.69%)	326 (18.59%)	136 (7.74%)	69(3.92%)	38(1.31%)	13 (0.74%)
100% traffic	Users	215.75	192.40	204.48	229.27	57.03	59.63	248.78
load	*Mbps*	52.49	46.98	49.13	53.03	243.10	245.30	61.85

Cells minimise transmit power and hence assign less power to those RBs allocated to users having good geometries or with lower demands, therefore neighbouring cells will 'see' low interference in such RBs and will allocate them to their bad geometry users. This kind of spatial reuse is not possible by making use of uniform power distributions when all network cells are highly loaded.

Stolyar's approach gave a good performance for the scenario with 9 users per cell, but the number of outages significantly increased when fully loading the network. Nevertheless, coRRA and auRRA were able to handle this traffic load growth better due to its interference avoidance properties. The reasons why they performed better than Stolyar's approach are:

- Due to the use of the mentioned DL-HII based inter-BS cooperation.
- They do not use frequency hopping.

  Assigning the least number of subcarriers within a RB, which involves assigning larger MCSs and hence power, to improve the efficiency of frequency hopping increases interference compared to solutions in which all subcarriers of a RB are modulated with the least possible MCS and power.

  Frequency hopping losses performance when network load and user throughput demands are large, i.e, when the number of subcarriers used in the serving and the interfering cells is large.
  Also, because when the least number of subcarriers is used to meet user demands, if one of them fails to provide its contribution to achieve the user throughput aim, users may suffer from service disruption. But, if all subcarriers of a RB are used, the communication is more robust because of the use of lower-order MCS and there may be a sort of bit rate back up.

Table 5.5 shows the network performance of coRRAA, auRRAA and above ap-

proaches in terms of outages, average number of network connected users and average network throughput. In this case, 12 user terminals attempted to connect per cell and the distance between neighbouring BSs was set to 1000 m. The increase in cell radius decreased inter-cell interference. Consequently, for almost all techniques considered, outages reduced and system capacity in terms of both average network connected users and average network throughout improved.

For coRRAA, because the number of outages was low in Table 4.8, increased user path losses had a larger impact in terms of outages at cell-edges than reduced inter-cell interference, hence increasing users outages very slightly from 23 to 38 occurrences. Nevertheless, because of the mentioned reduced inter-cell interference, in this case, the average network throughput increased with cell radius from 58.29 to 59.63 Mbps.

5.6.3.8 Signalling Overhead

In this section, the signalling overhead incurred by coRRAA due to DL-HII is analysed. Let us recall that every DL-HII contains two items, transmit power constraint $p_k^{m,max}$ and the index of its RB k. Assuming that 4 bits are utilised to encode k (12 RBs), the number of bits needed per exchanged DL-HII is $(4 + 10)\cdot D_u$ bits according to discussions in Section 5.5.1. Furthermore, let us note that according to our simulations, an average of 12.29, 18.18 and 24.28 DL-HIIs per second where sent per cell for the 6, 9 and 12 users per cell cases, respectively. Therefore, for these three distinct scenarios, the X2 bit rate required was in average of 0.4916, 0.7272 and 0.9212 kbps, respectively. As a result, it can be concluded that a small fraction of the available X2 bandwidth is needed for coRRAA signalling overhead.

5.7 Conclusions

In OFDMA literature, dynamic subcarrier assignments with equal power per subcarrier are usually preferred to complex joint subcarrier and power assignments due to mathematical tractability and easier implementation. Traditional wisdom assumes that capacity improvement due to the allocation of different powers to different subcarriers is low in scenarios with a wide range of users with diverse signal quality requirements. In this chapter, we have shown that this is not the case in realistic deployments with a limited user number, and that performance can be improved by allocating different

transmit powers to different RBs according to user throughput demands and positions.

This chapter has researched the joint allocation of MCS, RB and power to users in OFDMA networks. A new resource allocation model subjected to LTE constraints has been presented where cells independently allocate resources to users so that their total transmit powers are minimised while meeting their users demands. Also, a reduced-complexity approach has been devised to solve the intricate resource allocation problem. Based on the proposed assignment model, 2 network architectures have been proposed. In the first one, DL-HII are exchanged among cells to enhance interference coordination, whereas in the second one, cells operate based only on local knowledge of RB usage in neighbouring cells fed back by their users.

Conclusion 1: The implementation of a power controlled resource allocation scheme that minimises transmit power at each cell is the key to allow a better spatial reuse. Minimising transmit power independently at each cell reduces interference in those RBs allocated to users with good channel conditions or low throughput requirements, hence generating RB allocation opportunities that may be used by neighbouring cells for their cell-edge users.

Conclusion 2: The use of inter-BS coordination via DL-HIIs (coRRAA) has been shown to improve inter-cell interference mitigation with respect to a fully distributed operation (auRRAA). This inter-cell interference mitigation enhancement has been translated into an average network throughput improvement of 7 % and a significant reduction of the number of user outages. Also, the performances of the proposed decentralised architectures are not far from that of centralised ones such as eDFP, and even outperform some other proposed in literature, e.g., Ronald's, Hussain's schemes. Moreover, only a very small fraction of available back-haul or X2 interface bandwidth is required to carry signalling, i.e., DL-HIIs.

Conclusion 3: Simulations have shown that the proposed algorithms significantly improve network capacity with respect to a variety of allocation schemes in literature. coRRAA and auRRAA provided a performance improvement of 19 % and 11 % in terms of network throughput over cutting-edge techniques such as Stolyar's approach, while also dealing with fully loaded networks.

Conclusion 4: In real cellular networks, the problem of the joint allocation of MCS, RB and power to users becomes complex and cannot be solved using ILP solvers. On the contrary, the proposed two-level optimisation scheme based on TS and network simplex has been proved to be able to obtain well-performing solutions of this problem within affordable times.

Chapter 6

Radio Resource Management for Femtocells: Co-Tier Interference

Co-tier interference[1] among femtocells is described as the unwanted signal received at a femtocell because of the simultaneous transmissions of other surrounding femtocells. The term co-tier refers to the fact that all femtocells belong to the same network tier. This problem is thus independent of the disruption caused by/to the macrocell tier.

In the DownLink (DL), co-tier interference occurs when a given femtocell user is located in an area where the signal coming from its own femtocell is not strong enough with respect to the sum of the interference coming from its neighbouring femtocells. Nevertheless, Orthogonal Frequency Division Multiple Access (OFDMA) femtocells[2] can avoid co-tier interference by a proper allocation of frequency resources among users. For instance, two femtocell users could be located at the same geographical position and only one of them suffer from co-tier interference due to subchannel assignment. In order to depict this, Figure 6.1 shows an example situation where there are two users U_1^1 and U_2^1 connected to femtocell F_1 and one user U_1^2 connected to femtocell F_2. Femtocell F_1 has allocated subchannel 1 and 5 to its users U_1^1 and U_2^1, respectively. Meanwhile, user U_1^2 has been unfortunately allocated to subchannel 1 by femtocell F_2. As a result, user U_1^1 and U_1^2 interfere with each other and their services are disrupted,

[1] An extensive introduction and literature review about the state-of-the-art with regard to interference mitigation in femtocell scenarios is given in Section 1.4 and Section 2.2.

[2] In this chapter, when we refer to OFDMA femtocells, we refer to both Long Term Evolution (LTE) and Wireless Interoperability for Microwave Access (WiMAX) femtocells.

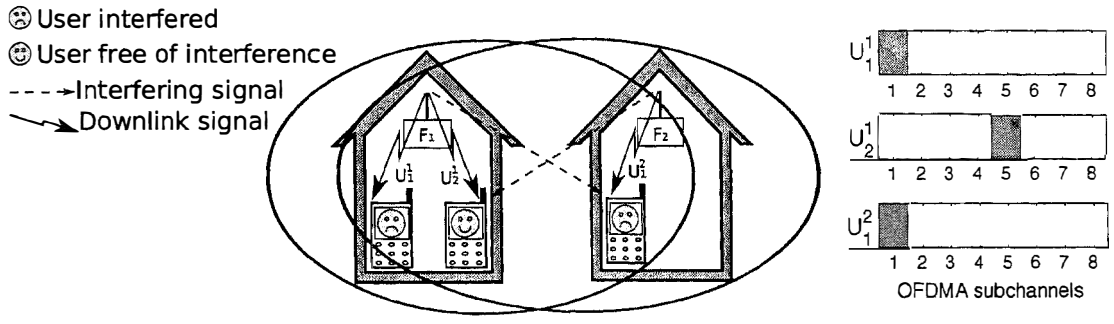

Figure 6.1: Co-layer downlink interference in an OFDMA femtocells network.

while user U_2^1 enjoys a good signal quality because subchannel 5 is free of interference.

Because the deployment of femtocells is user driven, it is very likely that several femtocells are installed in close locations. For instance, horizontally in terraces of adjacent houses or vertically in blocks of apartments, thus interfering one another. Furthermore, co-tier interference may also occur between immediate neighbouring femtocells due to low isolation of walls or windows between houses or apartments. Nevertheless, the most challenging case of co-tier interference takes place in enterprise and outdoor public femtocell deployments, e.g., offices, airport halls or train stations. In this case, a femtocell deployment could be very dense and sometimes there could be no isolation at all between femtocells.

Subchannel allocation is thus a key technology for successfully deploying femtocells. Nevertheless and due to the individualistic nature of Femtocell Access Points (FAPs), good femtocell resource allocations highly depend on their self-organising capabilities. In this chapter, we research the potential of applying the decentralised radio resource management architectures proposed in the previous chapter, i.e., cooperative Radio Resource Allocation Architecture (coRRAA) and autonomous Radio Resource Allocation Architecture (auRRAA), to femtocell scenarios in order to reduce co-tier interference. Motivation for the use of these two novel resource allocation architectures in FAPs steams from the fact that they involve a few or no signalling between base stations, therefore providing a practical approach to femtocell inter-cell interference mitigation. In particular, auRRAA may be specially useful due to its fully distributed nature, which may allow femtocells to self-organise into efficient resource allocation patterns independently of delay issues that may arise in femtocell user-provided back-hauls [108].

Let us note that in this chapter the nomenclature of WiMAX networks is utilised, and that without loss of generality with respect to our approach, we focus on the DL.

6.1 Radio Resource Management Issues in Femtocell Scenarios

Due to their user-deployed nature and user-provided Internet Protocol (IP) back-haul, femtocells can not rely on traditional Fractional Frequency Reuse Schemes (FFRSs) or centralised architectures to provide inter-cell interference mitigation (Section 1.4), but they still need to be aware of the presence of neighbouring cells and their spectrum and power allocations to perform optimal or at least good resource assignments that minimise cross- and co-tier interference. Thus, other schemes have been proposed to achieve this cognitive radio stage, in which each femtocell is able to learn by itself about the structure and behaviour of the network, traffic and channel conditions [37].

In this section, the main advantages and disadvantages of the most representative channel monitoring methods proposed in femtocell literature are summarised [16] [18]. Methods proposed in the following section for performance comparison with auRRAA and coRRAA will be based on such bases.

6.1.1 Network Listening Mode

A sensing or monitoring capability may be implemented in the femtocell device itself. In this way, a femtocell will be able to scan the air interface, detect neighbouring cells and tune its network and Radio Frequency (RF) parameters accordingly to this data.

The implementation of a network listening mode or sniffer is essential for automatising the tasks of network planning and optimisation within a femtocell network. Using this functionality, femtocells will periodically switch on their sniffers to check network settings, synchronisation and interference conditions [109].

Similarlyi, the information collected through sniffing can also be used in order to discover surrounding Base Stations (BSs)i identify the operator to which they belong, learn if they are macro BSs or femto BSs and also estimate their path losses to them.

Moreover, femtocells can also use their statistics (failed handover ratio, dropped

call ratio, uplink interference) in order to assess their own and other cell performances and trigger different configuration and/or optimisation procedures.

6.1.2 Message Passing

Femtocells could broadcast information messages that will be received by their neighbouring femtocells containing some interference measurements, e.g., interference power, or information related to the power and/or subchannel allocation of the broadcaster. In this way, a femtocell will be aware of the present actions and future intentions of its neighbouring femtocells, and thus they could act in a cooperative manner (Figure 6.2).

These messages can be exchanged over existing interfaces or over new ones:

- Femtocells may exchange these messages through the femtocell gateway [110].

  The source femtocell would send its message to the femtocell gateway, and the femtocell gateway would forward this message to the target femtocell/femtocells.

- Another solution is to establish a new link/interface between femtocells [110].

  This alternative has similarities to the X2 interface defined in LTE to allow communication between eNodeBs, but is not extended yet to femtocells [111].

Nevertheless, these two techniques, network listening mode and message passing, are limited by the coverage areas of femtocells. For example, if two femtocells are not in the range of one another, they will not be able to notice the presence of each other or exchange messages between them. As a result, these femtocells will not be able to coordinate their subchannel/power resource assignments, and users located in between cell-edges of these two overlapping cells will suffer from a large inter-cell interference. This special scenario is shown in Figure 6.3, and is known as *hidden femtocell* problem.

6.1.3 User Measurements

In order to solve the problem of hidden femtocells, measurements performed by user terminals and reported to femtocells can be utilised. In this way, a user in between two overlapping femtocells can indicate to its server the presence of neighbouring femtocells, and also their actions with regard to frequency and power assignments (Figure 6.4).

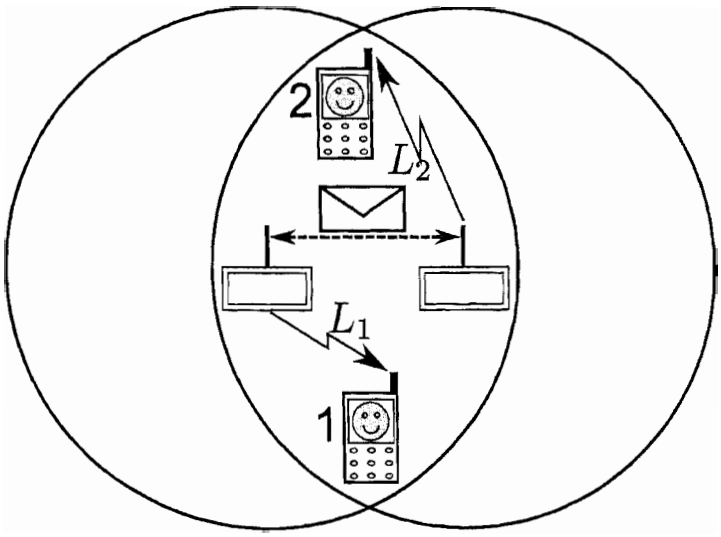

Figure 6.2: Message exchange.

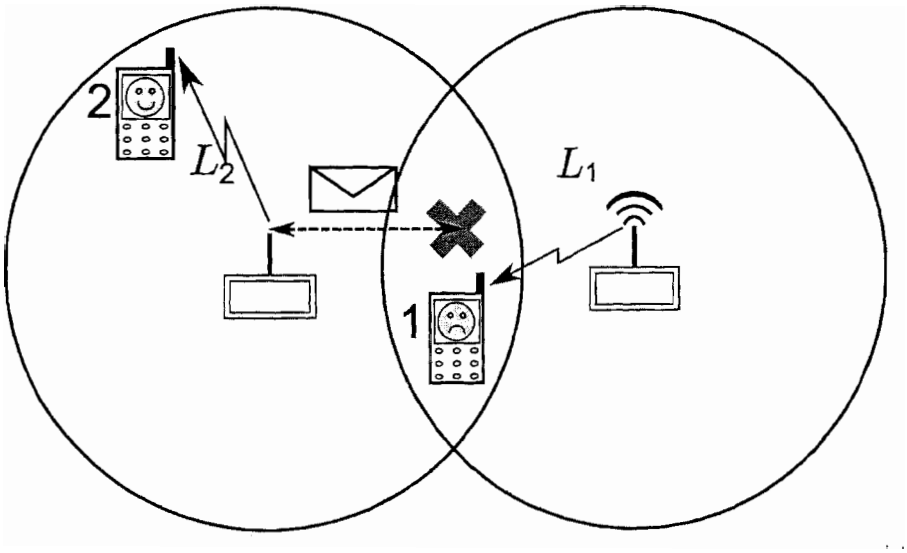

Figure 6.3: Hidden femtocell problem.

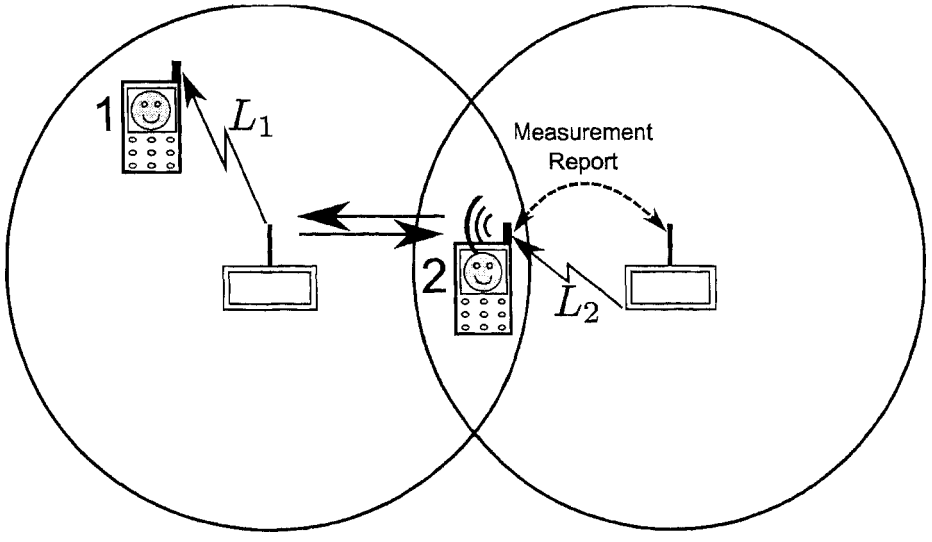

Figure 6.4: Measurement report.

These measurements are very useful because they provide information collected at user environments. Contrarily to the information collected by network listening mode or message passing, the information provided by user measurements help to assess the varying channel conditions at user locations, the ones who suffer from DL interference.

Figure 6.5 illustrates how the interference conditions of two subscribers of the same femtocell can vary according to their locations and surroundings. Users close to the femtocell will enjoy good signal qualities, while users located in opposite rooms far from their femtocells and close to neighbouring ones will suffer from a large interference.

6.2 coRRAA and auRRAA

As it was indicated earlier, in this chapter, we investigate the potential of applying the decentralised radio resource management architectures proposed in Chapter 5, i.e., auRRAA and coRRAA, to femtocell deployments to mitigate co-tier interference.

Let us briefly recall that:

- When using auRRAA, cells independently allocate resources to users based on Channel Quality Indicators (CQIs) fed back by its users.

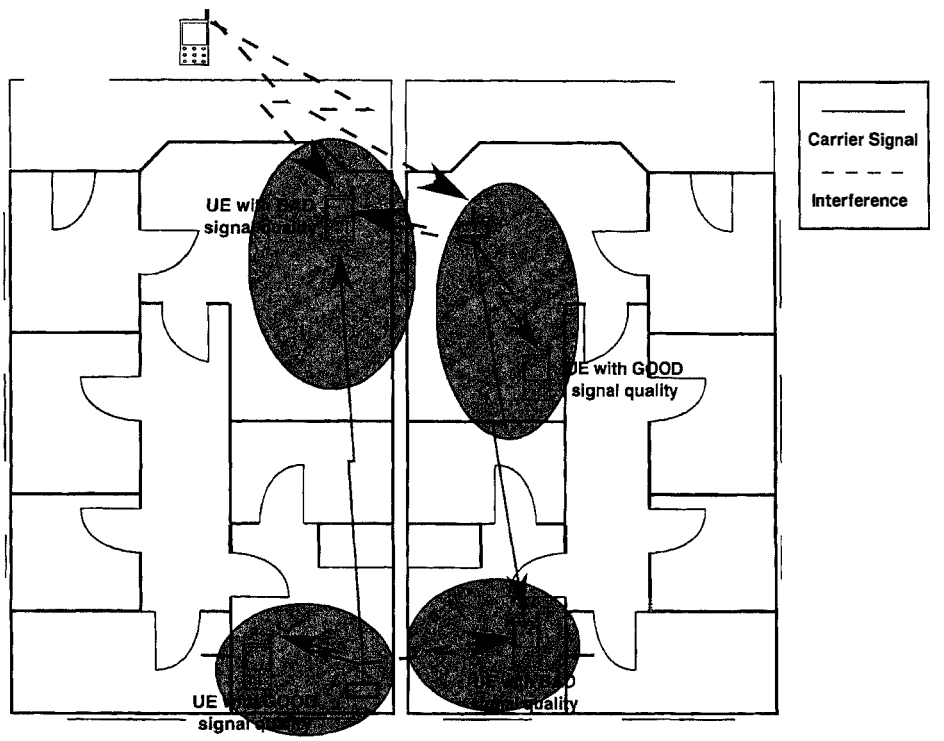

Figure 6.5: Users with different channel conditions within the same femtocell coverage.

- When using coRRAA, cells additionally are able to exchange information through a message passing technique to coordinate assignments.

In both cases, Modulation and Coding Schemes (MCSs) are assigned to users in a hundreds of frame basis by solving Resource Allocation Problem (xxRAP)[1](Section 5.4), whereas subchannels and power are allocated to users in a much more frequent basis, milliseconds basis, by solving RB and Power Allocation Problem (xxRPAP)(Section 5.3). Note that xxRPAP was solved making use of a minimum cost network flow approach, while xxRAP was solved using a combination of both Tabu Search (TS) and xxRPAP.

In coRRAA, control information is only exchanged among neighbouring femtocells, hence involving a few signalling overhead and also avoiding single points of failure. In this way, this decentralised architecture is more scalable than a centralised one, in which all network cells communicate periodically with a centralised resource broker.

In this chapter, exactly the same implementation of auRRAA and coRRAA is used, so refer to Chapter 5 for more information, but TS has been replaced for an heuristic able to obtain optimal solutions of xxRAP.

Let us recall that the target of xxRAP is to obtain an MCS assignment with its associated optimal subchannel and power allocation that minimises transmit power, and that a solution ρ consists of an MCS assignment to every user of femtocell F_f.

In this approach, the MCS h of every user U_u^f of cell F_f is selected according to a new heuristic rule, building a given MCS solution ρ. Thereafter, by solving xxRPAP, the optimal subchannel and power allocation related to this MCS assignment is found. Afterward, the quality of MCS assignment ρ is evaluated according to the cost value $f(\rho)$ of this optimal subchannel and power allocation obtained by xxRPAP, i.e., (5.5a*). Using this method, an exhaustive search can be used to find the MCS allocation that yields the lowest transmit power, i.e., minimum $f(\rho)$, safely excluding some MCS allocations from the search to accelerate it:

- If an MCS h_{max} can be obtained, which can satisfy the throughput demand TP_u^{req} of user U_u^f by using 1 subchannel, no higher-order MCSs are allocated to user U_u^f since allocating higher-order MCSs would unnecessarily increase transmit power.

- If an MCS allocation ρ is found, which requires more subchannels than there are available to satisfy the throughput demand of users, no other MCS allocation ρ'

[1]For the sake of simplicity, *xx* stands for autonomous in auRRAA or for cooperative in coRRAA.

that can be derived from ρ by lowering the selected MCS of a single user is tried. This is because $\rho\prime$ would also require more subchannels than there are available.

This heuristic solves xxRAP optimally and sufficiently fast due to the low number of connected users per femtocell and the speed of network simplex for solving xxRPAP.

6.3 Femtocell Radio Resource Management Techniques Proposed for Performance Comparison

In this section, two different approaches to the radio resource management of femtocells are presented, which will be used in the following section for performance comparison. Let us note that these methods were presented by the author of this thesis in [112]. The first one is based on a central sensing performed at the femtocell and referred to as *Network Listening Mode-based method*, whereas the second one is based on user CQIs and an Interference Minimisation (IM) process, and referred to as *IM-based method*. Since both methods uniformly distribute femtocell transmit power among subcarriers, and because the interference conditions in each subchannel may be assessed via CQIs, user MCSs are selected according to its Signal to Interference plus Noise Ratio (SINR). Furthermore, the number of subchannels D_u required to meet user U_u^f's throughput demand T_u^{req} can be calculated using (5.6).

6.3.1 Network Listening Mode-Based Method

In this approach, femtocells regularly switch on its network listening mode in order to check their inter-cell interference conditions and tune their resource assignments. In more detail, femtocell F_f frequently switches on its network listening mode and estimates the power $w_{f,k}$ of the inter-cell interference in every subchannel $k \in \mathcal{K}$. Thereafter, femtocell F_f reassigns its set of connected users $\mathcal{U}^f$ to those subchannels having the lowest inter-cell interference $w_{f,k}$.

This update event occurs in each femtocell after a time interval uniformly distributed in $[1, T^f_{NLM,up}]$ time units after its last update. In this way, the probability of several femtocells changing their subchannel allocations at the same time is reduced.

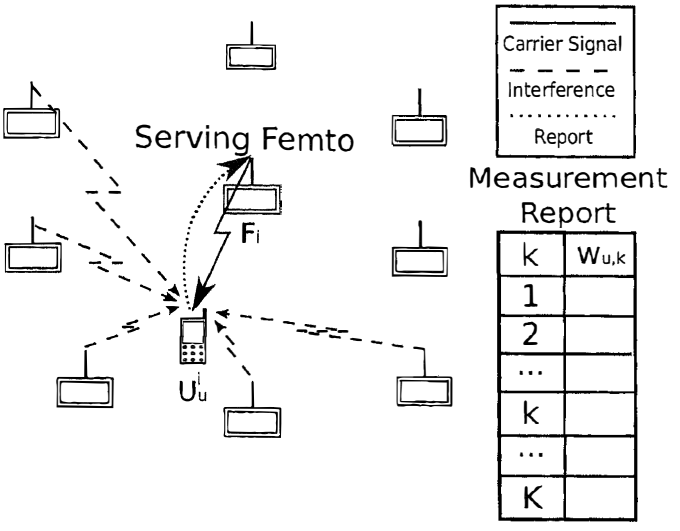

Figure 6.6: Diagram of the measurement report based method.

6.3.2 IM-Based Method

In this approach, user U_u^f sends regularly T_{cqi} a CQI, CQI_u, to its serving femtocell F_f. CQI_u depicts the power $w_{u,k}$ of the interference suffered by user U_u^f in all subchannels $\mathcal{K}$. Meanwhile, femtocell F_f frequently updates its subchannel assignment according to CQIs received from its users using the optimisation method presented in the following. Figure 6.6 depicts the idea of this approach and the structure of a CQI (Section 3.11).

In order to avoid frequent changes in the radio resource allocations of femtocells, they do not update their subchannel assignments every time they receive a CQI. However, they perform it on a regular basis. The time between consecutive updates of the resource allocation of a femtocell is uniformly distributed in $[1,T_{IM,up}^f]$ time units. This is done in order to prevent oscillation, i.e., several femtocell making changes in their resource allocations at the same time.

When an optimisation of the resource allocation is triggered in a femtocell, e.g., F_f, first of all, femtocell F_f gathers and processes the information fed back by its users via CQIs and builds interference matrix Ψ_f (6.1), where each element $w_{u,k}$ of Ψ_f indicates the power of the inter-cell interference suffered by user U_u^f in every subchannel $k \in \mathcal{K}$. The dimensions of Ψ_f are $U_f \times K$, where U_f is the number of users of femtocell F_f and K is the total number of subchannels.

$$\Psi_f = \begin{pmatrix} w_{1,1} & w_{1,2} & \cdots & w_{1,K} \\ w_{2,1} & w_{2,2} & \cdots & w_{2,K} \\ \vdots & \vdots & \ddots & \vdots \\ w_{U_f,1} & w_{U_f,2} & \cdots & w_{U_f,K} \end{pmatrix} \tag{6.1}$$

Once the interference matrix Ψ_f is built, F_f computes is new subchannel allocation using the following optimisation procedure, whose target is to minimise the sum of the inter-cell interference suffered by all its connected users in a non-cooperative manner. A cell targeted to minimise the inter-cell interference suffered by its users tends to choosing subchannels for transmission that are not being utilised by neighbouring cells.

$$\min_{\phi_{u,k}} \sum_{u=1}^{U_f} \sum_{k=1}^{K} w_{u,k} \cdot \phi_{u,k} \tag{6.2a}$$

subject to:

$$\sum_{u=1}^{U_f} \phi_{u,k} \leq 1 \qquad \forall k \tag{6.2b}$$

$$\sum_{k=1}^{K} \phi_{u,k} = D_u \qquad \forall u \tag{6.2c}$$

$$\phi_{u,k} \in \{0, 1\} \qquad \forall u, k \tag{6.2d}$$

where

- $\phi_{u,k}$ is a binary variable (6.2d) that is equal to 1 if user U_u^f is using subchannel k, or 0 otherwise.
- Constraint (6.2b) ensures that subchannel k is allocated to at most one user U_u^f.
- Constraint (6.2c) guarantees that each user U_u^f is allocated to exactly D_u RBs.

This problem is solved using the network simplex scheme proposed in Section 5.3.1. However, instead of minimising transmit power, we minimise inter-cell interference. The edge set in *Remark 3* should be utilised, because femtocells operate independently.

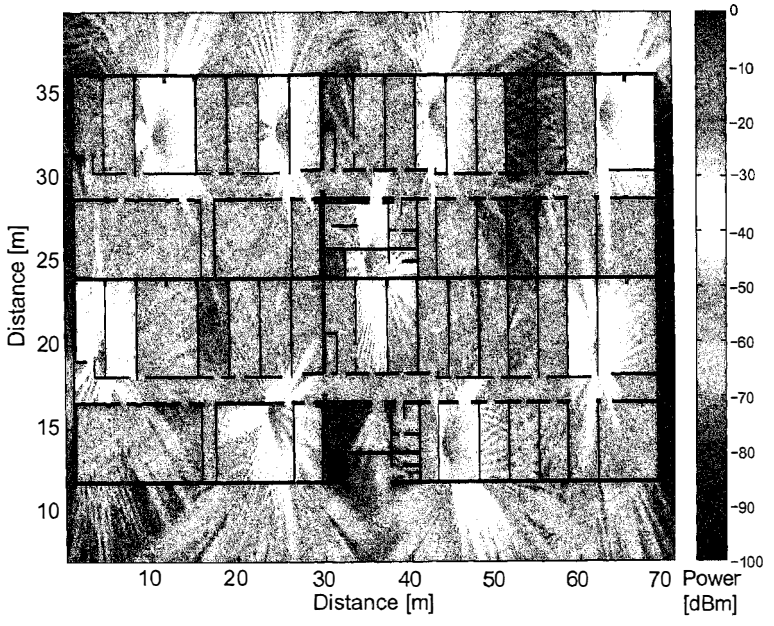

Figure 6.7: Office scenario with 9 femtocells: Coverage.

6.4 Simulation and Numerical Results

6.4.1 Scenario

We considered an enterprise WiMAX cellular network comprised of 9 femtocells. Figures 6.7 and 6.8 depict coverage and best server areas of this network, respectively. Different simulations with 4, 6 or 8 static users connected per cell were performed, representing in this case a femtocell user load of 50%, 75% and 100%, receptively, since the network had 8 subchannels per DL time slot in a bandwidth of 2.5 MHz. Users were uniformly distributed within the coverage area of each cell. A user held its connection for a time dictated by an exponential distribution of mean μ and then disconnected. After its disconnection, a new user was generated at a random location. A full buffer user traffic model was used and the demand of each user was 250 kbps. Users suffered from outage if they could not transmit at a throughput no less than their requirements[1] for a time period T_{outage}. When a given user suffered from outage, its resources were freed and a new user was not generated till its holding time expired.

[1]Applications based on real-time or streaming services are insensitive to bit rate slow downs if the expected Quality of Service (QoS), i.e., transmission rate, is achieved.

Table 6.1: SIMULATION PARAMETERS

Parameter	Value	Parameter	Value
Femtocells	9	UE Ant. Height	1.5 m
Simulation time	600 s	UE Noise Figure	9 dB
Scenario Size	72 m × 39 m	UE Body Loss	0 dB
Carrier Frequency	2.0 GHz	Path Loss Model	FDTD-based model
Channel Bandwidth	2.5 MHz	Shadowing	Predicted by FDTD
Frame Duration	5 ms	Users per sector (U)	4,6,8
Data subcarriers	192	User distribution	Uniform
Subchannels (K)	8	Min. dist. UE to FAP	1 m
DL OFDM data symbols	39	Mean Holding Time	45 s
FAP Tx Power (P_m^{tot})	20 dBm	Type of Service	Full buffer
FAP Ant. Base Gain	0 dBi	Min Service TP	250 kbps
FAP Ant. Pattern	Omni	T_{outage}	4 s
FAP Ant. Height	1.5 m	$T_{u,mr}$	480 ms
FAP Ant. Tilt	-	$T_{u,cqi}$	10 ms
FAP Noise Figure	5 dB	NLMr- $T^f_{NLM,up}$	100 ms
FAP Body Loss	0 dB	IM - $T^u_{IM,up}$	100 ms
Thermal Noise Density	-174.0 dBm/Hz	T_{aurap}/T_{corap}	1 s
UE Ant. Gain	0 dBi	T_{aurpap}/T_{corpap}	100 ms
UE Ant. Pattern	Omni	-	-

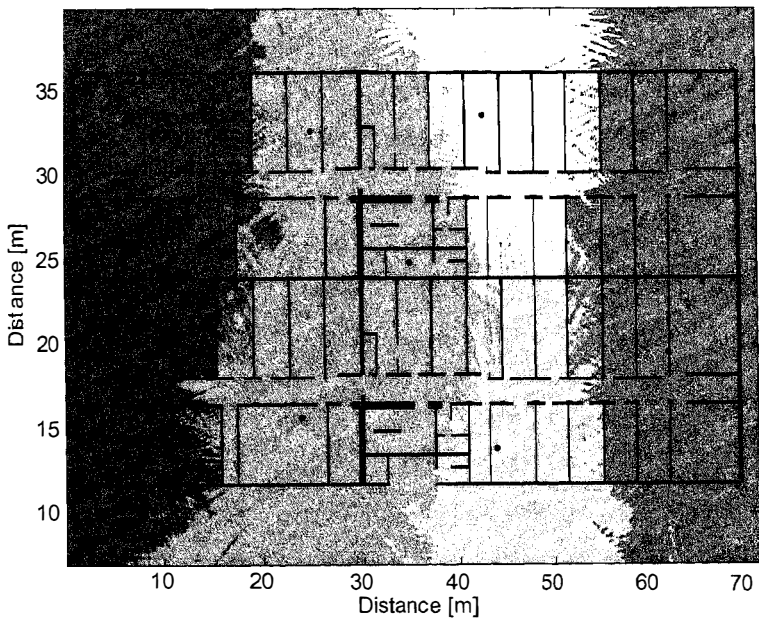

Figure 6.8: Office scenario with 9 femtocells: Best server.

T_{outage} has been set to 4 s in this case rather than the 9 s utilised in the macrocell case. Mean holding time μ has been changed from 90 s to 45 s to have a more dynamic load.

The system model was implemented as a subframe-level simulator using the event-driven simulation presented in Chapter 3. 600 s of network operation were simulated. User performance in terms of throughput, outage, transmit power and other indicators was assessed on a regular basis, every 1 s. Statistics were collected from all femtocells.

Path losses were modelled according to the Finite-Difference Time-Domain (FDTD)-based model presented in [89]. Subframe errors were modelled based on BLER Look Up Tables (LUTs) from Link-Level Simulations (LLSs) [85]. Further details about the models and parameters used in our simulations are presented in Chapter 3 and Table 6.1.

6.4.2 Optimisation Performance

6.4.2.1 Solving auRPAP

Similarly to Chapter 5, to analyse the performance of network simplex when solving auRPAP, we also extracted one million problem instances from our simulation scenario.

The running time[1] of one million auRPAP subchannel and power allocations in different cells was estimated to be 203.33 s. Thus, the average running time of network simplex for a single auRPAP subchannel and power assignment in one cell is around 0.20 ms.

In this case, the running time of network simplex is lower than in Chapter 5 because there are 8 instead of 12 subchannels and users connected per cell. Because auRPAP can be solved in less that one millisecond, it can be used to fight fast channel variations.

Note that very similar results were obtained with coRPAP.

6.4.2.2 Solving auRAP

To compare the running time of our proposed two-level exhaustive search approach to that of an Integer Linear Programming (ILP) solver when solving auRAP, we have also extracted 100 problem instances from the scenario introduced in Section 6.4.1. The ILP solver utilised was CPLEX [95], while in case of our two-level optimisation the proposed smart exhaustive search and network simplex algorithm were employed.

In this femtocell scenario, the average running time of the ILP solver was 23.43 s, while that one of our two-level exhaustive search approach was much less, i.e., 0.39 s. Our two-level exhaustive search approach found the optimal solution for all instances.

In this case, the running time of our approach is much lower than in Chapter 5 because there are 6 MCSs and 8 subchannels and users connected per cell instead of 15 MCSs and 12 subchannels and users.

Note that very similar results were obtained with coRPAP.

6.4.3 Network Performance

6.4.3.1 Techniques Used for Comparison

In order to evaluate the performance of auRRAA and coRRAA, the following decentralised radio resource management techniques were used for comparison:

Random assignment In this case, subchannels are randomly allocated to users and transmit power is uniformly distributed among subcarriers.

[1]It must be noted that the computer utilised for this simulation contained an AMD Opteron 275 dual-core processor running at $2.2\,GHz$ with $16\,GB$ of RAM.

Stolyar's approach This method was presented in Section 5.6.3.

Network listening mode-based method This method was presented in Section 6.3.1.

IM-based method This method was presented in Section 6.3.2.

6.4.3.2 Cell-Centre and Cell-Edge Zones: γ^{edge}

Similarly to the tuning procedure presented in Section 5.6.3.2 of the previous chapter, in order to derive an appropriate cell-edge and cell-centre boundary γ^{edge} for coRRAA, we run a number of simulations in the proposed scenario with 8 users per femtocell.

Table 6.2 illustrates that $\gamma^{edge} = 3$ dB provides the best network-wide performance. For instance, the number of user outages considerably decreased from 48 to 16 when γ^{edge} was fine tuned from 12.0 dB to 3.0 dB. (This results are inline with Section 5.1.2).

In the following simulations, the cell-centre and cell-edge boundary γ^{edge} is set to 3 dB.

Table 6.2: Network Performance vs. γ^{edge}

γ^{edge} [dB]	-3	0	3	6	9	12
User outage	25	19	**16**	34	38	48
Connected users	70.02	70.64	**71.00**	69.74	69.15	68.37
Network throughput [Mbps]	17.55	17.67	**17.84**	17.32	17.22	17.01

6.4.3.3 Transmit Power

Figure 6.9 shows the Cumulative Distribution Function (CDF) of the power allocated to subcarriers along the simulation. When making use of uniform power distributions, transmit power applied to subchannels does not vary according to the environment. On the contrary, when using auRRAA or coRRAA, the power applied to subchannels is adaptive and also becomes much smaller.

Because coRRAA results in less user outages and thus in a larger cell user load, it uses slightly more power than auRRAA to deal with the larger inter-cell interference.

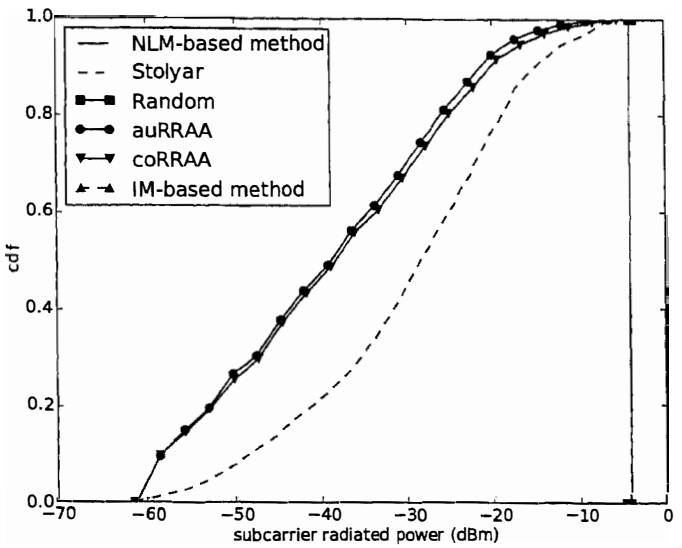

Figure 6.9: CDF of the radiated power per subcarrier during the simulation in the 12 user/sector scenario.

Details on network performance in terms of user outages are given in Section 6.4.3.6.

On the other hand, Stolyar's approach uses more transmit power per subcarrier because its objective was to allocate as less subcarriers as possible within a subchannel in order to satisfy user throughput demands, hence allocating larger MCSs and power.

6.4.3.4 Inter-Cell Interference

Figure 6.10 illustrates that the inter-cell interference suffered by subcarriers decreases when using the proposed coRRAA and auRRAA in comparison to the other approaches. This inter-cell interference reduction is significant with respect to techniques based on a uniform power distribution such as network listening mode and IM-based methods.

Since coRRAA results in a larger traffic load because it results in less user outages, inter-cell interference is slightly larger in the coRRAA case than in the auRRAA case. Details on network performance in terms of user outages are given in Section 6.4.3.6.

On the other hand, since in this case there are 24 subcarriers per subchannel, frequency hopping in Stolyar's approach becomes more effective than in Chapter 5.

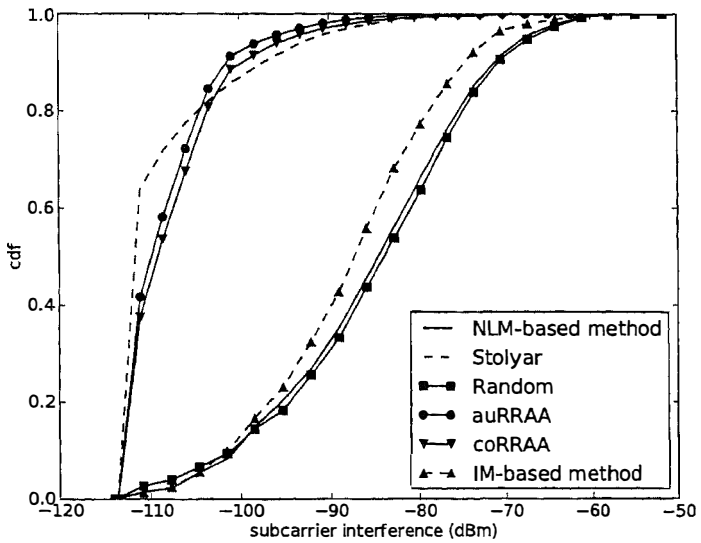

Figure 6.10: CDF of the interference suffered per subcarrier during the simulation in the 12 user/sector scenario.

However, some subcarriers still suffer from larger interference than in auRRAA and coRRAA.

6.4.3.5 Resource Block Allocation

Similarly to Section 5.6.3.6, Figure 6.11 shows the quantity of transmit power allocated by three neighbouring femtocells in each of the 8 subchannels at a given time instant. It can be observed that when using auRRAA, femtocells tend to allocate high powers in those subchannels in which the neighbouring cells assign low powers and vice versa. Even though cells operate independently, there is an implicit coordination among them in terms of radio resource allocations to their cell-edge and cell-centre users.

The same logic also applies to coRRAA.

6.4.3.6 System-Level Performance

Table 6.3 illustrates the network performance when making use of coRRAA, auRRAA and the presented schemes in terms of outages, average number of network connected

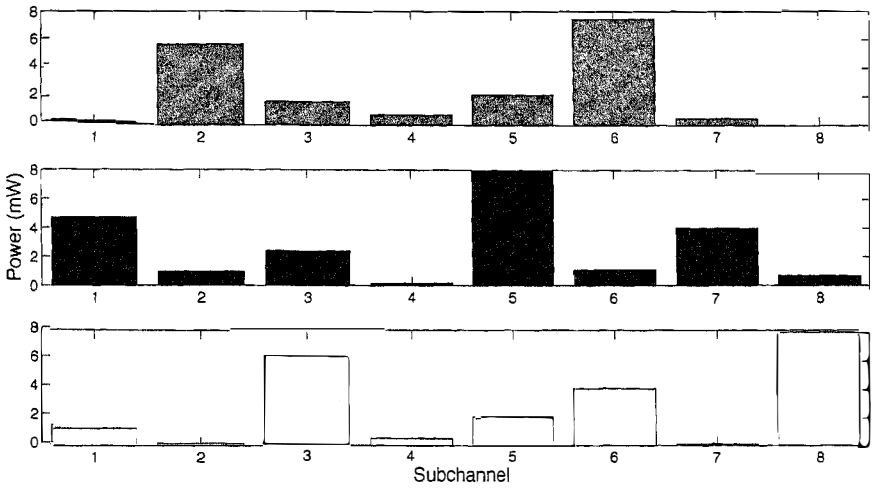

Figure 6.11: RB allocation of three neighbouring sectors with 8 users each.

Table 6.3: System-level simulation results.

Cell load	Scheme	Random	MNL	IM	Stolyar	auRRAA	coRRAA
4 users/cell 50 % load	Outage	70 (15.09 %)	40 (8.62 %)	12 (2.59 %)	25 (5.39 %)	4 (0.86 %)	1 (0.22 %)
	Users	31.13	33.11	35.20	34.44	35.75	35.87
	Mbps	7.65	8.24	8.77	8.56	8.83	8.91
6 users/cell 75 % load	Outage	141 (20.06 %)	114 (16.22 %)	55 (7.82 %)	47 (6.69 %)	15 (1.99 %)	14 (2.13 %)
	Users	43.65	45.15	49.64	49.92	52.71	52.79
	Mbps	10.73	11.18	12.35	12.33	12.87	13.02
8 users/cell 100 % load	Outage	187 (19.87 %)	186 (19.77 %)	146 (15.52 %)	77 (8.18 %)	30 (3.19 %)	16 (1.70 %)
	Users	58.36	58.59	60.47	65.93	69.63	71.00
	Mbps	14.40	14.48	14.98	16.23	16.78	17.45

users and average network throughput. Note that 8 subchannels were available and that 4, 6 or 8 users attempted to connect per cell, representing a 50 %, 75 % and 100 % cell user load of its maximum, respectively.

In these tables, columns denote proposed approaches, e.g., coRRAA, auRRAA, whereas rows represent the user load of cells.

An important fact that we can see in this table is that for all cell user loads, schemes based on a power controlled scheduling, i.e., Stolyar's, auRRAA and coRRAA, outperform those based on uniform power distributions, e.g., NLM, IM-based methods, For example, our auRRAA provided a performance improvement of 9.16 and 12.01 %

in terms of average connected users and average network throughput, respectively, compared to IM-based method.

Within the power controlled schemes, coRRAA resulted in the best performance since it allows inter-BS communication and therefore a better inter-cell interference mitigation through DL-HIIs. But, we can see that for the most challenging case, i.e., scenario with 8 users per cell, auRRAA performance is close to that of coRRAA, 1.37 and 3.99 % worse in terms of average connected users and network throughput. Because auRRAA does not require any signalling between FAPs, this technique may be more appealing for femtocell roll-outs where backhaul QoS may not be guaranteed.

auRRAA also outperformed Stolyar's approach. As explained in Section 5.6.3.7, this is mainly because Stolyar's approach allocates less subcarriers but with more power because of its frequency hopping, creating strong components of inter-cell interference.

In our architectures, the optimisation problem considers the allocation of MCSs, when minimising transmit power independently at cells, which implies modulating as many subcarriers as possible applying the least possible power to each one of them. This approach provides better results in terms of user outages in studied scenarios. Note that the performance of Stolyar's approach was now closer to that of auRRAA than in Chapter 5, because there are 24 rather than 12 subcarriers per subchannel, thus having a user transmission more free subcarriers for hopping within a subchannel.

6.4.3.7 Signalling Overhead

In this section, the signalling overhead incurred by coRRAA due to DL-HII is analysed. Let us recall that every DL-HII contains two items, transmit power constraint $p_k^{m,max}$ and subchannel index k. Assuming that 3 bits are utilised to encode k (8 subchannels), the number of bits needed per exchanged DL-HII is $(3 + 10) \cdot D_u$ bits according to discussions in Section 5.5.1. Furthermore, let us note that according to our simulations, an average of 9.32, 14.07 and 18.91 DL-HIIs per second where sent per cell for the 4, 6 and 8 users per cell cases, respectively. Therefore, for these three distinct scenarios, the back-haul bit rate required was in average of 0.28 0.42 and 0.57 kbps, respectively. A small fraction of the available back-haul bandwidth is needed for coRRAA signalling. But, since femto-to-femto interfaces may be handled via user-provided IP back-hauls, delay issues may arise during DL-HII exchange that could affect coRRAA performance.

6.5 Conclusions

This chapter has investigated the potential of applying the decentralised radio resource management architectures proposed in the Chapter 5, i.e., coRRAA and auRRAA, to femtocell scenarios in order to mitigate co-tier interference. Also, a new heuristic based on a smart search over the MCS solution space of xxRAP has been proposed, which is able to deliver optimum solution within reasonable times due to the reduced number of users per cell. Dynamic system-level simulations of a realistic femtocell enterprise deployment confirm that these two novel architectures are able to enhance network performance in comparison with advanced approaches proposed in literature.

Conclusion 1: Again, the adoption of a power controlled resource allocation scheme that minimises transmit power at each cell is the key to allow a better spatial reuse. Minimising transmit power independently at each cell reduces interference in those RBs allocated to users with good channel conditions or low throughput requirements, hence generating RB allocation opportunities that may be used by neighbouring cells for their cell-edge users.

Conclusion 2: The use of inter-BS coordination via DL-HIIs (coRRAA) has been shown to improve overall network performance with respect to a fully distributed operation (auRRAA). However, because this improvement is not really significant, i.e., coRRAA is 1.37 and 3.99 % better than auRRAA in terms of average connected users and network throughput, respectively, we may prefer auRRAA to coRRAA for femtocell deployments where QoS on the user-provided IP back-haul cannot be guaranteed for the exchange of control messages.

Conclusion 3: Simulations have shown that the proposed algorithms significantly improve network capacity with respect to a variety of allocation schemes in literature. coRRAA and auRRAA provided a considerable performance improvement of more than 50 % in terms of user outages over cutting-edge techniques such as Stolyar's approach, while also dealing with fully loaded networks.

Conclusion 4: In real femtocell networks, the problem of the joint allocation of MCS, RB and power to users becomes complex and cannot be solved using ILP solvers.

However, the proposed two-level optimisation scheme based on an heuristic search and network simplex has been proved to be able to obtain optimum solutions of this problem within affordable times.

Chapter 7

Radio Resource Management for Femtocells: Cross-Tier Interference

7.1 Introduction

Cross-tier interference[1] is described as the unwanted signal received at a femtocell because of the simultaneous transmissions of surrounding macroce .
The term cross-tier indicates that macrocells and femtocells belong .
Note that this problem differs from that of co-tier interference prese... in Chapter 6.

In the DownLink (DL), cross-tier interference occurs when a given macrocell user is located in an area where the signal coming from its own macrocell is not large enough with respect to the sum of the interference coming from its neighbouring femtocells. Cross-tier interference may be specially significant in Closed Subscriber Group (CSG) femtocell deployments, because macrocell users may not be allowed to connect to nearby femtocells at shorter path losses than their macrocells due to connectivity rights. Nevertheless, Orthogonal Frequency Division Multiple Access (OFDMA) femtocells[2] may avoid cross-tier interference by a proper allocation of frequency resources to users. For example, in Figure 7.1, user U_1^1 is at home receiving data from its CSG femtocell F_1. In order to allow this downlink connection, F_1 allocates subchannels 1 to 4 to user U_1^1.

[1] An extensive introduction and literature review about the state-of-the-art with regard to interference mitigation in femtocell scenarios is given in Section 1.4 and Section 2.2.

[2] In this chapter, when we refer to OFDMA femtocells, we refer to both Long Term Evolution (LTE) and Wireless Interoperability for Microwave Access (WiMAX) femtocells.

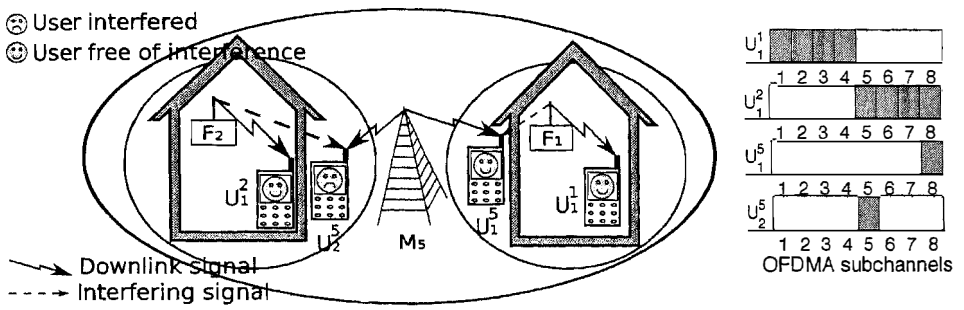

Figure 7.1: Cross-layer downlink interference in an OFDMA two-tier network.

Meanwhile, an outdoor user U_1^5 connected to macrocell M_5 is walking down the street and it passes by the front door of user U_1^1, therefore falling inside the coverage of F_1. In this case, macrocell M_5 had already assigned subchannel 8 to this mobile user U_1^5, which is not interfered because femtocell F_1 has not allocated subchannel 8 to any user. Nevertheless, this is not always the case. For example, Figure 7.1 also shows a case, in which macrocell user U_2^5 is allocated a subchannel, which is being simultaneously used by nearby femtocell F_2, and thus it is heavily interfered and its service disrupted.

Open access femtocells have been regarded as a feasible solution to mitigate cross-tier interference in two-tier networks [113]. However, open access femtocell roll-outs are hardly practical due to the large number of Handovers (HOs) associated to them. In fact, when outdoor users are permitted to connect to any macrocell or femtocell, it is likely that because of their mobile nature, their connections would be continuously transferred among adjacent femtocells, or among them and the umbrella macrocell. Indeed, it is also known that HOs are not always successful and user connections might be dropped because of their failures [114]. In addition, the large signalling that emanates from an open access femtocell tier increases the complexity of the access network, thus introducing the necessity for large and powerful femtocell gateways (FemtoGW).

Due to the above presented drawbacks and because of the sharing concerns of users, CSG femtocells still seem to be more appealing to most of mobile network operators. Thus, new solutions to the interference problem created by CSG femtocells are needed. In this chapter, we research the potential of applying the decentralised and cooperative Radio Resource Management Architecture (coRRAA) proposed in previous chapters, to hybrid macrocell-femtocell deployments in order to mitigate cross-tier interference. Through inter-Base Station (BS) cooperation is expected that both macrocells and femtocells can coordinate their radio resource allocations, so that cross-tier interference

towards higher priority macrocell users is mitigated and its service disruption is avoided.

Let us note that in this chapter the nomenclature of WiMAX networks is utilised, and that without loss of generality with respect to our approach, we focus on the DL.

7.2 Overview on Handover and Cross-Tier Interference Coordination in Femtocell Deployments

This section introduces the concepts of HO and cross-tier interference coordination, which are both fundamental in this chapter.

7.2.1 Handover

The aim of an HO is to transfer a mobile user from its serving cell to a target one (Figure 7.2).

In macrocellular networks, an HO is triggered every time the received signal strength $w_{u,m}^{pilot}$ of the pilot signal of the serving macrocell M_m at user U_u^m is lower than that $w_{u,n}^{pilot}$ of a neighbouring macrocell $N_b^m \in \mathcal{N}_m$. Serving cells indicate to connected users, which pilot signals should be measured through their Neighbouring Cell Lists (NCLs) and users report this information to serving cells via Measurement Reports (MRs)[1]. These pilot signal strength measurements are averaged over time by serving cells before triggering an HO in order to cope with time-dependent fast fading conditions. Furthermore, when a mobile user is located in between cells, it could occur that its transmission is ping-ponged from cell to cell. In order to avoid these ping-pong issues, averaged signal strengths relative to a hysteresis margin are utilised for HO decision. Furthermore, an umbrella cell system is normally deployed to reduce the large number of HOs incurred by high speed users [115]. If the HO condition is met (Figure 7.2), the serving cell then establish communication with the target one to initiate an HO.

However, in two-tier networks, performing an HO is not always the best solution or a possible option at all because:

- In closed access, it is not allowed that a nonsubscriber hands over from its serving

[1] The concepts of neighbouring cell list and measurement report were introduced in the introductory chapter (Section 1.3.3)

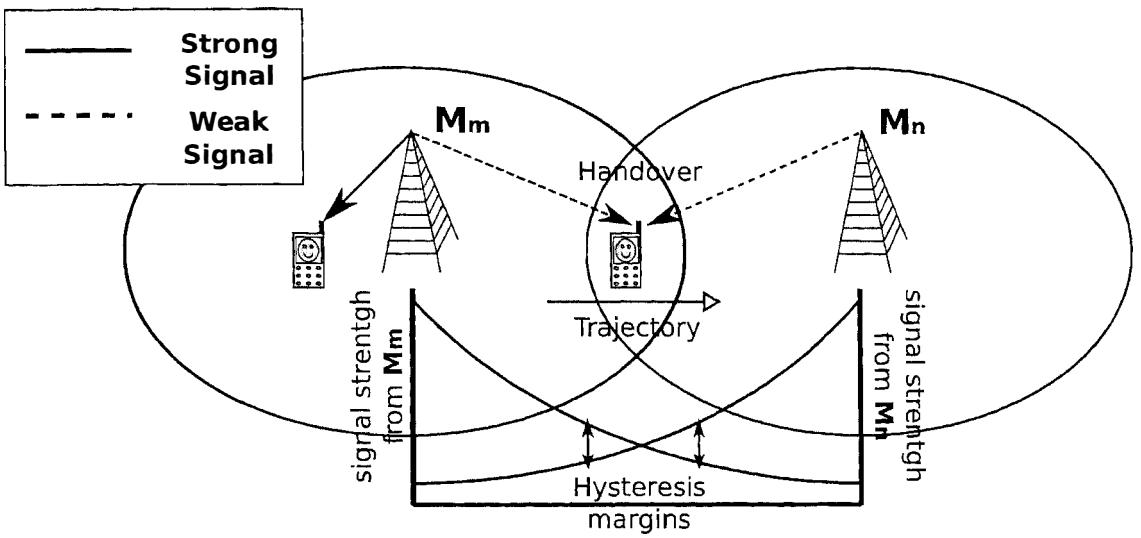

Figure 7.2: Diagram of a handover.

cell to a CSG femtocell.

- In open access, it is preferred to keep a mobile user connected to a macrocell rather than hand it over continuously between adjacent open access femtocells. In this case, the mobile user speed must be considered.

7.2.2 Cross-Tier Interference Coordination

In order to mitigate cross-tier interference, it is essential that users are able to sense, detect, and report information to their servers concerning potential interfering cells, being present in their vicinity. Serving cells in collaboration with potential interferers will then coordinate their resource allocations in terms of power, frequency, and time to enhance network capacity and mitigate user outages. In order to allow coordination, control information messages need to be exchanged between neighbouring cells, e.g., neighbouring macro BSs are interconnected via inter-BS interfaces for this reason [106].

While such message exchanged over inter-BS interfaces can help alleviating dominant interference scenarios for macrocells, they are not standardised for femtocells, therefore necessitating new approaches to provide inter-cell interference coordination.

One possible solution for enabling macrocell-femtocell coordination is the exchange of information messages via the backhaul. However, delay problems may appear because the wireline backhaul of femtocells may not be owned by femtocell network operators. To overcome this issue, the exchange of messages between macro BSs and femto BSs through the wireless broadcast channels or the use of users for relaying data between neighbouring cells are being investigated [116]. For instance, victim macrocell users can be determined by macrocells by utilising their user Channel Quality Indicators (CQIs), and their identity may be signalled by macrocells to femtocells via backhaul connection.

Making use of inter-BS coordination, transmissions of victim DL macrocell users may be scheduled in time-domain resources, e.g., subframe, or OFDM symbol, where interference from femtocells is mitigated [117]. For instance, when macro BS and femto BS subframes are aligned as in Figure 7.3(a), their control and data channels overlap. Hence, in order to avoid DL cross-tier interference from femto BSs to macrocell users, some form of inter-cell interference coordination should be implemented at femtocells.

One way to reach this is to utilise the so called Almost Blank Subframes (ABSF). In these ABSFs, no control or data signals, but pilot signals are emitted (Figure 7.3) In order to fully avoid cross-tier interference, DL macrocell users in the vicinity of femtocells can be scheduled within the subframes overlapping with femtocell ABSFs. This ASBF approach completely avoids femtocell to macrocell inter-cell interference at the expense of regularly 'switching off' femtocells and thus reduce their throughput. Similar approaches with the same drawback may also be used in the frequency domain.

In the following, we propose a power controlled inter-BS cooperation targeted to provide victim macrocell users with a given signal quality target in terms of Signal to Interference plus Noise Ratio (SINR), while allowing femtocell transmissions too. Like this, spatial spectrum reuse is enhanced.

7.3 Cooperative Radio Resource Allocation Architecture for Two-Tier Networks

As it was indicated earlier, in this chapter, we investigate the potential of applying the cooperative radio resource management architecture proposed in previous chapters, i.e., coRRAA, to hybrid macrocell-femtocell roll-outs to mitigate cross-tier interference.

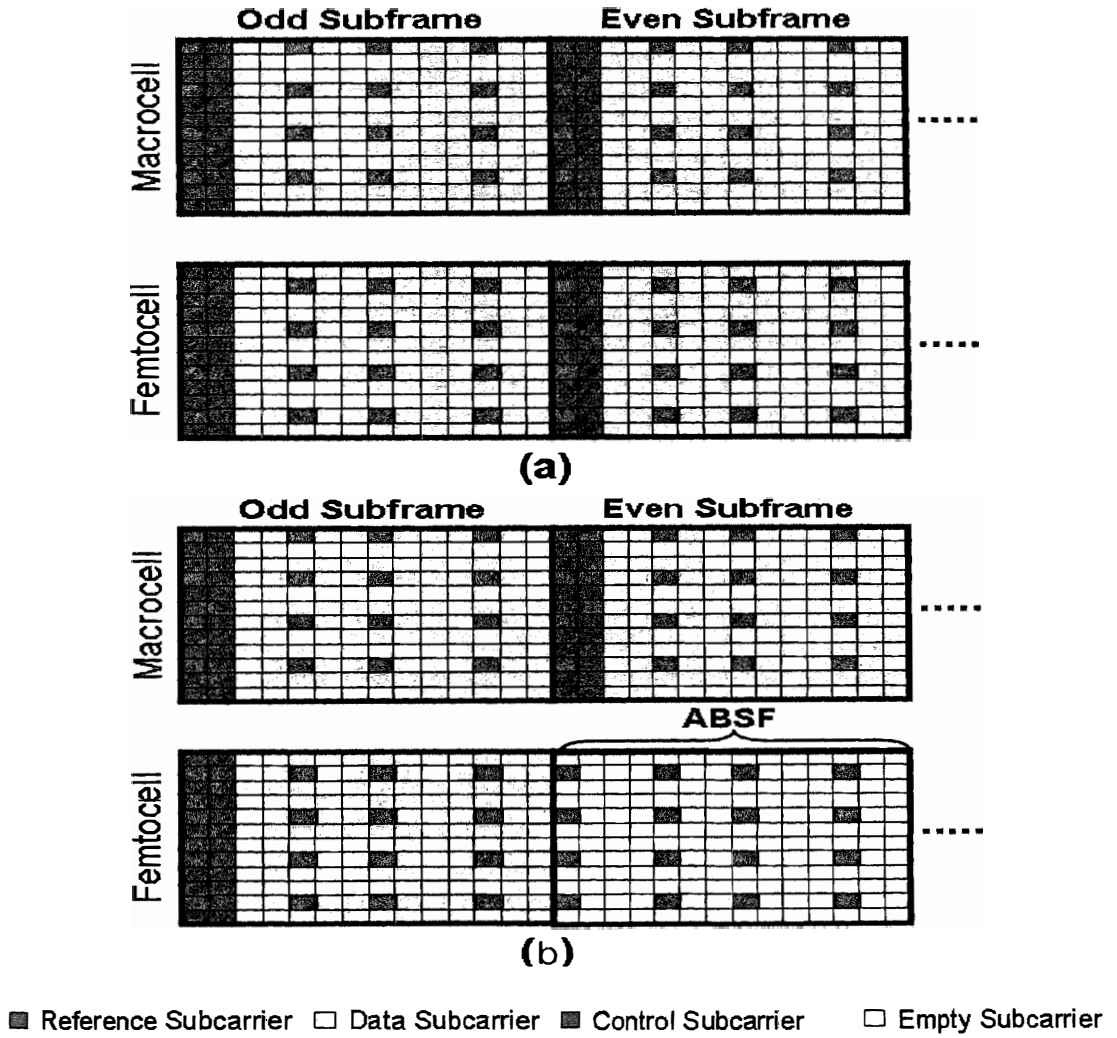

Figure 7.3: Illustration of ABSFs for time-domain: (a) Macrocell and femtocell subframes without any inter-cell interference coordination. (b) Macrocell and femtocell subframes with inter-cell interference coordination. This can address the interference problem, where the macrocell users close to the femtocell can be scheduled in the even subframes of femtocell.

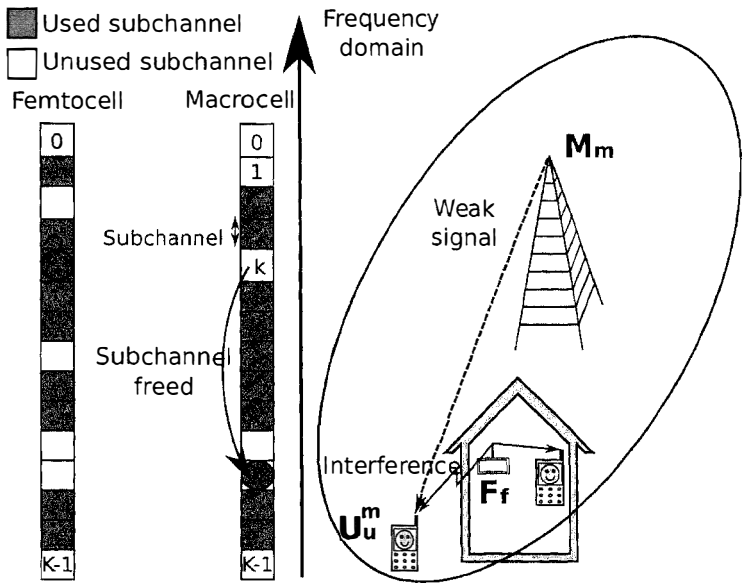

Figure 7.4: Operation of coRRAA in the presence of a low load femtocell.

Let us note that in the following, macrocell users are considered to have a higher service priority than femtocell users, thus mitigating their outages has priority with respect to maximise femtocell performance.

First of all, let us describe how the proposed coRRAA in Chapter 5 would operate in the following two scenarios:

Low loaded femtocell When a given nonsubscriber U_u^m connected to macrocell M_m suffers from cross-tier interference in subchannel k because of a nearby femtocell F_f, macrocell user U_u^m will report a large interference in subchannel k to macrocell M_m through a CQIs. Thereafter and because there are some subchannels in femtocell F_f that are unused, when macrocell M_m runs coRAP or coRPAP, it will automatically assign macrocell user U_u^m to a new less-interfered subchannel $k\prime$, in which it needs less transmit power to achieve the macrocell user SINR target γ_u. (Figure 7.4).

The proposed coRRAA will deal with this scenario with no problem, as long as it 'sees' some subchannels free of interference.

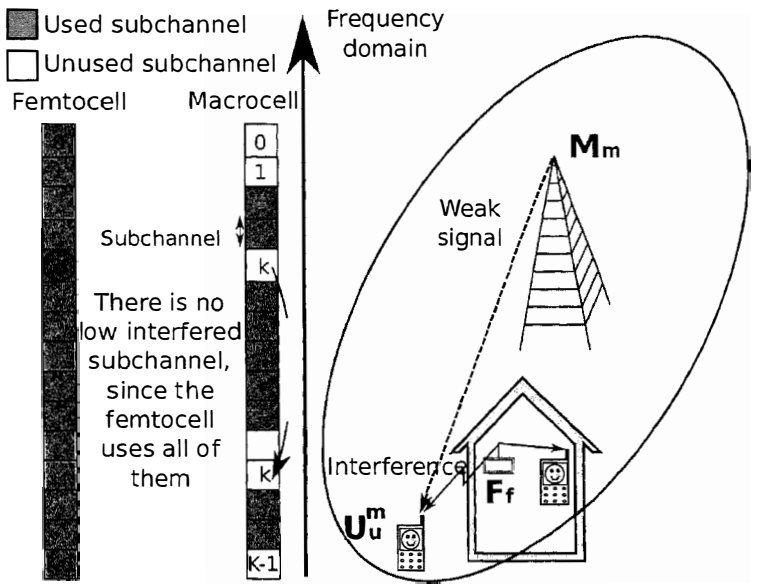

Figure 7.5: Operation of coRRAA in the presence of a high load femtocell.

High loaded femtocell On the contrary, if interfering femtocell F_f is fully loaded and therefore there is no subchannel k' where user U_u^m reports low inter-cell interference, coRRAA cannot deal with this scenario without using a form of inter-BS coordination. (Figure 7.5).

In the following, we describe our proposed inter-BS coordination procedure that allows coRRAA to cope with this scenario.

If the SINR $\gamma_{u,k}^m$ of user U_u^m connected to macrocell M_m in subchannel k is smaller than the SINR threshold γ_h of its targeted Modulation and Coding Scheme (MCS) h, and if an increase of transmit power $p_{u,k,h}^m$ is not feasible[1] to reach SINR threshold γ_h, serving macrocell M_m will then request a specific measurement report from user U_u^m.

$$\text{MR Triggering Condition} \rightarrow \gamma_{u,k}^m < \gamma_h \tag{7.1}$$

This measurement report indicates the power of the signal received by user U_u^m from its serving macrocell M_m and its neighbouring cells $N_b^m \in \mathcal{N}_m$ in subchannel k, i.e., $w_{u,k}^m$ and $w_{u,k}^b \ \forall N_b^m \in \mathcal{N}_m$.

[1]For example, if there is no more available transmit power at macrocell M_m to serve user U_u^m because it is being assigned to other users $\mathcal{U}^m/U_u^m$.

For the sake of simplicity, in the sequel, inter-macrocell interference is disregarded.

Then, femtocells $\Upsilon_u = \{A_1, ..., A_c, ..., A_{C_u^{intrf}}\}$ producing an interference $w_{u,k}^b$ larger than the noise σ^2 minus 10 dB[1] are considered as interferers.

Thereafter, in order to mitigate the cross-tier interference suffered by user U_u^m, serving macrocell M_m will establish communication with all interfering cells $A_c \in \Upsilon_u$ (Section 7.3.1) and commence coopetation.

One solution in order to mitigate cross-tier interference towards nonsubscriber U_u^m is to disconnect subscriber U_u^c of femtocell A_c from subchannel k for a period of time. Nevertheless, this could significantly reduce the throughput of interfering femtocell A_c. This scheme has similarities with the ABSF-based method introduced in Section 7.2.2, and it will be used for performance comparison under the name: *subchannel forbidding*.

Instead of disconnecting all subscribers U_u^c of all interfering femtocells $A_c \in \Upsilon_u$ from subchannel k, we propose to reduce the power applied by all these femtocells to this subchannel for a period of time ΔT_{PC}. The objective of this power control is to avoid cross-tier interference to nonsubscriber U_u^m in subchannel k, while also enhancing the throughput of femtocell subscriber U_u^c assigned by femtocell A_c to subchannel k. In this way, the reduction of user throughput in all interfering femtocells $A_c \in \Upsilon_u$ is mitigated compared to that of the above presented subchannel forbidding approach.

The target of this distributed power control is to set the power $p_{u,k}^c$ applied by each interfering femtocell $A_c \in \Upsilon_u$ in subchannel k to a value $p_{u,k}^{'c}$ that guarantees a given signal quality in terms of SINR γ_u^{pc} to nonsubscriber U_u^m.

In order to guarantee SINR target γ_u^{pc}, the maximum inter-cell interference $w_{u,k}^{max}$ that nonsubscriber U_u^m can suffer from is

$$w_{u,k}^{max} = (\frac{w_{u,k}^m}{\gamma_u^{pc}} - \sigma^2) + \Delta w \tag{7.2}$$

where σ is the background noise density, γ_u^{pc} is the aimed user MCS SINR threshold, $w_{u,k}^m$ is the power of the carrier signal received by user U_u^m from its serving cell M_m, and Δw represents an additional inter-cell interference protectation margin set to 3 dB.

Thereafter, macrocell M_m requests all interfering femtocells $A_c \in \Upsilon_u$ to decrease their transmit power in subchannel k from $p_{u,k}^c$ to $p_{u,k}^{'c}$ so that interference $w_{u,k}^{max}$ is respected for nonsubscriber U_u^m.

[1]This is a margin added to consider the effect of aggregated signals close to the noise power level.

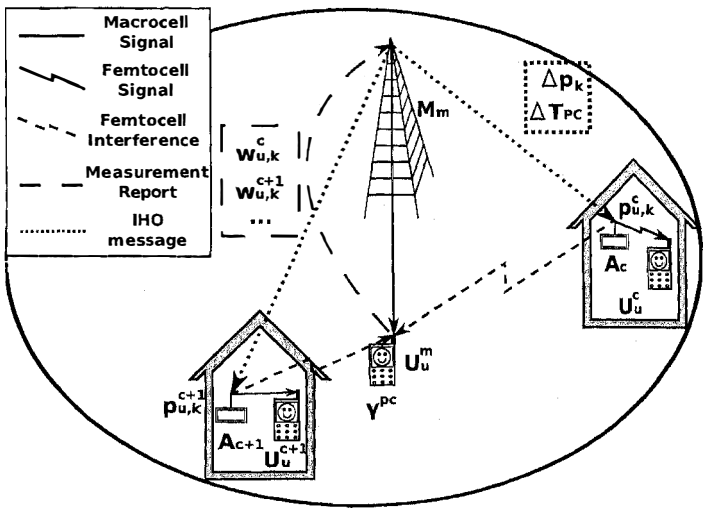

Figure 7.6: Macrocell-femtocell cooperation.

Furthermore and in order to avoid unfair power decrease requests among femtocells, this power decrease is weighted by macrocell M_m according to the following equation:

$$p'^{c}_{u,k} = \underbrace{w^{max}_{u,k} \cdot \frac{w^{c}_{u,k}}{\sum_{\forall c} w^{c}_{u,k}}}_{w^{C-max}_{u,k}} \cdot \underbrace{\frac{p^{c}_{u,k}}{w^{c}_{u,k}}}_{\delta_{c,u}} \tag{7.3}$$

where $w^{c}_{u,k}$ is the received signal strength measured by nonsubscriber U^{m}_{u} from each interfering femtocell $A_c \in \Upsilon_u$ in subchannel k, which was fed back in the measurement report used to trigger this power control, $w^{C-max}_{u,k}$ represents the maximum inter-cell interference that each femtocell $A_c \in \Upsilon_u$ is allowed to generate to nonsubscriber U^{m}_{u}, and $\delta_{c,u}$ is the path loss between interfering femtocell $A_c \in \Upsilon_u$ and nonsubscriber U^{m}_{u}.

Furthermore, equation (7.3) simplifies to:

$$(p'^{c}_{u,k})_{dB} = (p'^{c}_{u,k})_{dB} - (\Delta p_k)_{dB} \tag{7.4}$$

where

$$(\Delta p_k)_{dB} = 10 \cdot log_{10} \left(\frac{\sum_{\forall c} w^{c}_{u,k}}{w^{max}_{u,k}} \right) \tag{7.5}$$

being $(\Delta p_k)_{dB}$ the power reduction in decibels in subchannel k asked by macrocell M_m to each of its interfering femtocells $A_c \in \Upsilon_u$.

Figure 7.6 illustrates the idea and parameters used in this power control approach. When decreasing the power $p^c_{u,k}$ of femtocell A_c in subchannel k, let it be noted that:

- If femtocell A_c is already transmitting at low power in subchannel k, or
- If the targeted signal quality in terms of SINR γ^{pc}_u is too demanding,

power reduction Δp_k may have exactly the same effect as switching off subchannel k. In this case, subchannel k is forbidden in femtocell A_c for a period of time ΔT_{PC}. Nevertheless, it must be noted that subscriber U^c_u is only disconnected from subchannel k if and only if it can afford it, i.e., subscriber U^c_u has assigned some more subchannels, or it carries a service where delay is tolerated such as non-real time or best effort. Moreover, let us note that the decrease in the femtocell throughput when forbidding a subchannel is statistically small, because this power control is performed only from time to time when the femtocell is fully loaded and a nonsubscriber passes close to it.

In addition, because a femtocell can only be accessed simultaneously by a few users and because subchannel forbidding is only triggered when the femtocell is fully loaded (in order to fully use all available subchannels of a femtocell, it is likely that the femtocell subscribers are not only using VoIP (12.2 kbps) or video (256 kbps) but also intensive best effort peer-to-peer services), femtocells can generally afford to liberate a subchannel during a short period of time to prevent the outage of a nonsubscriber.

7.3.1 Macrocell and Femtocell Communication

To permit macrocell-femtocell cooperation, communication among them is necessary. In more detail, macrocells will send control messages to all interfering femtocell Υ_u in order to indicate the reduction of power Δp_k that has to be applied to subchannel k and for how long ΔT_{PC} it has to be applied.

These control messages may be sent from macrocells to femtocells as follows:

- Macrocells and femtocells can communicate through the femtocell gateway [110].

  The serving macrocell would send its message to the femtocell gateway, and the femtocell gateway would forward this message to the target femtocell/femtocells.

- Another solution is to establish a new link among macrocells and femtocells [110].

  This alternative has similarities to the X2 interface defined in LTE to allow communication between eNodeBs, but it is not extended yet to femtocells [111].

- The user could relay information from a macrocell to a femtocell and vice versa. This option has been suggested in [40]n

Once a given femtocell receives a control message, it will then set a power constraint in the specified subchannel, and it will allocate resources to its users accordingly. Since both macrocells and femtocells make use of the proposed coRRAA (Section 5.2), and because power constraints are considered in the formulation of coRPAP (5.3), i.e., the subroutine used to derive optimum subchannel and power assignments to users, femtocells only need to compute its power constraint after receiving a control message and continue running coRRAA as in Section 5.5.

Power constraint $p_k^{c,max}$ can be calculated as the current power $p_{u,k}^c$ applied by the interfering femtocell A_c to subchannel k minus the reduction of power Δp_k that this femtocell should apply to this subchannel.

7.4 Simulation and Numerical Results

7.4.1 Scenario

The scenario under scrutiny is a residential area within the town of Luton (U.K.), containing 438 premises of which 400 are dwelling houses within an area of 300×300 m. In this case, 64 of these houses were selected to potentially host an indoor femtocell. Assuming that 3 operators with equal customer share provide services in this area, these 64 femtocells represent an approximate femtocell penetration of by around 50%. Moreover, besides these 64 femtocells, the scenario also contains one outdoor macrocell. This macrocell was located out of the scenario of Figure 7.7 at position (400, -100) m.

It must be noted that simulations were carried out with different femtocell penetrations: 50% (= 64 femtocells), 25%(= 32 femtocells) and 12.5% (=16 femtocells). The WiMAX network had 8 subchannels per DL time slot in a bandwidth of 5 MHz. The scenario and the simulation parameters are shown in Figure 7.7 and Table 7.1, respectively.

Table 7.1: System-level simulation parameters.

Parameter	Value	Parameter	Value
Macrocells	1	FAP Body Loss	0 dB
Femtocells	16,32,64	Thermal Noise Density	-174.0 dBm/Hz
Simulation time	300 s	UE Ant. Gain	0 dBi
Scenario size	300 m× 300m	UE Ant. Pattern	Omni
Carrier frequency	3,500 MHz	UE Ant. Height	1.5 m
Bandwidth	5 MHz	UE Noise Figure	9 dB
Frame duration	5 ms	UE Body Loss	0 dB
Subcarriers	512	Macro path loss	Empirical
Data subcarriers	384	Femto path loss	FDTD
Subchannels (K)	8	Nonsubscribers per macro BS	8
DL OFDM data symbols	39	Subscribers per FAP	4,8
Macro BS Tx Power (P_m^{tot})	43 dBm	Nonsubscribers distribution	Predefined paths
Macro BS Ant. Base Gain	0 dBi	Subscribers distribution	Uniform
Macro BS Ant. Pattern	Omni	UE average speed	1.1 m/s
Macro BS Ant. Height	30 m	Min. dist. UE to Macro BS	35 m
Macro BS Ant. Tilt	0	Min. dist. UE to FAP	1 m
Macro BS Noise Figure	5 dB	Type of Service	Full buffer
Macro BS Cable Loss	3 dB	Min Nonsubscribers Service TP	250 kbps
FAP Tx Power (P_m^{tot})	20 dBm	Min Subscribers Service TP	750 kbps
FAP Ant. Base Gain	0 dBi	T_{outage}	200 ms
FAP Ant. Pattern	Omni	$T_{u,mr}$	480 ms
FAP Ant. Height	1.5 m	$T_{u,cqi}$	10 ms
FAP Ant. Tilt	-	ΔT_{PC}	15 s
FAP Noise Figure	5 dB	-	-

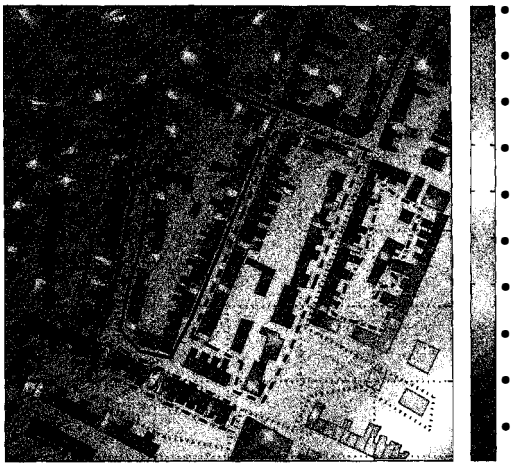

Figure 7.7: Performance evaluation scenario with 1 macrocell and 64 femtocells.

In these system-level simulations, two different propagation models were utilised:

- The macrocell coverage prediction was performed using the model given in [87]. This is an empirical model based on macrocell measurements taken at an urban environment at a frequency of $3.5\,GHz$.
- The femtocell coverage predictions were performed using a Finite-Difference Time-Domain (FDTD) based model [118] calibrated with indoor-to-outdoor measurements taken at a frequency of $3.5\,GHz$.

In these system-level simulations, users follow two different well-defined behaviours:

- Subscribers are located inside households with femtocell and do not move at all.
- Nonsubscribers are located outdoors and move along predefined paths according to the pedestrian model proposed in [119] (User paths are depicted in Figure 7.7).

Both femtocell and macrocell users were created at the beginning of the simulation and we kept them until the simulation ended.

A full buffer traffic model was used to simulate mobile and static user demands. In this case, the throughput demands TP_u^{req} of macrocell users were set to 250 kbps, while the requirements of femtocell users were set to a higher value, i.e., 750 kbps.

This is because femtocell users are indoors and protected by their household walls. Furthermore, larger demands create more challenging cross-tier interference conditions.

Macrocell users incurred outage if they could not transmit at a throughput no less than their demands for a time period T_{outage}. In this case, T_{outage} was fixed to 200 ms, a typical value for real time applications [88]. When macrocell users incurred outage, they attempted to reconnect after a random time uniformly distributed within [5, 10] s On the contrary, indoor femtocell users were assumed to carry best effort services and hence we did not consider their user outages.

The system model was implemented as a subframe-level simulator using the event-driven simulation presented in Chapter 3. 300 s of network operation were simulated. User performance in terms of throughput, outage, transmit power and other indicators was assessed on a regular basis, every 1 s. Statistics were taken from all network cells.

Subframe errors were modelled based on BLER Look Up Tables (LUTs) from Link-Level Simulations (LLSs) [85]. Further details about the models and parameters used in our simulations are presented in Chapter 3 and Table 7.1. This dynamic simulation also considers the Adaptive Modulation and Coding (AMC) nature of the network and its different MCSs are shown in Table 1.2.

7.4.2 Network Performance

7.4.2.1 Techniques Used for Comparison

In order to evaluate the performance of our enhanced coRRAA, the following techniques were used for comparison:

Closed-Access IM-based method In the closed access simulations, nonsubscribers are always connected to the macrocell, while subscribers are connected to femtocells. Nonsubscribers are likely to suffer from outage when they pass close to a femtocell that is making use of the same subchannel.

Open-Access IM-based method In the open access simulations, nonsubscribers, on the contrary, are allowed to connect to any serving cell, i.e., macrocells or femtocells. In this case, user terminals feed back measurement reports to their serving cells on a regular basis, i.e., every T_{mr} time units. A hard HO is performed if the received signal

strength of the strongest neighbouring cell is larger than that of the current server, and it cannot meet the user demands. In addition, it is assumed that there is a 2% probability of that an HO process fails, thus resulting this HO in a dropped call.

In both methods, macrocells and femtocells independently assign resources to users according to the Interference Minimisation (IM) procedure presented in Section 6.3.2. Let us recall that when using IM, power is uniformly distributed among subcarriers, each cell is targeted to minimise the sum interference suffered by its connected users, and CQIs assist this channel-dependent scheduling.

The proposed coRRAA with forbidding subchannel or power controlled macrocell-femtocell coopetation will also be compared.

Moreover, in all simulated schemes, the transmit power of femtocells is fine tuned depending on the macrocell signal level received where the femtocell was deployed [75]. In more detail, each femtocell sets its maximum femtocell transmit power per subcarrier to a value that is equal to the maximum power received from the closest macrocell at a targeted femtocell radius, here, 15 m.

7.4.2.2 coRRAA Basis

In order to analyse the functioning of the proposed macrocell-femtocell cooperation, Figure 7.8 illustrates the scenario used to study the performance of a nonsubscriber when it moves/walks across the scenario. Note that there are 2 femtocells, F_1 and F_2, and that they can be half or fully loaded according to the cases depicted in Section 7.3. Since pedestrians walk at an average speed of 1.1 m/s and because the femtocell radius is estimated to be 15 m [89], ΔT_{PC} has been tuned to 15 s, which is sufficient for a user to move across of a femtocell coverage.

Low loaded femtocell The macrocell is fully loaded (8 users), while the femtocells are half loaded (4 users).

Figure 7.9 shows that the SINR of a user connected to the macrocell is not affected by cross-tier interference from half-loaded femtocells. When this user moves close to femtocells F_1 and F_2, the macrocell can always find subchannels free of interference since femtocells are half loaded. Therefore, all schemes can solve potential cross-tier interference issues by subchannel allocation. Moreover, note that when using coRRAA,

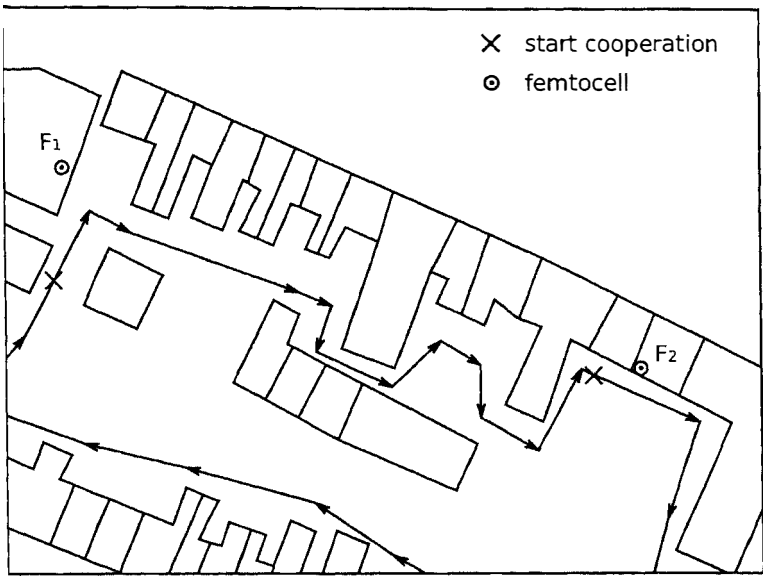

Figure 7.8: Route of a nonsubscriber within the performance evaluation scenario.

the user SINR adjusts to the aimed MCS, while methods based on uniform power distributions result in a much larger SINR, of which this user will not benefit from[1].

High loaded femtocell The macrocell and the femtocells are fully loaded (8 users).

Figure 7.10, on the contrary, shows that the SINR of a macrocell user is affected by cross-tier interference from fully-loaded femtocells. When this user moves close to femtocells F_1 and F_2, the macrocell cannot find now subchannels free of interference since femtocells are fully loaded. Thus, when using the closed-access IM-based method, this nonsubscriber falls into outage because its SINR has been significantly decreased and it is now smaller than the targeted one for a period of time longer than 200 ms. When using the open-access IM-based method, this user is handed over the femtocell, and cross-tier interference disappears at the expense of a HO procedure that may fail and reducing the subscribers' throughput to absorb the higher priority macrocell user.

When our coRRAA is applied making use of subchannel forbidding, i.e., the interfering femtocells are not allowed to use those subchannels utilised by the nonsubscriber, the SINR of the nonsubscriber does not suffer from femtocell cross-tier interference.

[1] A user will not benefit from a throughput larger than its demand.

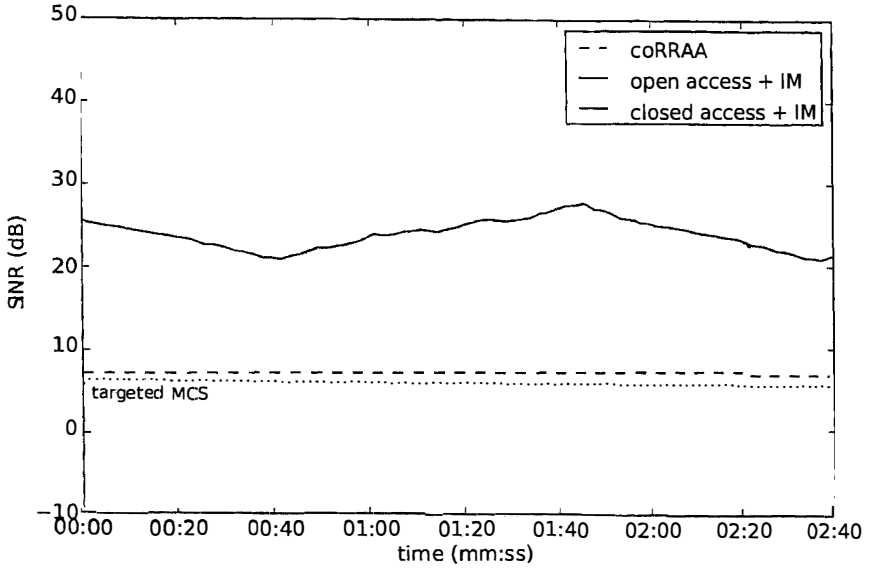

Figure 7.9: SINR of the nonsubscriber of Figure 7.8 versus time when it passes close to femtocells F_1 and F_2, and they are not fully loaded.

However, this is at the expense of reducing the throughput of the interfering femtocells, since they have to liberate for a given period of time a subchannel that was being used. This femtocell throughput reduction is depicted in Figure 7.11 and Figure 7.12 for femtocells F_1 and F_2, respectively.

However, when our coRRAA is applied making use of power control, i.e. the interfering femtocells reduce the power applied to those subchannels used by the nonsubscriber, the outage of the macrocell user is avoided and the femtocell throughput is enhanced. Unfortunately, power control cannot fully recover the femtocell throughput capacity compared to the CSG case, but it provides a gain compared to the forbidding case. This femtocell throughput enhancement is shown in Figure 7.11 and Figure 7.12 for femtocells F_1 and F_2, respectively.

7.4.2.3 Subroutine Updating Frequency: T_{corpap}

In this section, we investigate the impact in network performance of the updating frequency of coRPAP (Section 5.3), i.e., the subroutine able to compute optimum RB

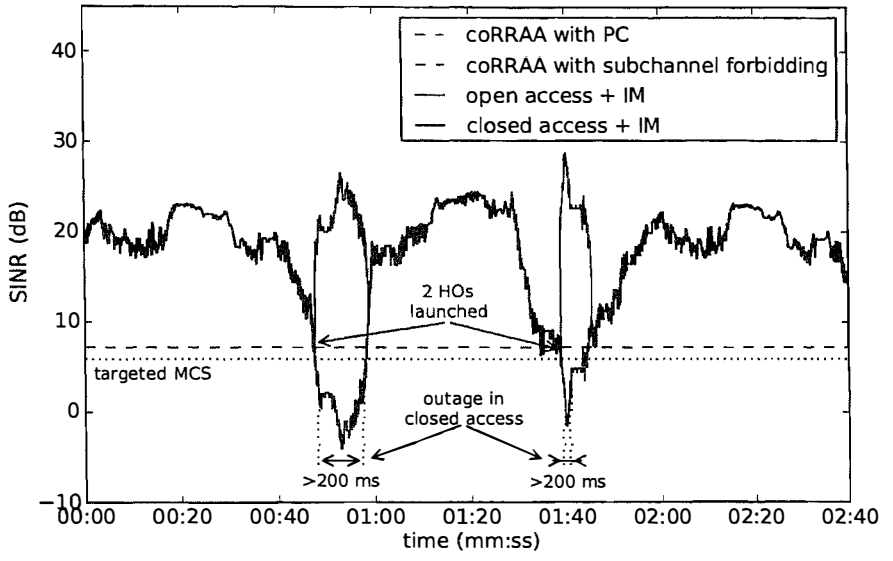

Figure 7.10: SINR of the nonsubscriber of Figure 7.8 versus time when it passes close to femtocells F_1 and F_2, and they are fully loaded.

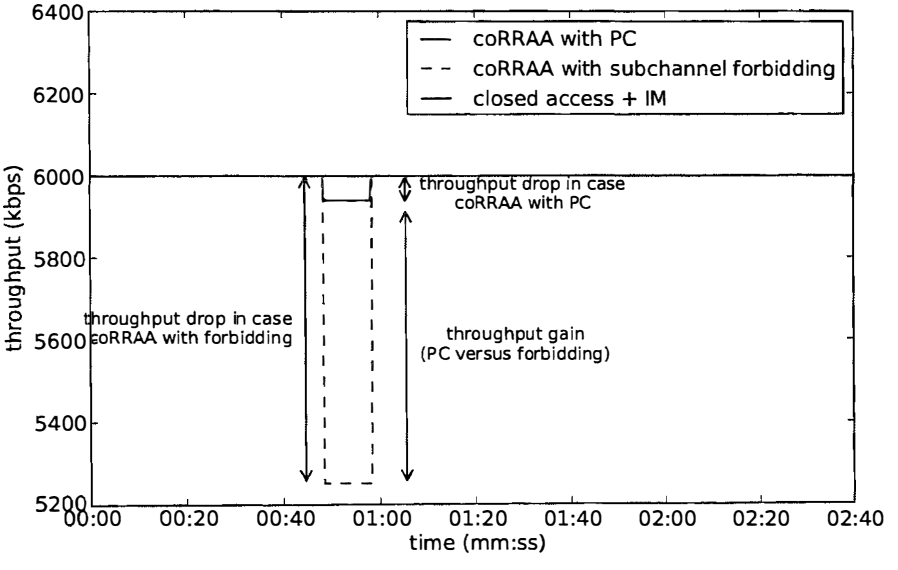

Figure 7.11: Throughput of femtocell F_1 versus time when the nonsubscriber passes close to it.

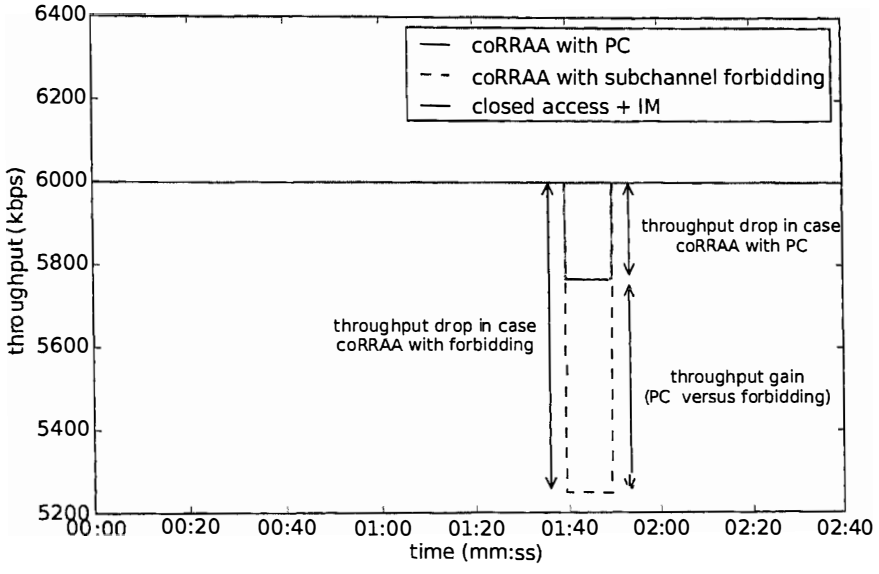

Figure 7.12: Throughput of femtocell F_2 versus time when the nonsubscriber of passes close to it.

and power allocations given a MCS assignment.

Recall that coRPAP updates are triggered in each network cell after a random time uniformly distributed within $[1, T_{corpap}]$ ms after the previous allocation (Section 5.5). Figures 7.13, 7.14 and 7.15 show that increasing T_{corpap} degrades system performance, since the RB and power allocation to users is updated less often. When using coRRAA, because the coverage provided by cells is not continuous due to multi-path (Figure 7.8), often updates of coRPAP are required in order to provide a constant user SINR and cope with user mobility. Figure 7.15 indicates that if T_{corpap} is too large, i.e., 500 ms, coRPAP cannot track the fast fluctuations of the radio channel because of multi-path, and it cannot guarantee that the user SINR will always be larger than the aimed one, thus making likely that users incur outage. On the contrary, Figure 7.13 indicates that, in this case, T_{corpap}=10 ms is sufficient to provide constant SINRs and deal with fading. Figure 7.14 shows that T_{corpap}=50 ms is not fast enough to track channel changes either. These results show that it is crucial to update the radio resource allocation to users as often as possible according to the user mobility and time-variant fading conditions. However, this is possible due to the speed of the proposed network simplex algorithm

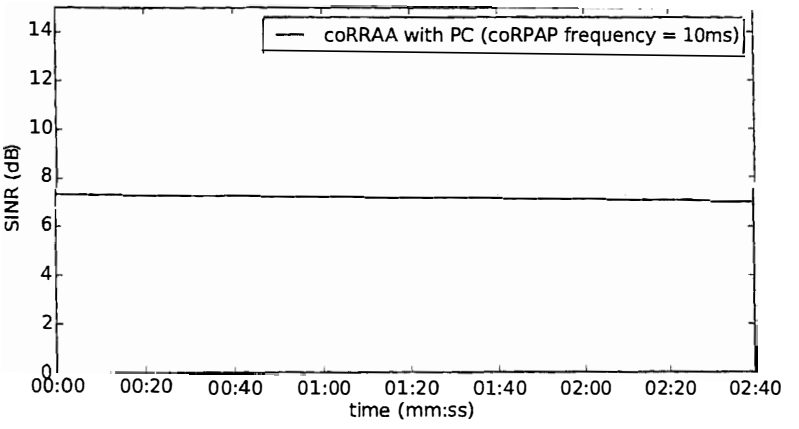

Figure 7.13: SINR of the nonsubscriber of Figure 7.8 versus time when the updating frequency of coRPAP is at most $10\,ms$.

(Section 5.3.1), which can solve coRPAP in less than 1 ms (Section 5.6.2 and 6.4.2).

According to these results, when running coRRAA, each cell independently solves coRPAP after a random time interval uniformly distributed in [1,10] ms after its previous coRPAP updating event. In addition, each cell solves coRAP after a random time interval uniformly distributed in [0.5,1] s after its previous coRAP updating event.

7.4.2.4 System-Level Performance

In this section, the performance of coRRAA with respect to that of closed and open IM-based methods is analysed. This is done under distinct femto penetration densities, i.e., 12.5 %, 25 % and 50 %, which correspond to 16, 32 and 64 femtocells, respectively, as well as femtocell traffic loads, i.e., presented low and high loaded femtocell scenarios. Note that results for low and high loaded femtocell scenarios are in Tables 7.2 and 7.3, respectively.

The performance analysis with regard to different performance metrics follows next:

Number of Handovers or Control Messages

First of all, it must be noted that in closed femtocells, HOs are not permitted. Therefore, these values are neglected in the tables of results, i.e., Tables 7.2 and 7.3.

In all setups, when using open access, the number of HOs increases when the

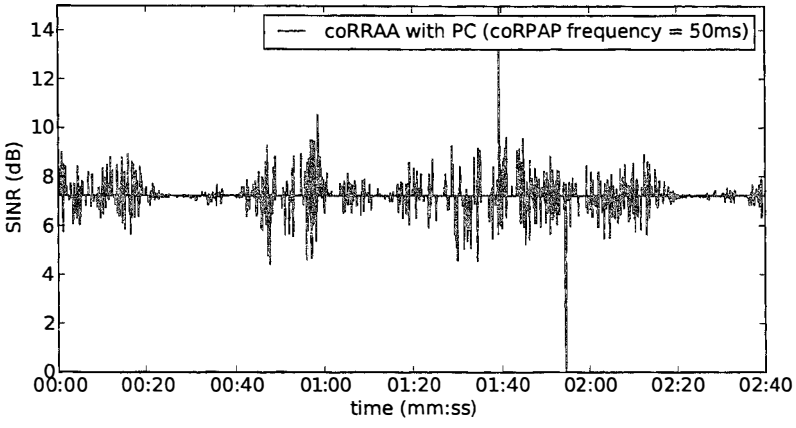

Figure 7.14: SINR of the nonsubscriber of Figure 7.8 versus time when the updating frequency of coRPAP is at most $50\,ms$.

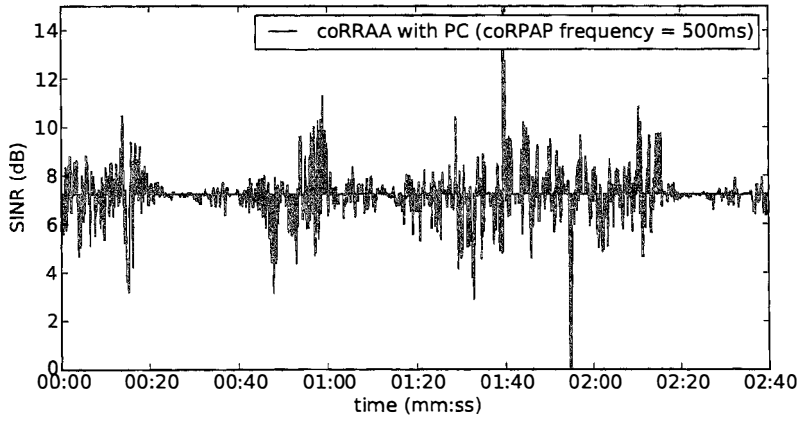

Figure 7.15: SINR of the nonsubscriber of Figure 7.8 versus time when the updating frequency of coRPAP is at most is $500\,ms$.

Table 7.2: Performance comparison for scenario with low loaded femtocells

Femtocell penetration	12.5%			25%			50%		
Access method	Closed + IM	Open + IM	coRRAA	Closed + IM	Open + IM	coRRAA	Closed + IM	Open + IM	coRRAA
HO attempts	-	0	0	-	0	0	-	70	0
Average HO attempts into femtos	-	0	0	-	0	0	-	2.19	0
HO attempts into macrocell	-	0	0	-	0	0	-	35	0
Outages due to HO failure	-	0	0	-	0	0	-	1	0
Outages due to interference	0	0	0	0	0	0	45	0	0
Avrg. nonsubscribers tier throughput [kbps]	2000	2000	2000	2000	2000	2000	1720	1811	2000

In this case, femtocells are not fully loaded. Hence, coRRAA approach can cope with interference without macrocell-femtocell cooperation.

femtocell penetration increases. The more femtocells a nonsubscriber finds in its route, the more hand-ins and hand-outs the network must perform to maintain its connection. Note that when femtocells are not fully loaded and the femtocell penetration is low, the macrocell can deal with cross-tier interference through radio resource management, and there is no need to hand users over from the macrocell to the femtocells (Table 7.2). The number of control messages in coRRAA also increases with femtocell penetration. Note that more messages are needed when using coRRAA with power control than with subchannel forbidding. This is because power constraint $p_k^{c,max}$ has to be recalculated when a user is moving from the femtocell edge and getting closer to the FAP location. (Δw was set to 3 dB for avoiding a continuous recalculation of power constraint $p_k^{c,max}$). However, this transmit power reduction tailored according to user mobility will provide a large gain in femtocell throughput compared to the subchannel forbidding approach, to be shown in this section.

Outages due to Cross-Tier Interference

In all setups, CSG deployments are significantly affected by cross-tier interference, thus resulting in a large number of outages. As soon as a nonsubscriber walks near by a CSG femtocell using the same subchannel, it is severely jammed and falls into outage.

Table 7.3: Performance comparison for scenario with high loaded femtocells

Femtocell penetration	**12.5%**				**25%**				**50%**			
Access method	Closed +IM	Open +IM	coRRAA (fb.)	coRRAA (PC)	Closed +IM	Open +IM	coRRAA (fb.)	coRRAA (PC)	Closed +IM	Open +IM	coRRAA (fb.)	coRRAA (PC)
HO attempts	-	270	64	74	-	628	169	233	-	1267	448	639
Average HO attempts into femtos	-	8.38	4.00	4.63	-	9.72	5.28	7.28	-	9.84	7	9.98
HO attempts into macrocell	-	134	0	0	-	311	0	0	-	630	0	0
Outages due to HO failure	-	2	0	0	-	12	0	0	-	24	0	0
Outages due to interference	110	0	0	0	210	3	0	0	273	10	0	0
Avrg. nonsubscriber tier throughput [kbps]	1307	1977	1999	1999	687	1860	1999	1999	279	1390	1998	1998

In this case, femtocells are now fully loaded. Hence, coRRAA uses the forbidding or power control approach to cope with interference.

:ms the need for new interference avoidance techniques in CSG deployments.

open access case, the number of outages due to cross-tier interference are ly reduced compared to that of the closed access case. This is because non- s are allowed to connect to the strongest cells, turning strong interferers into .ng cells. Nonetheless, when the femtocell penetration grows, some cases of ue to co-tier interference appear. This is because even if a nonsubscriber is to the strongest femtocell, the aggregate of co-tier interference from neigh- :mtocells can disrupt its service, thus creating new outages in the network. : noted that the signal strength of a femtocell outdoors is of the same order of e as the signal strengths of neighbouring femtocells located few meters away. the femtocell penetration is large, co-tier interference becomes a problem too. /er, when using coRRAA, the number of outages due to interference is zero. se, the number of outages does not depend on femtocell penetration density, RAA via message passing is able to 'switch off' multiple interferers at a time ently of their number or position. This user outage avoidance is the main ion of the proposed macrocell-femtocell collaboration.

ges due to Handover Failure

of all, it must be noted that in CSG femtocells, HOs are not permitted. :, these values are neglected in the tables of results, i.e., Tables 7.2 and 7.3.

e open access case, the number of HO failures increases with the femtocell ion and the number of subscribers. It must be noted that according to [114], a 2% probability that an HO attempt results in a dropped call, i.e., outage. e, the more HOs, the more outages. Nevertheless, the number of outages due ilure in open access is much smaller than those due to interference in CSG.)s are not triggered when using the proposed macrocell-femtocell collaboration, due to HO failure are avoided when utilising coRRAA.

subscribers' Throughput

: CSG deployments produce the largest number of nonsubscriber outages due to r interference, they result in the worse average sum nonsubscriber throughput. :ontrary and because it is able to completely avoid all nonsubscriber outages, \ gives the best performance in terms of average sum nonsubscriber throughput. spect to the open access case, because there were some user outages due to

Table 7.4: Average Throughput gain at the femtocells (PC vs. forbidding)

	16 femtocells	32 femtocells	64 femtocells
Average TP gain PC vs. forbidding [kbps]	655.97	610.68	483.60
Average TP gain PC vs. Closed Access [kbps]	-273.03	-311.31	-751.38

Average throughput gain at a femtocell when applying coRRAA with power control with respect to coRRAA with subchannel forbidding.

HO failure, it obtains a performance worse than coRRAA but better than closed-access.

Subscribers' Throughput and Power Control Performance

Table 7.4 indicates the average throughput gain at a given femtocell when utilising coRRAA with power control with respect to coRRAA with subchannel forbidding. These results were obtained from the scenario where all femtocells were fully loaded.

This table shows, in agreement with the results of Figure 7.11, that when power control is used, femtocell throughput is enhanced compared to the forbidding approach. The throughput gain in the interfering femtocell when applying the power control approach compared to the subchannel forbidding one is in average at least 483.60 kbps, which is enough to hold real time services, e.g., VoIP (12.2 kbps), streaming at 256 kbps.

This table also shows that using power control in the interfering femtocells for avoiding nonsubscribers outages comes at the expense of reduced femtocell throughput. In this case, the average femtocell throughput reduction was at most of 751.38 kbps, which is a 12.52 % of the maximum throughput carried per femtocell in closed access. However, since macrocells users have a higher service priority than femtocell ones, trading a 12.52 % femtocell throughput for the avoidance of 273 outages in 300 s is a good business (data in Tables 7.3 and 7.4).

7.4.3 Signalling Overhead

Our macrocell-femtocell cooperation implies the following signalling:

- In the UL, a measurement report in order to indicate to serving macrocell M_m the power of the signals received by nonsubscriber U_u^m from serving macrocell M_m and its neighbouring cells $N_b^m \in \mathcal{N}_m$ in subchannel k, i.e., $w_{u,k}^m$ & $w_{u,k}^b \forall N_b^m \in \mathcal{N}_m$. The size in bits of a measurement report is:

$$Overhead_{UL}^{IHO} = C_u^{intrf} \cdot (d_{ID} + d_w) \tag{7.6}$$

  where C_u^{intrf} denotes the number of interfering femtocells ($|\Upsilon_u|$), and d_{ID} and d_w indicate the number of bits required to encode the identifier of subchannel k and the received signal strength in subchannel k of a neighbouring cell, respectively.

- In the DL, a control message in order to indicate to all interfering femtocell Υ_u the reduction of power Δp_k that has to be applied to the specified subchannel k and for how long ΔT_{PC} it has to be applied.

  The size in bits of a cooperation message is:

$$Overhead_{DL}^{PC} = d_k + d_{\Delta p} + d_{\Delta T_{PC}} \tag{7.7}$$

  where d_k , $d_{\Delta P}$ and $d_{\Delta T_{PC}}$ represent the number of bits required to encode the identifier of subchannel k, and the values of both Δp_k and ΔT_{PC}, respectively.

Also, let us assume that 3 bits are used to encode the identifier of a subchannel d_k (8 subchannels), whereas 10 bits (1024 levels) are utilised for d_{ID}, d_w, $d_{\Delta p}$ and $d_{\Delta T_{PC}}$. Thus, the number of bits needed per measurement report and cooperative message are:

$$Overhead_{UL} = C_u^{intrf} \cdot (d_{ID} + d_w) = 32 \cdot (10 + 10) = 640\,\text{bit} \tag{7.8}$$

$$Overhead_{DL} = d_k + d_{\Delta p} + d_{\Delta T_{PC}} = 3 + 10 + 10 = 23\,\text{bit} \tag{7.9}$$

Note that a large number of interfering femtocells C_u^{intrf} is considered in (7.8), i.e., 32, which is the maximum number of cells that the NCL in UMTS can support.

The UL measurement report is triggered when the SINR $\gamma_{u,k}^m$ of a nonsubscriber U_u^m connected to macrocell M_m in subchannel k is lower than that of its targeted MCS. In the worst case scenario of our system-level simulations, i.e., high loaded femtocells, an average of 9.98 cooperation were triggered per femtocell (simulation time = 300 s). As a result:

- The average UL bandwidth required to carry 9.98 measurement reports of 640 bits each per femtocell in 300 s is 21.29 bps.
- The average DL bandwidth required to to carry 9.98 DL-HIIs of 23 bits each per femtocell in 300 s is 0.77 bps.

Thus, a small bandwidth is needed to carry signaling overhead when using coRRAA. It must also be noted that the signaling needed in coRRAA is lower than in an HO. When performing an HO, all packets stored in the source cell, which belong to the user that is to be handed over, have to be transferred from the source cell to the target cell. When utilising coRRAA, the macrocell only needs to indicate the reduction of power that has to be applied to a subchannel and for how long to all interfering femtocells Υ_u.

7.5 Conclusions

This chapter has presented a novel approach for the avoidance of cross-tier interference in OFDMA two-tier networks. In this approach, macrocells and femtocells make use of a combination of coRRAA and power control techniques. Dynamic system-level simulations confirm that this approach reduce cross-tier interference and user outages in comparison with open and closed access. The implementation details of this novel approach has also been discussed in detail.

The results of the system-level simulations presented above indicate the following facts with regard to our proposed approach:

Conclusion 1: Compared to CSG deployments, DL cross-tier interference towards nonsubscribers is significantly decreased through macrocell-femtocell cooperation.

Conclusion 2: With respect to the open access, since coRRAA does not use HOs, HO attempts, signalling, and thus the risk of outage due to HO failure disappear.

Conclusion 3: In order to reduce the impact of femtocells in existing macrocells, femtocells must be flexible when limiting the throughput of their own subscribers. The interference reduction of nonsubscribers must thus have greater priority than the throughput enhancement of their subscribers. Power control aids to handle interference,

while decreasing the impact to subscribers. The proposed scheme was able to avoid a large number of outages (273 in 300 s) compared to closed access, while reducing the average femtocell throughput only by 12.5 %.

Chapter 8

Discussion

8.1 Trade-offs

This thesis has proposed 3 different architectures for the allocation of radio resources to users in Orthogonal Frequency Division Multiple Access (OFDMA)-based networks. These 3 different architectures, which we will briefly summarise in the following, are based on the same principle, i.e., minimising total transmit power independently at each cell leads the network to self-organise into efficient resource allocation patterns. Also, spatial spectrum reuse is enhanced because users of neighbouring cells with different throughput demands and channel conditions can coexist in the same subchannel.

- In Chapter 4, we proposed a semi-distributed architecture, named enhanced Dynamic Frequency Planning (eDFP), in which subchannels for cell-edge use are allocated in a centralised manner to cells, and cells independently allocate radio resources to users, taking the commands of the central broker into account. The principle of minimising cell transmit power is only applied at the cell-level.

- In Chapter 5, we proposed an autonomous Radio Resource Allocation Architecture (auRRAA), where cells independently allocate resources to users based on local knowledge of subchannel usage in neighbouring cells fed back by associated users. In Chapter 5, the performance of auRRAA was analysed for macrocell roll-outs, while in Chapter 6 for femtocell deployments.

- In Chapter 5, we proposed a cooperative Radio Resource Allocation Architecture

(coRRAA), where cells are also able to exchange information through a message passing approach in order to coordinate their cell-edge radio resource assignments. In Chapter 5, the performance of coRRAA was analysed for macrocell roll-outs, while in Chapter 6 for femtocell deployments.

In Chapter 7, this cooperative approach was extended to deal with cross-tier interference in macrocell-femtocell scenarios.

Because these 3 different approaches are based on different network architectures, from a centralised architecture (eDFP) to a fully distributed one (auRRAA) passing by a cooperative one that involves message exchange only between neighbouring cells (coRRAA), the proposed approaches have a different performance-cost trade-off and they may be used for distinct roll-out types.

In macrocell scenarios and according to Table 5.4, the performance improvement of eDFP over coRRAA was of 2.37 average connected users and 0.88 Mbps (1.51 %), whereas over auRRAA was of 8.54 average connected users and 4.71 Mbps (8.64 %).

coRRAA provided a significant improvement in network performance over all methods used for comparison. Specifically, coRRAA gave an average performance improvement over FFRS3-B of 48.29 connected users and 9.86 Mbps (20.36%). Also, the average performance improvement over Stolyar's approach was about 35.55 connected users and 9.28 Mbps (18.96%).

auRRAA also provided a large improvement in network performance over all methods used for comparison. Specifically, auRRAA gave an average performance improvement over FFRS3-B of 42.12 connected users and 6.03 Mbps (12.45%). Also, the average performance improvement over Stolyar's approach was about 29.38 connected users and 5.46 Mbps (11.14%).

However, although eDFP provided the best performance, coRRAA and auRRAA may be more practical for network roll-outs because they require a few or no signalling among cells, respectively. Moreover, they do not require a centralised resource broker, avoiding threatening single points of failure and bottle necks. This fact may facilitate the network planning and deployment to Radio Frequency (RF) engineers and may also reduce both CAPital EXpenditure (CAPEX) and OPerational EXpenditure (OPEX). More information on the overhead incurred by coRRAA and auRRAA can be found in Section 5.6.3.8.

In femtocell scenarios and according to Table 6.3, coRRAA also resulted in a best performance than auRRAA since it allows inter-cell communication and therefore a better inter-cell interference mitigation through High Interference Indicators (HIIs). (Note that the signalling overhead incurred by coRRAA is small (Section 6.4.3.7)). But, the performance of auRRAA was close to that of coRRAA, i.e., it was 1.37 and 3.99 % worse in terms of average connected users and network throughput, respectively.

coRRAA and auRRAA significantly outperformed other method proposed in literature, e.g., network listening mode and Interference Minimisation (IM)-based methods, For example, our auRRAA provided a performance improvement of 9.16 and 12.01 % in terms of average connected users and average network throughput, respectively, compared to IM-based method.

Since auRRAA does not require any signalling between femtocells, this technique may be more appealing for pure femtocell roll-outs where back-haul capacity may not be guaranteed. However, Chapter 7 has shown that macrocell-femtocell cooperation via message exchange may help to significantly reduce cross-tier interference and outages. Hence, it may be better to use an inter-cell cooperative approach whenever is possible. Indeed, providing a reliable cooperation among macrocells and femtocells is currently a hot research topic in Long Term Evolution (LTE)-Advanced standardisation [116]. For example, the exchange of control messages between macro BSs and femto BSs through the wireless broadcast channels or the use of users for relaying data between neighbouring cells are being investigated [116]. For instance, victim macrocell users can be determined by macrocells by utilising their user Channel Quality Indicators (CQIs), and their identity may be signalled by macrocells to femtocells via back-haul connection. This method is inline with the proposed cooperative approach in this thesis (Chapter 7).

Figure 8.1 summarises the performance-signalling trade-offs described above, while Figure 8.2 indicates our recommendation for the use of eDFP, coRRAA and auRRAA.

8.2 Limitations

The proposed architectures here, as mentioned earlier, are based on the same objective, i.e., minimising transmit power independently at each cell while meeting user demands.

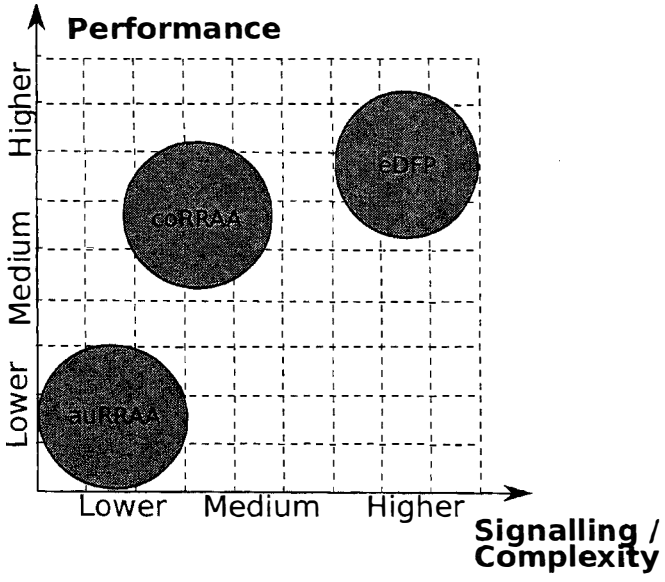

Figure 8.1: Performance-Signalling trade-off of the proposed schemes. Note that in this case a larger signalling also involves a more complex and costly network architecture.

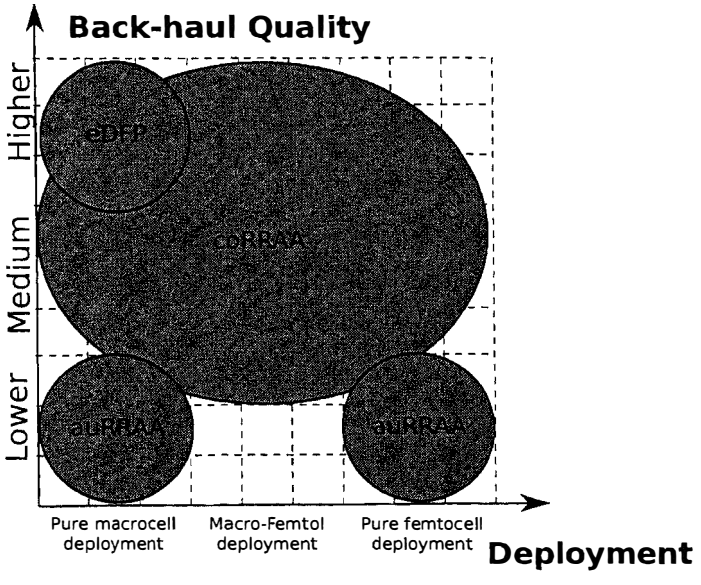

Figure 8.2: Recommendation for the use of eDFP, coRRAA and auRRAA in different scenarios with different back-haul quality.

In the following, we discuss the limitations of this optimisation approaches.

User distribution If users are not uniformly distributed within cells, but they are pushed towards their cell-edges, users will require high powers to deal with increased path losses, and therefore, neighbouring cells will not identify scheduling opportunities, i.e., subchannel with low interference, for their own cell edge-users. In this situation, under high load conditions, users will be dropped because they cannot co-exist in the same subchannel.

Let us note that in our experiments, users were uniformly distributed within cell coverage areas, which seems to be more realistic than having all user at the cell-edge. Also, note that operators tend to deploy their macro BS as close as possible to hot spots to provide better user experience.

Our resource allocation approach could be enhanced with a time domain scheduler that ensures that all users simultaneously scheduled do not have bad channel conditions.

User throughput If a large percentage of users requires a large throughput, e.g., due to peer to peer applications, users will require high powers to achieve high-order modulations, and hence, neighbouring cells will not identify scheduling opportunities, i.e., subchannel with low interference, for their own cell edge-users. In this situation, under high load conditions, users will be dropped because they cannot co-exist in the same subchannel.

Let us note that in our experiments, all users had a throughput demand of 250 kbps. This user throughput is adequate to carry standard video and streaming applications and is larger than the demanded by common Voice over IP (VoIP) services (12.2 kbps) or real-time radio streaming (64 kbps).

Our resource allocation approach could be enhanced with a time domain scheduler that ensures that all users simultaneously scheduled do not require large throughputs.

Updating time of Modulation and Coding Schemes (MCSs) Let us recall that coRAP and auRAP, when solved using Tabu Search (TS) in macrocell scenarios or using a smart exhaustive search in femtocell scenarios, could be solved in about 0.5 s. Therefore, the updating time of user MCSs is no less than 0.5 s. On the other hand, subchannels and power are assigned to users in a much more regular basis (milliseconds)

to deal with the fast channel fluctuations.

It may occur that updating user MCSs every 0.5 s might be not responsive enough for vehicular users moving at high speds, e.g., 60 km/h. Therefore and as future work, we will attempt to solve coRAP and auRAP utilising faster optimisation approaches, which will allow the updating of user MCSs in a much more frequent basis.

Chapter 9

Conclusions and Future Work

9.1 Conclusions

This thesis has shed new light on the development of novel self-organising techniques for the fourth generation of mobile networks, in particular for the avoidance of inter-cell interference in Orthogonal Frequency Division Multiple Access (OFDMA) networks. This thesis has presented new practical approaches to the inter-cell interference problem for both macrocell and femtocell systems and for the deployment of two-tier networks by means of the design of novel frameworks and the usage of mathematical optimisation.

Our contributions are structured in three blocks that deal with different types of inter-cell interference problems that arise in both macrocell and femtocell deployments and their combination in two-tier networks. First of all, the fundamental concepts of self-organisation, OFDMA-based networks and femtocell deployments were introduced. Thereafter, an overview of the different approaches existing in literature for the avoidance of inter-cell interference in macrocell and femtocell deployments was presented. Moreover, our discussion concluded that the available resource allocation schemes cannot reasonably satisfy user requirements for the fourth generation of mobile networks. Thus, in order to overcome the shortcomings of the available approaches in literature, different models, architectures and optimisation schemes were proposed in this thesis.

In literature, dynamic subchannel assignments with equal power per subcarrier are usually preferred to complex joint subchannel and power assignments due to mathematical tractability and easier implementation. Traditional wisdom also assumes that the

capacity improvement due to the allocation of different powers to different subchannels is low in scenarios with a wide range of users with diverse signal quality requirements. In this thesis, we have shown that this is not the case in realistic deployments with a limited user number, and that performance can be improved by allocating different transmit powers to different subchannels according to user requirements and positions.

This thesis has researched the joint allocation of Modulation and Coding Schemes (MCSs), subchannels and transmit power to users in macrocell and femtocell networks, and has shown that minimising transmit power independently in each network cell leads the entire system to self-organise into an efficient radio resource assignment pattern. Following this principle, three different architectures have been proposed:

- A semi-distributed architecture, named enhanced Dynamic Frequency Planning (eDFP), where subchannels for cell-edge use are allocated in a centralised manner to cells, and then cells independently allocate radio resources to users.
- An autonomous Radio Resource Allocation Architecture (auRRAA), where cells independently allocate resources to users based on local knowledge of subchannel usage in neighbouring cells fed back by their associated users.
- A cooperative Radio Resource Allocation Architecture (coRRAA), where cells additionally are able to exchange information via a message passing approach to coordinate assignments.

eDFP has been shown more powerful from an optimisation viewpoint due to its centralised nature, providing a better inter-cell interference avoidance across the network. However, decentralised architectures that involve much less signalling and simpler network roll-outs, i.e., coRRAA and auRRAA, gave a performance not far from eDFP. coRRAA outperformed auRRAA due to its better inter-cell interference coordination provided by message exchange among cells. However, auRRAA may be more practical in scenarios where cells cannot rely on back-haul or inter-BS interfaces, e.g., femtocells. Moreover, in two-tier networks, the need of inter-BS cooperation has been shown important to mitigate cross-tier interference. Utilising a form of inter-BS coordination, the transmissions of higher priority macrocell users are scheduled in resources where cross-tier interference from femtocells is mitigated through power control commands.

According to system-level simulations, the proposed self-organising architectures provide a high degree of inter-cell interference mitigation in OFDMA-based networks.

They outperformed random assignments as well as traditional frequency reuse schemes. They also significantly outperformed cutting-edge approaches such as [53], [63] and [68] in macrocell and femtocell environments where the loads of cells were high and dynamic. These results in conjunction with the reduced amount of time incurred by the proposed optimisation methods when computing the solutions of intricate optimisation problems, make these approaches an efficient option for the self-organisation of cellular networks.

9.2 Future Work

Although much time was spent on developing these models and self-organising approaches further possible improvements and applications remain to be investigated. Future research directions are introduced in the following:

Convergency/stability With regard to coRRAA and auRRAA, distributed resource allocation algorithms may lead to unstable decisions among interfering entities [120], e.g., cells may continuously change their resource allocations as response to changes in resource allocations of neighbouring cells, hence leading to unstable assignments. Future work will attempt to analyse the convergence of the proposed decentralised transmit power optimisation towards efficient solutions, and derive under which conditions stability can be guaranteed. Power control theory could be useful in this task.

Optimisation methods With regard to coRRAA and auRRAA, future work will attempt to find even faster solutions for the joint MCS, subchannel and transmit power allocation problem that allow proposed architectures to work on the basis of feedback, i.e., milliseconds. Thus, we are interested in replacing metaheuristics by faster methods and studying possible enhancements based on basic principles of optimisation theory such as the duality and convexity properties.

Fundamental limits Stochastic geometry is a powerful modelling tool that has been used in literature to derive fundamental limits of femtocell deployments [121] [122], e.g., minimum macro BS-to-femto BS distance in co-channel roll-outs to ensure a given outage probability to macrocell and femtocell users, maximum femtocell transmit power, impact of sectorised antennas, etc. However, due to the nature of stochastic geometry

only simple allocation schemes can be considered, e.g., random, aloha, time hopping. We are interested in quantifying the improvements that sophisticated algorithms such as coRRAA or auRRAA can have in fundamental limits derived by stochastic geometry.

Coordinated Multi-Point transmission/reception (CoMP) Future work will attempt to enhance the proposed inter-BS coordination adding CoMP into our model. Making use of CoMP, several cells may coordinate their data transmissions to serve those users located in between cells and therefore suffering from low signal qualities. Utilising this approach, cell-edge inter-cell interference could be significantly mitigated, because neighbouring cells are turned from being interferers to becoming serving cells. In a similar way, macrocells and femtocells may also coordinate resource assignments utilising CoMP principles to enhance network performance and mitigate user outages. However, because the same information should be transmitted and/or received at the same time in the same subchannel in neighbouring cells, CoMP represents a challenge from the coordination view point. Thus, CoMP schemes involving both macrocells and femtocells are an interesting research topic.

Appendix A

Techniques Used for Comparison

A.1 Ronald's Approach

In this section, we describe the algorithm presented in [53] referred to as Ronald's approach. For further details refer to [53].

In this case, the channel assignment problem has been studied in the context of graph multi-colouring.

The first step in this graph-based approach is to construct an interference graph, which is comprised of nodes representing users and edges representing the interference between two users. Whether two nodes are connected by an edge is determined by the topology of users and the used fractional frequency reuse scheme. For instance, since FFRS-A and FFRS-B (Section 2.1.2) have different resource assignment strategies, they also have different interference graphs.

The graph construction rule for FFRS-A and FFRS-B is described in Figure A.1 and Figure A.2, respectively.

Thereafter, the second step in this graph-based approach is to colour the nodes in the interference graph. A colour corresponds to a subchannel, and the colouring of nodes is equivalent to the assignment of subchannels to users. A colouring is proper if the colouring constrain is met: any two neighbouring nodes, i.e., nodes connected by an edge in the graph have different colours.

The graph colouring rule for both FFRS-A and FFRS-B is described in Figure A.3.

THE GRAPH CONSTRUCTION RULE FOR FFR-A

Node a and node b in the interference graph are connected by an edge if:

A1e MS a and MS b are users of the same cell; or

A2. MS a is a cell-edge user of cell i and MS b is a cell-edge user of cell j, where cell i and cell j are neighbors[a]; or

A3. MS a is a cell-center user of cell i and MS b is a cell-edge user of cell j, or, MS a is a cell-edge user of cell i and MS b is a cell-center user of cell j, where cell i and cell j are neighbors.

Otherwise, node a and node b are not connected by an edge.

[a]Two cells are *neighbors* if they are physically adjacent to each other. In a typical hexagonal deployment, a cell has six neighbors.

Figure A.1: Graph construction rule for FFRS-A [53].

THE GRAPH CONSTRUCTION RULE FOR FFR-B

Node a and node b in the interference graph are connected by an edge if:

B1. MS a and MS b are users of the same cell; or

B2. MS a is a cell-edge user of cell i and MS b is a cell-edge user of cell j, where cell i and cell j are neighbors.

Otherwise, node a and node b are not connected by an edge.

Figure A.2: Graph construction rule for FFRS-B [53].

THE MODIFIED BRÉLAZ'S ALGORITHM FOR COLORING GRAPHS

1. Select from the unexamined subgraph (or initially, the entire graph) a node x whose available color set, $a(x)$, is of minimum size. The $a(x)$ is defined as the set of colors that may be used to color node x such that the coloring constraint is respected.
2. If there are ties, break ties by selecting one whose degree[a] is maximum in the unexamined subgraph. If there are still ties, break ties arbitrarily.
3. Color the selected node x with color randomly selected from $a(x)$. If $a(x)$ is empty, leave the node uncolored.
4. Repeat 1–3 until all nodes are examined.

[a]The *degree* of a node is the number of edges incident to the node

Figure A.3: Graph colouring rule for both FFRS-A and FFRS-B [53].

A.2 Hussain's Approach

In this section, we describe the algorithm presented in [63] referred to as Hussain's Approach. For further details refer to [63].

Unlike the static Fractional Frequency Reuse Schemes (FFRSs), where users and subcarriers are partitioned into two groups, in [63], known as super and regular groups, Hussain's dynamic FFRS only partitions subcarriers into two different physical groups. Among users, there are no rigid boundaries between the super and the regular group. Therefore, all users of a Base Station (BS) are virtual members of both user groups. The super group covers the whole BS coverage area and the subcarriers allocated to it can be assigned to any user in the BS coverage area. The regular group also covers the whole BS coverage area, however it is further partitioned into 3 sectors (Figure A.4). The subcarriers assigned to a sector are available for scheduling to the inner and the cell edge users falling within the boundaries of the sector.

Subcarriers are distributed between the groups and the sectors belonging to the regular group by Hussain's centralised algorithm. Subcarriers assigned to the super and the sectors within the regular groups are orthogonal.

Note that in our implementation, the minimum resource scheduling unit is the subchannel rather than the subcarrier. The distribution of subchannels to geographical regions is replicated for all the BSs in the grid. The scheme uses a greedy approach that performs assignments so that system throughput for the whole grid is increased. Furthermore, the algorithm considers the minimum data rate requirements of users so that the allocated subchannels are able to satisfy the load in their respective regions. The pseudo-code of the proposed centralised algorithm is presented in Figure A.5, where i, j, l and k are iterators for users, subchannels, sectors and cells, respectively. In the following discussion, reference to step number is to line numbers in Figure A.5. The scheme requires, as input, average achievable rates for all users on all subchannels in the super and regular group settings, that is, $R_{i,j}^{sup}$,$R_{i,j}^{reg}$, and the minimum data rate demands C_i for each user i in the network.

The scheme initialisation phase declares variables and computes utility values of the subchannels. Note that variable g_l is the assigned rate of a sector. Its value is updated after assigning each subchannel in the main loop, exactly, in steps 5 and 7.

The utility parameters, W_j^{sup} and $W_j^{l,reg}$, measure the utility of a generic subchannel j assigned to either the super group or lth sector of the regular group, respectively. These values are computed assuming that subchannels are time multiplexed between users and summed for all BSs in the grid.

Variable $U_j^{l,reg}$ is the fractional utility gain if subchannel j is removed from the super group and allocated to sector l of the regular group. Thus, a negative value of $U_j^{l,reg}$ for all l means that the allocation of the subchannel to any sector of the regular group lowers the system data rate. Then, the scheme assigns it to the super group (step 5). Because of the overlap of users, the assigned subchannel is available to the users of all sectors in the regular group. As a result, the assignment to the super group increases the allocated data rates of the regular group sectors. The scheme incorporates this fact in step 5 when it updates g_l by a fraction of W_j^{sup} assuming time multiplexing of the subchannel by the respective users.

The main part of the algorithm consists of a loop that iterates on the subchannels. During the initialisation phase, the scheme assigns all subchannels to the super group. In the main loop, it iterates on subchannels, according to descending order of $U_j^{l,reg}$, and attempts to assign the subchannel that increases the system data rate the most to a sector in the regular group. If this sector exits, it assigns the subchannel to it, increases the rate for the sector and updates output variable $x_j^{l,reg}$ (steps 6 and 7). Otherwise, the algorithm leaves the subchannel to the super group (step 5).

The fairness measure is added in step 2 and 3 by a simple condition. During every iteration, the algorithm first looks for the sectors which are lacking in radio resources such that their allocated data rates are less than their required demand. If such sectors are found, then it considers only them in the next allocation steps during the iteration. However, if all sectors have sufficient radio resources to satisfy their required load, then it behaves as greedy scheme and considers all sectors in the next allocation steps. Therefore, when all sectors are considered, then the one that increases the most system data rate will be assigned the subchannel.

Finally, the central algorithm forwards the subchannel assignments to every BS, where a copy of RB and Power Allocation Problem (RPAP) (Section 4.3) operates, in order to allow a fair comparison with enhanced Dynamic Frequency Planning (eDFP).

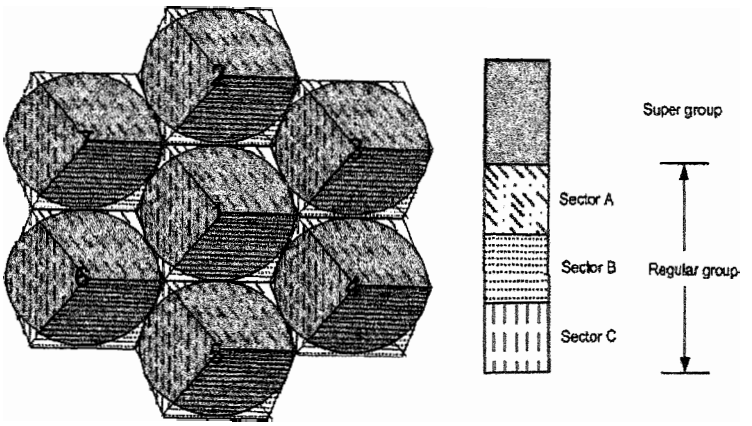

Figure A.4: Fractional Frequency Reused based cell models[63].

Inputs: $R_{i,j}^{sup}$, $R_{i,j}^{reg}$, $C_i \quad i = 1 \cdots M_c, \quad j = 1 \cdots N$

Outputs: x_j^{sup}, $x_j^{l,reg}, \quad j = 1 \cdots N, \quad l = 1 \cdots L$

Initialization: $x_j^{l,reg} = 0, \; g^l = 0, \quad j = 1 \cdots N, \quad l = 1 \cdots L$

$$W_j^{sup} = \sum_{k=1}^{K} \left(\frac{\sum_{i \in \Upsilon_k} R_{i,j}^{sup}}{M_k} \right), \quad \forall j \quad \text{and} \quad W_j^{l,reg} = \sum_{k=1}^{K} \left(\frac{\sum_{i \in \Upsilon_k^l} R_{i,j}^{reg}}{M_k^l} \right), \quad \forall j, \; l$$

$$U_j^{l,reg} = \frac{W_j^{l,reg} - W_j^{sup}}{\max_l \left(W_j^{l,reg} \right)}, \quad l = 1 \cdots L, \quad j = 1 \cdots N$$

$C^l = \sum_{k=1}^{K} \sum_{i \in \Upsilon_k^l} C_i \quad \forall l$ //rate requirements per sector

$Z = \{1, \cdots, N\}, \quad \mathcal{L} = \{1, \cdots, L\}$ //sets of subcarriers and sectors, respectively

1. FOR j=1 : N do //channel iteration
2. Find set of sectors, $\mathcal{L}'$, that satisfy $C^l - g^l > 0, \quad l \in \mathcal{L}$
3. IF $\mathcal{L}' == \{\}$ THEN $\mathcal{L}' = \mathcal{L}$ ENDIF
4. Find sector subcarrier pair (l^*, j^*) that satisfies $\max_{l', j} (U_j^{l', reg}), \quad l' \in \mathcal{L}', \quad j \in Z$
5. IF $U_{j^*}^{l^*, reg} < 0$ THEN $g^l = g^l + W_{j^*}^{sup} \frac{M^l}{M_c}, \quad l \in \mathcal{L}$
6. ELSE $x_{j^*}^{l^*, reg} = 1$ //assign j^* subcarrier to l^* sector
7. $g^{l^*} = g^{l^*} + W_{j^*}^{l^*, reg}$ //update assigned rate for l^* sector
8. ENDIF
9. Remove j^* from Z
10. End FOR
11. $x_j^{sup} = \vee \left(x_j^{l,reg} \right), \quad j = 1 \cdots N, \quad \forall l$

Figure A.5: Pseudocode for centralised dynamic subchannel allocation algorithm [63].

A.3 Stolyar's Approach

In this section, we describe the algorithm presented in [68] referred to as Stolyar's approach. For further details refer to [68]s

In this scheme and similarly to our proposed schemes coRRAA and auRRAA, cells target at minimising their transmit powers, whereas meeting the rate demands of their users. However, the authors use a different system model and also frequency hopping.

Because Stolyar's approach was devised for a general OFDMA framework in which subcarriers are grouped into sub-bands, adaptation to LTE constraints was needed. In our implementation of Stolyar's approach, we considered a sub-band to be an RB, i.e., instead of 16 subcarriers per sub-band, in our case we used 12 subcarriers per RB. Random frequency hopping was implemented by permuting in every subframe the sub-carrier indices independently across the distinct RBs and sectors. Frequency hopping for a given transmission is restricted to be across subcarriers within the RB to which it is assigned to. Moreover, users are assigned only to subcarriers in a single sub-band.

In a given cell, for each user, the cell's BS can choose which RB to assign it to. Thus, given the inter-cell interference levels, currently 'observed' by user terminal U_u^m, the BS knows, i.e., it can estimate from user feedback, that it would need to allocate $m_{u,k}$ subcarriers and average power $p_{u,k}$, if this user U_u^m is to be assigned to RB k. Note that the same power $p_{u,k}$ is allocated to every subcarrier assigned to user U_u^m. User Channel Quality Indicators (CQIs) are utilised to derive the transmission MCSs, number of subcarriers $m_{u,k}$, and transmit power $p_{u,k}$ required in RB k to satisfy a user. In more details, among the various combinations of $m_{u,k}$ and $p_{u,k}$ that can satisfy the user rate demand, the one that requires the least number of subcarriers is used [68]. Note that less subcarriers implies using more power per subcarrier and higher MCSs.

A good user-to-RB assignment, from the overall system performance point of view, would be one producing user-to-RB assignments in the cells, allowing the system to support as many users as possible. Hence, since $m_{u,k}$ and $p_{u,k}$ can be pre-computed, the optimisation problem assigns users to RBs so that the sum transmit power of the cell for all users/RBs is minimised, while meeting the throughput demands of its users. Any user-to-RB assignment should be such that the RB capacities are not exceeded, and the total power used in all sub-bands is below the maximum cell available power.

References

[1] "ETSI GSM specifications," Series 01-12.

[2] A. Eisenblätter, "Frequency assignment in GSM networks: Models, heuristics, and lower bounds," Ph.D. dissertation, Technische Universität Berlin, Fachbereich Mathematik, Berlin Germany, 2001.

[3] A. Eisenblätter, H.-F. Geerdes, T. Koch, A. Martin, and R. Wessäly, "UMTS Radio Network Evaluation and Optimization Beyond Snapshots," *Mathematical Methods of Operations Research*, vol. 63, no. 1, pp. 1–29, February 2006.

[4] H.-H. Chen, *The Next Generation CDMA Technologies.* John Wiley and Sons, LTD, July 2007.

[5] H. Holma and A. Toskala, *WCDMA for UMTS: Radio Access for Third Generation Mobile Communications.* John Wiley and Sons, LTD, July 2004.

[6] J. Laiho, A. Wacker, and T.Novosad, *Radio Network Planning and Optimisation for UMTS*, 2nd ed. John Wiley and Sons, LTD, December 2006.

[7] H. Holma and A. Toskala, *HSDPA/HSUPA for UMTS: High Speed Radio Access for Mobile Communications.* John Wiley and Sons, LTD, April 2006.

[8] IEEE Standard for Local and metropolitan area networks Part 16: Air Interface for Fixed and Mobile Broadband Wireless Access Systems Amendment 2: Physical and Medium Access Control Layers for Combined Fixed and Mobile Operation in Licensed Bands and Corrigendum 1, IEEE Std 802.16e-2005 and IEEE Std 802.16-2004/Cor 1-2005 (Amendment and Corrigendum to IEEE Std 802.16-2004) Std., 2006.

[9] 3GPP TR 25.913, "Requirements for evolved UTRA (E-UTRA) and evolved UTRAN (E-UTRAN)," v.8.0.0, January 2009.

[10] H. Lui and G. Li, *OFDM-Based Broadband Wireless Networks Design and Optimization.* John Wiley and Sons, LTD, 2005.

[11] A. Parkin-White, "Femtocell opportunities in 3G network evolution scenarios," in *Femtocell Europe 2008*, London, UK, June 2008.

[12] Institute of Electrical and Electronics Engineers (IEEE), http://www.ieee.org.

[13] 3rd Generation Partnership Project (3GPP), http://www.3gpp.org.

[14] Next Generation of Mobile Networks (NGMN), http://www.ngmn.org.

[15] Self Optimisation and self-ConfiguRATion in wirelEss networkS (SOCRATES), http://www.fp7-socrates.eu.

[16] INFSO-ICT-216284 SOCRATES, "Use Cases for Self-Organising Networks, D2.1," SOCRATES Project, SOCRATES, Tech. Rep., 2008.

[17] O. Linnell, M. Amirijoo, H. van den Berg, R. Litjens, A. Eisenblatter, C. Blondia, T. Kurner, N. Scully, J. Oszmianski, and C. Schmeltz, "Self-Organisation in Future Mobile Communication Networks," in *ICT Mobile Summit 2008*r, Stockholm, Sweden, June 2008.

[18] NGMN, "NGMN Informative List of SON Use Cases," Tech. Rep., April 2007.

[19] — , "NGMN Recommendation on SON and O&M Requirements," Tech. Rep., December 2008.

[20] 3GPP TS 36.211, "Long Term Evolution physical layer; General description," v.1.0.0, March 2009.

[21] E. Lawrey, "The suitability of OFDM as a modulation technique for wireless telecommunications, with a CDMA comparison," Master's thesis, Computer Systems Engineering at James Cook University, Tropical Northern Queensland, Australia, October 1997.

[22] H. Lui and G. Li, *OFDM-Based Broadband Wireless Networks Design and Optimization.* John Wiley and Sons, LTD, 2005.

[23] 3GPP TR 25.913, "Requirements for Evolved UTRA (E-UTRA) and Evolved UTRAN (E-UTRAN)," v.8.0.0, December 2008.

[24] 3GPP TR 25.912, "Feasibility Study for evolved Universal Terrestrial Radio Access (UTRA) and Universal Terrestrial Radio Access Network (UTRAN)," v.8.0.0, December 2008.

[25] 3GPP TS36.211, "Evolved universal terrestrial radio access (EUTRA); Physical channels and modulation," v.8.0.0, September 2007.

[26] H. Holma and A. Toskala, *LTE for UMTS - OFDMA and SC-FDMA Based Radio Access.* John Wiley and Sons, Ltd., 2009.

[27] E. Dahlman, S. Parkvall, J. Sköld, and P. Beming, *3G EVOLUTION HSPA and LTE for Mobile Broadband*, 2nd ed. Elsevier, August 2008.

[28] J. G. Andrews, A. Ghosh, and R. Muhamed, *Fundamentals of WiMAX Understanding Broadband Wireless Networking.* Prentice Hall, 2007.

[29] K.-C. Chen and J. R. B. de Marca, *Mobile WiMAX.* John Wiley and Sons, LTD, February 2008.

[30] 3GPP TS 25.331, "Radio resource control (RRC); Protocol specification," v.8.2.0, April 2008.

[31] R. Kwan, C. Leung, and J. Zhang, "Multiuser Scheduling on the Downlink of an LTE Cellular System," in *Research Letters in Communications*, vol. 2008, Article ID 323048, 2008, p. 4.

[32] 3GPP TS 36.133, "Evolved Universal Terrestrial Radio Access (E-UTRA); Requirements for support of radio resource management," v.8.8.0, 3GPP, December 2009.

[33] Ericssson, "Introduction of automatic neighbour relation function," 3GPP R3-072014, Tech. Rep., September 2007.

[34] M. Amirijoo, P. Frenger, F. Gunnarsson, H. Kallin, J. Moe, and K. Zetterberg, "Neighbor Cell Relation List and Physical Cell Identity Self-Organization in LTE," in *IEEE International Conference on Communications Workshops (ICC)*, New Orleans, USA, May 2008, pp. 37 – 41.

[35] G. Mansfield, "Femtocells in the US Market - Business Drivers and Consumer Propositions," in *FemtoCells Europe*. London, UK: ATT, June 2008.

[36] J. Cullen, "Radioframe presentation," in *FemtoCells Europe*, London, UK, June 2008.

[37] J. Zhang and G. de la Roche, *Femtocells: Technologies and Deployment*. John Wiley and Sons, LTD, January 2010.

[38] D. N. Knisely, T. Yoshizawa, and F. Favichia, "Standardization of Femtocells in 3GPP," *IEEE Communications Magazine*, vol. 47, no. 9, pp. 68–75, September 2009.

[39] V. Chandrasekhar and J. G. Andrews, "Femtocell networks: A survey," *IEEE Communication Magazine*, vol. 46, no. 9, pp. 59–67, September 2008.

[40] D. López-Pérez, A. Valcarce, G. de la Roche, and J. Zhang, "OFDMA Femtocells: A Roadmap on Interference Avoidance," *IEEE Communications Magazine*, vol. 47, no. 9, pp. 41–48, September 2009.

[41] Femto Forum, "Interference Management in UMTS femtocells," Tech. Rep., December 2008.

[42] 3GPP TS 22.220, "Technical Specification Group Services and System Aspects; Service requirements for Home NodeBs and Home eNodeBs," V.9.0.0, March 2009.

[43] A. Valcarce, D. López-Pérez, G. De La Roche, and J. Zhang, "Limited Access to OFDMA femtocells," in *IEEE Personal, Indoor and Mobile Radio Communications (PIMRC)*, Tokyo (Japan), September 2009.

[44] D. Choi, P. Monajemi, S. Kang, and J. Villasenor, "Dealing with Loud Neighbors: The Benefits and Tradeoffs of Adaptive Femtocell Access," in *IEEE Global Telecommunications Conference (GLOBECOM)*, December 2008, pp. 1–5.

[45] M. Beach, *et al.*, "A Study into the Application of Interference Cancellation Techniques," Ofcom, Tech. Rep., Apr. 2006, Report No: 72/06/R/038/U.

[46] A. B. Carleial, "A case where interference does not reduce capacity ," *IEEE Transactions on Information Theory*, vol. IT-21, pp. 569–570, September 1975.

[47] J. G. Andrews, "Interference Cancellation for Cellular Systems: A Contemporary Overview," *IEEE Wireless Communications*, vol. 12, no. 2, pp. 19–29, 2005.

[48] E. Celal, K. Mutlu, and D. Hakan, "Iterative Joint Tone-Interference Cancellation and Decoding for MIMO-OFDM," *IEEE Transactions on Vehicular Technology*, vol. 57, no. 5, pp. 2843–2855, September 2008.

[49] W. Webb, *Wireless Communications: The Future*. John Wiley and Sons, LTD, 2007, chi 6, pp. 73–74.

[50] S. E. Elayoubi and B. Fourestie, "On frequency allocation in 3G LTE systems," in *Personal, Indoor and Mobile Radio Communications, 2006 IEEE 17th International Symposium on*, 2006, pp. 1–5. [Online]. Available: http://dx.doi.org/10.1109/PIMRC.2006.254118

[51] S.-E. Elayoubi, O. B. Haddada, and B. Fourestié, "Performance Evaluation of Frequency Planning Schemes in OFDMA-based Networks," *IEEE Transactions on Wireless Communications*, vol. 7, no. 5, pp. 1623–1633, May 2008.

[52] H. Jia, Z. Zhang, G. Yu, P. Cheng, and S. Li, "On the Performance of IEEE 802.16 OFDMA System under Different Frequency Reuse and Subcarrier Permutation Patterns," in *IEEE International Conference on Communications (ICC)*, vol. 24, june 2007, pp. 5720–5725.

[53] R. Chang, Z. Tao, J. Zhang, and C.-C. J. Kuo, "A Graph Approach to Dynamic Fractional Frequency Reuse (FFR) in Multi-Cell OFDMA Networks," in *IEEE International Conference on Communications Workshops (ICC)*, Dresden, Germany, June 2009.

[54] M. Necker, "Interference Coordination in Cellular OFDMA Networks," *IEEE Network*, vol. 22, no. 6, pp. 12–19, November/December 2008.

[55] G. Song and Y. Li, "Cross-layer optimization for OFDM wireless networks-part I: theoretical framework," *IEEE Transactions on Wireless Communications*, vol. 4, no. 2, pp. 614–624, 2005.

[56] J. Jang and K. B. Lee, "Transmit power adaptation for multiuser OFDM systems," *IEEE Journal on Selected Areas in Communications*, vol. 21, no. 2, pp. 171–178, February 2003.

[57] S. Das, H. Viswanathan, and G. Rittenhouse, "Dynamic load balancing through coordinated scheduling in packet data systems," in *IEEE Conference on Computer Communications (INFOCOM 2003)*, San Francisco USA, April 2003.

[58] A. Gjendemsjo, D. Gesbert, G. E. Oien, and S. G. Kiani, "Optimal power allocation and scheduling for two-cell capacity maximization," in *in Proceedings of the IEEE RAWNET (WiOpt)*, April 2006.

[59] G. Li and H. Liu, "Downlink Radio Resource Allocation for Multi-Cell OFDMA System," *IEEE Transactions on Wireless Communications*, vol. 5, no. 12, pp. 3451–3459, December 2006.

[60] F. Bernardo, R. Agustí, J. Pérez-Romero, and O. Sallent, "Temporal and Spatial Spectrum Assignment in Next Generation OFDMA Networks through Reinforcement Learning," in *IEEE 69th Vehicular Technology Conference (VTC 2009)*, Barcelona, Spain, April 26-29 2009.

[61] L. Venturino, N. Prasad, and X. Wang, "Coordinated Scheduling and Power Allocation in Downlink Multicell OFDMA Networks," *IEEE Transactions on Vehicular Technology*, vol. 58, no. 6, pp. 2835–2848, July 2009.

[62] S. Hamouda, C. Yeh, J. Kim, S. Wooram, and D. S. Kwon, "Dynamic hard fractional frequency reuse for mobile wimax," *Pervasive Computing and Communications, IEEE International Conference on*, vol. 0, pp. 1–6, 2009.

[63] S. Hussain and V. C. M. Leung, "Dynamic Frequency Allocation in Freactional Frequency Reuse OFDMA Networks," *IEEE Transactions on Wireless Communications*, vol. 8, no. 8, pp. 4286–4295, August 2009.

[64] E. Altman, K. Avrachenkov, and A. Garnaev, "Closed form solutions for water-filling problem in optimization and game frameworks," in *IEEE Conference on Computer Communications (INFOCOM 2008)*, Phoenix USA, April 2008.

[65] S. T. Chung, S. J. Kim, J. Lee, and J. Cioffi, "A game theoretic approach to power allocation in frequency-selective Gaussian interference channels," in *Proceedings of the IEEE International Symposium on Information Theory*, July 2003, pp. 316–316.

[66] S. Kumar, G. Monghal, J. Nin, I. Ordas, K. Pedersen, and P. Mogensen, "Autonomous Inter Cell Interference Avoidance under Fractional Load for Downlink Long Term Evolution," in *IEEE Vehicular Technical Conference (VTC 2009-Spring)*, Barcelona Spain, April 2009.

[67] P. A., T. Kolding, and P. Mogensen, "Performance of Downlink Frequency Domain Packet Scheduling for the UTRAN Long Term Evolution," in *IEEE Personal, Indoor and Mobile Radio Communications Symposium (PIMRC)*, Helsinki Finland, September 2006.

[68] A. Stolyar and H. Viswanathan, "Self-organizing Dynamic Fractional Frequency Reuse in OFDMA Systems," in *IEEE Conference on Computer Communications (INFOCOM 2008)*, April 2008, pp. 691–699.

[69] J. D. Hobby and H. Claussen, "Deployment Options for Femtocells and their Impact on Existing Macrocellular Networks," *Bell Labs Technical Journal*, vol. 13, pp. 145–160, 2009.

[70] I. Güvenc, M.-R. Jeong, F. Watanabe, and H. Inamura, "A Hybrid Frequency Assignment for Femtocells and Coverage Area Analysis for Co-Channel Operation," *IEEE Communications Letters*, vol. 12, pp. 880–882, december 2008.

[71] G. de la Roche, A. Valcarce, D. López-Pérez, and J. Zhang, "Access Control Mechanisms for Femtocells," *IEEE Communications Magazine*, vol. 48, no. 1, pp. 33–39, January 2010.

[72] H. Claussen, L. T. W. Ho, and L. G. Samuel, "An overview of the femtocell concept," *Bell Labs Technical Journal - Wiley*, vol. 3, no. 1, pp. 221–245, May 2008.

[73] G. de la Roche, A. Valcarce, D. López-Pérez, and J. Zhang, "Access Control Mechanisms for Femtocells," *IEEE Communications Magazine*, vol. 48, no. 1, pp. 33–39, January 2010.

[74] S. P. Weber, J. Andrews, X. Yang, and G. de Veciana, "Transmission capacity of wireless ad hoc networks with successive interference cancellation," *IEEE Transactions on Information Theory*, vol. 53, no. 8, pp. 2799–2814, 2007.

[75] H. Claussen, "Performance of Macro- and Co-Channel Femtocells in a Hierarchical Cell Structure," in *IEEE Personal, Indoor and Mobile Radio Communications (PIMRC)*, Athens, Greece, September 2007, pp. 1–5.

[76] H. Claussen, L. T. W. Ho, and L. G. Samuel, "Self-optimization of coverage for femtocell deployments," in *Wireless Telecomunications Symposium (WTS)*, April 2008, pp. 278–285.

[77] H. Claussen and F. Pivit, "Femtocell Coverage Optimization using Switched Multi-element Antennas," in *IEEE International Conference on Communications (ICC)*, Dresden, Germany, June 2009.

[78] V. Chandrasekhar and J. G. Andrews, "Uplink Capacity and Interference Avoidance for Two-Tier Femtocell Networks," *IEEE Transactions on Wireless Communications*, vol. 8, no. 1, pp. 3498–3509, 2009.

[79] ——, "Spectrum Allocation in Tiered Cellular Networks," *IEEE Transactions on Communications*, vol. 57, no. 10, pp. 3059–3068, 2009.

[80] J. Ling, D. Chizhik, and R. Valenzuela, "On Resource Allocation in Desne Femtodeployments," in *IEEE International Conference on Microwaves, Communications, Antennas and Electronics Systems (COMCAS 2009)*, Tel Aviv, 2009.

[81] Q. Su, A. Huango, Z. Wu, G. Yu, Z. Zhang, K. Xu, and J. Yang, "A distributed dynamic spectrum access and power allocation algorithm for Femtocell networks," in *International Conference on Wireless Communications and Signal Processing (WCSP 2009)*, Nanjing, China, November 2009.

[82] D. P. Bertsekas, A. Nedic, and A. E. Ozdaglar, *Convex analysis and optimization.* Athena Scientific, 2003.

[83] T. Kwon, H. Lee, S. Choi, J. Kim, and D.-H. Cho, "Design and Implementation of a Simulator Based on a Cross-Layer Protocol between MAC and PHY Layers in a WiBro Compatible IEEE 802.16e OFDMA System," *IEEE Communications Magazine*, vol. 43, no. 12, pp. 136–146, December 2005.

[84] J. Chen, C.-C. Wang, F. C.-D. Tsai, C.-W. Chang, S.-S. Liu, J. Guo, W.-J. Lien, J.-H. Sum, and C.-H. Hung, "The Design and Implementation of WiMAX Module for ns-2 Simulator," in *Workshop on ns-2: the IP network simulator (WNS2)*, Pisa, Italy, October 2006.

[85] Forsk Atoll-Global RF Planning Solution, http://www.forsk.com.

[86] L. Häring, B. K. Chalise, and A. Czylwik, "Dynamic System Level Simulations of Downlink Beamforming for UMTS FDD," in *IEEE Global Telecommunications Conference (GLOBECOM)*, vol. 1, December 2003, pp. 133 – 137.

[87] A. Valcarce, H. Krauss, J. Hauck, M. Buchholz, and F. Aguado, "Empirical propagation model for WiMAX at 3.5 GHz in an urban environment," *Wiley Microwave and Optical Technology Letters*, vol. 50, no. 2, pp. 483–487, February 2008.

[88] NGMN, "NGMN radio access performance evaluation methodology," A White Paper by the NGMN Alliance, Tech. Rep., January 2008.

[89] A. Valcarce, G. de La Roche, A. Jüttner, D. López-Pérez, and J. Zhang, "Applying FDTD to the coverage prediction of WiMAX femtocells," *EURASIP Journal of Wireless Communications and Networking. Special issue on Advances in Propagation Modelling for Wireless Systems*, February 2009.

[90] J.-M. Gorce, K. Jaffres-Runser, and G. de la Roche, "Deterministic approach for fast simulations of indoor radio wave propagation," *IEEE Transactions on Antennas and Propagation*, vol. 55, pp. 938–942, March 2007.

[91] F. Gunnarsson, M. Johansson, A. Furuskar, M. Lundevall, A. Simonsson, C. Tidestav, and M. Blomgren, "Downtilted Base Station Antennas - A Simulation Model Proposal and Impact on HSPA and LTE Performance," in *Vehicular Technology Conference, 2008. VTC 2008-Fall. IEEE 68th*, Calgary, BC, September 2008.

[92] *TS 36.420, X2 general aspects and principles*, 3GPP Std.

[93] C. E. Shannon, "A mathematical theory of communication," *Bell System Technical Journal*, vol. 27, pp. 379–423, July 1948.

[94] *Optimization in Operations Research.* upper Saddle River, NJ, USA: Prentice Hall, 1998.

[95] "IBM ILOG CPLEX," http://www.ibm.com/software/integration/optimization/cplex/.

[96] "FICO Xpress Optimization Suite 7," http://www.fico.com/en/Products/DMTools/Pages/FICO-Xpress-Optimization-Suite.aspx.

[97] "GNU Linear Programming Kit," http://www.gnu.org/software/glpk/.

[98] "COIN-OR Linear Program Solver," http://www.coin-or.org/Clp/.

[99] B. Hajek, "A Tutorial Survey of Theory and Applications of Simulated Annealing," in *24th Conference on Decision and Control*, 1985.

[100] F. Glover and M. Laguna, *Tabu search.* Hingham: F. Glover and M. Laguna, 1997.

[101] R. K. Ahuja and T. L. M. J. B. Orlin, *Network Flows: Theory, Algorithms, and Applications.* Prentice Hall, 1993.

[102] G. B. Dantzig, *Linear Programming and Extensions.* Princeton University Press, 1963.

[103] "Library for Efficient Modeling and Optimization in Networks (LEMON)," http://lemon.cs.elte.hu.

[104] Z. Xie and B. Walke, "Enhanced Fractional Frequency Reuse to Increase Capacity of OFDMA Systems," in *New Technologies, Mobility and Security (NTMS), 2009 3rd International Conference on*, Cairo, Egypt, December 2009.

[105] C. Oliveira, J. B. Kim, and T. Suda, "An adaptive bandwidth reservation scheme for high-speed multimedia wireless networks," *IEEE Jour. Select. Areas in Comm.*, vol. 16, no. 6, pp. 858–874, August 1998.

[106] S. Sesia, I. Toufik, and M. Baker, *LTE: The UMTS Long Term Evolution, From Theory to Practice.* John Wiley & Sons Ltd, Feb. 2009.

[107] Séroul R., *Programming for Mathematicians.* Berlin: Springer-Verlag, p. 162, 2000.

[108] V. Chandrasekhar, J. G. Andrews, and A. Gatherer, "Femtocell Networksr A Survey," *IEEE Communications Magazine*, vol. 46, no. 9, pp. 59–67, September 2008.

[109] 3GPP TR 25.967, "FDD Home Node B (HNB) Radio Frequency (RF) requirements (FDD)," v.9.0.0, July 2009.

[110] Alcatel-Lucent, "HNB to HNB Handover Architecture," 3GPP TSG RAN3 63bis, Tech. Rep., March 2009.

[111] 3GPP TS 36.420, "Evolved Universal Terrestrial Radio Access Network (E-UTRAN); X2 general aspects and principles," v.8.0.0, December 2007.

[112] D. López-Perez, A. Ladanyi, A. Juttner, and J. Zhang, "OFDMA femtocells: A self-organizing approach for frequency assignment," in *Personal, Indoor and Mobile Radio Communications Symposium (PIMRC)*, Tokyo, Japan, September 2009.

[113] H. Claussen, "Co-Channel Operation of Macro- and Femtocells in a Hierarchical Cell Structure," *International Journal of Wireless Information Networks*, vol. 15, no. 3, pp. 137–147, December 2008.

[114] H. Claussen, L. T. W. Ho, and L. G. Samuel, "An overview of the femtocell concept," *Bell Labs Technical Journal*, vol. 13, no. 1, pp. 221–245, May 2008.

[115] M. Gudmundson, "Analysis of Handover Algorithms," in *IEEE 41st Vehicular Technology Conference (VTC 1991)*, St.Louis, MO, May 1991, pp. 537–542.

[116] *R1-101369, Considerations on interference coordination in heterogeneous networks*, 3GPP Std., San Francisco, CA, Feb. 2010.

[117] *R1-104661, Comparison of Time-Domain eICIC Solutions*, 3GPP Std., Madrid, Spain, Aug. 2010.

[118] A. Valcarce, G. de la Roche, A. Jüttner, D. López-Pérez, and J. Zhang, "Applying FDTD to the coverage prediction of WiMAX femtocells," *EURASIP Journal of Wireless Communications and Networking*, vol. 2009, 2009.

[119] C. Bettstetter, "Smooth is better than sharp: A random mobility model for simulation of wireless networks," in *Proceedings of the 4th ACM international workshop on Modeling, analysis and simulation of wireless and mobile systems*, Rome, Italy, 2001, pp. 19–27.

[120] P. Coucheney, C. Touati, and B. Gaujal, "Fair and efficient user-network association algorithm for multi-technology wireless networks," in *IEEE INFOCOM 2009, IEEE*, Rio de Janeiro, Brazil, April 2009, pp. 2811 – 2815.

[121] X. Chu, Y. Wu, D. López-Pérez, and X. Tao, "On Providing Downlink Services in Collocated Spectrum-Sharing Macro and Femto Networks," *Submitted to IEEE Transactions on Wireless Communications*, 2011.

[122] V. Chandrasekhar and J. Andrews, "Uplink Capacity and Interference Avoidance for Two-Tier Femtocell Networks," in *IEEE Global Telecommunications Conference (GLOBECOM)*, Washington, DC, November 2007, pp. 3322–3326.